CRANFIELD UNIVERSITY

T I R MATKO

TWO-PHASE FLOW IN CIRCULAR SECONDARY SEDIMENTATION TANKS

SCHOOL OF INDUSTRIAL AND MANUFACTURING SCIENCE

PhD THESIS

CRANFIELD UNIVERSITY

SCHOOL OF WATER SCIENCES

PhD THESIS

Academic Year 1997-8

T I R MATKO

Two-Phase Flow in Circular Secondary Sedimentation Tanks

Supervisor: Professor Tom Stephenson

December 1997

This thesis is submitted in partial fulfilment of the requirements
for the Degree of Doctor of Philosophy

ABSTRACT

The main objective of this work was to optimise a numerical model to predict the flow in circular secondary sedimentation tanks. The numerical models in the literature were reviewed and the new opportunities for research were identified. Single-phase flow characteristics of two circular sedimentation tanks were investigated using the CFD program, CFX-F3D. The flow in the circular clarifiers were modelled in two dimensions (axial and radial) and using the standard k-ϵ turbulence model. Results indicated that a vertical inlet instead of a horizontal inlet did not improve the correlation with the experimental data in a pilot-scale tank. Modelling the diurnal variation in flow to a full-scale tank significantly improved the correlation with experimental data. The 'Eulerian multi-fluid' model in the program, CFX-F3D was modified to predict the flow in circular secondary sedimentation tanks. The model compared quite closely with the measured residence time of the effluent and return activated sludge (RAS) in a conventional secondary clarifier. The residence time of the effluent in another secondary clarifier with a turbulent jet, was over-predicted. The mean particle diameter in the model was found by comparing the numerical predictions with experimental data. The particle diameter was between 100 to 190 μm for the secondary clarifiers, which was in agreement with the experimental data in the literature. The flow patterns in the conventional secondary clarifier were affected by the particle density, particle diameter, axial slip velocity, colloids settling parameter, axial turbulent Prandtl number, inlet flow rate and inlet solids concentration. A 3-D simulation of the conventional secondary clarifier was in agreement with a 2-D simulation. Recommended values were given for all these parameters. However, the drag force between the phases was not formulated correctly and the water surface was modelled as a symmetry plane. Therefore, some more work is still required to make suitable modifications to the model.

ACKNOWLEDGEMENTS

I would like to dedicate my PhD thesis to my late father, who sadly passed away in August 1995. Up to a few years ago he was still working at Glasgow University, as a lecturer in the Department of Soviet and East European Studies. He received his Masters Degree many years ago and would have really appreciated me receiving my PhD title.

There are many people I would like to thank for the help and support they have given me during the time I spent at Cranfield. I have had three supervisors at the British Hydromechanics Research Group. The first two were Dr. Joe Hannon and Dr. Yong-Fu Xu, who were my supervisors for the first six months of my studies. For the rest of my time I was managed by Anthony Sharp, who's managing capabilities and fluid dynamics knowledge kept me on the right path. He was the head of the Process Technologies section at BHR Group. The original visionary of the project was Dr. Nick Fawcett, who is the head of the Process Modelling team at Yorkshire Water, and was my industrial supervisor. I always looked forward to my quarterly meetings with him. Professor Tom Stephenson is the head of the School of Water Sciences at Cranfield University and has been my academic supervisor throughout. His extensive knowledge of water and wastewater treatment processes and good writing ability was appreciated. His constant supervision right up to when I submitted my thesis helped me a lot. Dr. Raz Esfandiari is a friend, who was working at BHR Group as a CFD engineer. His knowledge of CFD has been inspirational to me and he has taught me so much, which has also been due to his thoughtful and thought provoking personality! I must acknowledge my other CFD colleagues at BHR Group, who understand very well what I have been through!

I visited some of Yorkshire Water's wastewater treatment plants to carry out tests on their sedimentation tanks. Yorkshire Water provided me with the equipment and the members of the Process Modelling team helped me with some of the experiments. The CFD software I was using was CFX-F3D and I would like to thank all the technical support staff at Computational Fluid Dynamics Services, who were able to answer my questions without much trouble. From a financial point of view, the Engineering and Physical Sciences Research Council provided me with a student grant and Yorkshire Water gave me an industrial bursary.

Finally, it gives me the most pleasure to remember the people dearest to me, who have been very understanding, patient and wise during the last 4 years. My mother, father, grandmother, brother Andrew and sister Stella have been very supportive and all deserve a special award! My girlfriend, Emal, who I was fortunate enough to meet at Cranfield University has been my main source of strength during my PhD. She has been extremely helpful and considerate, especially during the last 10 months when I have been writing up my thesis.

LIST OF CONTENTS

LIST OF TABLES

LIST OF FIGURES

Page

Chapter 4 Numerical model of single-phase flow

Chapter 5 Numerical model of two-phase flow

Chapter 6 Sensitivity investigation on the two-phase flow model

NOTATION

a	Stoke's settling velocity, m/s
A	settling area of tank, m^2
A_E, A_W, A_S, A_N	finite difference coefficients
c	concentration of Lithium ion, mg/l
C, C_i, C_1, C_2	suspended solids concentration, kg/m^3
C_d	dimensionless drag coefficient
C_{eff}	effluent suspended solids concentration, kg/m^3
C_{inl}	inlet suspended solids concentration, kg/m^3
C_{min}	suspended solids concentration of poorly settling particles, kg/m^3
C_p	suspended solids concentration at boundary, kg/m^3
C_{p1}, C_{p2}	turbulent constants
C_{RAS}	return activated sludge suspended solids concentration, kg/m^3
C_1, C_2, C_μ	turbulent constants
$C_{\alpha\beta}$	rate of mass transfer caused by momentum from phase α to β, kg/m^3s
°C	degrees celsius
d	distance from wall to boundary layer, m
d, d_p	particle diameter, m
D	hydraulic diameter, m
E	roughness coefficient
F_i	body force, N/m^3
Fr	inlet densimetric Froude number
g	gravitational acceleration, m/s^2
H	local water depth in the tank, m
H_b	water depth of the reaction baffle, m
H_{in}, H_{inl}	water depth of the inlet aperture, m
H_w	height of the effluent weir, m

$H-y_p$ thickness of the suspended solids boundary layer on the tank floor, m

i i direction

j j direction

k, k_{inl}, k_α mean (inlet) turbulent kinetic energy for phase α, m^2/s^2

k_r resuspension (scouring) parameter

K floc settling parameter, m^3/kg

K_1 colloids settling parameter, m^3/kg

Li^+ Lithium ion

LiCl Lithium Chloride

l_m mixing length, m

m mass flow rate of Lithium Chloride, kg/s

n, n^i distance, m

p mean pressure, N/m^2

P production of turbulent kinetic energy by the mean velocity gradients, m^2/s^3

Q flow rate, m^3/h

Q_e, Q_{eff} effluent flow rate, m^3/h

Q_i, Q_{inl}, Q_o inlet flow rate, m^3/h

$Q_r, Q_{RAS.} Q_u$ return activated sludge flow rate, m^3/h

r radial distance, m

r_{inl} inlet pipe radius, m

R tank radius, m ; residual of a variable

R_{in} baffle radius, m

R_o inlet pipe radius, m

R_s settling zone radius, m

r_α volume fraction of phase α

r_β volume fraction of phase β

$r_{\alpha inl}, r_{\beta inl}$ inlet volume fraction of phase α and β

R_e relative Reynolds number

S_C , S_P linearised source term components

SF_g gravity solids flux, kg/m^{2}s

SF_t downward solids flux, kg/m^{2}s

SF_u underflow solids flux, kg/m^{2}s

S_s specific gravity of particles

t time, s

u,v mean flow velocities in two directions, m/s

U mean flow velocity in axial direction, m/s

U^i increment to mean flow velocity, m/s

u_{inl}, u_o inlet flow velocity, m/s

u_p flow velocity parallel to the wall, m/s

u^* friction velocity, m/s

u_{slip} slip velocity, m/s

$u_{\alpha i}$, $u_{\beta i}$ mean flow velocity of phases α and β in i direction, m/s

$u_{\alpha j}$ mean flow velocity of phase α in j direction, m/s

V tank volume, m^3 ; mean flow velocity in radial direction, m/s

V_b bulk downward flow velocity, m/s

V_h horizontal velocity, m/s

V_o surface overflow rate, m^3/m^{2}day

V_p vertical velocity component in the bottom boundary layer at $y = y_p$

V_s average settling velocity of solids suspension, m/s

V_s, V_o Stoke's velocity of design particle, m/s

V_s, V_i, V_h hindered terminal settling velocity of particle, m/s

V_v vertical velocity, m/s

X_i suspended solids concentration of mixed liquor, kg/m^3

x_i, x_j distance in the i and j directions, m

y axial distance, m ; normal distance from wall, m

y_p normal distance between point p and the wall, m ; thickness of the suspended solids boundary layer on the tank floor, m

y_p^+ dimensionless wall distance

Greek Letters

α liquid (or solid) phase ; under-relaxation factor

β solid phase

Γ_α turbulent mass diffusivity of phase α, kg/ms

Δy thickness of boundary layer near tank base, m

∂ differential

ϵ, ϵ_{inl}, ϵ_α mean (inlet) turbulent kinetic energy dissipation rate for phase α, m^2/s^3

θ tangential angle, radians

κ von Karman constant

λ a constant

μ_α dynamic viscosity of phase α, kg/ms

$\mu_{\alpha eff}$ effective dynamic viscosity of phase α, kg/ms

$\mu_{t\alpha}$ turbulent eddy viscosity of phase α , m^2/s

μ_w dynamic viscosity of water, kg/ms

ν kinematic viscosity, m^2/s

ν_t turbulent eddy viscosity, m^2/s

ν_{sr} eddy diffusivity of suspended solids in the radial direction, kg/ms

ν_{sy} eddy diffusivity of suspended solids in the axial direction, kg/ms

ρ density, kg/m^3 ; local density of mixture, kg/m^3

ρ_s solids density, kg/m^3

ρ_w/ρ_r density of water (reference density), kg/m^3

ρ_α density of phase α, kg/m^3

ρ_β density of phase β, kg/m^3

σ_k turbulent Prandtl number for k

σ_{sr} turbulent Schmidt number in the radial direction

σ_{sy} turbulent Schmidt number in the axial direction

σ_α turbulent Prandtl number for volume fraction of phase α

σ_ϵ turbulent Prandtl number for ϵ

τ	nominal residence time, s
ϕ	a variable

Acronyms

BOD	Biochemical Oxygen Demand
CFD	Computational Fluid Dynamics
CFX-F3D	Computational Fluid Dynamics software
CSTR	Continuous Stirred Tank Reactor
MLSS	Mixed Liquor Suspended Solids
MW	Molecular Weight
NRT	Nominal Residence Time
RAS	Return Activated Sludge
RNG	Reynolds Normalisation Group
RSM	Reynolds Stress Model
RTD	Residence Time Distribution
SIMPLEC	Semi-Implicit Method for Pressure Linked Equations Correction
SVD	Settling Velocity Distribution
TPN	Turbulent Prandtl Number

CHAPTER I

INTRODUCTION

Sedimentation tanks or clarifiers are used traditionally in the treatment of industrial and municipal wastewaters. They remove solid particles by gravitational settling and produce an effluent with a reduced solids loading; for further treatment at the next unit process. In almost every wastewater treatment plant sedimentation tanks are still being used at several stages in the process, and are therefore one of the most important unit processes. However, wastewater treatment plants can fail to satisfy the legislated suspended solids concentration allowed in liquid wastes. It is important therefore to improve the design of sedimentation tanks.

The traditional design methods for sedimentation tanks use rules of thumb or empirical mathematical models, which normally do not consider the fluid dynamics. They are designed on simple criteria, such as the volume and settling area of the tank and assume that the fluid distribution and particle settling in the clarifier is uniform. Many clarifiers fail to satisfy their performance criteria because they have a poor flow distribution. A knowledge of the fluid dynamics can therefore be used to improve their performance. The most cost effective method will be to use a numerical model, as changes can be made more easily to the tank geometry, than using pilot-scale or full-scale tanks.

Computational fluid dynamics (CFD) is the most accurate numerical technique to predict the flow pattern and suspended solids concentration distribution in sedimentation tanks. The fundamental equations of fluid flow for the conservation

of mass, momentum and energy are solved. Turbulence models are used to predict the turbulent flow field, and additional equations may be used to solve the chemical and biological reactions and multi-phase flows. A computational grid is generated in two or three dimensions, to represent the tank geometry. The flow variables are solved in each cell (or cell node) to determine the velocity, turbulence, temperature and concentration profiles in the tank.

In the literature two dimensional models have been used to predict the fluid flow in secondary circular clarifiers with flat floors. The models have been validated successfully with experimental measurements of the velocities and the suspended solids concentrations. These models use a single phase flow model, with a density stratified model for the transport of the suspended solids. They include a term for the density of the solid particles and the local fluid density; and the drag of the particles on the fluid is ignored.

It is the intention of this project that some of the gaps in this work are addressed. The CFD program, CFX-F3D (version 4.1) has been used; which was written by Computational Fluid Dynamics Services (i.e. part of the Atomic Energy Authority). The Eulerian multi-fluid model in the program has been modified, to simulate the flow in circular secondary clarifiers with sloped floors. This work also involved the flow modelling around a deflector plate in a secondary clarifier, the study of the inlet velocity boundary condition and a three dimensional simulation of a secondary clarifier. Studies were also conducted on some of the properties of the solid particles, which include their density, viscosity, diameter and turbulent mass diffusion. These are all new areas of research. A literature review was conducted and found that CFD models were the most appropriate model to use for this work; and it identified the opportunities for new research. It is presented in Chapter 3 of the thesis.

The main objective of this project was to optimise the Eulerian multi-fluid model to predict the fluid flow in circular secondary clarifiers. A sensitivity study was undertaken on the numerical parameters in the model, to understand their importance and find their optimum values. This will make the model easier to use it in the future. It is intended that the model should be used in the future to reduce the final effluent solids concentration in wastewater treatment plants and make cost savings for sedimentation tanks.

Before progressing to a model of a secondary clarifier, a single-phase flow model was tested, to ensure that the flow patterns were accurate when there were no solids present. The model was validated with a laboratory tank and a full-scale humus tank. Two inlet velocity boundary conditions (horizontal and vertical) were simulated for the pilot-scale clarifier and the average inlet flow rate was compared to the variable inlet plant flow rate for the full-scale clarifier, using a user defined subroutine. The residence time distributions (RTD) of the effluent were validated with experimental measurements. This work is described in Chapter 4.

The Eulerian multi-fluid model uses different equations to the current models in the literature. Each phase occupies a fraction of the total control volume in each cell, and the conservation equations are applied to each phase to give separate velocity fields. The effect of drag on the fluid is accounted for by a source term, for the transfer of momentum between the phases. The multi-fluid model was modified to predict the flow in two full-scale secondary clarifiers. The experimental settling velocities of the particles were measured in settling columns and entered into the model, using a user defined subroutine. The anisotropic turbulent mass diffusion of the particles was also entered using a user defined subroutine. In one of the clarifiers there was a deflector plate which induced a turbulent jet. The models predictions of the residence time distribution and

suspended solids concentration of the effluent and return activated sludge (RAS) were compared to experimental measurements for both secondary clarifiers. This work is in Chapter 5.

Investigations were conducted on the multi-fluid model for the physical properties of the solids, i.e. density, viscosity and diameter; the settling and resuspension of the solids, i.e colloids settling parameter, axial slip velocity and turbulent Prandtl number, and the flow properties, i.e. inlet flow rate and inlet suspended solids concentration. A grid dependency check was conducted. A three dimensional model of the clarifier without the deflector plate was carried out. Further 3-D simulations were restrictive, because of the large computational effort required. The instability of the model when simulating the turbulent jet prevented a 3-D simulation of the secondary clarifier with the deflector plate. The sensitivity study is presented in Chapter 6.

The overall discussion of the thesis is given in Chapter 7, the conclusions are in Chapter 8 and the recommendations for future work are in Chapter 9. In Appendix A, the convergence history of the computed parameters are given for some of the secondary clarifier simulations. Appendix B discusses the numerical boundary conditions. Appendix C has some details about the experimental salt tracer test. Chapters 3 and 4 contain published papers and chapters 5 and 6 are also written as papers. The overall objectives are given in the next chapter.

CHAPTER II

OBJECTIVES

1. To validate a single-phase flow model of a circular clarifier with experimental measurements of the residence time distribution of the effluent from two clarifiers.

2. To determine whether a horizontal or vertical inlet velocity boundary is preferable in the single-phase flow model of a pilot-scale clarifier.

3. To determine if a single-phase flow prediction of a full-scale humus clarifier is more accurate when using the actual variable plant flow rate.

4. To validate a two-phase flow model with experimental measurements of the residence time distribution of the effluent and return activated sludge from two full-scale secondary circular clarifiers.

5. To predict the mean particle diameter in the two-phase model by comparing the predicted and experimental effluent solids concentration.

6. To validate a two-phase flow model with experimental measurements of the suspended solids concentration of the return activated sludge and solids contours within two secondary clarifiers.

7. To study the parametric sensitivity of the two-phase flow model on the flow pattern and suspended solids concentration in a secondary clarifier.

CHAPTER III

This chapter of the thesis has been refereed and published in a journal and the reference of the paper is as follows : Matko, T., Fawcett, N., Sharp, A. and Stephenson, T. (1996). 'Recent progress in the numerical modelling of wastewater sedimentation tanks'. Transactions of the Institution of Chemical Engineers, Part B3, vol. 74, 245-258. A literature review was conducted to determine what is the most appropriate numerical model for this work. The review briefly describes the traditional design methods and the more sophisticated computational modelling techniques, which are now being employed to improve sedimentation tank design. Progress from researchers in this area are reported, and the current opportunities for new research are identified, to enable the work in this thesis to make a contribution to research.

LITERATURE REVIEW

3.1 Introduction

Sedimentation is the 'workhorse' process for wastewater treatment (Figure 3.1). In fact, at most sewage treatment works sedimentation is the last process before the effluent is discharged to the river. Thus, a sedimentation tank which performs well is crucial for meeting the ever tightening effluent quality standards. Typically,

sedimentation is used for: the separation of heavy particles at the works inlet (grit removal) ; the removal of light organic matter from the incoming sewage (primary sedimentation); the separation of biomass from biological treatment processes (secondary or activated sludge sedimentation); and the thickening of sludge to facilitate its treatment and disposal.[1] The performance of the primary and secondary sedimentation stages, in particular, are central to the whole works performance, and thus form the focus of this review.

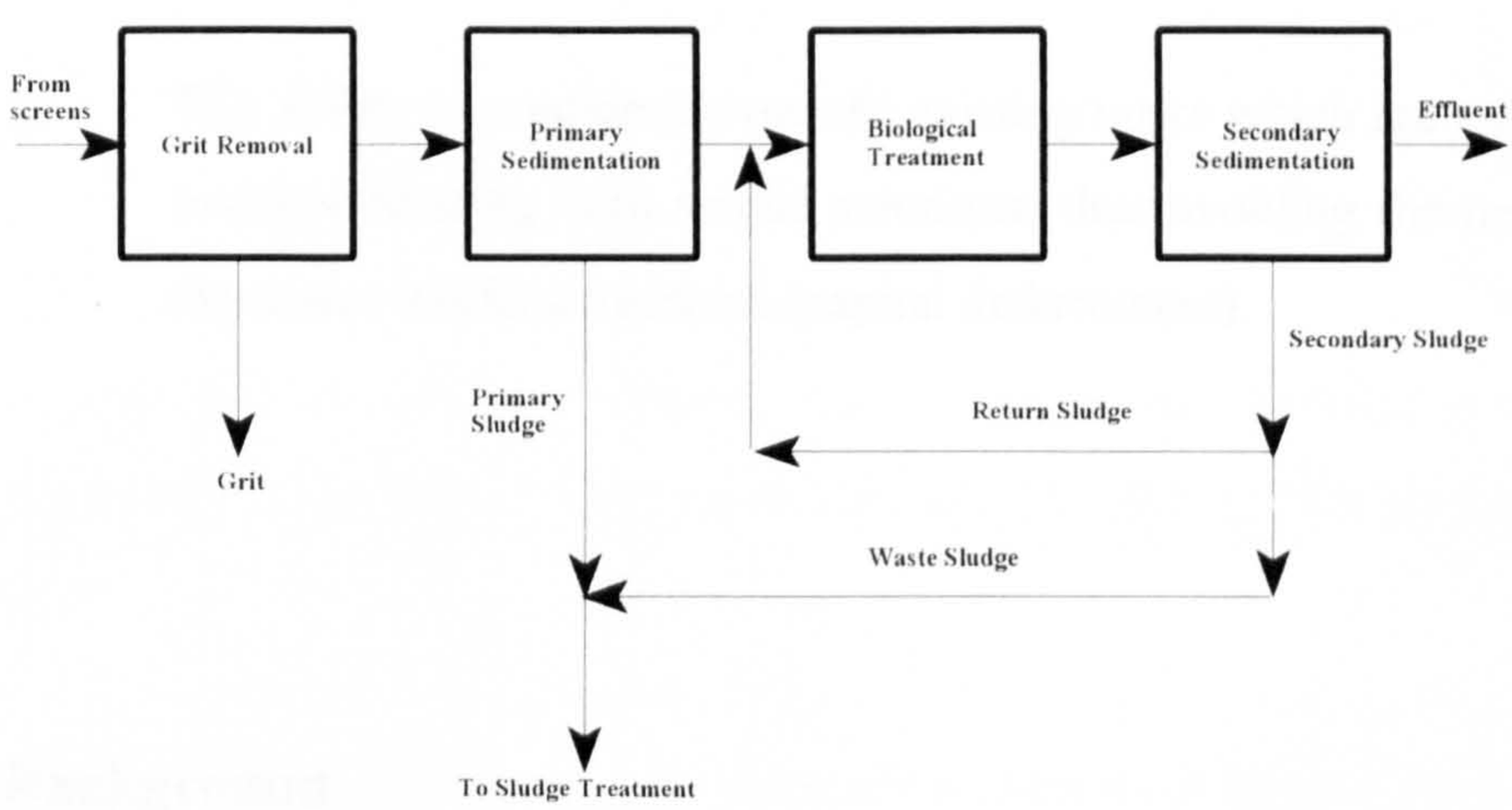

Figure 3.1 Schematic of typical wastewater treatment process.

The design methodologies for both primary and secondary sedimentation are based on simple mechanistic models, and operational experience. In all the design approaches the effect of the fluid mechanics on the performance are not considered. Consequently, failure of such tanks is often connected with poor flow distribution.

A better understanding of the sedimentation process, and in particular the influence of the fluid mechanics, could lead to two key benefits :

1. Improved design of new tanks, leading to fewer consent failures, or less tanks to achieve the consent with attendant capital savings ;

2. The ability to confidently retrofit existing tanks which are currently underperforming with simple solutions, thus avoiding the need for expensive works extensions (capital deferrement).

3.2 Background

The design of sedimentation tanks is normally based on the surface overflow rate[2], V_o and flow rate, Q, to determine the settlement area of the tank, A, as follows :

$$A=\frac{Q}{V_O} \qquad \text{- (3.1)}$$

The solids removal rate is assumed to be the fraction of solid particles with terminal settling velocities greater than the surface overflow rate.[2] Stoke's law gives the terminal settling velocity, V_s, for discrete spherical particles in quiescent conditions, as :

$$V_s=\frac{gd^2(\rho_s-\rho_w)}{18\mu_w} \qquad \text{- (3.2)}$$

where V_s is the terminal settling velocity in m/s, d is the particle diameter in m, ρ_s is the particle density in kg/m^3, ρ_w is the fluid density in kg/m^3 and g is the gravitational acceleration.

The terminal settling velocity is normally selected by experience (e.g. V_s = 10 m/hr). Alternatively Stoke's velocity is determined by settling column tests, in a laboratory on a particular wastewater. The test is used to determine the real settling characteristics of the wastewater, but it is still undertaken in quiescent flow conditions. Equation 3.2 has no expression for volume and the settling area is the important design variable. The volume is also set by operational experience (e.g. 2

hours retention time at the maximum flow). Thus, the 3rd dimension (depth) is often found, by dividing the volume, with the area calculated from equation 3.1. Guidelines also exist for the depth of sedimentation tanks.

The residence time and tank volume are calculated with no real consideration of the fluid dynamics (Table 3.1)[3]. Early studies only considered plug flow, meaning that all elements of the fluid reached the outlet in the same residence time[4,5]. Hazen[2] assumed that the flow from surface to base was uniformly distributed, and in theory the particle was carried horizontally by the motion of the fluid and settled vertically (Figure 3.2). However in practise, flow short-circuiting can reduce the residence time to typically 10-30 % of the expected value, and allow particles less time to settle and be removed[6]. Fluid mixing and turbulent flow in sedimentation tanks detrimentally disturb quiescent settling conditions. On the one hand, this can cause particle breakup, or conversely it can increase particle flocculation.

During settling, flocculation of the particles occur as soon as their concentration is higher than about 50 mg/l. The particles make contact with each other and stick together to form flocs (i.e. the process of flocculation) and consequently they increase in size and mass. The average settling velocity of the particles increase. As soon as the concentration of flocculated matter become substantial, interaction between flocs become important. They adhere together and form an interface between the particles and the supernatant liquid. Fluid is forced upwards between the particles which make them settle slower. This is referred to as 'hindered' settling and is typical when suspended solids concentrations exceed 500 mg/l. The path line of the particles in the clarifier is also affected (Figure 3.2).

Table 3.1 Hydraulic characteristics of sedimentation tanks.

Hydraulic Characteristic	**Description**
Recirculating flow	The flow re-circulates by its impact on solid boundaries rather than flowing slowly across the surface. There will be rapid flow along the base of the tank, causing resuspension of sedimented material. Noticeably there are 'dead-zones' (no flow zones) causing a reduction in the effective volume, and thereby reducing the effective solids removal.
Jet flow	The inlet flow behaves as a jet, causing free stream turbulence in the inlet region and turbulent mixing of the influent with the flow in the tank. Thus, in the inlet region there is the most swirling flow.
Wall boundaries	The impact of the flow on the solid boundaries causes flow turbulence and a change in the flow path direction. which will cause separation or re-attachment of flow at the boundary.
Stratification	The density difference between the inlet wastewater and the existing flow in the tank causes density currents. Either the influent floats along the top surface or plunges downwards. This may cause the solids to pass more quickly to the effluent, thus reducing the solids removal. Stratification reduces flow turbulence.
Flow impingement	The aim of the in-tank baffle is to diffuse the horizontal velocities and thereby reduce boundary turbulence. It also tangentially distributes the flow more evenly.
Turbulent parameters	The turbulent kinetic energy and dissipation of energy are distributed, causing local areas of mixing and a reduction in the solids removal.
Wind shear	The effect of wind on the water surface causes flow turbulence near the surface and swirling flow.
Re-entrainment	The solid particles re-entrain into the flow and cause solid-liquid turbulence. which is not ideal for quiescent particle settling.

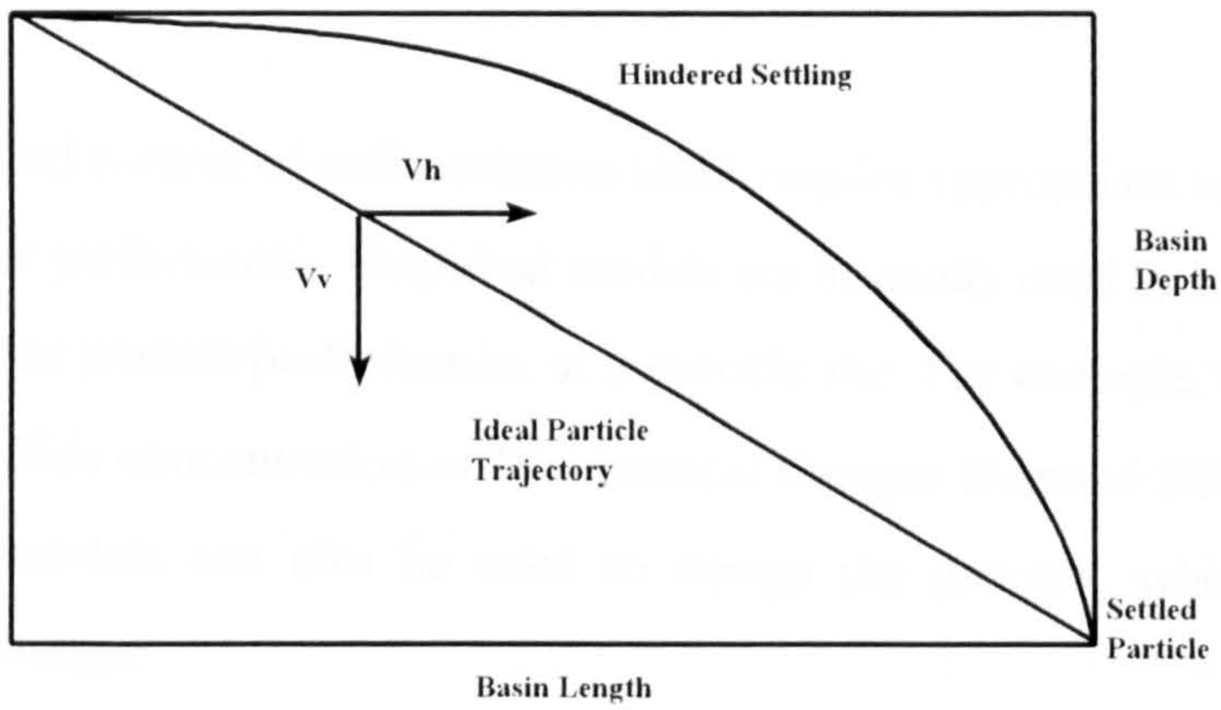

Figure 3.2 Idealised and hindered particle settling path in settling basins[4-5]

Discrete particle settling will take place at low suspended solids concentrations. This behaviour is predominant in grit removal, where particles are large and dense (1300 - 2700 kg/m^3), and also in the upper regions of primary sedimentation tanks (inlet solids concentrations from 100-500 mg/l)[1]. When solids concentrations are sufficiently high then flocculent and hindered settling occur (Table 3.2). This is predominant in the lower regions of primary sedimentation tanks, and especially in the high mixed liquor suspended solids (MLSS) concentrations in secondary sedimentation tanks. In the lower regions of secondary clarifiers, where suspended solids concentrations exceed 3000 mg/l, the particles compact when in close contact, and compressive settling occurs. The fluid dynamics and settling characteristics of the wastewater are clearly not ideal.

3.3 Empirical design methods

Efficient design and control of sedimentation tanks require appropriate tools for the evaluation of their performance. Empirical models are normally used to monitor and thereby improve the process performance, at a specific site. For example, to monitor the suspended solids concentration or Biochemical Oxygen Demand (BOD) in the effluent. These models can also be used to design the process, when there is insufficient knowledge.

Empirical models are developed by gathering sets of experimental data and identifying the linear relationships between process variables by regression analysis. By dimensional analysis, empirical constants can be determined, and help to determine the crucial variables in sedimentation tank design. The overflow rate and inlet solids concentrations have been identified as two important parameters that effect the performance of primary sedimentation tanks[7-9]. These studies found that the solids removal rate increased with increasing inlet solids concentration, and decreased with increasing surface overflow. Voutchkov concluded similarly, that the settling characteristics, MLSS and the sidewater depth were important variables for secondary clarifiers[10]. Roche *et al.*[11] developed a semi-empirical model, to account for the compressive settling of activated sludge, by taking samples from industrial, municipal and pilot-scale plants. They identified a power law relationship between the biomass concentration and the hydraulic residence time. The model agreed with experimental data obtained from a full scale secondary clarifier.

Empirical models have been used in process design which is based on an oversimplification of the fluid dynamics[4-5]. Billmeir's model, with a simplified flow pattern, sized a secondary clarifier using a series of zone depths (clarifying depth, separation depth, storage depth and thickening and scraping depth), and assumed there was full utilisation of the tank volume[12]. More recently Haltunnen[13] developed a model, to prevent high effluent concentrations in the pulp and paper industry. The clarifier was divided into four different zones (inlet, settling, thickening and separation), to estimate sludge volumes which were close to the measured values. Another study assumed plug flow for each unit process in an activated sludge plant, and calculated its flow and mass balances. This highly empirical approach found the least-cost design of the treatment plant, and especially for the aeration tank and the secondary clarifier[14,15].

Table 3.2 Types of settling phenomena in wastewater treatment[1].

Type of settling phenomenon	Description	Application/occurrence
Discrete particle (type 1)	Refers to the sedimentation of particles in a suspension of low solids concentration. Particles settle as individual entities.	Removes grit and sand particles from wastewater
Flocculant (type 2)	Refers to a rather dilute suspension of particles that coalesce, or flocculate, during the sedimentation process. By coalescing, the particles increase in mass and settle at a faster rate.	Removes a portion of the suspended solids in untreated wastewater in primary settling facilities, and in upper portions of secondary settling facilities. Also removes chemical floc in settling tanks.
Hindered, also called zone (type 3)	Refers to suspensions of intermediate concentration, in which inter-particle forces are sufficient to hinder the settling of neighbouring particles. The particles tend to remain in fixed positions with respect to each other, and the mass of particles settle as a unit. A solids-liquid interface develops at the top of the settling mass.	Occurs in secondary settling facilities used in conjunction with biological treatment facilities.
Compression (type 4)	Refers to settling in which the particles are of such concentration that a structure is formed, and further settling can occur only by compression of the structure. Compression takes place from the weight of the particles which are constantly being added.	Usually occurs in the lower layers of a deep sludge mass, such as in the bottom of deep secondarysettlingfacilities and in sludge-thickening facilities.

3.4 Solids mass flux model

The solids mass flux or limiting mass flux model is applied to activated sludge clarifiers, where the solids loadings are higher than other types of clarifiers. It recognises that the total mass of solids through the secondary clarifier and the return sludge flow is limited[16]. The mass flux model is normally used as a design tool, to select the return sludge flow and find the solids concentration in the sludge blanket and in the return sludge flow[17-18]. Its other use is to control the return sludge flow, by monitoring the sludge blanket in a working treatment plant. For activated sludge processes, the secondary sedimentation tank has two functions: to clarify and meet effluent standards, and as an integral part of the activated sludge process (i.e. for sludge storage, to provide biomass and reduce the size of the activated sludge plant).

Thickening of the mixed liquor is caused by the downward solids flux[19]. The mass flux model has been used to model the downward solids flux in the secondary clarifier, by dividing the tank into a number of volumes and calculating a mass balance across each element[20-21]. The one-dimensional multi-layered model (Figure 3.3) of Chi-Howell[22] has been used by others. If the flow rates are unknown, then it is sometimes assumed that the return activated sludge flow is 50% of the inlet flow[23].

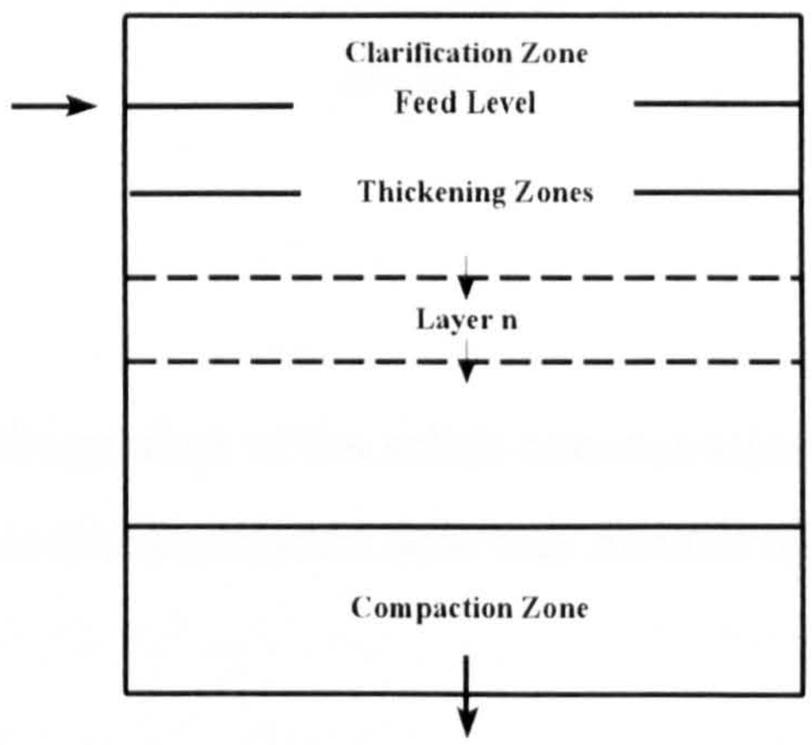

Figure 3.3 Schematic of Chi-Howell settler model after Chi[22].

For the transport of solids, the total solids flux, SF_t is the sum of the settling flux due to the gravitational floc settling, SF_t , and a bulk flow caused by the pumped underflow, SF_u[1] :

$$SF_t = SF_u + SF_g$$

- (3.3)

The gravity flux is the product of the average solids concentration, C_i , and the hindered settling velocity, V_i :

$$SF_g = C_i V_i \qquad \text{- (3.4)}$$

The underflow flux is the product of the solids concentration, C_i , and the downward velocity, V_b, defined as the downward flow rate divided by the settling area, A.

$$SF_u = C_i V_b \qquad \text{- (3.5)}$$

At the limiting solids flux, the tank performs at its maximum solids loading for a given tank area, and an increase in solids loading will cause the sludge blanket to rise and enter the settling zone. Consequently, the sludge blanket hinders the particle settling velocity and may over reach the weir, causing the effluent quality to deteriorate. To overcome this problem it is often desirable to determine whether the tank is underloaded or overloaded and this can be determined using Kynch's solid (or batch) flux curve[20].

The curve shows the solids concentration, X on the x-axis and the total flux, SF_t on the y-axis. Balslev[23] presented an analysis of the batch flux curve which was based on real data (Figure 3.4). Operating lines are plotted on the graph. The slope of line (C) is equal to the negative value of the underflow, Q_u , divided by the total area of the clarifiers, and the slope of line (B) is equal to the incoming flow, Q_i , divided by the total area of the clarifiers (note: line (B) starts at the origin). The lines intersect at the operating point, where the corresponding x-coordinate of intersection gives the MLSS in the aeration tanks, and the y-coordinate gives the solids flux to the clarifier as a result of the incoming flow. The range of the suspended solids concentration in the clarifier will be in the interval between C_1 and C_2 , where C_2 is the suspended solids concentration in the return sludge. In Balslev's clarifier (Figure 3.4), the tank is underloaded because line (C) does not cross the batch flux curve (A) between C_1 and C_2. Consequently the return sludge flow could be lowered (and concentration C_2 increased) in order to save energy. Note that the dotted line (C) represents an overloaded clarifier.

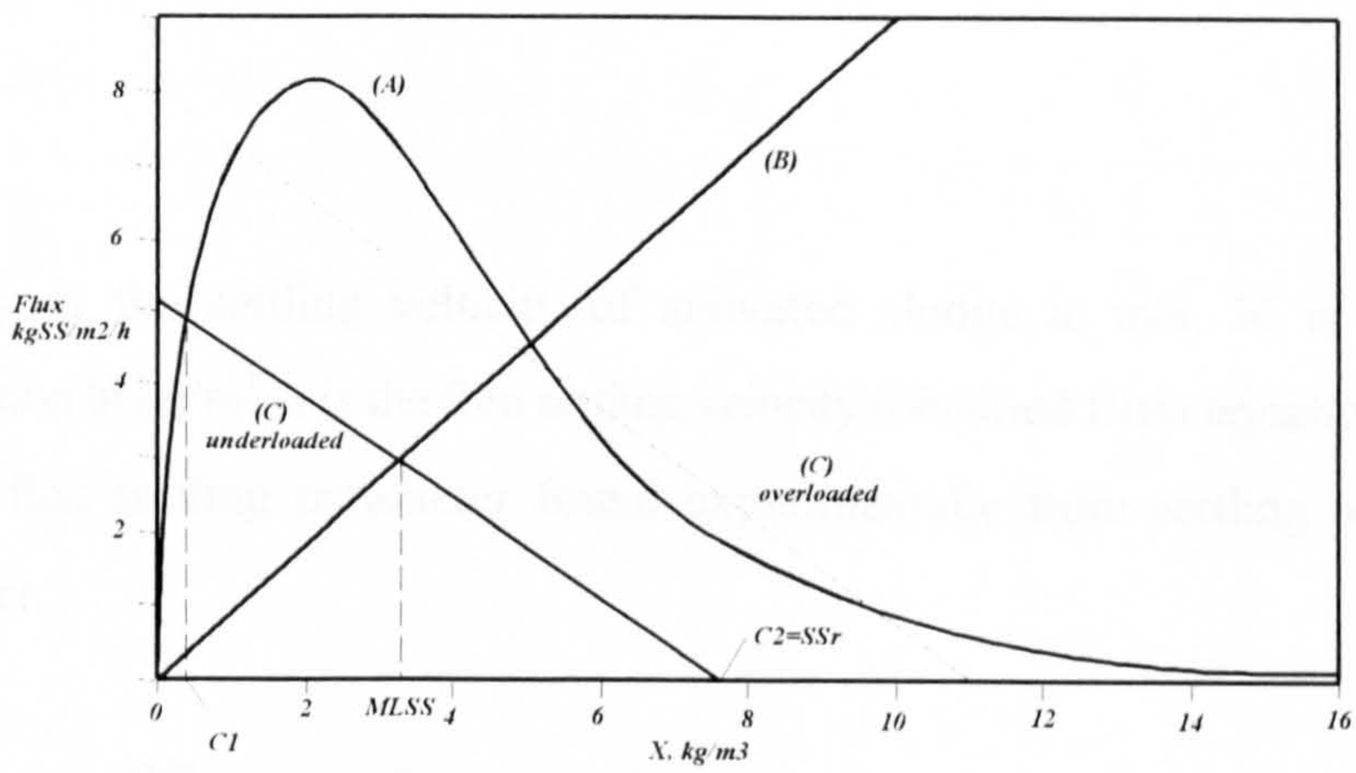

Figure 3.4 Batch mass flux curve of Balslev[23].

The activated sludge process can experience large changes in feed flow and concentrations, and may require process control. Therefore, the mass flux model can also be used for this purpose to determine the hydraulic behaviour of the sludge blanket interface (sometimes identified at a solids concentration of 3000 mg/l[24]). Several authors have used a dynamic interpretation of the model, to monitor the height and suspended solids concentration of the sludge blanket; for on-line process control[23,25-32]. They assumed that the clarification process in the settling zone and the thickening process in the sludge zone behave independently.

The hindered settling velocity, V_i is the most important parameter in the mass flux model[33]. Vesilind[34] proposed a single exponential function between the hindered settling velocity and the suspended solids concentration as follows:

$$V_i = ae^{-KX_i} \qquad \text{- (3.6)}$$

where V_i is the settling velocity of activated sludge in m/s, X_i is the MLSS concentration in kg/m^3, a is the free settling velocity (obtained from equation 3.2), and K is the floc settling parameter found experimentally from settling tests on the wastewater.

Vesilind's model[33-38] is generally accepted as the best model of the settling velocity for high suspended solids concentrations, but does not consider low solids

concentrations, such as in the upper regions of secondary clarifiers. Here the particle settling velocity increases directly with the suspended solids concentration as a result of particle flocculation (Figure 3.5). For low suspended solids concentrations the settling velocity reaches a maximum upper limit, which corresponds to the transition from flocculent to hindered settling. For all suspended solids concentrations above this point the interaction between particles causes the settling velocity to decrease; which is referred to as hindered settling. The y-axis in Figure 3.5 is the average settling velocity, V_s (obtained from equation 3.7) divided by the Stoke's velocity, V_o calculated by equation 3.2.

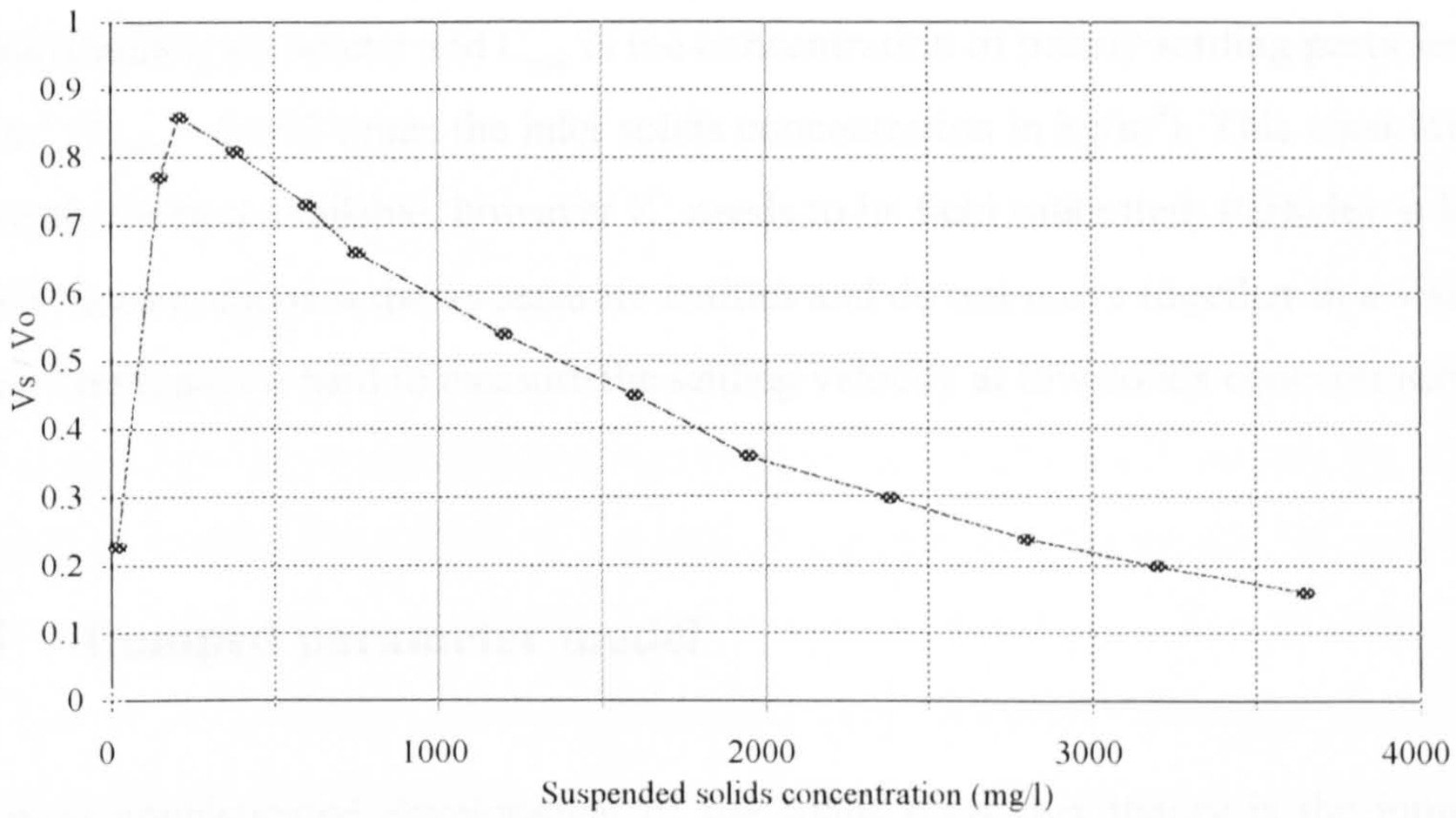

Figure 3.5 Relationship between particle settling velocity and suspended solids concentration[27].

To consider fully the range of suspended solids concentrations in activated sludge clarifiers, the best model, proposed by Takacs *et al.* [27] is the difference between two exponential terms :

$$V_s = V_o[\exp^{-K(C-C_{min})} - \exp^{-K_1(C-C_{min})}] \quad \text{- (3.7)}$$

where V_o is the free settling velocity in m/s, K is the floc settling parameter, K_1 is the colloids settling parameter and C_{min} is the concentration of poorly settling particles in kg/m^3 (C_{min} = 0.002 times the inlet solids concentration in kg/m^3). This equation is currently the best available; however K_1 needs to be field calibrated. Particles at low solids concentrations settle as separate entities and do not move together in a visible layer. This makes it hard to measure the settling velocity at low solids concentrations.

3.5 Lumped parameter model

A more sophisticated development of the solids mass flux theory is the lumped parameter model, which divides the clarifier into vertical layers. A mass balance is calculated across the boundaries of each layer (Figure 3.6)[27]. Perfect mixing is assumed in each layer by a continuous stirred tank reactor (CSTR) which has a uniform suspended solids concentration and volume. The whole clarifier is

represented by a train of continuous stirred tank reactors (an optimum number of 5 CSTR's has been identified[39,40]). The clarifier can be represented by CSTR's in series or in parallel, or in a combination of both[41]. Therefore the overall flow pattern is determined from the fluid dynamics in the CSTR's. The lumped parameter model uses a first order differential equation to model the dynamic feed flow or the steady-state behaviour of the flow. Mass balances are calculated across each layer to generate equations for solids, BOD, ammonia (NH_3), nitrates (NO_3) etc., and biological reactions can be included in the mass balance equations to simulate real biological clarifiers. This gives the dynamic relationships between the influent and effluent process variables. The lumped parameter model is often used to see what effect changes in the influent flow and solids concentration have on the effluent. The model is most often used to monitor existing processes on-line, but can be used for the design of a new plant.

Javed and Ahmad used a series of CSTR's to dynamically simulate primary clarifiers[40]. The model predicted the performance of a primary clarifier, by the response of the effluent suspended solids concentration to the inlet flow rate and solids concentration. Although their model was less representative of the actual conditions than the more sophisticated dispersion models, it was able to indicate sound trends in the clarifier's performance. The number of CSTR's in the model was increased to 5, until only small changes in the effluent solids concentration were noticeable. Although the model showed differences between the simulated and measured effluent solids concentration, it was able to predict values which were closer to the measured values than the regression models in the literature. Lumped parameter models have been widely applied to storm tanks (used during wet weather conditions to store large volumes of wastewater)[42], primary clarifiers[39-41,43,44] and sometimes for secondary clarifiers[38,45].

They have been used in industry in the form of computer programs[45] to predict the suspended solids concentration in the effluent.

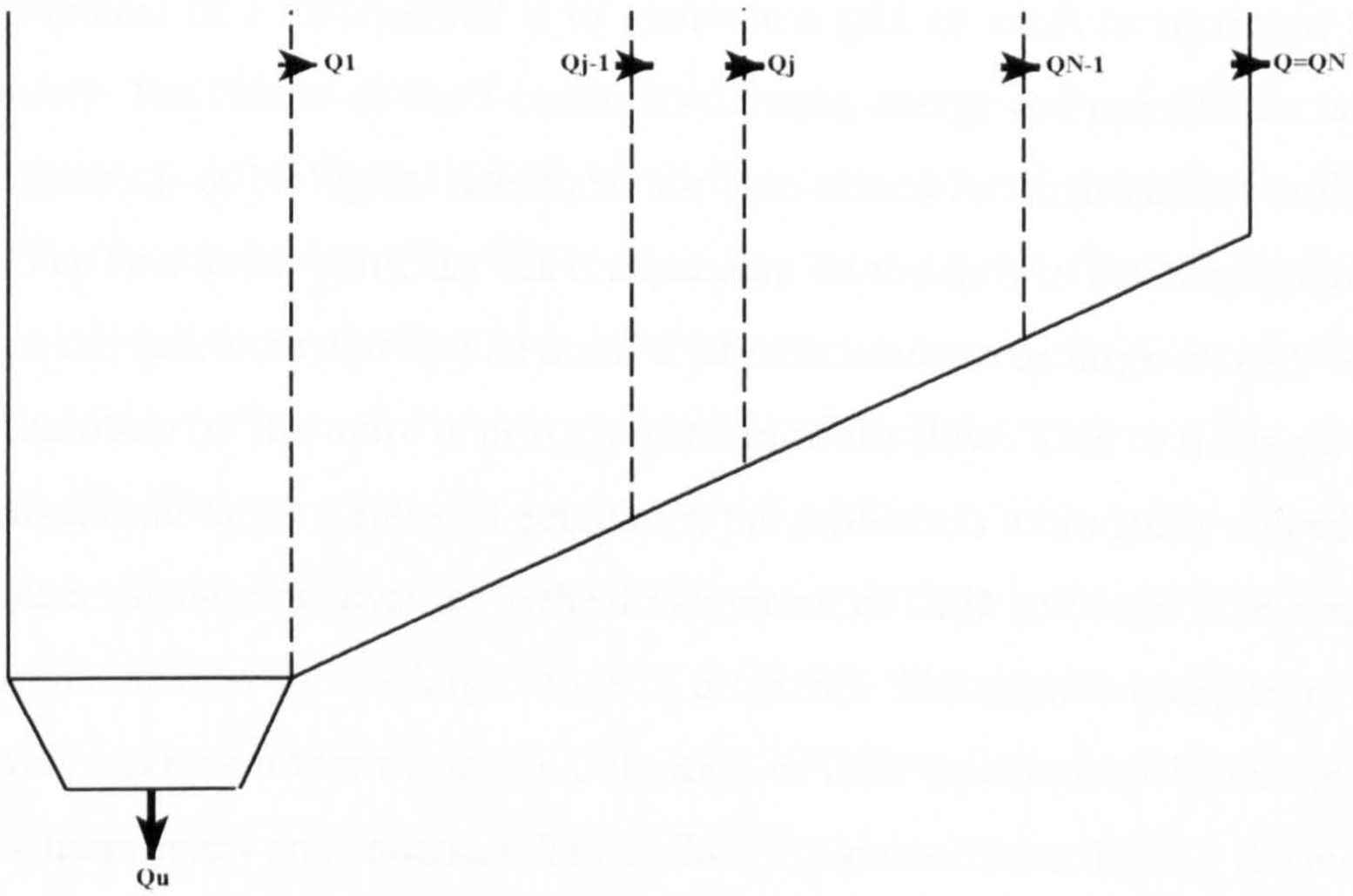

Figure 3.6 Schematic of primary tank (five CSTR's)[27].

3.6 Computational Fluid Dynamics models

3.6.1 Introduction

More sophisticated modelling techniques, notably Computational Fluid Dynamics (CFD), have been applied to sedimentation tank design to overcome some of the limitations of the simpler modelling approaches, described earlier. The first step of the development of a CFD model is to generate a grid or mesh to represent the tank geometry. The Navier-Stoke's equations of mass, energy and momentum, including any chemical or biological reactions, are then solved for each cell (or node) in the grid. The flow in any particular cell is dependent on the flow in the neighbouring cells and on the tank boundaries. The number of cells needs to be large enough to enable the resolution of the more important features of the flow. Due to the large number of cells and the large number of equations, the problem is more easily solved using a computer. Significant advances in the development of CFD software have made these programs able to solve a large range of problems. The relative complexity of CFD software has meant that the useful utilisation of CFD techniques will always depend on the users ability and understanding of fluid dynamics. Nevertheless, the increasing accessibility of the software to more users and the faster computing hardware available, allows changes to be made to the tank geometry, more quickly and cheaply than pilot-scale and full scale testing[47].

This description of CFD is of course simplistic. Turbulent flow is found in the majority of fluid systems and has been studied for a long time, to find meaningful mathematical equations to describe it. The unsteady turbulent nature of the fluid in a sedimentation tank brings with it a multitude of influences that affect all transport

mechanisms within the fluid. The time dependent Navier-Stoke's equations, which were developed about 150 years ago, provide the most accurate method of describing turbulent flow. Unfortunately to resolve these equations requires Direct Numerical Simulations (DNS) of turbulent shear flow, which need extremely powerful computers and even today these computations are prohibitive for routine use.

Consequently, the computations of fluid flow are based on the time-averaging of the Navier-Stoke's equations which result in the emergence of extra unknowns, i.e. Reynolds stresses. There are too many of these unknowns for the number of equations, and therefore 'turbulence models' are used to overcome this problem. The time-averaged variables of fluid flow are solved. First order turbulence models do not solve for the Reynolds stresses and therefore ignore the turbulent fluctuations in three dimensions. At the most, they solve two equations (i.e. the k-ϵ models) in addition to the mean flow equations. Second order turbulence models (i.e. the Reynolds and Algebraic Stress models) perform an accurate calculation of the mean flow properties and all the Reynolds's stresses. They have an additional five equations to solve. All turbulence models can however only be considered as an approximate description of turbulence.

In sedimentation tanks, even though the mean flow velocities are relatively low compared to other processes, the Reynolds number is high enough to cause turbulent flow. In fact, turbulent flow in clarifiers can be caused by several factors: the mixing of the influent with the flow in the tank, impact of the flow on the solid boundaries and the effect of wind on the water surface[48]. The modelling of the flow in clarifiers has used a range of turbulence models, from simple equations (constant eddy-viscosity models[48-58]) to more complex differential equation models (e.g. standard k-ϵ model[59-80] and Reynolds Stress Model[81]).

Constant eddy-viscosity models[48-58] or zero equation models were unable to predict the recirculating flow in sedimentation tanks. Therefore this problem was treated rather unsatisfactorily by excluding the inlet zone of the clarifier, and defining the inlet boundary below the internal baffle[48]. The zero equation models calculate the mixing length, l_m, and do not consider the transport of kinetic energy, k. When l_m is calculated, it is not accurate for recirculating flow and 3-D flows. The effect of streamline curvature, buoyancy or swirling flow is entirely empirical in the constant eddy-viscosity models[82]. These models can therefore often only be used for free shear flow layers and wall boundary layers. Next in complexity is the one-equation model, which can predict the transport of turbulent kinetic energy, but performs only marginally better than the zero equation models.

Therefore more complex turbulence models were developed. Two equation models are the most widely used equations to solve industrial problems, because they represent a reasonably accurate description of turbulence without being too computationally demanding[47]. The standard k-ϵ model describes the turbulent stresses only in terms of the kinetic energy due to the fluctuating components, and the viscous dissipation rate of the turbulent kinetic energy. Because of the linear isotropic limitation of the eddy viscosity, the model is unable to relate to flows with anisotropic turbulent stresses. Therefore flows where the Reynolds stresses play an important part are not well represented by the standard k-ϵ model. Even simple swirling flows can result in the model overestimating turbulent stress, such that axial and tangential velocity profiles may be poorly predicted. The weaknesses of the standard k-ϵ model are usually an insufficient response to streamline curvature and buoyancy forces, an insufficient breadth of generality in different types of shear flows, an incorrect response to adverse pressure gradients, difficulties for separated flows, and an

inapplicability to the low Reynolds viscous region[82].

Some modified versions of the standard k-ϵ model have allowed the model to be applied to various classes of flows of engineering importance. The low Reynolds number modification extends the standard k-ϵ model to regions of flow near to the wall, transitional flow, strongly accelerating flow, stable stratified buoyant flow and some strongly swirling flows in which curvature damps turbulence. The RNG k-ϵ turbulence model is derived using a mathematical Renormalisation Group method. Swirl or high streamline curvature effects are taken into account more accurately, by modifying a turbulent parameter as a function of curvature. The RNG model has given good results for weakly and mild swirling flows. The principal advantage of the RNG model is that the constants used in it are determined theoretically, and that the model includes corrections for low-Reynolds number effects. The RNG model is not much more expensive than the standard k-ϵ model to run because there are still only two equations.

Higher order turbulence models (e.g. Reynolds Stress Models) come closest to the ideal. They can be applied more generally than the standard k-ϵ model to most practical problems without any adjustment to the parameters. The advantage of this type of model is that it can capture many of the complex effects encountered,without having to incorporate ad-hoc modifications, necessary in lower order turbulence models. The RSM model gives accurate accounts of the streamline curvature, rotation and swirl. The main reason that it is less used than the k-ϵ models is the large computational effort required. Algebraic stress models were developed to reduce the workload and were found to be especially suitable when secondary flows were present. For example, in non circular ducts with an unequal height and width, the flow

normal to the axial direction has unequal vertical and horizontal components. The normal shear stresses are strong which suggest anisotropic turbulence.

The CFD models of sedimentation tanks have assumed that the flow is two dimensional (for instance axial and radial in circular clarifiers), which saves a large amount of computational effort. Three dimensional models have been prohibitive so far, because of the numerical instabilities associated with modelling 3-D multi-phase flow. Three dimensional phenomena may occur mainly in the inlet region of the clarifier, where intense eddy dissipation occurs[58]. In rectangular clarifiers, corner and side effects will produce recirculation[62]. Swirling flow in circular clarifiers can also be induced by the rotating sludge scraper. However Montens[83] has shown by direct measurement on full-scale circular clarifiers, that the flow is nearly radial in the absence of wind. Larsen[53] and Tay and Heinke[84] have made point velocity measurements in circular clarifiers, which have indicated that the flow is essentially 2-D in the vertical plane. In fact, due to the dominating driving force induced by density currents, 3-D effects were assumed to be negligible in secondary clarifiers, because the inlet solids concentration is much higher than in other clarifiers[58]. Two dimensional axi-symmetric models (i.e. no swirling flow) have therefore been used in all the reported clarifier models in the literature. Moreover, the 'standard' k-ϵ model has been the most widely used turbulence model, when swirling flow has been neglected. It is normally coupled with the wall layer models for detailed modelling of the near wall region. The standard k-ϵ model[82] calculates the eddy viscosity, ν_t from the turbulent kinetic energy, k and the dissipation of energy, ϵ, where C_μ=0.09.

$$\nu_t = C_\mu \frac{k^2}{\epsilon}$$

- (3.8)

It requires two additional semi-empirical equations for the transport of turbulent kinetic energy, k and the dissipation of turbulent kinetic energy, ϵ as follows :

$$\frac{\partial k}{\partial t} + u\frac{\partial k}{\partial r} + v\frac{\partial k}{\partial y} = \frac{\partial}{\partial r}\left(\frac{\nu_t}{\sigma_k}\frac{\partial k}{\partial r}\right) + \frac{\partial}{\partial y}\left(\frac{\nu_t}{\sigma_k}\frac{\partial k}{\partial y}\right) + P - \epsilon$$

- (3.9)

$$\frac{\partial \epsilon}{\partial t} + u\frac{\partial \epsilon}{\partial r} + v\frac{\partial \epsilon}{\partial y} = \frac{\partial}{\partial r}\left(\frac{\nu_t}{\sigma_\epsilon}\frac{\partial \epsilon}{\partial r}\right) + \frac{\partial}{\partial y}\left(\frac{\nu_t}{\sigma_\epsilon}\frac{\partial \epsilon}{\partial y}\right) + C_1\frac{\epsilon}{k}P - C_2\frac{\epsilon^2}{k}$$

rate of generation + convection = diffusion + generation + destruction

- (3.10)

in which P is the production of turbulent energy by the mean velocity gradients, i.e.

$$P=\nu_t[2(\frac{\partial u}{\partial r})^2+2(\frac{\partial v}{\partial y})^2+2(\frac{u}{r})^2+(\frac{\partial u}{\partial y}+\frac{\partial v}{\partial r})^2]$$

- (3.11)

The constants for the standard k-ϵ model are $C_1 = 1.44$ and $C_2 = 1.92$ and for the turbulent Prandtl numbers of k and ϵ are $\sigma_k = 1.0$ and $\sigma_\epsilon = 1.30$.

3.6.2 Model development

Most of the work reported in the literature tried to predict the flow in circular secondary clarifiers, where the feed enters the tank by a central vertical pipe and effluent is withdrawn over a peripheral weir. To avoid lengthy 3-D simulations, the circular clarifier has been modelled in two dimensions (Figure 3.7); i.e the water depth and the tank radius. The model developed by Zhou and McCorquodale[74] is probably the most advanced model in the literature. It consists of two parts: a flow model providing the velocity and turbulent viscosity field (unsteady, turbulent flow) and a suspended-sediment transport model for determining the particle concentration field. Density driven flow is defined by a density-sediment term, where the effect of the solid particles on the flow pattern is a function of the difference between the density of the solid particles and the local fluid density.

The local fluid density (ρ) is related to the local value of the solids concentration by

$$\rho=\rho_r+C(1-S_S^{-1})$$

- (3.12)

where ρ_r is the reference fluid density (water) in kg/m^3, C is the suspended solids concentration in kg/m^3 , and S_s is the specific gravity of solid particles. Transport of the suspended solids concentration, C was solved in the paper[74] using the following solids transport equation:

$$\frac{\partial C}{\partial t}+u\frac{\partial C}{\partial r}+v\frac{\partial C}{\partial y}=\frac{1}{r}\frac{\partial}{\partial r}(r\upsilon_{sr}\frac{\partial C}{\partial r})+\frac{1}{r}\frac{\partial}{\partial y}(r\upsilon_{sy}\frac{\partial C}{\partial y}+rV_sC)$$

- (3.13)

where ν_{sr} is the eddy diffusivity of suspended solids in the radial direction, ν_{sy} is the eddy diffusivity of suspended solids in the axial direction, and V_s is the particle settling velocity. Two equations for the relationship between the particle settling velocity and the suspended solids concentration were compared[74], and the double exponential equation was preferred (equation 3.7), because it gave the best agreement with

experimental data. Using the Reynolds analogy between mass transport and momentum transport, the sediment diffusion coefficients, defined in the radial and vertical directions, were related to the turbulent viscosity of the fluid, ν_t and the Schmidt number, σ_s[74] (or Prandtl number) as follows :

$$\nu_{sr} = \frac{\nu_t}{\sigma_{sr}} \qquad \text{- (3.14)}$$

$$\nu_{sy} = \frac{\nu_t}{\sigma_{sy}} \qquad \text{- (3.15)}$$

The boundary conditions of the secondary circular clarifier (Figure 3.7) were as follows. At the inlet, uniform profiles for the flow and solids concentration were assumed. To improve numerical convergence and save computational effort a radial flow was assumed for the influent (above the vertical pipe in the centre of the tank), instead of modelling the flow in the inlet pipe. The water surface was modelled as a symmetry plane, in which all the vertical gradients are set to zero and no mass diffusion across the liquid surface is allowed. On the wall boundaries, there were zero velocities normal to the boundary, and for the other parameters the standard wall function of Launder and Spalding[85] was used. The outflow over the effluent weir

assumed that stream-wise gradients for all variables were set to zero. The transfer of suspended solids across the wall boundaries and liquid surface were also set to zero.

Secondary clarifiers in wastewater treatment plants will usually withdraw sludge continuously from the base of the tank, and the underflow geometry will depend on the method of sludge withdrawal (Figure 3.8). For modelling purposes, the removal of sludge from secondary clarifiers has either been represented by a constant downward velocity across the floor of the tank (when the sludge is removed by suction and the tank base is flat) or as a constant downward velocity in the tank hopper (when the sludge is removed by a scraping mechanism and there is a sloping floor). Krebs *et al.*[58] included the effect of a bridge scraper on the removal of sludge, by including a radial velocity near the tank base in the direction of the sludge hopper.

The transport of solids within a clarifier was modelled by the momentum equation (equation 3.13) of the solids phase, which contained the vertical settling velocity and the turbulent mass diffusion, represented by the turbulent Schmidt number. However, this model was limited, because it was not possible to find agreement between the predicted and measured solids concentration distribution in the clarifier. To overcome this problem, a boundary condition was used to represent the resuspension of the suspended solids near the base of the tank.

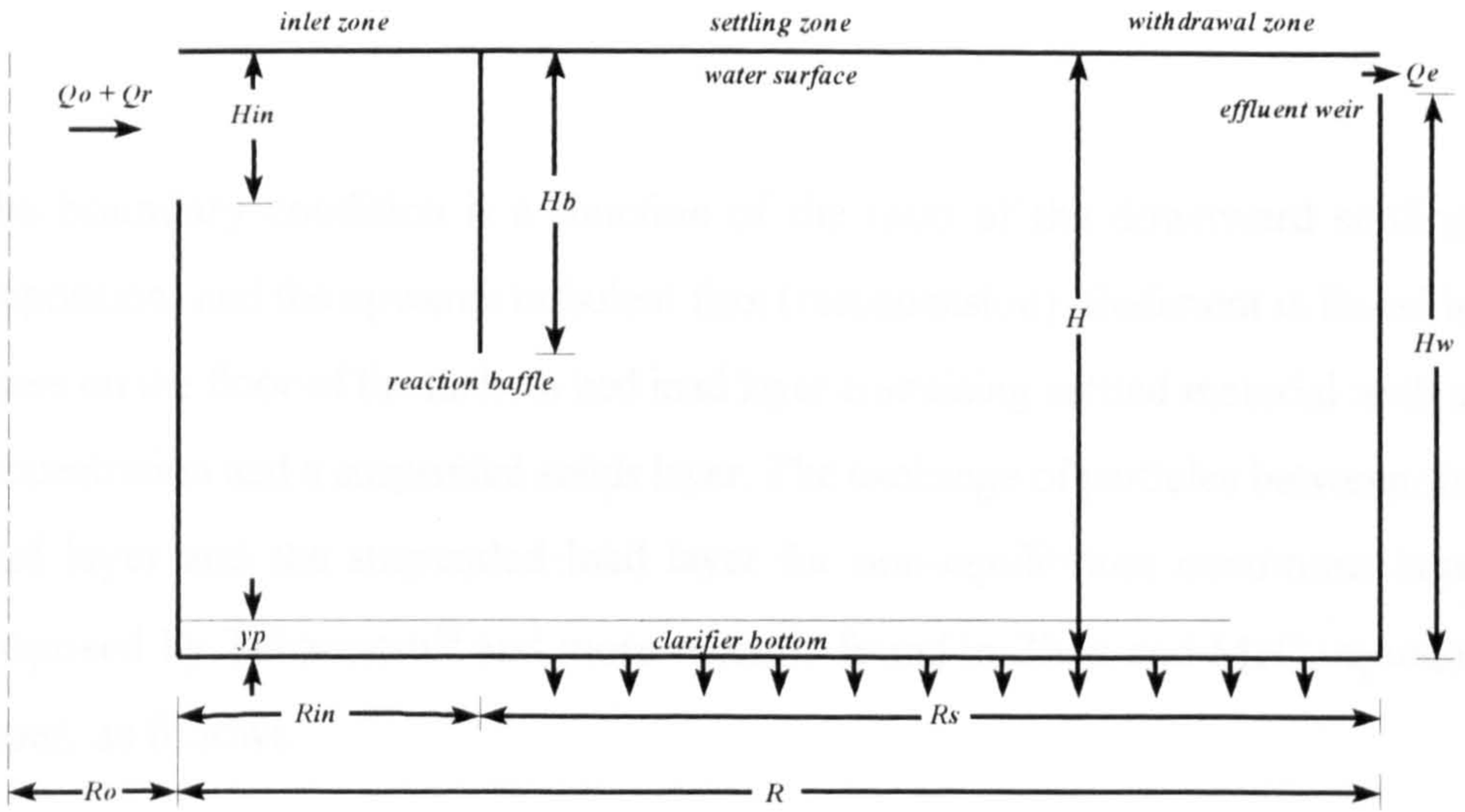

Figure 3.7 Two-dimensional circular tank geometry[74].

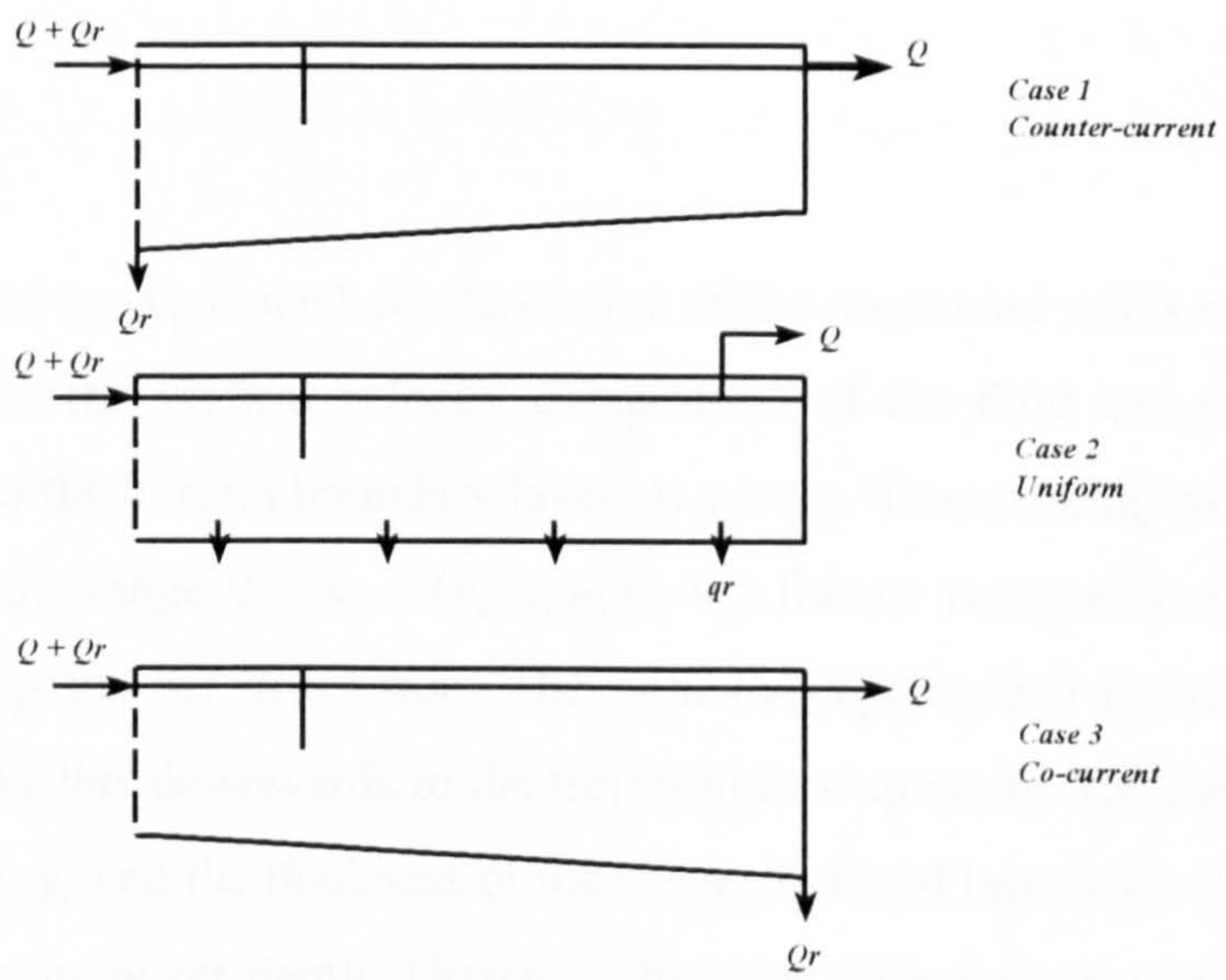

Figure 3.8 Schematic of sludge withdrawal methods[57].

The boundary condition is a function of the ratio of the downward settling flux (deposition) and the upwards turbulent flux (resuspension). Sediment is found in two layers on the floor of the tank: a bed load layer containing settled material with a high concentration and a suspended solids layer. The exchange of particles between the bed load layer and the suspended load layer for non-equilibrium conditions was first proposed by Takamatsu[86] and more recently found in Zhou and McCorquodale's[74] paper, as follows :

$$C_p = \frac{C}{[1 - k_r \frac{(V_s - V_p)}{\upsilon_{sy}/\Delta y}]} \qquad \text{-(3.16)}$$

where $\nu_{sy} = \nu_t / \sigma_{sy}$, C_p is the boundary value of the suspended solids concentration, V_p and V_s are the vertical velocity components of the fluid and solid particles respectively in the bottom boundary layer, at $y = y_p$. The scouring parameter, k_r is restricted to the range $0 < k_r < (\nu_{sy}/y_p)/(V_s - V_p)$ for net resuspension and $1 < k_r < (\nu_{sy}/y_p)/(V_s - V_p)$ for net deposition. The term $(V_s - V_p)/(\nu_{sy}/\Delta y)$ is the ratio of the resultant settling flux downwards to the turbulent flux upwards. The thickness of the bed load layer, y_p and the thickness of the suspended load layer were defined as H - y_p, where H is the water depth. Therefore, by using different values of the scouring parameter the model was validated with the measured solids concentration distribution in the clarifier.

More recent work by McCorquodale *et al.*[78] has made further progress, by modelling the compressive settling near the base of the tank and excluding the resuspension of solids near the tank floor (equation 3.16). This has allowed the suspended solids concentration distribution to be predicted correctly, using only the turbulent mass diffusion of the solids to represent particle resuspension.

3.6.3 Model application

Computational Fluid Dynamics models were first used for sedimentation tank design by modelling two-phase flows, with the solids transport equation effectively decoupled from the flow equations[59,61-63,65,66,70]. This approach was only used for primary clarifiers, where solids concentrations are low and density effects can be neglected. As progress was made, CFD models were used to predict density driven flows, allowing for an approach to secondary sedimentation tank design[6,57-58,71-78].

Previously, rectangular tanks were more common than circular tanks in wastewater treatment plants, and therefore the flow modelling in rectangular sedimentation tanks was more prevalent[54-56,58-66]. Although the corners in rectangular tanks may have an effect on the flow pattern, two-dimensional models have been used, and have given a fairly good agreement between numerical and experimental flow patterns. However, the use of circular tanks has become increasingly widespread in U.S. and U.K. wastewater treatment plants and become particularly popular for secondary clarifiers[74]. Two dimensional models of circular clarifiers (without tangential flow) have also shown good agreement with experimental data.

One approach to include tangential flow in a two-dimensional model was to model an idealised flight bridge scraper, using an additional vector near the base of the tank[58]. In another study, a single-phase flow model[79] of a circular tank had swirl vanes attached to the inlet baffle, a still on the tank base and the sludge scraper was modelled by a rotating bed. The inclusion of swirl in the numerical model caused the numerical residence time distribution (RTD) curves to be further from the experimental RTD curves. This was because the sludge scraper was modelled poorly. However, solids removal was increased with added swirling flow because the radial velocities were reduced in the withdrawal zone of the clarifier.

The effect of the density on the flow pattern has been defined as a function of the inlet solids concentration, hydraulic loading, influent temperature and the tank geometry. Zhou *et al.*[6] studied the effect of the inlet densimetric Froude number, F_r (which characterises the density effect) on the flows and suspended solids profiles in secondary circular clarifiers, in order to find the optimum densimetric Froude number (i.e. for the minimum effluent concentration), as follows :

$$F_r=\left(\frac{u_o^2}{gH_{inl}(\rho-\rho_r)/\rho_r}\right)^{1/2} \qquad \text{- (3.17)}$$

where u_0 is the horizontal inlet velocity in m/s and H_{inl} is the depth of the influent stream opening in m. The optimum inlet densimetric Froude number was found at a constant surface loading. A low densimetric Froude number (i.e. with a large density

effect) produced a strong bottom density current in the clarifier that rebounded off the wall in the withdrawal zone of the clarifier. The strong upward flow on the effluent wall of the clarifier increased the effluent solids concentration. McCorquodale and Zhou[77] also investigated the effect of the inlet solids concentration and inlet flow on the efficiency of a secondary circular tank. The clarifier efficiency was found to be dependent on the inlet densimetric Froude number and the return activated sludge flow, rather than the Reynolds number of the influent.

Another important phenomena was identified as the temperature induced currents in both primary and secondary clarifiers[87-90]. In the winter season, the influent is generally warmer than the contents of the tank, causing flow to be directed towards the water surface from the flow under the lip of the baffle. In fact, the short circuiting across the water surface was found to be more sensitive to temperature than the short circuiting across the tank floor and even small temperature differences of 0.2°C were significant in primary clarifiers[87,88]. Zhou *et al.*[81] investigated the effect of warm influents on a primary rectangular tank, and identified a strong surface density current towards the effluent. Researchers have observed that primary clarifiers are subject to diurnal temperature variations, that experience both bottom and surface density currents during a 24-h period[81,90]. In secondary clarifiers density stratification is mostly caused by the high inlet suspended solids concentration[58].

Some research has been applied to single-phase flows only. Several authors modelled rectangular tanks and verified their models against salt tracer testing[65-68,91]. Examples of single-phase flow modelling of circular sedimentation tanks have also been reported[69,79,92-93]. Quarini *et al.*[92] have compared their 3 dimensional model of a circular pilot-scale clarifier with measurements of radial velocities. Matko *et al* [93]

compared their model with salt tracer testing carried out on pilot-scale and full-scale circular clarifiers.

Flocculent and hindered settling have been modelled by substituting Stoke's law (equation 3.2) with an expression for the variable settling velocity. Vesilind's single exponential relationship (equation 3.6)[34] and the double exponential relationship (equation 3.7) of Takacs[27] were included in several secondary sedimentation models[6,57,73-78]. The mechanisms for particle flocculation are quite complicated (i.e. statistical in nature), which makes them difficult to model. Instead, authors have assumed that flocculation takes place before the clarifier and the settling of particles in the clarifier is discrete[54,70].

Analysis of a typical wastewater can give a density for the dry solids between 1.32 to 1.4 g/ml[27] and a normal distribution of particle sizes between 150-500 μm^2. A study on the effect of the particle density or particle size on the flow pattern has not been published.

Sedimentation tanks operate with variable hydraulic and solids loadings. The variable flow to a rectangular tank[68] and the density-driven variable flow to a secondary circular clarifier (McCorquodale *et al.*[73]) were modelled. For the latter study, two cases were simulated: a daily variation in flow at a constant MLSS concentration and a sudden increase in the MLSS. The steady maximum flow gave lower effluent concentrations than either the variable flow or the step increase in the MLSS. The effect of variable flow was found to be greater for peripheral weirs than in-board launders.

The underflow geometry in a circular secondary clarifier was studied by Samstag[57]. The differences between a countercurrent (centre fed, centre withdrawal), a uniform (centre fed, uniform withdrawal over the tank base) and a co-current (centre fed, peripheral withdrawal) sludge withdrawal system were investigated (Figure 3.8). Profiles in the tank of the solids concentrations and the injected dye concentrations, for the numerical model agreed with the results from pilot-scale and full scale experiments. A highly loaded circular sedimentation tank with a relatively poor settling sludge was insensitive to the changes made to the underflow geometry.

The internal baffle radius in a secondary circular clarifier was studied by Zhou and McCorquodale[75]. With a large radius baffle and a high solids loading, a significant density waterfall was found and verified by pilot-scale modelling. A small skirt radius gave a reduction in the density waterfall for a highly loaded clarifier by reducing the subsequent rebound strength at the effluent weir and significantly improving the efficiency of the clarifier.

McCorquodale and Zhou[78] modelled a secondary circular clarifier to determine the baffle depth for the highest solids removal with dry and wet weather flows. A deep baffle during a dry weather flow and a well compressed sludge blanket increased the solids removal from the tank. An optimum baffle depth of 70-80% of the water depth was found, which depended on the solids loading and settling characteristics within the sludge layer. In wet weather conditions a deep baffle was found to cause inadequate sludge storage and induce a sludge blanket above the baffle lip, resulting in a detrimental effect on the flow pattern. A 50% baffle depth provided the most efficient wet weather conditions.

The inlet geometry of a secondary rectangular clarifier was studied by Krebs *et al.*[58]. Design improvements to the position of the inlet aperture were related to reductions to the inlet velocities and density currents, and which reduced short circuiting. Using the numerical model, the improved inlet structure increased the dissipation of kinetic energy after the inlet, and thereby improved the flocculation behaviour of the inlet chamber, thus increasing the overall solids removal in the tank. The flow-improving measures were verified by pilot-scale models.

3.7 Discussion

Sedimentation may seem to be a simple process but it is complex in practise. As a consequence, modelling the process is difficult and therefore no simple, reliable model has been universally used. Factors such as the inlet position, side water depth and the sludge removal mechanism can all influence a model[3]. To make the correct selection of a numerical model (Table 3.3), it is necessary to know what is being modelled, what is the accuracy of the model and how long it takes for each simulation.

Empirical or regression-based models are the most simple. Empirical modelling methods are still widely used today because they are well documented, easy to use and can reliably predict the quality of the effluent. They are normally used to calculate, for example, the settling area or volume of the tank[12]. However empirical models are not useful for optimising the tank configuration, because they do not consider the details of the tank geometry, nor the flow patterns and solids concentration distributions in the tank. Next in complexity are the mass flux models, which describe the fluid mechanics by dividing the tank into a number of horizontal

'layers'. These models have been widely applied to the design of secondary clarifiers to determine their mass balance, although they are only a one-dimensional model[32], which has been poorly validated in the past[20]. Flow patterns and solids concentration distributions cannot be determined. Because the solids mass flux model considers only the downward flow in the clarifier, then it can only be used to find the return activated sludge flow rate, the height of the sludge blanket and the suspended solids concentration in the return activated sludge. It can not be used to determine the effluent suspended solids concentration[17,18]. The mass flux model is most commonly used in industry as a check on tank design, or as a simple tool in an audit of a poor process, and it is widely used in sewage treatment simulation software[22]. The lumped parameter model is similar to the mass flux model except that it divides the tank into vertical layers (still one-dimensional) and is not applicable to density-driven flows. Predictably then, both the mass flux and lumped parameter models are less accurate and powerful to use than computational fluid dynamics models. Nevertheless they can be run quite easily on personal computers[45] and are easier to learn.

Computational Fluid Dynamics models have the associated costs of computer hardware (but these costs are decreasing), software licences, and the requirement for a highly skilled workforce to operate them efficiently. However the software is being developed to cope with a wide range of engineering problems in many industrial sectors[47]. Particular areas being improved are easier mesh generation, better graphics for pre and post-processing, improvements in the numerical boundary conditions, turbulence models and chemical and biological models. Most reported CFD models of clarifiers have used 2-dimensional axi-symmetric flow models for circular tanks, which can be used with enough accuracy. For rectangular tanks it is however advisable to compare 2-dimensional with 3-dimensional simulations because of the

effect of the tank width. The water surface has been modelled using a symmetric plane which neglected the effect of wind[74]. There is no consideration of the movement of the water surface by using a symmetry plane and the flow on the symmetry plane is rebounded. Wind modelling could be represented by an additional shear force on the water surface and by modelling the free surface. Flow stratification takes place not only as a result of high solids concentrations but also because of the difference in temperature between the influent and the fluid within the tank. In some cases, knowing the temperature of the influent during experimental testing can be useful, in order to enter this data into the numerical model. In fact, some research on temperature effects has been published[81,87-90].

Numerical models for multi-phase flows require a greater understanding of the numerical parameters than single phase flow models. The terminal settling velocity of the solid particles has been represented by a source term in the solids transport equations (e.g. Zhou and McCorquodale[74]). In practice, settling column tests on real samples of wastewater should be undertaken to determine the settling velocities of the wastewater, for the range of particle concentrations within the clarifier. This is even more important for secondary clarifiers, where flocculent, hindered and compressive settling occur and the range of suspended solids concentrations are wider[21]. The mass transfer from the solids phase to the liquid phase, caused by the solids concentration gradient, can be neglected for the purposes of most wastewater treatment modelling, as long as the transportation of solids only considers the suspended solids and not the dissolved solids. However inter-phase mass transfer from the solids to the fluid does occur and is caused by the transfer of turbulence from the fluid. Increased turbulence causes the solids to resuspend into the fluid and this is especially true in regions of high mixing. To account for this an anisotropic dimensionless number, the turbulent

Schmidt (or Prandtl) number has been used throughout the clarifier (e.g. Zhou and McCorquodale[74]). Turbulent mass diffusion is dependent therefore on the localised turbulence of the background fluid and a constant value of the Schmidt number. However in several models of secondary clarifiers the resuspension of solids near the tank base has also been included to obtain the correct solids distribution. This has meant that the model has been validated with experimental data, by adjusting the value of the scouring parameter, k_r (e.g. Zhou and McCorquodale[74]). Nevertheless, in one more recent paper[78] the compressive settling near the base of the tank was modelled correctly and the scouring parameter was not needed. This paper signified an important improvement to the multi-phase flow models.

For the CFD modelling of wastewater sedimentation tanks there are several important factors to consider, as follows: particle density, particle size, the settling velocity distribution of the suspended solids, the velocity distribution of the fluid (water in this case), turbulent mass diffusion of the solids and the resuspension of solids near the tank floor. There are other factors caused by the environmental conditions in wastewater treatment plants which can affect the tanks performance considerably. These are the temperature of the influent, the variability of the flow, the effect of the flow on floc growth or breakup, denitrification, the wind effect on the water surface and the movement of the sludge scrapers. Experiments should be undertaken to determine the transport properties of the wastewater and the environmental effects. Experiments are also important to validate numerical models. Therefore measurements should be made of the flow rates and suspended solids concentrations of the influent, effluent and return activated sludge; the distribution of suspended solids within the tank, velocities within the tank and possibly the residence time distributions of the effluent and return activated sludge in secondary clarifiers.

Table 3.3 The numerical models of sedimentation tanks.

Model name	**Settling basin**	**Fluid dynamics**	**Settling**	**Density effects**	**Steady/ dynamic**
Empirical	Primary/ Secondary	Plug flow	Hindered	No	S / D
Solids mass flux	Secondary	Partially mixed	Hindered	Yes	S / D
Lumped parameter	Primary	Partially mixed	Discrete	No	S / D
CFD	Primary/ Secondary	Dispersion of flow, turbulence and solids	Hindered	Yes	S / D

There are new opportunities for research using CFD models to study the particle density, particle size, particle flocculation, the turbulent mass diffusion of the solids, the effect of flow on particle growth and breakup, denitrification and the effect of wind on the water surface. The other new topics are to improve the design of the internal baffle, side wall depth, slope of the tank, sludge hopper, the internal structures in the tank and the peripheral and launder weirs.

3.8 Conclusions

1. Empirical models are still widely used today to predict the suspended solids concentration in the effluent and return activated sludge but cannot model the flow pattern or solids distribution within the tank.

2. The mass flux model is normally used to perform a mass balance on secondary sedimentation tanks and determine the return activated sludge flow rate for new designs, to audit a poor process and monitor the height of the sludge blanket.

3. The lumped parameter model is normally used to determine the characteristics of the effluent in primary sedimentation tanks.

4. CFD models can predict the flow pattern in sedimentation tanks more accurately.

5. The most important factors reported in the literature in the CFD modelling of clarifiers are the particle density, settling velocity distribution of suspended solids, the velocity distribution of the fluid (water in this case), turbulent mass diffusion of solids and the resuspension of the suspended solids.

6. There are new areas for research using CFD models, to study the particle density, particle size, particle flocculation, turbulent mass diffusion of solids, the effect of flow on particle growth or breakup, denitrification and the effect of wind and variable flow on the water surface.

7. The other new opportunities are to improve the design of the internal baffle, the side wall depth, slope of the tank, sludge hopper, the internal structures in the tank and the peripheral and in-board launders.

This chapter has identified that a CFD model is the most accurate model for predicting the flow in sedimentation tanks. However, before progressing to the multi-phase model of the secondary clarifier, it is more sensible to first determine whether a single-phase flow model is accurate by comparing it to experimental data. This is the work presented in the next chapter of the thesis. The work outlined in the next three chapters of the thesis will also include new research topics, which have not been addressed before in the literature.

3.9 References

1. Burton, F.L. and Tchobanoglous, G. (1991). Wastewater engineering: treatment, disposal, reuse. 3rd edition. McGraw-Hill Inc.
2. Hazen, A. (1904). 'On sedimentation'. Transactions of the American Society of Civil Engineers, vol. 53, 45-88.
3. Anderson, N.E. (1945). 'Design of final settling tanks for activated sludge'. Sewage Works Journal, vol. 17, 50-65.
4. Camp,T.R. (1945). 'Sedimentation and the design of settling tanks'. Transactions of the American Society of Civil Engineers, vol. 94, 895-958.
5. Dobbins,E.W. (1943), 'Effect of turbulence on sedimentation'. Proceedings of the American Society of Civil Engineers. New York, N.Y.
6. Zhou,S., McCorquodale,J.A. and Vitasovic,Z. (1992c). 'Influences of density on circular clarifiers with baffles'. Journal of Environmental Engineering (American Society of Civil Engineers), 829-847.
7. Abuzeid,N.S., Vellioglu,S.G. and Nakhla,G.F. (1990). 'Simulation modelling of primary clarifiers (case study of Doha treatment plant)'. Journal of Environmental Science and Health, vol. 7, 799-820.
8. Voshel,D. and Sak,J. (1968). 'The effect of the primary effluent suspended solids and BOD on activated sludge production'. Journal of Water Pollution Control, vol. 40, R203-R212.
9. Tebbutt,T. and Christaulas,D. (1975). 'Performance relationships for primary sedimentation'. Water Research , 348-356.
10. Voutchkov,N.S. (1992). 'Relationship for clarification efficiency of circular secondary clarifiers'. Water Science Technology, vol.26, nos. 9-11, 2539-2542.

11. Roche, N., Vaxelaire, J. and Prost,C. (1995). 'A simple empirical model for hindered settling in activated sludge clarifier'. Water Environmental Research, vol. 67, 775-780.

12. Billmeier,E. (1992). 'Dimensioning of final settling tanks of large activated sludge plants for high quality effluent'. Water Science Technology, vol.25, nos. 4-5, 23-33.

13. Halttunen,S. (1994). 'Clarifier performance in activated sludge process treating pulp and paper mill effluents'. Water Science Technology, vol. 29, nos. 5-6, 313-328.

14. Tyteca,D. (1981). 'Nonlinear programming model of wastewater treatment plant', Journal of Environment Engineering (American Society of Civil Engineers), 747-767.

15. Akca,L., Kinaci, C. and Karpuzcu,M. (1993). 'A model for optimum design of activated sludge plants'. Water Research, vol. 27,1461-1468.

16. Coe,H.S. and Clevenger,G.H. (1916). 'Methods of determining the capacities of slime settling tanks'. Transactions of the American Institution of Mining Engineers, vol.55, 356-384.

17. Dixon,D.C. (1977a). 'Momentum-balance aspects of free settling theory, I : batch thickening'. Separation Science, vol. 12, 171.

18. Dixon,D.C. (1977b). 'Momentum-balance aspects of free settling theory, II :continuous, steady-state thickening'. Separation Science, vol.12, 193.18.

19. Dick, R.I. (1980). 'Analysis of the performance of final settling tanks'. Tribology Cebedeau, vol. 33, 359.

20. Kynch,J.A. (1952). 'Theory of sedimentation'. Transactions of the Faraday Society, vol. 48, 166-167.

21. White,M.J.D. (1975). Settleability of activated sludge. WRc technical report, TR11, May.

22. Chi,J. (1974). Optimal control policies for the activated sludge process. PhD dissertation, State University, New York at Buffalo.

23. Balslev, P., Nickelsen, C., Lynggaard-Jensen, A. (1994). 'On-line flux-theory based control of secondary clarifiers'. Water Science Technology, vol. 30, 209-218.

24. Vitasovic,Z.Z. (1986). An integrated control strategy for the activated sludge process. PhD dissertation, Rice University, Houston, Texas.

25. Attir,U. and Denn,M.M. (1978). 'Dynamics and control of the activated sludge wastewater process'. Journal of the American Institution of Chemical Engineers, vol. 24, 693-698.

26. Tracy,K.D. and Keinath,T.M. (1974). Dynamic model for thickening of activated sludge. American Institution of Chemical Engineers Symposium Series. No. 136, vol. 70, 291.

27. Takacs,I., Patry,G.G. and Nolasco,D. (1991). 'A dynamic model of the clarification-thickening process'. Water Research, vol. 25, 1263-1271.

28. Bryant,J.O. (1972). Continuous time simulation of the conventional activated sludge wastewater renovation system. PhD dissertation, Clemson University, Clemson, S.C.

29. Busby,J.B. (1973). Dynamic modelling and control strategies for the activated sludge process. PhD dissertation, Clemson University, Clemson, S.C.

30. Stenstrom,M.K. (1976). A dynamic model and computer compatible control strategies for wastewater treatment plants. PhD dissertation, Clemson University, Clemson, S.C.

31. Hill,R.D. (1985). Dynamics and control of solids-liquid separation in the activated sludge process. PhD dissertation, Rice University, Houston, Texas.

32. Laikari,H., (1989). 'Simulation of the sludge blanket of a vertical clarifier in an activated sludge process'. Water Science Technology, vol. 21, nos. 6-7, 621-629.

33. Alderman,B.J., Theis,T.L., Collins, A.G. (1994). 'Numerical approach to clarifier operation according to flux theory'. Journal of Environmental Engineering, vol. 120, no. 3, 670-675.

34. Vesilind, P.A. (1974). Treatment and disposal of wastewater sludges. Ann Arbor Science Publishers, Inc., Ann Arbor, Michigan.

35. Salem,A.B.S.H. (1988). Simulation algorithm for sedimentation basin design and analysis. ISA Transactions, vol. 27, 25-29.

36. Daigger,G.T. and Roper,R.E.,Jr. (1985). 'The relationship between SVI and activated sludge settling characteristics'. Journal of the Water Pollution Control Federation, vol. 57, 859.

37. Dupont,R. and Henze,M. (1992). 'Modelling of the secondary clarifier combined with the activated sludge model no. 1'. Water Science Technology, vol. 25, no. 6, 285-300.

38. Cho,S.H., Colin,F., Sardin,M. and Prost,C. (1993). 'Settling velocity model of activated sludge'. Water Research, vol. 27, 1237-1242.

39. Tanthapanichakoon,W. and Himmelblau,D.M. (1981). 'Simulation of a time dependent activated sludge wastewater treatment plant'. Water Research, vol. 15, 1185-1195.

40. Javed,K.H. and Ahmad,S. (1991). 'Computer simulation of full scale primary settling tanks'. Transactions of the Institution of Chemical Engineers, Part B, vol. 69,107-112.

41. Roche, N., Bendounan,R., Prost,C. (1994). 'Wastewater treatment plant primary clarifier hydrodynamic modelling'. Revue des Sciences de l'eau, vol. 7 , 153-167.

42. Lessard,P. and Beck,M.B. (1991b). 'Dynamic simulation of storm tanks'. Water Research, vol. 25, 375-391.

43. Lessard,P. and Beck,M.B. (1988). 'Dynamic modeling of primary sedimentation'. Journal of Environmental Engineering, vol. 114, 753-769.

44. Paraskevas,P., Kolokithas,G. and Lekkas,T. (1993). 'A complete dynamic model of primary sedimentation'. Environmental Technology, vol. 14, 1037-1046.

45. Pons,M.N., Potier,O., Roche,N., Colin,F. and Prost,C. (1993). 'Simulation of municipal wastewater treatment plants by activated sludge'. Computers and Chemical Engineering, vol. 17 (suppl.), S227-S232.

46. Olsson,G. and Chapman,D. (1985). Modelling the dynamics of clarifier behaviour in activated sludge systems, In: Instrumentation and Control of Water and Wastewater Treatment and Transport Systems, Proceedings 4th IAWPRC: 405-412.

47. CFD comes to the desktop. (1991). The Chemical Engineer, 13th June, 23-25.

48. Abdel-Gawad,S. and McCorquodale,J.A. (1985). 'Simulation of particle concentration distribution in primary clarifiers'. Canadian Journal of Civil Engineering, vol. 12, 454-463.

49. Valioulis,I.A. and List,E.J. (1984). 'Numerical simulation of a sedimentation basin - 1. Model development 2. Design application'.Environmental Science and Technology, vol. 18, 242-253.

50. Bechteler, W. and Schrimpf, W. (1984). 'Improved numerical model for sedimentation'. Journal of Hydraulic Engineering (American Society of Civil Engineers), 234-247.

51. Ostendorf,D.W. and Botkin,B.C. (1987). 'Sediment diffusion in primary shallow rectangular clarifiers'. Journal of Environmental Engineering (American Society of Civil Engineers, vol. 113, 595-611.

52. Guetter,A.K. and Jain,S.C. (1991). 'Analytical solution for density currents in settling basins.' Journal of Hydraulic Engineering, vol. 117, no.3.

53. Larsen,P., (1977). On the hydraulics of rectangular settling basins, experimental and theoretical studies. report no. 1001, Department of Water Resources Engineering, Lund Institute of Technology, Lund University, Lund, Sweden.

54. Imam,E. (1981). Numerical modelling of rectangular clarifiers. PhD thesis, University of Windsor, Windsor, Ontario.

55. Imam,E., McCorquodale,J.A. and Bewtra,J.K. (1983). 'Numerical modeling of sedimentation tanks'. Journal of Hydraulic Engineering (American Society of Civil Engineers), vol. 109, 1740-1754.

56. Imam,E. and McCorquodale,J.A. (1983). 'Simulation of flow in rectangular clarifiers'.Journal of Environmental Engineering, vol. 109, 713-730.

57. Samstag, R.W., Dittmar,D.F., Vitasovic,Z., McCorquodale, J.A. (1989). 'Underflow geometry in secondary sedimentation'. Water Environmental Research, vol. 64, no. 3, 204-212.

58. Krebs, P., Vischer,D. and Gujer,W. (1995). 'Inlet-structure design for final clarifiers'. Journal of Environmental Engineering, vol. 121, no. 8, 558-564.

59. Stamou,A.I., Adams,E.W. and Rodi,W. (1989). 'Numerical modeling of flow and settling in primary rectangular clarifiers'. Journal of Hydraulic Research, vol. 27, 665-682.

60. Schamber,D.R. and Larock,B.E. (1978). A finite element model of turbulent flow in primary sedimentation basins. Proceedings of Finite Element in Water Resources. Imperial College.

61. Schamber,D.R. and Larock,B.E. (1981). 'Numerical analysis of flow in sedimentation basins'. Journal of the Hydraulic Division (American Society of Civil Engineers), vol. 107, 575-591.

62. Schamber,D.R. and Larock,B.E. (1983). 'Particle concentration predictions in settling basins'. Journal of Environmental Engineering, vol. 109, no. 3.

63. Larock,B.E., Chun,W.K.C. and Schamber,D.R. (1983). 'Computation of sedimentation basin behavior'. Water Research, vol. 17, 861-867.

64. Cenedese,A., Gallerano,F. and Misiti,A. (1987). Turbulence effect in the primary settling tank. International Conference on New Technology in Model Testing in Hydraulic Research. Central Board, Irrigation & Power, September 24-26, Pune, India. Session III, Paper II: 143-146.

65. Celik,I. and Rodi,W. (1985a). Simulation of hydrodynamic and transport characteristics of rectangular settling basins. In: Transport of suspended solids in open channels. June 11-15, Munich/Neubiberg, University Karlruhe, Germany.

66. Celik,I., Rodi,W. and Stamou,A.I. (1985b). Prediction of hydrodynamic characteristics of rectangular settling tanks. Proceedings of the International Symposium for Refined Flow Modelling and Turbulence Measurements. Iowa City, Iowa.

67. Adams,E.W. and Rodi,W. (1990). 'Modelling flow and mixing in sedimentation tanks'. Journal of Hydraulic Engineering (American Society of Civil Engineering), vol. 116, 895-911.

68. Lowe,S.A. and Sivakumar,M. (1991). 'A penalty finite difference model for Navier-Stokes flow problem in sedimentation basins'. Advances in Water Research, vol. 14, 318-312.

69. Lyn,D.A. and Zhang,Z. (1989). Boundary-fitted numerical modelling of sedimentation tanks. Proceedings of the 23rd International Association for Hydraulic Research (IAHR). Ottawa, Canada, A331-A338.

70. Casonato,M. and Gallerano,F. (1990). 'A finite difference self-adaptive mesh solution of flow in a sedimentation tank'. International Journal of Numerical Methods in Fluids, vol. 10, 697-711.

71. DeVantier,B.A. and Larock,B.E. (1986). 'Modelling a recirculating density-driven turbulent flow'. International Journal of Numerical Methods in Fluids, vol. 6, 241-253.

72. DeVantier,B.A. and Larock,B.E. (1987). 'Modeling sediment-induced density currents in sedimentation basins'. Journal of Hydraulic Engineering, vol. 113, 80-94.

73. McCorquodale,J.A.,Yuen,E.M., Vitasovic,Z. and Samstag,R. (1991). 'Numerical simulation of unsteady conditions in clarifiers'. Water Pollution Research Journal of Canada, vol. 26, 201-222.

74. Zhou,S. and McCorquodale,J.A. (1992a). 'Mathematical modelling of a circular clarifier'. Canadian Journal of Civil Engineering, vol. 19, 365-374.

75. Zhou,S. and McCorquodale,J.A., (1992b). 'Influence of skirt radius on performance of circular clarifier with density stratification'. International Journal of Numerical Methods in Fluids, vol. 14, 919-934.

76. Lyn,D.A., Stamou,A.I. and Rodi,W., (1992). 'Density currents and shear-induced flocculation in sedimentation tanks'. Journal of Hydraulic Engineering, vol. 118, 849-867.

77. McCorquodale, J.A. and Zhou, S. (1994). 'Effects of hydraulic and solids loading on clarifier performance'. Journal of Hydraulic Research, vol. 31, no. 4, 461-478.

78. McCorquodale, J.A. and Zhou,S.P. (1994). Use of numerical models in clarifier design - Optimization of inlet structures. 67th Annual Conference of the Water Environment Federation. Chicago.

79. Szalai,L., Krebs, P. and Rodi, W. (1994). 'Simulation of flow in circular clarifiers with and without swirl'. Journal of Hydraulic Engineering, vol. 120, no. 1, 4-21.

80. Dahl,C., Larsen,T., Petersen,O. (1994). 'Numerical modelling and measurement in a test secondary settling tank'. Water Science Technology, vol. 30, 219-228.

81. Zhou, S. and McCorquodale, J.A. (1994). 'Short circuiting and density interface in primary clarifiers'. Journal of Hydraulic Engineering, vol. 120, no. 9, 1060-1080.

82. Rodi, W. (1980). Turbulence models and their application in hydraulics, a state of the art review. Book publication of the International Association for Hydraulic Research, Delft, Netherlands.

83. Montens, A. (1954). 'The use of radioactive isotopes for water flow and velocity measurement,'. Radioisotope Conference. J.E. Johnston, ed., Butterworths, London, England, 169-180.

84. Tay, A.J. and Heinke, G.W. (1983). 'Velocity and suspended solids distribution in settling tanks.' Journal of the Water Pollution Control Federation., vol. 55, 261-269.

85. Launder, B.E., and Spalding, D.B. (1974). 'The numerical computation of turbulent flows'. Computer Methods in Applied Mechanics and Engineering, vol. 2, 207-209.

86. Takamatsu,T., Naito,M., Shiba,S. and Ueda,Y. (1974). 'Effects of deposit resuspension on settling basin'. Journal of the Environmental Engineering Division (American Society of Civil Engineers), vol. 100, 883-903.

87. Heinke, G.W. (1974). Design and performance criteria for settling tanks for the removal of physical-chemical flocs. Summary Report. University of Toronto.

88. Heinke, G.W., Qazi, M.A. and Tay,A. (1975). Design and performance criteria for settling tanks for removal of physical-chemical flocs. Research report. University of Toronto.

89. McCorquodale, J.A. (1987). Density currents in clarifiers. Proceedings of the National Conference on Hydraulic Engineering. ASCE. New York. N.Y.

90. McCorquodale, J.A. (1976). Hydraulic study of the circular settling tanks at the West Windsor pollution control plant. Report submitted to Lafontaine, Cowie, Buratto and Associates limited, consulting engineers. Windsor, Ontario.

91. Kabza,Z., Dobrowolski,B. and Spyra,A. (1983). Numerical modelling of the flow phenomena in the settling tanks. In: Applied Chemistry Unit Operations and Processes. Proceedings of the 4th Conference of the Hungarian Chemical Society. Paper 1.4.2: 135-140.

92. Quarini, G., Innes, H., Smith, M. and Wise, D. (1995). 'Hydrodynamic modelling of sedimentation tanks'. Proceedings of the Institution of Mechanical Engineers, vol. 210, 83-91.

93. Matko,T., Fawcett, N., Sharp, A. and Stephenson, T. (1996). 'A numerical model of flow in circular sedimentation tanks'. Transactions of the Institution of Chemical Engineers, Part B, vol. 74, 197-204.

CHAPTER IV

This chapter of the thesis has been refereed and published in a journal, and the reference of the paper is as follows : Matko, T., Fawcett, N., Sharp, A. and Stephenson, T. (1996). 'A numerical model of flow in circular sedimentation tanks'. Transactions of the Institution of Chemical Engineers, Part B3, vol. 74, 197-204. This work intends to validate a single-phase flow model, before progressing to the complexities of a multi-phase flow model. It has not been investigated before whether a horizontal or vertical facing inlet is the best inlet boundary condition for a centre-fed circular clarifier. The effects of modelling the real plant flow rates have also not been studied. These issues are addressed in this chapter. The single-phase flow model in the computational fluid dynamics program, CFX-F3D has been suitably modified to predict the flow in two circular clarifiers.

NUMERICAL MODEL OF SINGLE-PHASE FLOW

4.1 Introduction

Numerical methods for the design of primary and secondary sedimentation tanks in wastewater treatment plants are mostly based on simple mechanistic models and operational experience. Traditional numerical models[1] assume a uni-directional flow. The effect of the fluid mechanics within these tanks, their interaction with the solids, and the effect on the tank performance are not considered.

Consequently, failure of such tanks is often associated with poor flow distribution. Nevertheless, progress in computational fluid dynamics (CFD) allow the flow pattern and solids concentration distribution within the tank to be accurately modelled[2].

Primary sedimentation, for the removal of light organic matter from the incoming sewage, and humus tanks, for the clarification of the effluent from biological trickling filters have low inlet suspended solids concentrations (100-500 mg/l). It is a reasonable assumption that the solids do not affect the flow patterns in these tanks, and therefore for modelling purposes the fluid dynamics can be solved using a single phase flow model. Prior to modelling the solids concentration distribution, a single-phase CFD model can also be useful in understanding the major flow characteristics within these clarifiers. Nevertheless, before a numerical model can be used as a design tool, it needs to be validated against experimental data.

Several authors have modelled turbulent single-phase flows in sedimentation tanks and used the standard k-ϵ turbulence model[3-9]. These studies have compared numerical and experimental results, either by measuring the flow velocities[3-6] or by chemical tracer methods[3-6,8]. Indeed, in all these studies there were satisfactory comparisons with experimental data. Celik *et al*[3-4] modelled a rectangular clarifier in two dimensions and positioned the horizontal inlet flow below the reaction baffle. The computed flow pattern and residence time distribution were compared with experimental data, by adjusting the inlet velocity profile. Adams and Rodi[5] modelled two rectangular pilot-scale clarifiers with different inlet arrangements, namely an inlet flow below the reaction baffle and an inlet slit at a variable water depth. Flow velocities were measured inside the tank and the RTD's of fluorescent dye were measured at the tank outlet. Lowe and Sivakumar[6] compared flow patterns between a numerical model and the experimental data obtained by

McCorquodale et al[10], in two rectangular pilot-scale tanks. Szalai, Krebs and Rodi[8] tested a numerical model of single-phase flow in a centre-fed circular tank, with and without swirling flow. Tracer studies and flow streamline measurements in a pilot-scale tank by McCorquodale[11] were compared to this model.

In the present work, the RTD's from the numerical models of a full-scale and a pilot-scale circular clarifier were compared to salt tracer experiments. The vertical and the horizontal inlet velocity boundary condition in the numerical simulations of the pilot-scale tank were compared, to investigate any differences in the simulated flow pattern. The horizontal inlet neglected the region of the clarifier above the vertical inlet pipe. Computer simulations were undertaken for the steady flow rate to the pilot-scale tank and the variable and mean flow rates to the full-scale tank. The simulation of the variable flow accounted for the diurnal changes in flow (during the salt tracer test) to the treatment plant.

4.2 Theory

4.2.1 Flow and turbulence equations

Fluid flow is described by three conservation laws of mass, momentum and energy. For the modelling of rectangular clarifiers these equations have been presented by Lyn *et al* [12] in a cartesian coordinate system. Circular tanks are modelled here using cylindrical polar coordinates, where y denotes the downward axial direction, r is the radial direction and θ is the circumferential direction. It can be assumed that there is no swirling flow and the flow is axi-symmetric about the central axis of the circular tanks. In fact, there was no rotating sludge scraper in both the pilot-scale and full-scale clarifiers. Previous investigators had also

observed: by velocity measurements in full-scale circular clarifiers, that the flow is essentially 2-D in the vertical plane, in the absence of wind[13-14].

The conservation equations for mass and momentum can be expressed in cylindrical co-ordinates (here presented in the radial direction only) :

$$\frac{1}{r}\frac{\partial}{\partial r}(rV)+\frac{\partial U}{\partial y}=0 \qquad \text{- (4.1)}$$

$$\frac{\partial V}{\partial t}+V\frac{\partial V}{\partial r}+U\frac{\partial V}{\partial y}=-\frac{1}{\rho}\frac{\partial p}{\partial r}+\frac{\partial}{\partial r}(\nu_t(\frac{\partial V}{\partial r}+\frac{V}{r}))+\frac{\partial}{\partial y}(\nu_t\frac{\partial V}{\partial y}) \qquad \text{- (4.2)}$$

In these two equations, the real time dependent flows have already been converted into U and V, the mean velocities in the y and r directions, respectively. In order to solve the real fluid's behaviour, extremely long computations are required even using today's computers. Therefore, a time averaging procedure known as the Reynolds decomposition is carried out, where the turbulent velocity is split into a mean component and a fluctuating velocity. When this term is substituted into the original Navier-Stoke's equations, the same form of equations are generated,

except that an extra term appears in the momentum equations known as the Reynolds Stress. There are too many unknowns for the number of equations: the so called 'closure problem'[15].

The way out of this seemingly untreatable problem is to use a 'turbulence model'. The aim of these models is to replace the extra terms in the momentum equations (the Reynolds stresses). First order or Boussinesq turbulence models use the eddy viscosity concept, which relate the Reynolds stresses to the mean velocity gradients, thereby reducing the number of equations to solve. The mixing length model is the most common of these models in general use, however among computational fluid dynamics models, the most often used is known as the standard k-ϵ model. It calculates the turbulent kinetic energy, k and the eddy dissipation, ϵ from the mean flow velocities and solves two semi-empirical equations, for the transport of k and ϵ. It was used in this study using standard turbulent constants[15] : $C_1 = 1.44$, $C_2 = 1.92$, $\sigma_\epsilon = 1.22$, $\sigma_k = 1.0$ and $C_\mu = 0.09$.

4.2.2 Boundary conditions

The flow domain of a centre-fed circular sedimentation tank is bounded by the flow inlet, water surface, the exit flow over the effluent weir and solid boundaries to represent the inlet pipe wall, tank bottom, effluent wall and reaction baffle, as shown in Figures 4.1a and 4.1b. The inlet flow boundary can be represented in two ways. Firstly, by a uniform horizontal flow positioned between the top of the inlet pipe and the water surface, and secondly by a uniform vertical flow at the top rim of the inlet pipe.

To calculate the inlet horizontal velocity, u_{inl} the influent flowrate, Q_{inl} is divided by the cross sectional area that is normal to the flow, as follows :

$$u_{inl}=\frac{Q_{inl}}{2\pi r_{inl}H_{inl}} \quad \text{- (4.3)}$$

The inlet vertical velocity is found by dividing the influent flow rate by the cross sectional area of the vertical inlet pipe, as follows :

$$u_{inl}=\frac{Q_{inl}}{\pi r^{2}_{inl}} \quad \text{- (4.4)}$$

The equations to solve the inlet conditions for k and ϵ in the standard k-ϵ model are as follows (Celik et al[4]) :

$$k_{inl}=C_{pl}u^{2}_{inl} \qquad \text{-(4.5)}$$

$$\epsilon_{inl}=\frac{k^{1.5}_{inl}}{C_{p2}D} \qquad \text{-(4.6)}$$

where $C_{p1} = 0.002$, $C_{p2} = 0.3$ and D is the hydraulic diameter.

On the wall boundaries, the conditions are related to the dependent variables in the viscous sub layer by a logarithmic wall function. The tangential velocity at the grid node p, next to the wall, follows the log law of the model[4], as follows:

$$\frac{u_p}{u^*}=\frac{1}{K}\ln(Ey_p^*) \qquad \text{-(4.7)}$$

where $y_p^+ = y_p u^* / \nu$ (dimensionless wall distance). The rate of production of turbulence near the wall is equal to its rate of dissipation, which gives a single boundary condition :

$$\epsilon = \frac{C_\mu^{3/4} k^{3/2}}{K(d-y)} \qquad \text{- (4.8)}$$

Disturbance of the liquid surface in a sedimentation tank can be caused by the shear forces acting from the wind and the behaviour of the fluid below the surface. This is particularly noticeable above the inlet vertical pipe in a centre-fed circular clarifier, where the jet coming from the pipe impacts the water surface. Another reason is that the variation in flow rate to the full-scale humus tank will affect the water depth in the tank. To account for the effect from wind, additional mathematical models are required, whereas the movement of the water surface can be modelled using the 'homogeneous' model in the program CFX-F3D. This model requires an additional fluid phase to be calculated (i.e. air) and will be therefore a multi-phase flow, which makes it harder to solve. Therefore, instead the model was simplified to solving a single-phase flow only by representing the water surface by a symmetry plane, which assumes that there is no disturbance of the water surface. It will behave like a horizontal lid (there is no net transfer of momentum or turbulence across a symmetry plane).

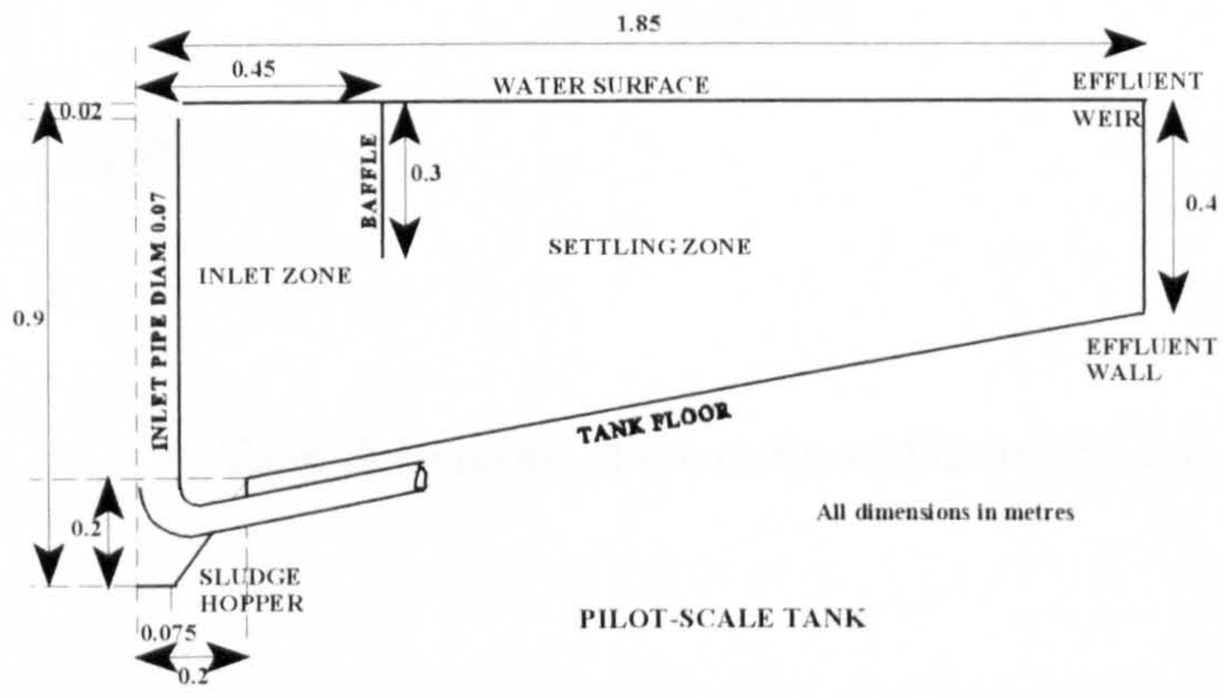

Figure 4.1a Tank dimensions of the cross-section of the pilot-scale tank.

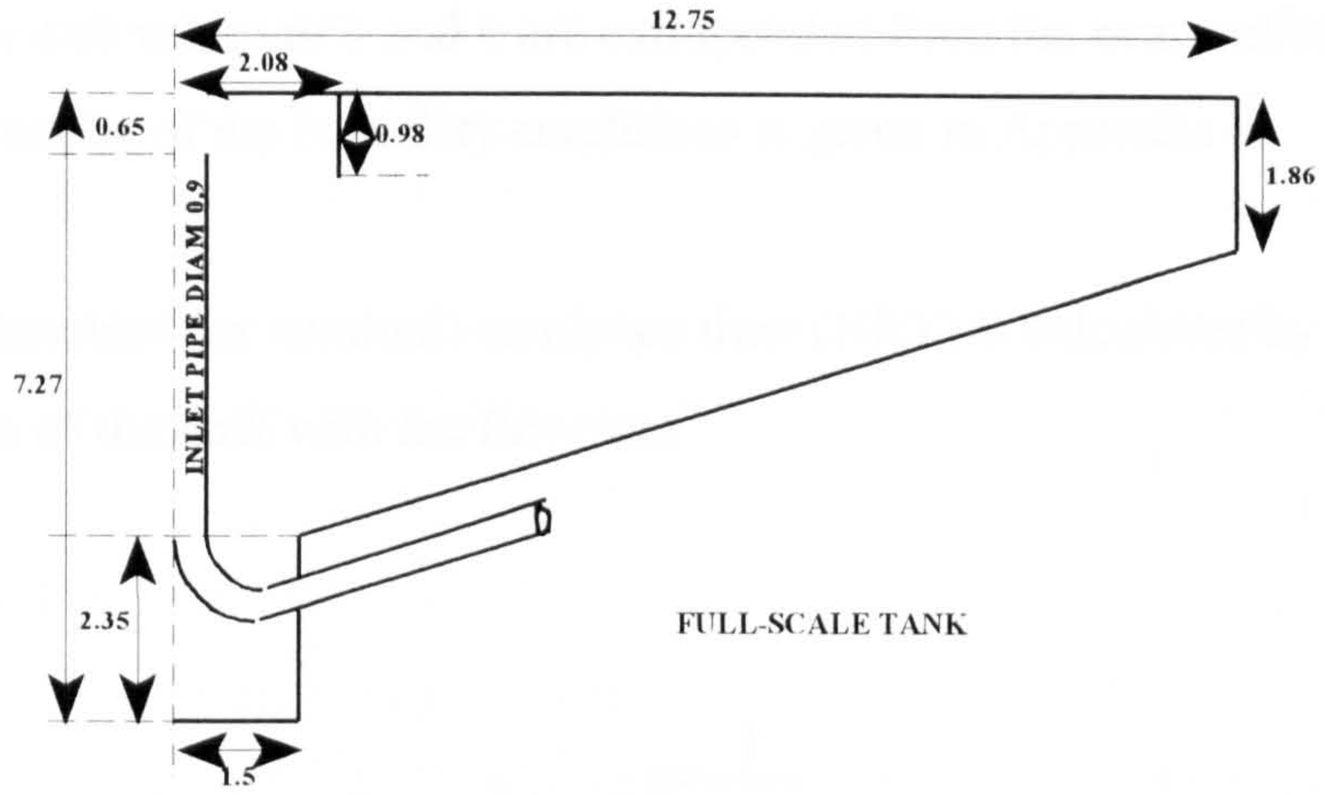

Figure 4.1b Tank dimensions of the cross-section of the full-scale tank.

For a centre-fed circular sedimentation tank it was assumed that there is axi-symmetric flow from the central vertical axis (r=0). This is modelled by a symmetry plane also. There was no sludge removal from the bottom of either of the clarifiers and therefore a wall boundary condition was used to represent the floor of the sludge hopper. The effluent flows over a circular weir into a channel surrounding the clarifier. However, the flow domain was not extended to include the channel and the effluent outlet was instead defined by one cell thickness above the effluent weir. At this boundary, mass conservation is imposed and therefore the mass flow rate of the effluent must be equal to the mass flow rate of the influent. The effluent mass flow rate is divided by the fluid density to give the volumetric flow rate. The radial velocity of the effluent is computed by dividing the volumetric flow rate by the cross sectional area normal to the flow. This

boundary condition is referred to as a 'mass flow boundary' in the program CFX-F3D. The condition for the outlet velocity in the vertical direction is set to zero and the exit values of k and ϵ are extrapolated from the near-outlet values.
A discussion of the boundary conditions is given in Appendix B.

The theoretical (or nominal) residence time (NRT) is calculated by dividing the volume of the tank with the flow rate[16] :

$$\iota = \frac{V}{Q_{inl}} \qquad \text{- (4.9)}$$

The dimensionless time is the measured residence time of the tracer divided by the NRT of the tank[16].

4.3 Numerical method

To decrease the length of each simulation there were several simplifications made to the model. Firstly, it was assumed that there was no heat transfer in the system and therefore no temperature difference between the influent and the fluid in the tank and also between the tank walls and the fluid. Therefore, the energy conservation equation was neglected. Secondly, the tank was modelled as a two-dimensional system (Figures 4.1a and 4.1b), with respect to the water depth and tank radius. Thirdly, the water surface was simplified by a symmetry boundary plane and therefore a multi-phase 'free surface' model was not used. The computational grid had a non-uniform distribution of cells near the solid boundaries, where velocity gradients were expected to be greater. The horizontal direction of the grid in Figure 4.2, pointing to the right is the radial co-ordinate system, and the vertical direction pointing downwards is the axial co-ordinate system. A 'finite difference' method was used to interpolate the computed cell centre values of the variables to the computational mesh.

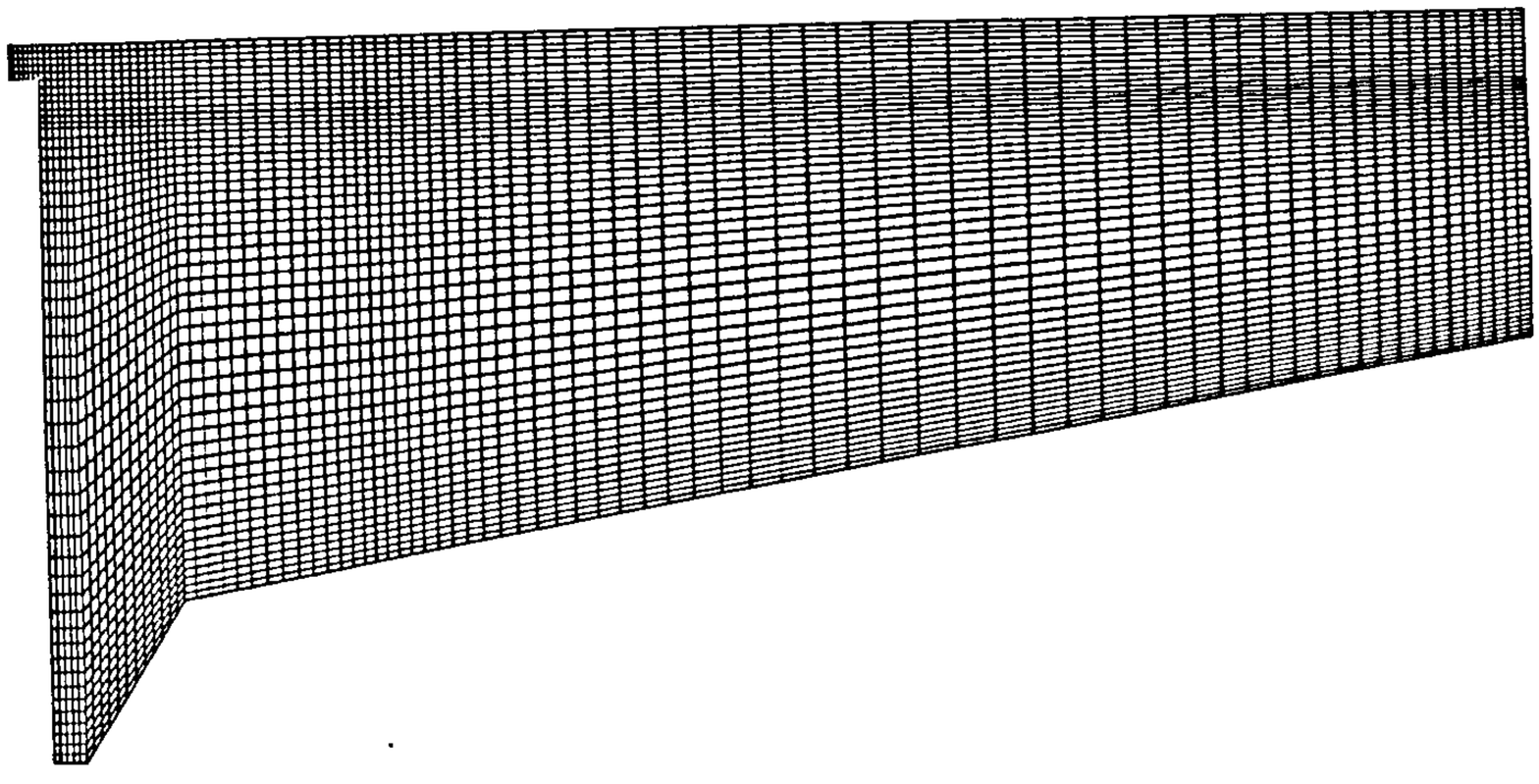

Figure 4.2 Computational grid of the pilot-scale sedimentation tank.

Two simulations were undertaken, for both the pilot-scale tank in the BHR Group laboratory and the full-scale humus tank at the Marley wastewater treatment plant. A steady inlet flow simulation was run for each case until the computed residuals for each variable were less than 0.001, and a steady-state flow pattern had been found. Using the steady-state solution as a restart a time dependent simulation was run, with a pulse of inert scalar (during the first time step) 'injected' into the inlet of the clarifier, to mimick the salt tracer in the experiments. The concentration of the scalar was monitored at the outlet with time and represented the RTD of the tank. During the time-dependent calculations the conservation equations for mass

and momentum were not solved. Therefore the residence time of the scalar was calculated from a steady-state velocity field. The constant time step in the simulations were the same as the frequency of sampling the salt tracer during the experiments. The conditions of the computer simulations are summarised in Table 4.1.

Table 4.1 Computer model conditions for the pilot and full-scale sedimentation tanks.

Clarifier	Pilot-scale	Pilot-scale	Full-scale	Full-scale
Inlet geometry	horizontal	vertical pipe	horizontal	horizontal
Inlet flow	constant	constant	constant	variable
Inlet water depth, cm	2	2	65	65
Inlet velocity, cm/s	45.5	52.0	4.96	4.47 - 5.51
Iterations	6000	6000	6000	6000
Time step, s	30	30	600	600

Both clarifiers had an upflow inlet through a solid vertical pipe in the centre, and a solid ring baffle positioned vertically in the tank. The tanks were divided by the internal baffle into two functional zones, namely the inlet zone and the settling zone. Effluent exited over the weir and there was no sludge withdrawal from the base of the tanks. In the pilot-scale tank there were no suspended solids (i.e. only water was used as the test fluid) and therefore there was no need to remove solids from the floor of the clarifier. The humus tank has a low inlet suspended solids concentration and during its normal operation it removes the settled sludge periodically to ensure that the tank does not accumulate solid matter. During the salt tracer test however the automatic periodic removal of sludge was turned off so that steady state flow conditions were maintained in the humus tank.

The salt tracer experiment, conducted to find the RTD of the effluent from the pilot-scale tank had the exit from the vertical inlet pipe at the same height as the water surface. This could have been modelled by extending the flow domain above the water surface to include the air above the clarifier and represent the interface between the water and the air with a free surface boundary. Instead, a symmetry boundary was used to define the water surface and the height of the inlet pipe was modelled 2 cm below the water surface. The predicted RTD's of the effluent were compared to experimental data for two inlet velocity boundary conditions, i.e a uniform radially outwards velocity between the inlet pipe and the water surface and a uniform vertically upwards velocity at the exit of the inlet pipe. This comparison was done to determine whether the vertical inlet jet impacting on the symmetry plane was a more accurate simulation than a horizontal inlet.

The full-scale tank had the end of the inlet pipe below the water surface and therefore the real height of the inlet pipe could be modelled with the single-phase flow model. A uniform radial velocity boundary condition above the inlet pipe

was simulated. Consequently, the flow pattern directly above the inlet pipe was ignored which made the solution easier to converge.

To consider the effects of a variable inlet flow rate on the flow pattern in the humus tank, two transient simulations were undertaken : the mean flow rate and the variable flow rate. In the latter case, a steady-state simulation was run at the inlet flow rate which corresponded to the beginning of the salt tracer test. Using the steady-state solution, a time-dependent simulation was run with a variable inlet velocity and a short pulse of scalar to the inlet of the clarifier. On every time step (at 10 minute intervals) the variable inlet velocity was interpolated from the raw velocity data (every 15 minutes) using a user defined subroutine. The velocity data had been calculated by dividing the measured inlet flow rate by the inlet cross sectional area. The RTD's of the effluent for the mean and variable inlet flow simulations were compared to the results from the experimental tracer studies.

The standard k-ϵ turbulence model, devised by Launder and Spalding[17], is very popular for modelling turbulent flows in sedimentation tanks because it is computationally inexpensive compared to the Reynolds stress models. It can also calculate recirculating flows more accurately than simpler models such as the zero or one equation eddy-viscosity models. The accuracy of the calculation can be improved by increasing the number of cells. To consider this, a grid dependency test was undertaken, which carries on from the previous work done by the author on a flat based clarifier[18]. The number of cells for a flat based clarifier had been increased from 1500 to 6000 and then to 12000 cells. The flow pattern changed significantly, upon an increase to 6000 cells, but the flow pattern was relatively unchanged from 6000 to 12000 cells. Therefore, the number of cells selected for this study was 6000 (see Figure 4.2), to keep the length of each simulation to a minimum. However, it would have been desirable to have tested a grid with 3000 cells and then possibly use fewer cells in the simulations.

A higher mesh density was used in the regions of the clarifier, near the wall boundaries, to compensate for the following factors. Firstly, the conservation of mass is poorer in the regions of the tank where there are high velocity gradients, for instance, where the flow collides with the walls of the tank. Secondly, the equations used to calculate the mean normal velocities and the turbulent parameters near the tank boundaries are an approximation based on the principles of boundary layer flows. Therefore, having more grid lines near the wall boundaries will improve the models accuracy.

4.4 Experimental method

Tracer studies were undertaken on both the pilot-scale tank and the full-scale tank. Schematic diagrams of the equipment are shown in Appendix C. The pilot-scale tank drew tap water from a laboratory sump by a service pump. Sodium chloride tracer was injected into the horizontal pipe upstream of the tank as a pressurised pulse. A steady flow was metered by a rotameter in this pipe between the injection point and the entry pipe to the clarifier. One conductivity probe located in the weir channel of the clarifier (near to the outlet pipe) measured the voltage charge of the salt going into the outlet. The probe was calibrated using samples with known salt concentrations in water. The outputs from the probe were processed by a data acquisition system, consisting of a six channel signal conditioning box and a personal computer with a data acquisition card, and software to configure the system. The concentration of tracer needed to be low so that its density was similar to water but it could not be too low, otherwise the conductivity equipment would not produce a clear signal. A high flow rate was chosen to reduce the density effect of the salt tracer.

To validate the CFD model for single-phase flow, a full-scale clarifier with a low inlet suspended solids concentration was chosen. The full-scale tank had a deep, flat based sludge hopper and there was no de-sludging during the salt tracer test. Lithium chloride tracer was dosed as a pulse to the square inlet distribution chamber upstream of the tank. The variable plant flow rate was metered automatically using a flume and an ultrasonic level measuring device, further upstream of this chamber. The flow rate was measured at the inlet to the 4 humus tanks at the works. It was assumed that there was an even flow split to each of the humus tanks to give the flow rate to the test tank. An automatic sampler was programmed to extract samples periodically in the weir channel of the clarifier for the duration of the test. Samples were analysed for trace concentrations of lithium chloride using an 'inductivity coupled plasma' test, which had first been spiked with caesium chloride. To allow a high fraction of tracer to reach the outlet, testing lasted for several nominal residence times for both tanks. Experimental conditions for both tanks are summarised in Table 4.2.

Table 4.2 Experimental conditions for the pilot and full-scale sedimentation tanks.

Sedimentation tank	Pilot-scale (1:10 scale to prototype)	Full-scale
Tank diameter, m	3.7	25.5
Tank volume, m^3	5.5	1518
Pipe radius, cm	3.5	45
Inlet flow, m3/hr	7.2	328
Surface overflow rate, m^3/m^2d	68	63
Mean residence time clarifier, min	46	279
Mean time lag from salt dosing point, min	0.4	2
Mean time lag from flow measure, min	0.2	4
Inlet solids concentration, mg/l	0	mean : 50 range : 20-150
Salt tracer	sodium chloride	lithium chloride
Flow measurement	rotameter (metric 65x series)	flume / ultrasonic head measurement
Sampling rate, Hz	2	1/600
Test duration, hr	2 hrs 20 min	8 hrs
Salt dosing	pressurised pulse (100 psig) to inlet pipe	inlet distribution chamber
Concentration measurement	conductivity	salt concentration

4.5 Results and Discussion

The predicted flow patterns in the pilot-scale tank are shown in Figures 4.3a and 4.3b (i.e. with the horizontal and vertical inlets). No discernible difference was observed, except for the flow profile in the upper region of the inlet zone of the clarifier. It should be noted that the large vertical vectors in Figure 4.3b are a feature of the graphics, and do not imply a vertical jet leaving from the water surface. It was also noticeable that the speed of convergence for the model was better with a horizontal inlet because there were fewer grid cells. Moreover, the vertical inlet jet in the pipe collided with the symmetry boundary plane and caused velocity gradients, which made the conservation of mass worse in the region above the inlet pipe. However, the modelling of the water surface as a symmetry plane caused the flow pattern above the vertical pipe to be predicted incorrectly. The buoy on the water surface was ignored and the largest radial velocity was predicted next to the symmetry boundary. In reality, the largest radial velocity will be below the water surface. It is not surprising therefore that the only difference in the flow pattern was in the top region of the inlet zone of the clarifier. In other regions of the clarifier the influence of the inlet velocity profile will be diminished.

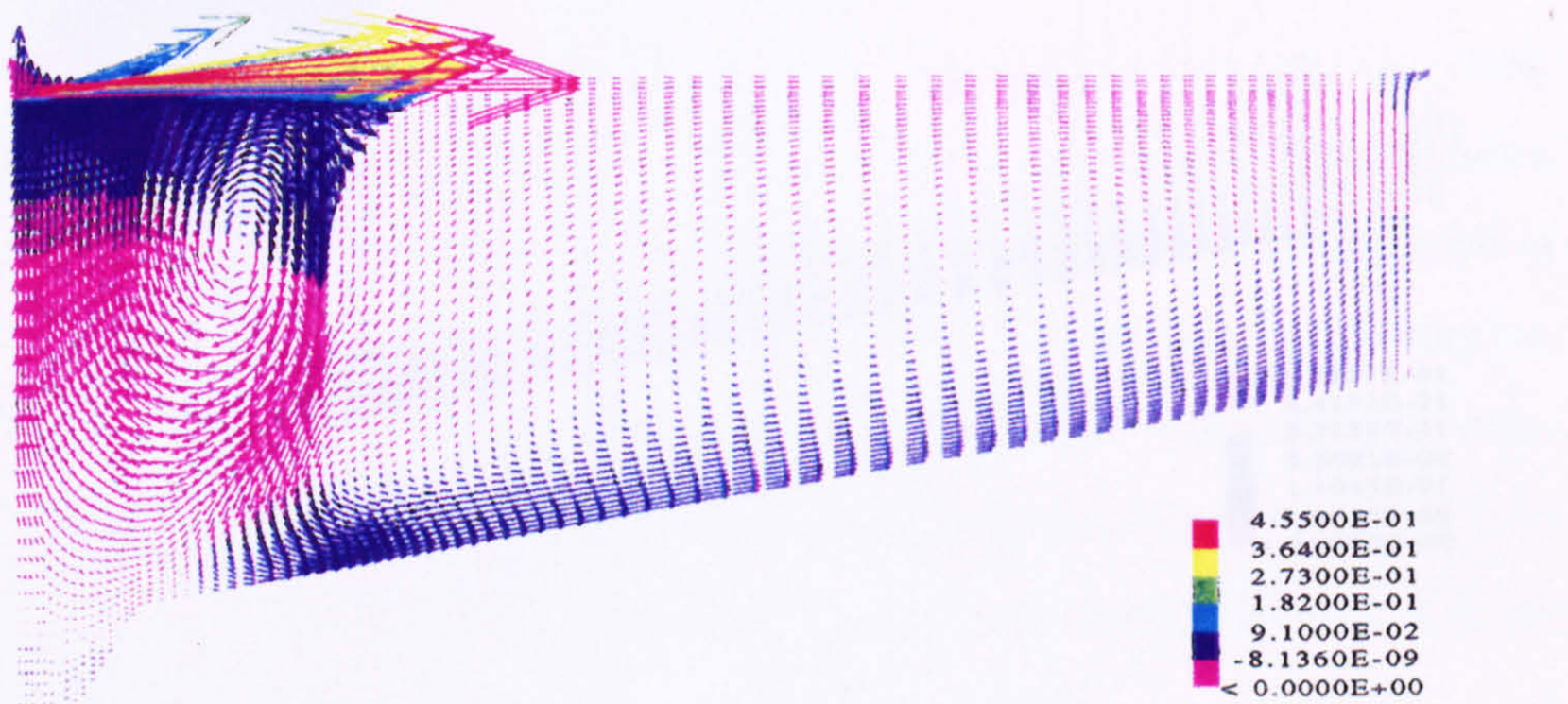

*Figure 4.3(*a) Flow pattern in the pilot-scale sedimentation tank with a horizontal inlet (the scale is the radial velocity in ms^{-1}).

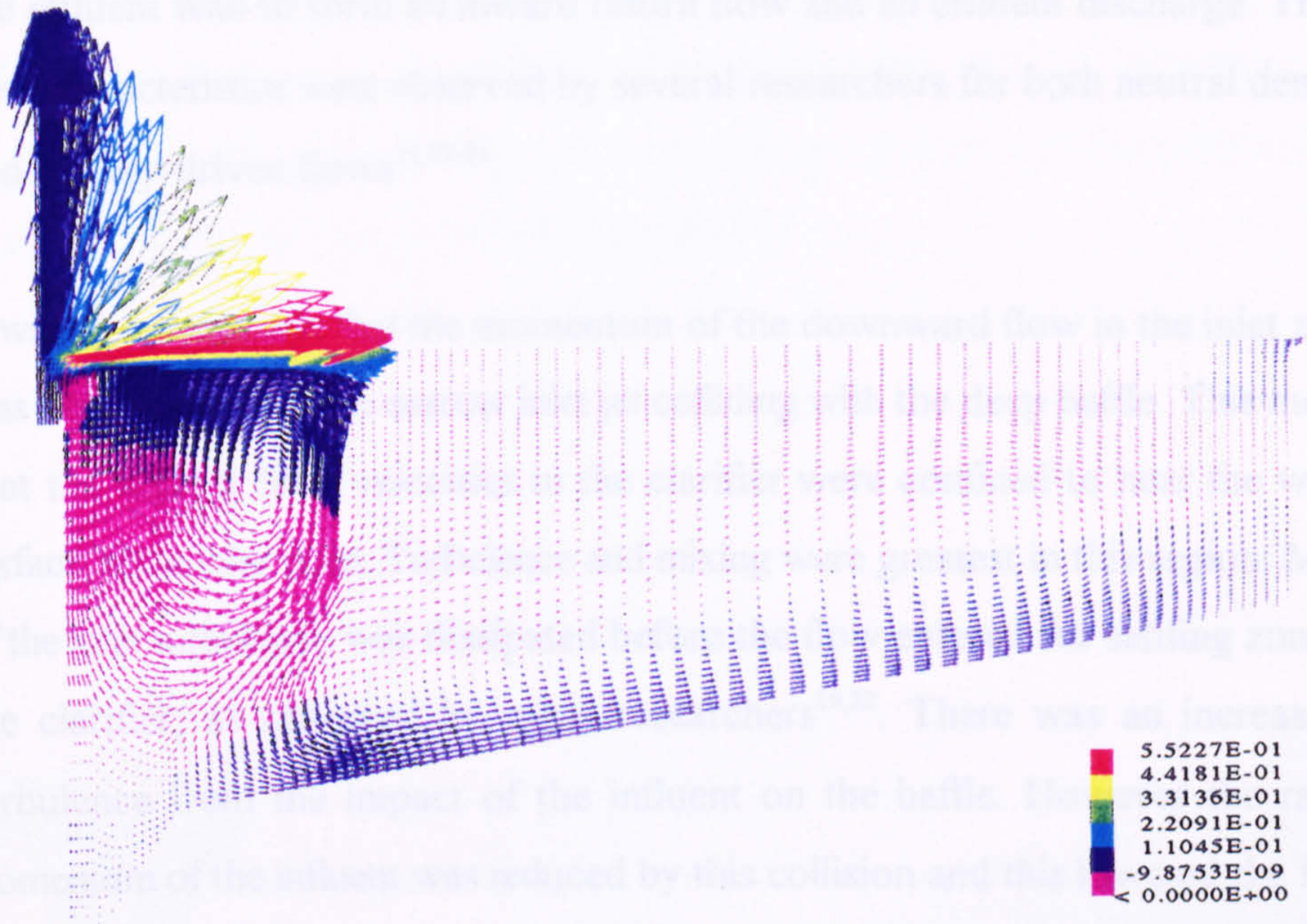

Figure 4.3(b) Flow pattern in the pilot-scale sedimentation tank with a vertical inlet (the scale is the radial velocity in ms^{-1}).

In both simulations, the narrow influent stream near the water surface was deflected downwards, due to impingement on the reaction baffle. It was noticeable that the downward flow migrated slightly towards the centre of the tank, caused by the re-entrainment of fluid from the settling zone. The downward current impinged on the tank floor below the reaction baffle. At this point, the flow split

to form a strong current along the tank floor radially outwards and a weak current to the sludge hopper. The current along the tank floor decreased in velocity, collided with the effluent wall and flowed upwards. This upward flow split near the effluent wall to form an inward return flow and an effluent discharge. These flow characteristics were observed by several researchers for both neutral density and density-driven flows[11,19-21].

It was also noticeable that the momentum of the downward flow in the inlet zone was small; caused by the narrow inlet jet colliding with the deep baffle. This meant that the highest flow velocities in the clarifier were confined to near the water surface in the inlet zone. Turbulence and mixing were greatest in this region. Most of the inlet turbulence was dissipated before the flow entered the settling zone of the clarifier, as observed by other researchers[19,22]. There was an increase in turbulence from the impact of the influent on the baffle. However the radial momentum of the influent was reduced by this collision and this lowered the flow velocities in the settling zone. Generally, as expected there was a radial decreasing velocity, with the distance from the centre of the clarifier[19-22].

The main flow characteristics of the Marley tank simulation (Figure 4.4) were the same as the pilot-scale tank. However a wider influent jet, in relation to the position of the baffle, caused more downward flow in the full scale tank. The most mixing in the full- scale tank was found in the centre of the inlet region. As before, the downward flow split on the tank base. The outwards current along the tank floor was stronger (a quarter of the inlet velocity) in the full scale tank, but decreased up the tank slope. A strong upward flow near the effluent wall, caused flow separation into two streams on the water surface, namely the effluent discharge and the return current in the settling zone. There was no re-entrainment of flow from the settling zone to the inlet zone.

The flow simulations of both circular clarifiers showed a region with high velocities and kinetic energy in the inlet zone, which should encourage mixing and particle flocculation[21]. Elsewhere, the relatively low velocities, especially in the settling zone should allow particles to settle quiescently, as desired[23-25]. The inlet and the baffle designs are critical to the distribution of fluid turbulence in sedimentation tanks and will affect the magnitude and direction of the influent jet, as also observed by Zhou and McCorquodale[19].

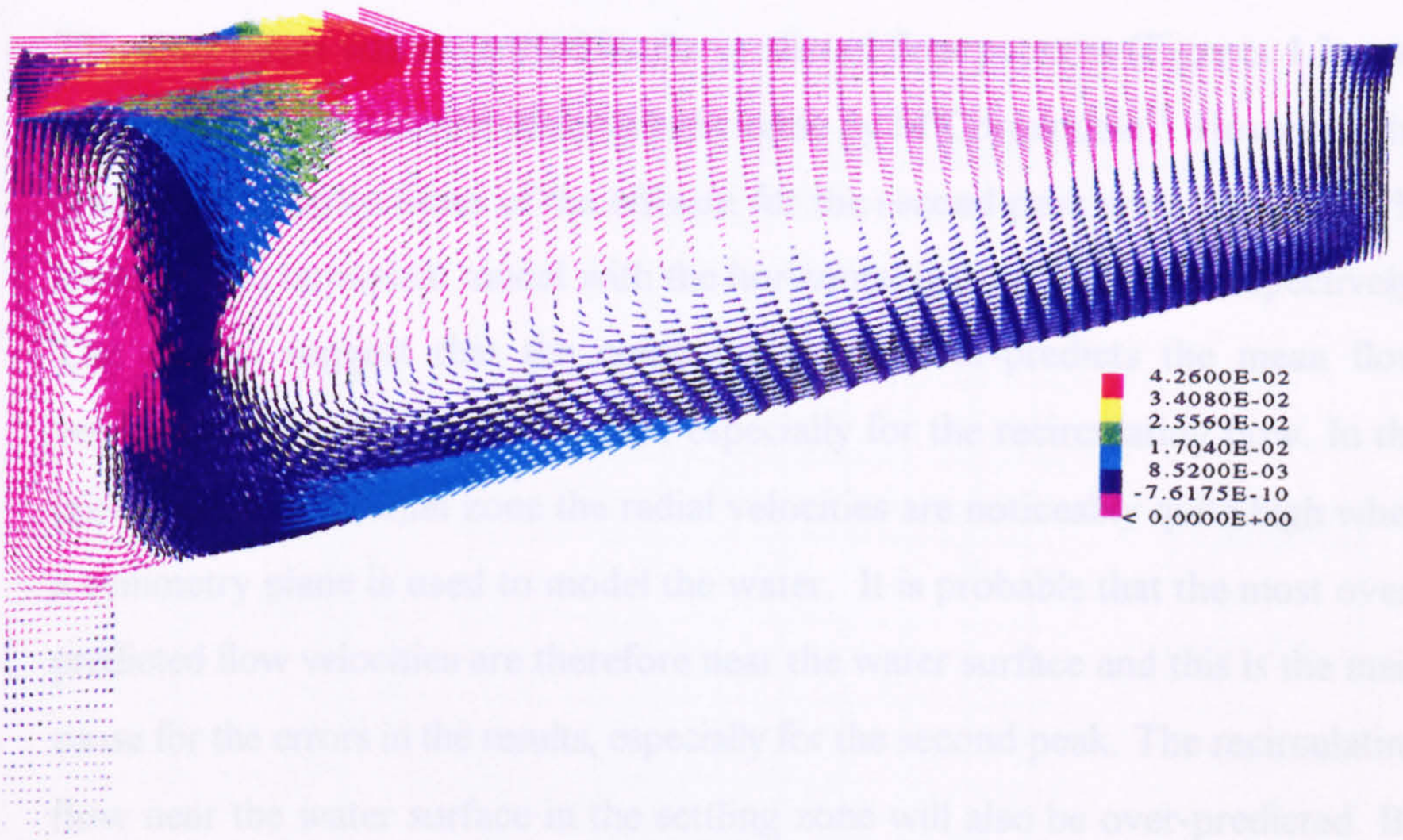

Figure 4.4 Flow pattern in the full-scale sedimentation tank (the scale is the radial velocity in ms^{-1}).

Figure 4.5 shows the RTD's of the numerical model and the experimental tracer study for the pilot-scale tank. The vertical axis denotes the dimensionless tracer concentration, which is found by dividing the instantaneous tracer concentration with the total area under the concentration-time curve[16]. The RTD's from the computations were in agreement with the experimental RTD, in terms of the shape of the curve and its tail. Tracer peaks for the predicted and experimental RTD's were seen to occur about 0.1 of the nominal residence time, indicating severe short circuiting of flow within the tank (ideal flow = 1). The percentage error between the numerical and experimental results for the peak concentrations and residence times of the RTD's (Table 4.3) were -3 % and -18 % respectively for the horizontal inlet and +6 % and -24% for the vertical inlet. The simulations showed a second peak indicating that there was recirculating flow in the clarifier. This observation was supported by the predicted flow patterns (Figures 4.3a and 4.3b) and the experimental observations made by M^{c}Corquodale[11]. However, the predicted residence times of the effluent for the second peak were 29 and 38 % lower for the numerical model with the horizontal and vertical inlet respectively. The results suggest that the computer model over-predicts the mean flow velocities in the pilot-scale clarifier, especially for the recirculating flow. In the upper region of the inlet zone the radial velocities are noticeably quite high when a symmetry plane is used to model the water. It is probable that the most over-predicted flow velocities are therefore near the water surface and this is the main cause for the errors in the results, especially for the second peak. The recirculating flow near the water surface in the settling zone will also be over-predicted. By looking at Figure 4.5, qualitatively there is a good agreement between the numerical and experimental RTD but quantitatively the error for the residence time of the effluent at the peak concentration was up to 24 %. There may have been a reduction in the radial velocities in the clarifier if swirling flow had been included in the model, however there was no rotating scraper.

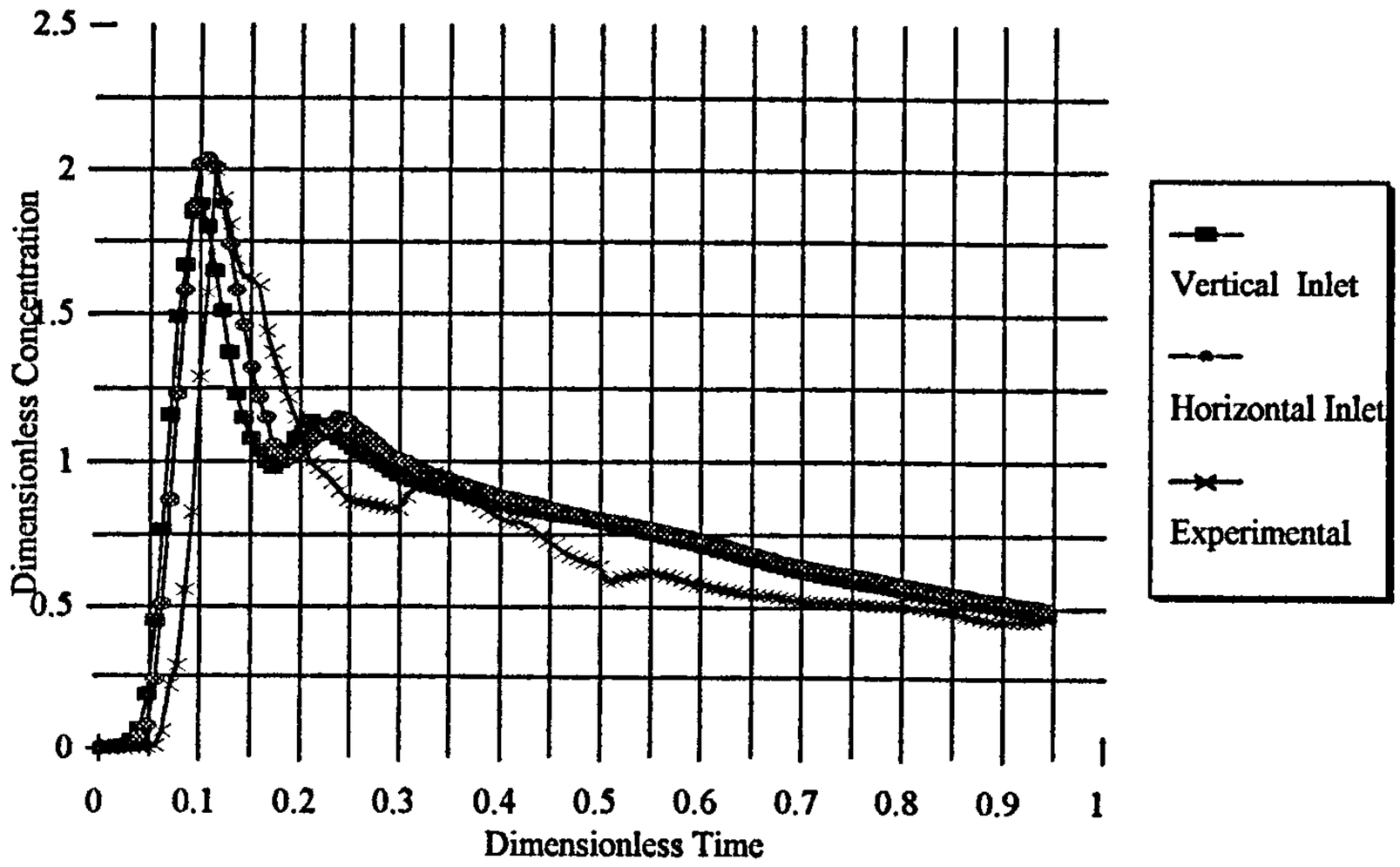

Figure 4.5 Residence time distributions of the effluent in the pilot-scale sedimentation tank.

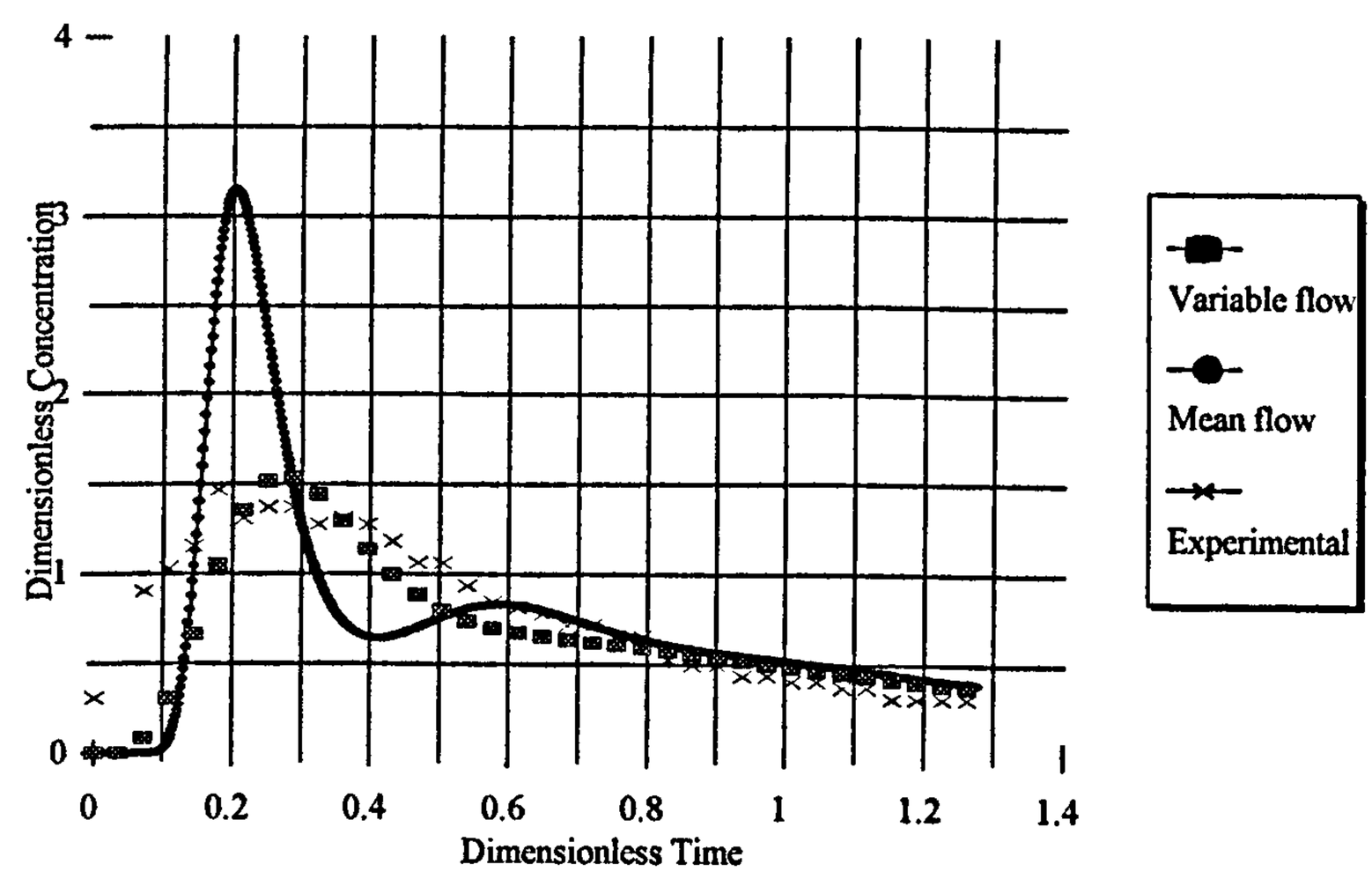

Figure 4.6 Residence time distributions of the effluent in the full-scale sedimentation tank.

Table 4.3 Characteristics of the residence time distributions of the effluent for the pilot and full-scale sedimentation tanks.

System	**Peak dimensionless tracer concentration**	**Dimensionless time at peak tracer concentration**
Pilot-scale tank (computer model): horizontal inlet	2.06	0.098
Pilot-scale tank (computer model): vertical inlet	1.88	0.090
Pilot-scale tank: salt tracer	2.00	0.119
Full-scale tank (computer model): mean flow	3.15	0.207
Full-scale tank (computer model): variable flow	1.53	0.291
Full-scale tank: salt tracer	1.46	0.182 - 0.364

When using a tracer or simulant in water, the ratio of the inertial to gravitational forces for water and the tracer should be the same, by the laws of dynamic similarity[26]. The inlet densimetric Froude number is used in the similarity law for the downscaling of full-scale sedimentation tanks (equation 3.14). Two operational parameters affected this law during the experiments, namely the salt concentration and the water flow rate. The concentration of sodium chloride should ideally be the same density as the water[26]. However, in the experiments very low salt concentrations were not detectable by the conductivity equipment and so a higher salt concentration (10 mg/l) was chosen. The gravitational force on the salt was therefore greater than the water. It was necessary, to increase the inertial force on the salt, by increasing the water flow rate and this meant that the model could only be validated at a high flow rate.

The inlet densimetric Froude number is directly proportional to the inlet velocity divided by the square root of the density difference between the salt and the water. Therefore to increase the water flow rate in the pilot-scale tank it should be in proportion to the density difference to keep the Froude number constant. The experiment did not consider this but instead only carried out the experiment at the highest flow rate which did not disturb the water surface. This was done because the single-phase flow model was unable to predict the free water surface.

In practise, all the dimensionless numbers used for similarity laws cannot be kept constant. This is a common problem when scaling down equipment from a full-scale prototype. The inlet densimetric Froude number may be the most important dimensionless number used for sedimentation tanks but the Reynolds number should also not change from one flow regime to another (e.g.. transitional to turbulent flow). This may have happened in some places in the pilot-scale clarifier, when the flow rate was increased in the experiment. The standard k-ϵ turbulence

model is more accurate when predicting the mean flow velocities when the flow is only in the fully turbulent flow. This was a possible reason why there was not a bad agreement between the predicted and experimental RTD's using a high flow rate.

Figure 4.6 compares the predicted RTD's with the tracer studies for the full-scale tank. The CFD simulation with the mean inlet flow rate did not agree with the experimental data from the full-scale tank. However, when a variable inlet flow rate was simulated there was a marked improvement in the correlation with experimental data. This RTD agreed with the experimental results in terms of the peak residence time, peak concentration (+ 5%) but the shapes of the curves were different. However, the results show that there is a need to model the variation in flow rate (Figure 4.7) to a sedimentation tank in a treatment plant, because the variability of the flow rate does affect the flow patterns.

Severe flow short circuiting was indicated by the tracer peak concentrations for both the experimental and numerical results of the humus tank. Dimensionless peak residence times of 0.25 - 0.3 times the nominal residence time were found for the variable flow simulation and the experiment. However, differences between the computational and experimental results in the detection of the first tracer at the outlet were noticeable (Figure 4.6). The site test showed that the salt tracer was already present at the outlet, at the beginning of the test, which suggested that there was a background concentration of lithium chloride at the works. However, there was no reason that lithium should be present in the wastewater. A possible explanation was that the deposition of suspended solids formed a boundary layer of solids on the tank base. This may have caused flow to pass more quickly to the effluent because some of the tank was blocked by settled matter and the tank's effective volume was reduced. Another explanation was that the measurements of

lithium chloride were inaccurate. To test this the first measurement (0.1 mg/l) was zeroed by deducting this concentration from all the measurements. However, this gave a greater overall difference between the experimental and computational RTD's.

There are some concerns about the variable flow data used for the inlet velocity boundary condition in the model of the humus tank. The flow rate to the humus tank was measured upstream of the location where the salt was injected. The time lag between the flow at the measuring location and the flow at the inlet to the clarifier was 4 minutes. Therefore, the percentage change in flow rate (Figure 4.7) in this time interval was 2 % which will be the experimental error caused by the time lag. The time lag for the salt tracer to travel from the inlet distribution box to the inlet of the clarifier is 2 minutes. Therefore, the measured salt concentration curve should be shifted to the left along the x-axis by 2 minutes to account for the time lag, which would have made the comparison with the predicted RTD worse.

Another concern is that the variable flow rate measured upstream of the clarifiers will be damped and smoothened before reaching the inlet of the humus tank. This will happen as the flow progresses through the treatment works. Therefore, the variation in flow rate will be in reality lower than is shown in Figure 4.7.

The water level in the full-scale clarifier will change with the variation in flow rate and could significantly affect the outlet conditions. This is not accounted for by the numerical model which models the water surface as a rigid plane. At the maximum flow to the clarifier the disturbance to the water surface will be at its greatest and the vertical velocities up the effluent wall and the radial velocity over the weir will be increased. This will carry suspended solids over the weir which is detrimental to the performance of the tank in terms of the solids removal.

Therefore, the errors in this study were partly caused by the accuracy of the inlet flow data to the full-scale clarifier which were due to its measurement location, the time lag to reach the clarifier and the smoothing of the variable flow rate. Another concern was the use of the symmetry boundary plane to model the water surface. The comparisons to experimental data were therefore qualitatively quite good but quantitatively less good.

The most important finding of this work was the significance of modelling the variable influent flow rate to the sedimentation tank. When field data is gathered it should be checked whether the flow rate is variable or steady. Computer simulations should be compared for a mean flow rate and a real plant flow rate. This is especially important when modelling with solids present (i.e. applying the model to real plants), and could show that the effluent solids concentration is affected by the inlet flow rate.

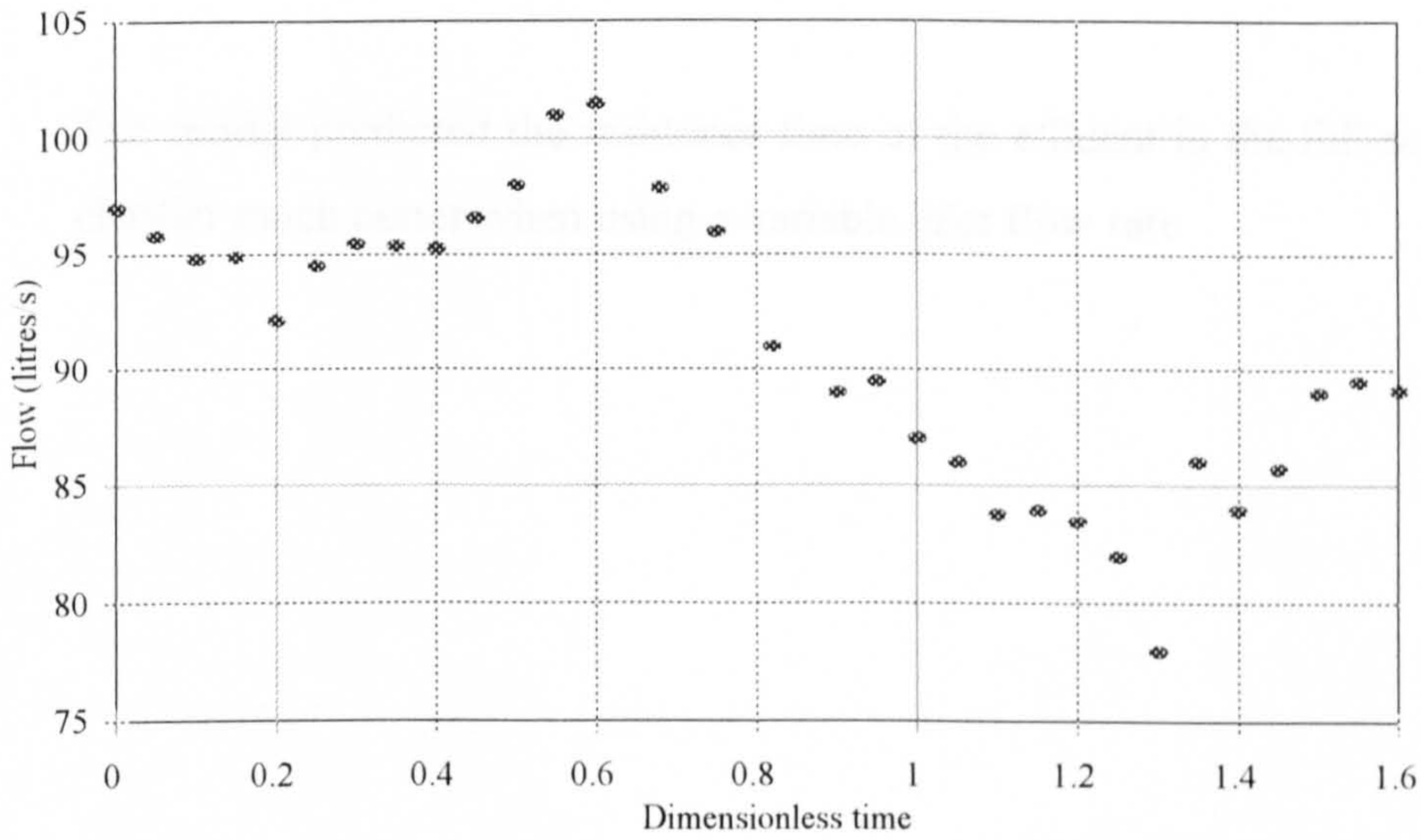

Figure 4.7 Plant flow rates to the full-scale sedimentation tank.

4.6 Conclusions

1. The predicted and experimental residence times of the effluent in the pilot-scale tank at the peak of the RTD differed by 29 and 38% respectively for the horizontal and vertical inlet simulations.

1. 2. The inlet boundary represented as a vertical flow showed no added value to the single-phase flow prediction in the pilot-scale tank, and therefore a horizontal inlet flow was preferred.

3. The flow rate measurements upstream of the full-scale clarifier did not account for the time lag to the clarifier and the smoothening of the flow.

4. The symmetry plane boundary condition did not account for the movement of the water surface which is affected by the vertical inlet jet, variation of flow and the wind.

5. The model predicted the residence time of the effluent in the full-scale clarifier much better when using a variable inlet flow rate.

This chapter of the thesis has shown that the single-phase flow model was valid when qualitative comparisons were made to experimental data from both a pilot-scale and a full-scale clarifier. Even though there were some suspended solids in the full-scale clarifier, the effect of the solids was negligible because of the low inlet solids concentration. However, the quantitative comparisons of the model to experiments were less good and this can be accounted for by the boundary condition of the water surface and the flow measurements taken upstream of the humus tank. The study has shown that a horizontal velocity was a reasonable simplification of the inlet boundary condition. It was especially important to simulate the transient flow conditions, which implied that diurnal changes in flow will also affect the modelling of secondary clarifiers. Consequently, the next stage of the project intends to validate a multi-phase flow model for secondary clarifiers by comparing it to experimental data. This is presented in the next chapter of the thesis.

4.7 References

1. Camp,T.R. (1945). 'Sedimentation and the design of settling tanks'. Transactions of the American Society of Civil Engineers., part III, 895-396.
2. McCorquodale, J.A. and Zhou, S. (1994). 'Effects of hydraulic and solids loading on clarifier performance'. Journal of Hydraulic Research, vol. 31, no. 4, 461-478.
3. Celik, I. and Rodi, W. (1985). Simulation of hydrodynamic and transport characteristics of rectangular settling basins. In : Transport of Suspended Solids in Open Channels. June 11-15, Munich/Neubiberg, University of Karlsruhe, Germany.
4. Celik,I., Rodi,W. and Stamou,A.I. (1985). Prediction of hydrodynamic characteristics of rectangular settling tanks. Proceedings of the International Symposium on Refined Flow Modelling and Turbulence Measurements. Iowa City, Iowa.
5. Adams, E.W. and Rodi, W. (1990). 'Modelling flow and mixing in sedimentation tanks. Journal of Hydraulic Engineering (American Society of Civil Engineers), vol. 116, 895-911.
6. Lowe, S.A. and Sivakumar,M. (1991). 'A penalty finite difference model for Navier-Stokes flow problem in sedimentation basins, Advances in Water Research, vol. 14, 318-312.
7. Lyn, D.A. and Zhang, Z. (1989). Boundary-fitted numerical modelling of sedimentation tanks. Proceedings of the 23rd International Association for Hydraulic Research (IAHR). Ottawa, Canada, A331-A338.
8. Szalai,L. , Krebs, P. and Rodi, W. (1994). 'Simulation of flow in circular clarifiers with and without swirl. Journal of Hydraulic Engineering (American Society of Civil Engineers), vol. 120, no. 1, 4-21.

9. Kabza,Z., Dobrowolski, B. and Spyra,A. (1983). Numerical modelling of the flow phenomena in the settling tanks. In: Applied Chemistry Unit Operations and Processes. Proceedings of the 4th Conference of the Hungarian Chemical Society. Paper 1.4.2, 135-140.

10. McCorquodale, J.A., Moursi,A.M. and El-Sebakhy,I.S. (1988). 'Experimental study of flow in settling tanks'. Journal of Environmental Engineering, (American Society of Civil Engineers), vol. 114, 1160-1174.

11. McCorquodale, J.A. (1976). Hydraulic study of the circular settling tanks at the West Windsor pollution control plant. Report submitted to Lafontaine, Cowie, Buratto and Associates limited, consulting engineers. Windsor, Ontario.

12. Lyn, D.A., Stamou,A.I. and Rodi,W. (1992). 'Density currents and shear-induced flocculation in sedimentation tanks'. Journal of Hydraulic Engineering, vol. 118, 849-867.

13. Montens, A. (1954). 'The use of radioactive isotopes for water flow and velocity measurement'. Radioactive Conference. J.E. Johnston, ed., Butterworths, London, England, 169-180.

14. Tay, A.J. and Heinke, G.W. (1983). 'Velocity and suspended solids distribution in settling tanks'. Journal of the Water Pollution Control Federation, vol. 55, 261-269.

15. Rodi,W. (1980). Turbulence models and their application in hydraulics, a state of the art review. Book publication of the International Association for Hydraulic Research. Delft, Netherlands.

16. Levenspiel,O. (1988). Chemical reaction engineering, Second Edition, 253-259.

17. Launder, B.E. and Spalding, D.B. (1972). Mathematical models of turbulence. (Academic press, London).

18. Matko,T., Sharp,A. and Stephenson,T. (1995). Simulation of the flow in a circular sedimentation tank. Proceedings of the 1st European Conference for Young Researchers in Chemical Engineering, 5-6 January 1995, Edinburgh, UK, 808-810.

19. Zhou,S. and McCorquodale,J.A (1992). 'Influence of skirt radius on performance of circular clarifier with density stratification'. International Journal of Numerical Methods in Fluids, vol. 14, 919-934.

20. Zhou,S. and McCorquodale,J.A. (1992). 'Mathematical modelling of a circular clarifier.' Canadian Journal of Civil Engineering, vol. 19, 365-374.

21. Zhou,S., McCorquodale, J.A. and Vitasovic,Z. (1992). 'Influence of density on circular clarifiers with baffles'. Journal of Environmental Engineering (American Society of Civil Engineers), 829-847.

22. Krebs, P., Vischer, D. and Gujer, W. (1995). 'Inlet structure design for final clarifiers'. Journal of Environmental Engineering, (American Society of Civil Engineers), vol. 121, no. 8, 558-564.

23. Hazen, A. (1904). 'On sedimentation'. Transactions of the American Society of Civil Engineers, vol. 53, 45-88

24. Dobbins,E.W. (1944). 'Effect of turbulence on sedimentation'. Transactions of the American Society of Civil Engineers, vol. 109, 629-656.

25. Kawamaru,S. (1981). 'Hydraulic scale-model simulation of the sedimentation process'. Journal of the American Water Works Association, 372-379.

26. Silveston,P.L. (1979). 'On the use of residence time distributions for the design of clarifiers.' Canadian Journal of Chemical Engineers, vol. 57, 83-87.

CHAPTER V

It is the intention that this chapter will be submitted to a journal, and therefore it has been written here in the format of a paper. This work aims to validate a multi-phase flow model, by comparing it to experimental data from two full-scale circular secondary sedimentation tanks. The numerical models in the literature treated the flow in secondary clarifiers as single-phase and density stratified. However, in this work the Eulerian multi-fluid model, from the computational fluid dynamics programme CFX-F3D, has been modified to predict the flow in secondary clarifiers. One of the circular secondary clarifiers has a deflector plate, which is quite unusual. The model was compared to experimental residence time distributions which has not been done before for secondary clarifiers.

NUMERICAL MODEL OF TWO-PHASE FLOW

5.1 Introduction

Secondary clarifiers are one of the last process stages in wastewater treatment before the final effluent is discharged and therefore, it is important to design and operate them correctly. In these clarifers the inlet solids concentration is usually much higher than in primary clarifiers, which leads to density currents as well as hindered settling[1]. Numerical models of secondary clarifiers often do not consider the fluid dynamics within these tanks[2], and consequently failure is often associated with poor flow distribution. A computational fluid dynamics (CFD) model can be used to predict the flow patterns and suspended solids concentrations in secondary

clarifiers[1]. However, a numerical model needs to be verified by comparing it to experimental data.

Several authors have modelled the flow in secondary clarifiers[3-11]. Predicted radial velocities[3-4,6,7,10] and contour lines of suspended solids concentrations[5,8] were compared with experimental data[5,12,13,14,15]. For all instances, a two dimensional representation of the clarifier was sufficient to give a reasonable agreement with experimental data

The Eulerian multi-fluid model was validated, by comparing it to measurements of the residence time distribution (RTD) of the effluent and return activated sludge (RAS) coming from two full-scale secondary circular clarifiers. It was also compared to the measured suspended solids concentrations within these clarifiers, and the solids concentrations of the effluent and RAS coming from the tanks.

5.2 Theory

5.2.1 Flow equations

The flow is represented by a Eulerian multi-fluid model, which divides the wastewater into its two constituents, namely the clear fluid and the solid particles. Each constituent is treated as a fluid with distinct physical properties and assigned a volume fraction equal to the fraction of the control volume occupied by it. The standard conservation laws for mass, momentum and energy are solved for each phase to give separate velocity fields. There are extra terms for the exchange of mass, momentum and energy between the phases. It was assumed that the fluid entering the clarifier had the same temperature as the fluid already in the clarifier,

the walls were adiabatic and there was no convective or radiative heat transfer. Therefore the energy conservation equation was neglected because the flow was isothermal. The terms for the transfer of mass between the phases caused by molecular diffusion were neglected from the mass continuity and solids transport equations because the dissolved species in wastewater (e.g nitrates) were ignored in the model (i.e. only the suspended solids were modelled). However, the term for the mass transfer between the phases in the momentum conservation equation was included, in order to represent the drag force acting on the fluid by the particles.

In the programme, CFX-F3D, the governing equations for unsteady, two-phase, turbulent mean flow for the conservation of mass and momentum are :

$$\frac{\partial}{\partial t}(r_\alpha \rho_\alpha)+\frac{\partial}{\partial x_i}(r_\alpha \rho_\alpha u_{\alpha i})=0$$

$$\frac{\partial}{\partial t}(r_\alpha \rho_\alpha u_{\alpha i})+\frac{\partial}{\partial xi}(r_\alpha \rho_\alpha u_{\alpha i} u_{\alpha j})=r_\alpha(F_i-\frac{\partial p}{\partial xi})+\frac{\partial}{\partial xj}(\mu_{\alpha eff}\frac{u_{\alpha i}}{\partial xj})+C_{\alpha\beta}(u_{\beta i}-u_{\alpha i})$$

- (5.1)

$$\frac{\partial}{\partial t}(r_\alpha \rho_\alpha u_{\alpha i})+\frac{\partial}{\partial xi}(r_\alpha \rho_\alpha u_{\alpha i} u_{\alpha j})=r_\alpha(F_i-\frac{\partial p}{\partial xi})+\frac{\partial}{\partial xj}(\mu_{\alpha eff}\frac{u_{\alpha i}}{\partial xj})+C_{\alpha\beta}(u_{\beta i}-u_{\alpha i})$$

- (5.2)

where the phases are denoted by α and β, the volume fraction and mean density for each phase are r_α, and ρ_α, directions are labelled by subscripts i and j, mean velocities are denoted by $u_{\alpha i}$, $u_{\beta i}$, $u_{\alpha j}$ and $u_{\beta j}$, distances are given as x_i and x_j, and time is t. The body force is given as F_i, the mean pressure is p and the effective viscosity is written as $\mu_{\alpha eff}$. In equation 5.1 the first term describes the time dependency of the solution. It is necessary to include this term to improve the numerical stability when solving multi-phase flows. The second term in each equation describes the convection of each phase in space. On the right hand side of the momentum equation are the sink terms for the momentum of each phase which include the body force and the pressure gradient. The second term on the right hand side is the momentum lost due to viscous forces.

The third term is the exchange of momentum between the phases, which is a product of the inter-phase momentum coefficient, $C_{\alpha\beta}$ and the difference between the liquid and solid velocities (i.e. the slip velocity). This term defines the drag force (per unit volume of liquid), being exerted on the moving fluid by the solid particles, and the coefficient, $C_{\alpha\beta}$ is calculated as follows :

$$C_{\alpha\beta}=\frac{3}{4}\frac{C_d}{d_p}r_\beta\rho_\alpha(u_{\beta i}-u_{\alpha i}) \qquad \text{- (5.3)}$$

where α and β represent the liquid and solid phases respectively, C_d is the dimensionless drag coefficient, d_p is the mean diameter of the spherical particles and r_β is the volume fraction of the solids phase.

Circular tanks are modelled in two dimensions using cylindrical coordinates, where y is the downward axial direction and r is the radial direction. The geometries of both secondary clarifiers were axially symmetric and it was assumed that the tangential flow was negligible, even though there was turbulent mixing in the inlet zone of the clarifier, and there will be the effects from wind and the rotating bridge scraper. Indeed, it has been stated that due to the high inlet solids concentration, the density driven flow in a secondary clarifier is directed in a longitudinal direction, and swirling flow can be neglected[7]. However, in the Blackburn Meadows clarifier, the presence of the deflector plate induces a free turbulent jet. Three dimensionality is essential to the creation and maintenance of turbulence and the shape of the jet. Therefore, a 3-D simulation of the Blackburn Meadows clarifier was undertaken but unfortunately due to numerical instabilities the solution of the model diverged.

5.2.2 Turbulence model

The inter-phase terms in the two semi-empirical transport equations (Rodi[16]) for k and ϵ, in the standard k-ϵ model, are not usually known for multi-phase flows and hence are ignored. Because there is no standard turbulence model for multi-phase flows, the general form of the single-phase k-ϵ model is applied. For both the liquid and solid phases turbulent flow is assumed and therefore the eddy viscosity hypothesis holds for each turbulent phase, α. Hence molecular and turbulent diffusion of momentum is governed by an effective viscosity :

$$\mu_{\alpha eff}=\mu_{\alpha}+\mu_{t\alpha} \qquad \text{- (5.4)}$$

where the turbulent viscosity, $\mu_{t\alpha}$ is calculated from the turbulent kinetic energy and eddy dissipation :

$$\mu_{t\alpha}=C_{\mu}\rho_{\alpha}\frac{k_{\alpha}^{2}}{\epsilon_{\alpha}}$$

- (5.5)

Standard constants (Celik *et al*)[17] were used in this study : $C_1 = 1.44$, $C_2 = 1.92$, $\sigma_\epsilon = 1.22$, $\sigma_k = 1.0$ and $C_\mu = 0.09$.

5.2.3 Transport of suspended solids

Turbulent dispersion of the volume fraction for phase α is modelled using the eddy diffusivity hypothesis :

$$\frac{\partial}{\partial t}(r_{\alpha}\rho_{\alpha})+\frac{\partial}{\partial xi}(r_{\alpha}\rho_{\alpha}u_{\alpha i}-\Gamma_{\alpha}\frac{\partial r_{\alpha}}{\partial xi})=0$$

- (5.6)

where

$$\Gamma_{\alpha}=\frac{\mu_{t\alpha}}{\sigma_{\alpha}}$$

- (5.7)

In these two equations, Γ_α denotes the turbulent mass diffusion and σ_α is the turbulent Prandtl number of the volume fraction (also known as the turbulent Schmidt number[1]). The turbulent Prandtl number is a dimensionless number, which defines the ratio of the diffusion of the flow properties and the solid particles. Different values are needed in the axial and radial directions, because the anisotropic nature of turbulence causes the turbulent mass diffusion rates to be anisotropic. Experiments by McCorquodale et al[14] have shown that the turbulent Prandtl number can affect a buoyant flow. The concentration gradients for the suspended solids are larger in the vertical direction of a clarifier and they suppress the dispersion of particles between stratified layers, e.g. heavy laden flow is hindered as it encounters less dense flow. Stratification also hinders turbulence and therefore the turbulent mass diffusion of the particles is lower in the vertical direction. Therefore, a higher value for the turbulent Prandtl number is used in the axial direction than in the radial direction. The diffusion of the particles is normally set to be the same as the fluid in the vertical direction because the particles have a negligible effect on turbulence. This is because there is a relatively small density difference between the water and the solids phase; and the particles are small. For sedimentation tanks, the values chosen by other researchers were between 0.5 and 1.0 (Samstag *et al*[5], M^{c}Corquodale *et al*[6], Zhou and M^{c}Corquodale[8], M^{c}Corquodale and Zhou[11] and Lyn *et al*[18]). Values of 1.0 and 0.5 were chosen for the axial and radial turbulent Prandtl numbers in this work.

5.2.4 Drag coefficient

The drag force exerted on a moving Newtonian, incompressible fluid (phase α), by a solid particle is expressed in terms of a non-dimensional drag coefficient, C_d which depends on the relative Reynolds number, Re, as follows :

$$Re = \frac{\rho_\alpha u_{slip} d_p}{\mu_\alpha}$$

- (5.8)

The flow is split into two directions in the circular clarifier, i.e. axially and radially. The difference in velocity between the phases (i.e. the slip velocity) is calculated separately in each direction and is by default found directly from the conservation of momentum (5.2). The slip velocity is used to calculate the relative Reynolds number and the drag coefficient in each direction. However, in this work the slip velocity in the axial direction was substituted in equation 5.8 by the average settling velocity of the particles, V_s, which was determined from measurements taken in a settling column. The slip velocity in the radial direction was calculated from the momentum conservation equation. Therefore, the axial drag coefficient, C_d was found directly from the particle settling velocity. The inter-phase momentum transfer coefficient, $C_{\alpha\beta}$ is found from the directional drag coefficient and multiplied by the slip velocity calculated from the momentum conservation equation to give the total drag force.

The particles are assumed to have a spherical shape and can be represented by their mean diameter. If a particle size distribution is modelled then an additional

dispersed phase is needed for each of the discrete particle sizes. The model was however simplified to a mean particle size to make considerable savings in the computational effort. The relationship between the drag coefficient and the Reynolds number can be split into three distinct regions, i.e. the Stoke's or laminar regime ($0 < Re < 0.2$),

$$C_d = \frac{24}{Re} \qquad \text{- (5.9)}$$

the Allens, viscous or transitional regime ($0.2 < Re < 500$),

$$C_d = \frac{24}{Re}(1 + 0.15Re^{0.687}) \qquad \text{- (5.10)}$$

and the Newton or turbulent regime ($Re > 500$) : $C_d = 0.44$. Super critical fluids at higher Reynolds numbers are not present in sedimentation tanks. The radial drag coefficient was calculated, for all sub-critical Reynolds numbers, from the following equation :

$$C_d = \frac{24}{Re} + \frac{5.48}{Re^{0.573}} + 0.36 \qquad \text{- (5.11)}$$

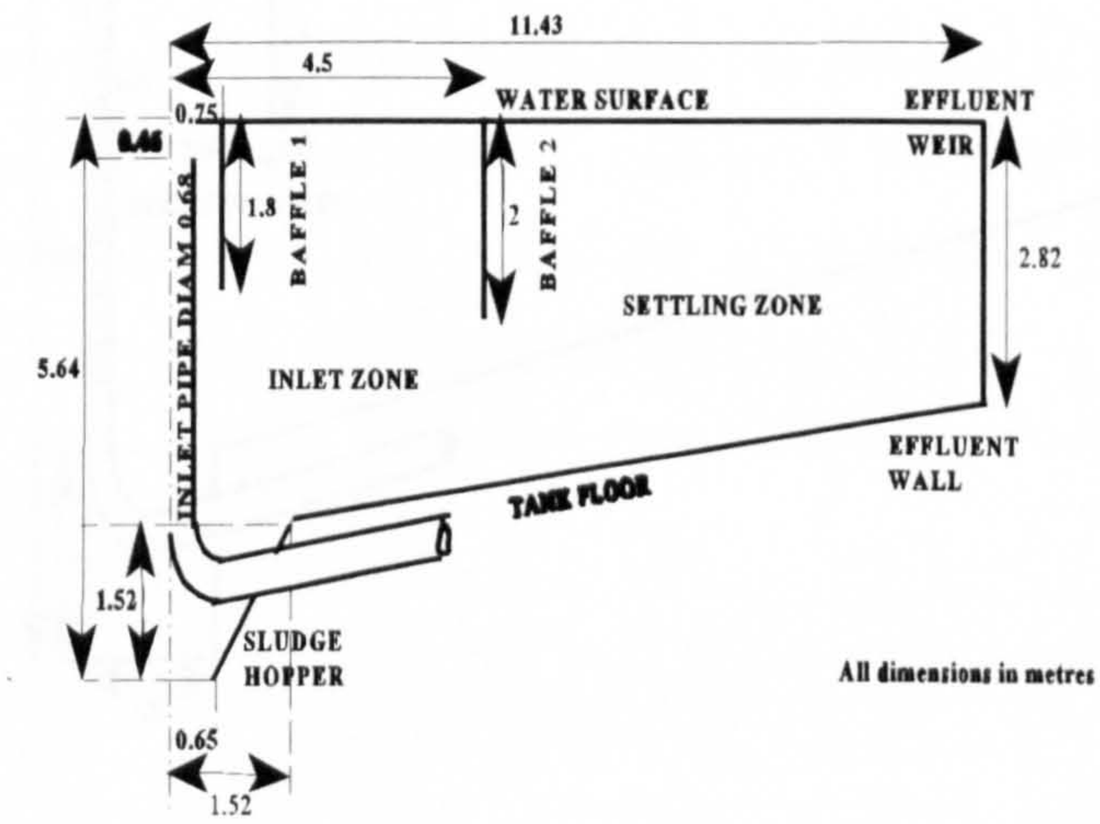

Figure 5.1a Tank dimensions of the cross section of the Copley clarifier.

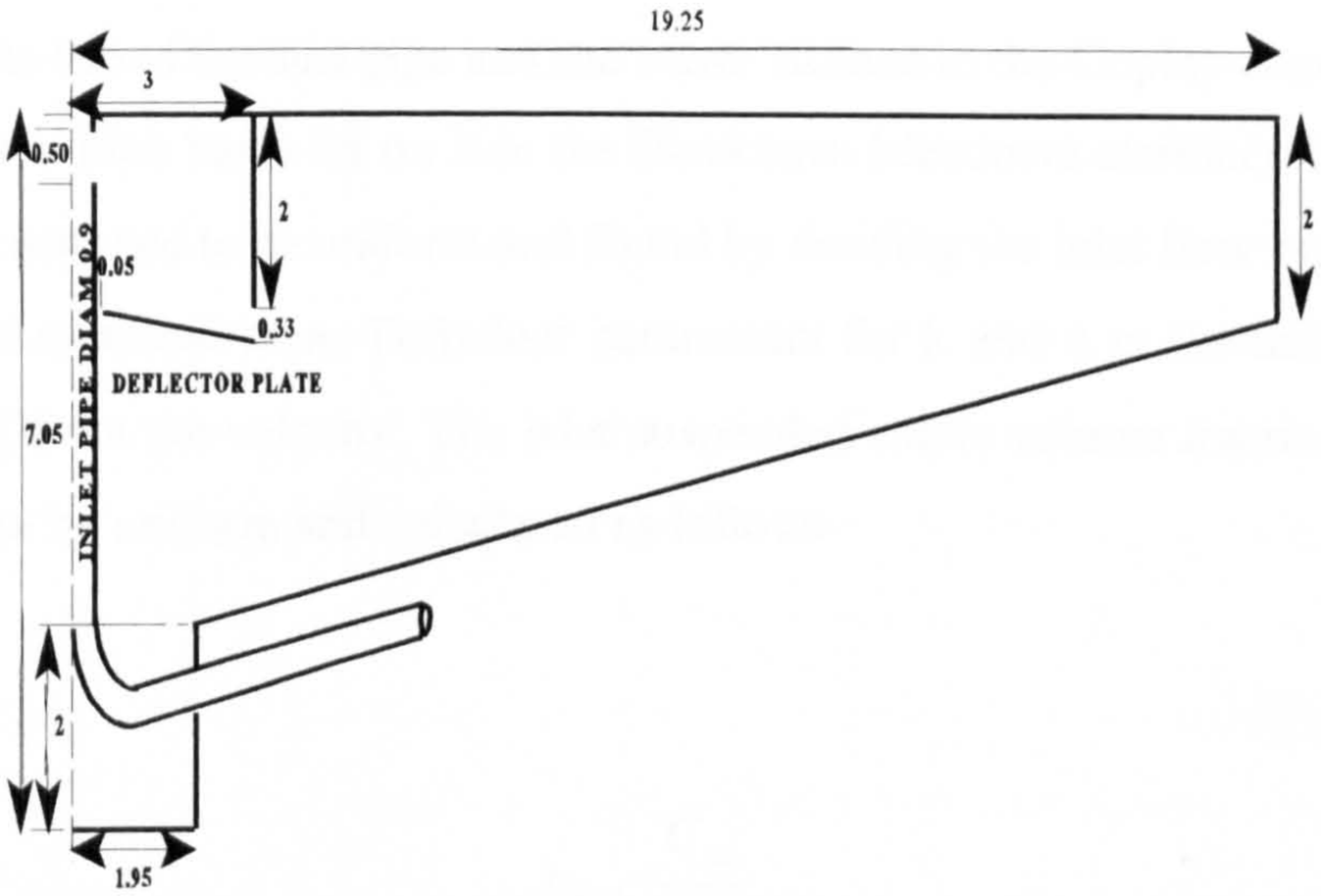

Figure 5.1b Tank dimensions of the cross section of the Blackburn Meadows clarifier

5.2.5 Boundary conditions

The boundary conditions in the computational fluid dynamics programme, CFX-F3D were unmodified. The flow domain in a circular secondary sedimentation tank is bounded by the flow inlet, water surface, two flow outlets and wall boundaries to represent the inlet pipe wall, tank bottom, effluent wall, baffle and deflector plate (Figures 5.1a and 5.1b). The deflector plate in the Blackburn Meadows clarifier is positioned at an angle of 6°, with a gap to the inlet pipe wall and a gap to the bottom of the baffle. The horizontal influent flow is positioned between the top of the inlet pipe and the water surface in the Copley clarifier (the vertical inlet pipe has a lid on it in the Blackburn Meadows clarifier). The inlet velocity is assumed to be uniform and found by dividing the inlet flow rate by the inlet cross sectional area. Turbulent parameters for k and ϵ in the influent are calculated from the velocity. The inlet suspended solids volume fraction is also assumed to be uniform and calculated as follows :

$$r_{\beta inl} = \frac{C_{inl}}{\rho_{\beta}} \qquad \text{- (5.12)}$$

$$r_{\alpha inl} = 1 - r_{\beta inl} \qquad \text{- (5.13)}$$

where $r_{\beta inl}$ and $r_{\alpha inl}$ denote the volume fraction of the solids phase and the liquid phase respectively for the influent, C_{inl} is the suspended solids concentration of the influent and ρ_β is the mean density of the particles. The sum of the inlet volume fractions of the liquid and solid phases must be equal to 1. One cell between the top of the effluent wall and the liquid surface represents the effluent flow boundary and the RAS flow boundary is across the floor of the sludge hopper (Figure 5.1). Mass flow boundaries are used to define the outlets, where the sum of the liquid and solid mass flow rates leaving the clarifier must be equal to that entering the clarifier, to satisfy mass conservation. The ratio of the total mass flow rate in an outlet compared to the inlet is specified, and the sum of the ratios in all the outlets must be equal to 1. The total mass flow rate in the outlet is corrected every iteration to satisfy mass conservation. The mass flow rates of each phase are divided by their densities to give their volumetric flow rates. The sum of the volumetric flow rates are divided by the cross sectional area of the outlet to give the total velocity. Volume fractions of each phase in an outlet are calculated from the values in the adjacent cells upstream to determine the velocities of each phase. In the outlets the velocity normal to the main flow direction is set to zero and the outflow conditions for k and ϵ are extrapolated from near-outlet values. The boundary conditions of each phase on a wall boundary are the same as those used for the single-phase flow model in Chapter 4[19]. A symmetry plane was used again for the boundary condition at the water surface and the gradients for the volume fraction of each phase are therefore zero across the water surface. The boundary conditions are discussed in Appendix B.

5.3 NUMERICAL METHOD

5.3.1 Numerical scheme

The numerical methods are found in the CFD program, CFX-F3D. Numerical grids (Figures 5.2a and 5.2b) of the clarifiers compute the flow variables in the cell centres and interpolate them to the nearby cell nodes. To define the Copley clarifier, a two dimensional grid was used containing 5800 cells, which was similar to the grid used for the humus tank (see Chapter 4). A number of different sized grids were compared for the Blackburn Meadows clarifier (i.e. 1383, 2405, 3499, 5607, 6148, 9335, 12642 and 17201 cells) to find out the dependency of the flow pattern on the grid size. Moreover, they were used to find out whether more cells around the deflector plate would improve the modelling of the turbulent jet.

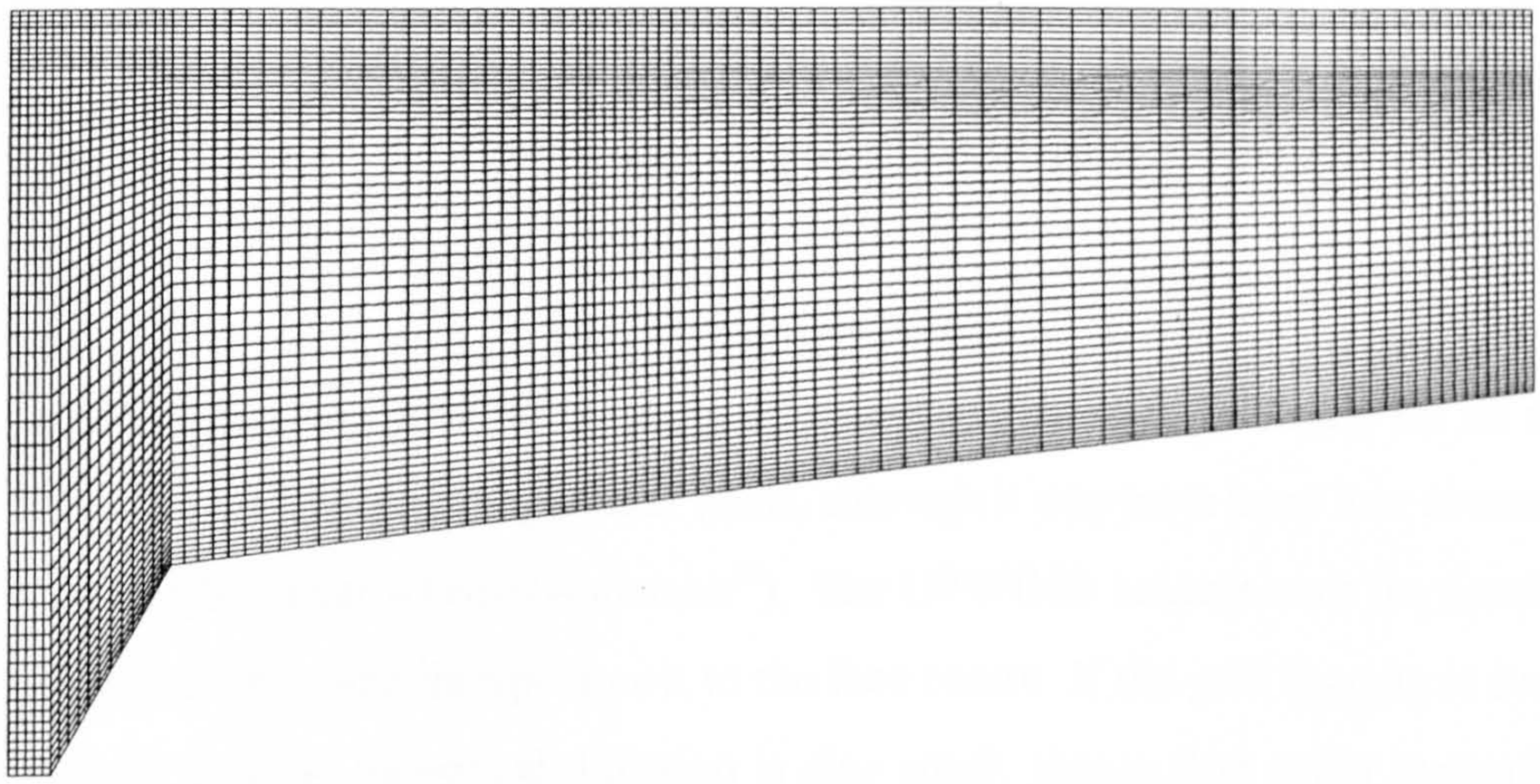

Figure 5.2a Computational grid of the Copley clarifier.

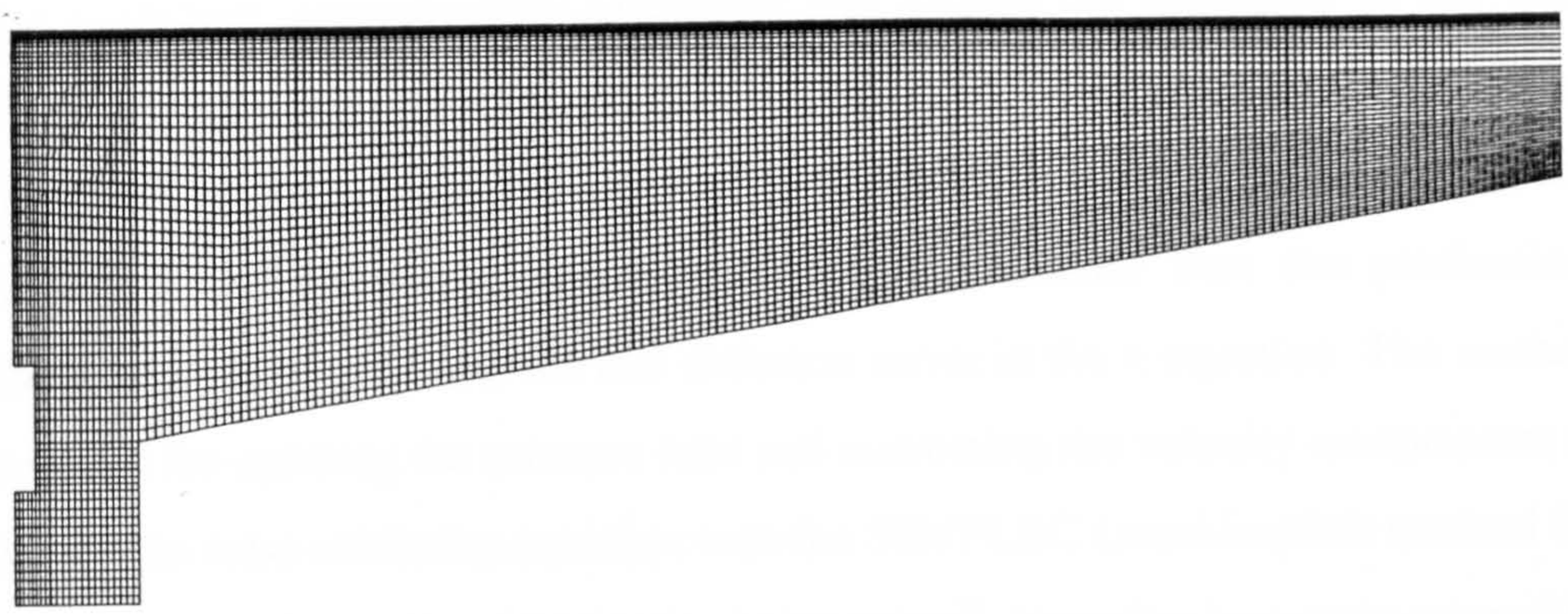

Figure 5.2b Computational grid of the Blackburn Meadows clarifier.

A first order numerical differencing scheme was chosen (UPWIND) for all the equations, to keep the computation stable, although it may have been less accurate than a higher order scheme (Anderson[20]). The UPWIND scheme uses the upwind cell centre value and interpolates it to the face centre. If the grid spacing is small enough and the numerical diffusion is also small, then a first order numerical differencing scheme may be accurate enough. The default differencing scheme in the program CFX-F3D that is used to model the convective terms of all transport equations is HYBRID. However, it has been reported in the literature that the

HYBRID scheme is numerically diffuse[6]. UPWIND has been recommended for calculating the density and the volume fraction in the multi-fluid model.

Misalignment of the cells with the flow path can cause numerical (false) diffusion, however this error should be smaller using quadrilateral cells than triangular cells. Nevertheless, a very small value of the eddy dissipation and a very high value of the turbulent viscosity was calculated and caused the instability of the axial velocity calculation. This problem was overcome by omitting the cross-derivative terms in the k and ϵ equations (referred to as 'deferred correction' in the program CFX-F3D). These terms were anyhow, much smaller than the production, dissipation, advection and normal diffusion terms in the ϵ equation. The method selected for updating the pressure field and correcting the velocity components to satisfy the mass continuity equation was the SIMPLEC (semi-implicit method for pressure-linked equations correction) algorithm[20]. Negative buoyancy caused by the higher density of the solids phase was another cause for the instability of the axial velocity calculation. For the clarifier without the deflector plate, low values were used for the under-relaxation factors of the axial and radial velocities. The under-relaxation equation is as follows :

$$\phi = \alpha\phi(new) + (1-\alpha)\phi(old) \qquad \text{- (5.13)}$$

where ϕ denotes the variable and α is the under-relaxation factor. False time steps of 0.05 and 0.02 seconds were used to compute the axial and radial velocities in the Blackburn Meadows clarifier, because even with very low under-relaxation

factors (0.02) the model was numerically unstable. This was caused by the high velocity gradients around the deflector plate, because of the presence of the turbulent jet. Time dependent simulations were undertaken for both secondary clarifiers, using a small initial time step (0.1 seconds) to keep the solution stable, then an incremental increase to a larger time step (1200 s), and thereafter kept constant. For each time step there were 40 iterations for the pressure-correction equation. The residuals of each variable were monitored every time step and a converged solution was based on all the residuals falling below 0.001. A steady-state solids concentration distribution in the clarifier was based on the solids volume fraction residual reaching a low enough value which was also at steady-state (~ 1e-06).

Experimental measurements of the inlet suspended solids concentration and the flow rates of the influent, effluent and RAS were entered into the model. The models prediction of the effluent solids concentration was compared to the average daily measurement. The mean particle diameter was difficult to measure in an experiment, because although the particles in the numerical model were spherical, in reality they formed flocs with irregular shapes. It was also difficult to find a reliable value for the particle diameter in the literature because of the different experimental methods reported. Therefore, different values of the particle diameter were tested in the model until there was agreement between the predicted and measured effluent solids concentration. This meant that the effluent solids concentration was really being used as an input to the model in order to predict the particle diameter.

The theoretical RAS solids concentration was calculated, using the following solids mass balance on the clarifier which contains only experimental measurements :

$$C_{RAS}=\frac{Q_{inl}C_{inl}-Q_{eff}C_{eff}}{Q_{RAS}} \qquad \text{- (5.14)}$$

where the flow rates and suspended solids concentrations of the influent, effluent and RAS were denoted by Q_{inl}, Q_{eff}, Q_{RAS}, C_{inl} C_{eff} and C_{RAS} respectively. The predicted, theoretical and measured RAS solids concentrations were compared, to test the accuracy and solids mass conservation of the model. The predicted and measured levels of the sludge blanket were also compared.

In most biological reactors prior to the secondary clarifier, tissue cells are produced and need to be wasted because they increase the BOD of the effluent (Figure 3.1). Sludge is either wasted directly from the biological reactor or as a fraction of the settled sludge coming from the bottom of the secondary clarifier. The remaining portion of the settled sludge is returned back to the inlet of the biological reactor or to the secondary clarifier and is normally referred to as return activated sludge (RAS). It was assumed that there was no cell production in the secondary clarifier and that the portion of settled sludge that was wasted was negligible. The sludge coming from the bottom of the clarifier is normally referred to as secondary sludge. However, in this case it is more convenient to refer to it as RAS, when none of it is portioned of as waste sludge.

5.3.2 Physical properties

Standard properties of the density and viscosity of water, at 20 °C and 1 atmospheric pressure were used for the liquid phase. The dry solids density of activated sludge flocs have been reported in other CFD models of secondary clarifiers, e.g. 1300 kg/m^3 by Samstag *et al*[5] and M^{c}Corquodale *et al*[10]; and 1240 to 1650 kg/m^3 in the experiments reported in the literature[5,12,21-25]. The median solids density (1450 kg/m^3) was taken from the experimental literature. It was assumed that an activated sludge floc has an equivalent diameter of a spherical particle and the same density as the sphere.

The molecular viscosity of the solids phase is not easily found, yet a value for it is required in the multi-fluid model. Fluids deform continuously under the action of a shear stress but solids can resist shear stress in a static condition. Consequently, the proportionality factor for a viscous fluid is the viscosity and for a solid it is the shear modulus. Without knowing the value of the solids viscosity, a much lower value (0.000001 kg/ms) than the viscosity of water was chosen. Therefore, in the calculation of the effective viscosity (equation 5.4) the molecular viscosity of the particles should be ignored.

5.3.3 Residence time distribution

The residence time distribution (RTD) of the effluent and RAS were found from a steady-state flow solution. An inert massless numerical scalar was released into the inlet of the clarifier. The concentration of the scalar in the liquid phase was monitored above the effluent weir and at the bottom of the sludge hopper for 3 nominal residence times. Fluid flow was not solved, so that the residence time of the scalar could be calculated from a steady-state velocity pattern. A constant time

step was used to match the sampling rate of the experimental data (5 and 10 minutes respectively for the Blackburn Meadows and Copley clarifiers). The concentration curves for the experimental tracer were extrapolated to 3 nominal residence times. The normalisation method (see Appendix C) was applied to the numerical and experimental concentration curves to derive their RTD's. The RTD's were plotted as graphs of dimensionless time against dimensionless concentration[19]. The dimensionless time is the elapsed time divided by the nominal residence time (i.e. the volume of the tank divided by the flow rate of the effluent or RAS). It was checked how much of the numerical scalar and experimental tracer had reached the effluent and RAS outlets in 3 nominal residence times. A mass balance was carried out on both of the secondary clarifiers to determine how much scalar and tracer had passed to the effluent channel and the RAS distribution box (see Table 5.2 and Appendix C). Therefore, by integrating under the area of the RTD curve it was possible to find the mean residence time of the scalar and tracer in each of the outlets (i.e. the time for 50% of the cumulative area under the curve). The predicted and measured RTD's were compared for both the effluent and the return activated sludge.

5.4 EXPERIMENTAL METHOD

Data was collected at the wastewater treatment sites for comparison with the numerical model, as follows :

5.4.1 Residence time distribution

A solution of lithium chloride was dosed as a pulse to the inlet distribution chamber upstream of the secondary clarifiers and the salt concentrations in the effluent channel and the RAS distribution box were monitored. The same testing method was used on the full-scale circular humus tank (Chapter 4 and Appendix C).

5.4.2 Suspended solids concentration

Wastewater samples were taken of the influent over the inlet weir upstream of the clarifier, the effluent in the weir channel and the RAS in the distribution box downstream of the clarifier (Figure C2 in Appendix C). Suspended solids concentrations of the influent, effluent and return activated sludge were measured at time intervals during the salt tracer test, using a standard technique[26] with gravimetric filter paper, and the average daily suspended solids concentration was calculated. Sludge blanket detectors were used to measure the solids concentration contours within the clarifiers, and these were calibrated by lowering them into samples of wastewater which had known suspended solids concentrations. The detectors were subsequently lowered into the full-scale tanks, to measure the water depth and radial position at the calibrated solids concentration (i.e. 865 mg/l and 600 mg/l in the Copley and Blackburn Meadows clarifiers respectively).

5.4.3 Settling velocity of suspension

A double-exponential equation is the best relationship between the average settling velocity of the suspension and the suspended solids concentration[1,5,6,8-11,27-28]:

$$V_s = V_0[e^{-K(C-C_{min})} - e^{-K_1(C-C_{min})}] \quad \text{- (5.15)}$$

where K denotes the floc settling parameter, K_1 is the colloids settling parameter, V_o is the free (or Stoke's) settling velocity, C is the suspended solids concentration and C_{min} is the concentration of poorly settling particles (0.002 times the inlet solids concentration). A settling column test was carried out on wastewater samples taken from the secondary clarifiers and the settling velocity distribution (SVD) was found, by a standard method outlined in a report by White[29]. Because the settling velocities at low solids concentrations were difficult to measure, it was assumed that the maximum settling velocity (i.e. the transition from flocculent to hindered settling) occurred at a concentration of 500 mg/l[26], in order to derive the colloids settling parameter. The measured settling velocity of the solids suspension was substituted for the difference between the downward velocity of the fluid and the particles, in order to calculate the source term for inter-phase momentum transfer. Therefore, the double exponential settling velocity equation above was substituted for the slip velocity in the axial direction only of the circular secondary clarifier. Experimental conditions and numerical parameters are summarised in Table 5.1.

Table 5.1 Experimental conditions and numerical parameters.

Case	A	B Copley	C	D Blackburn	E
Tank volume,m^3		1365		3665	
Inlet flow, m^3/hr	435	702	677	2552	1959
RAS flow, m^3/hr	213	213	213	796	747
Effluent flow, m^3/hr	222	489	464	1756	1212
Surface overflow rate, m^3/m^2d	13	34	32	37	26
Mean residence time RAS, min	385	385	385	276	295
Mean residence time effluent, min	369	167	177	125	182
Time lag from salt dosage, min	2.0	1.25	1.25	0.5	0.75
Time lag from flow meas, min	3	2	2	1.5	1.3
Time lag to RAS, min	1.0	1.0	1.0	0.4	0.5
Inlet solids concentration, mg/l	2260	1700	1700	2790	2949
Stoke's velocity, m/hr	9.73	9.73	9.73	12.64	12.64
Colloids settling parameter, m^3/kg	4.2	4.2	4.2	4.8	4.8
Floc settling parameter, m^3/kg	0.703	0.703	0.703	0.600	0.600
Fluid density, kg/m^3	Fluid viscosity, kg/m^3	Solids density, kg/m^3	Solids viscosity kg/ms	Axial turbulent Prandtl number	Radial turbulent Prandtl number
998	0.001	1450	0.00001	1.0	0.5

5.5 RESULTS

5.5.1 Settlement tests

The equation (5.15) for the settling velocity distribution of the wastewater in both secondary clarifiers agreed with the measurements taken at high suspended solids concentrations (Figure 5.3). However, the settling velocity measurements taken at low solids concentrations (from the Blackburn Meadows clarifier) were higher than the settling velocity model, because it had been difficult to observe the settling of smaller particles. The derived values for K, K_1 and V_0 were 0.703 m^3/kg, 4.2 m^3/kg and 9.73 m/hr for the Copley clarifier and 0.600 m^3/kg, 4.8 m^3/kg and 12.64 m/hr for the Blackburn Meadows clarifier.

5.5.2 Flow patterns

For the small baffle radius in the Copley clarifier (case A), the influent was deflected sharply downwards upon impingement with the baffle (Figure 5.4a). The downward flow was attached to the baffle and the inlet pipe. It formed a radially outwards current which moved upwards under the lip of the baffle because of buoyancy. The radial current decreased in velocity because of the increasing tank area and split on the effluent wall, to form an upward flow and a strong return current along the sloping tank floor. The upwards flow near the effluent wall split to form an inward return flow and the effluent discharge. The return current on the floor of the clarifier was caused by the removal of sludge in the hopper.

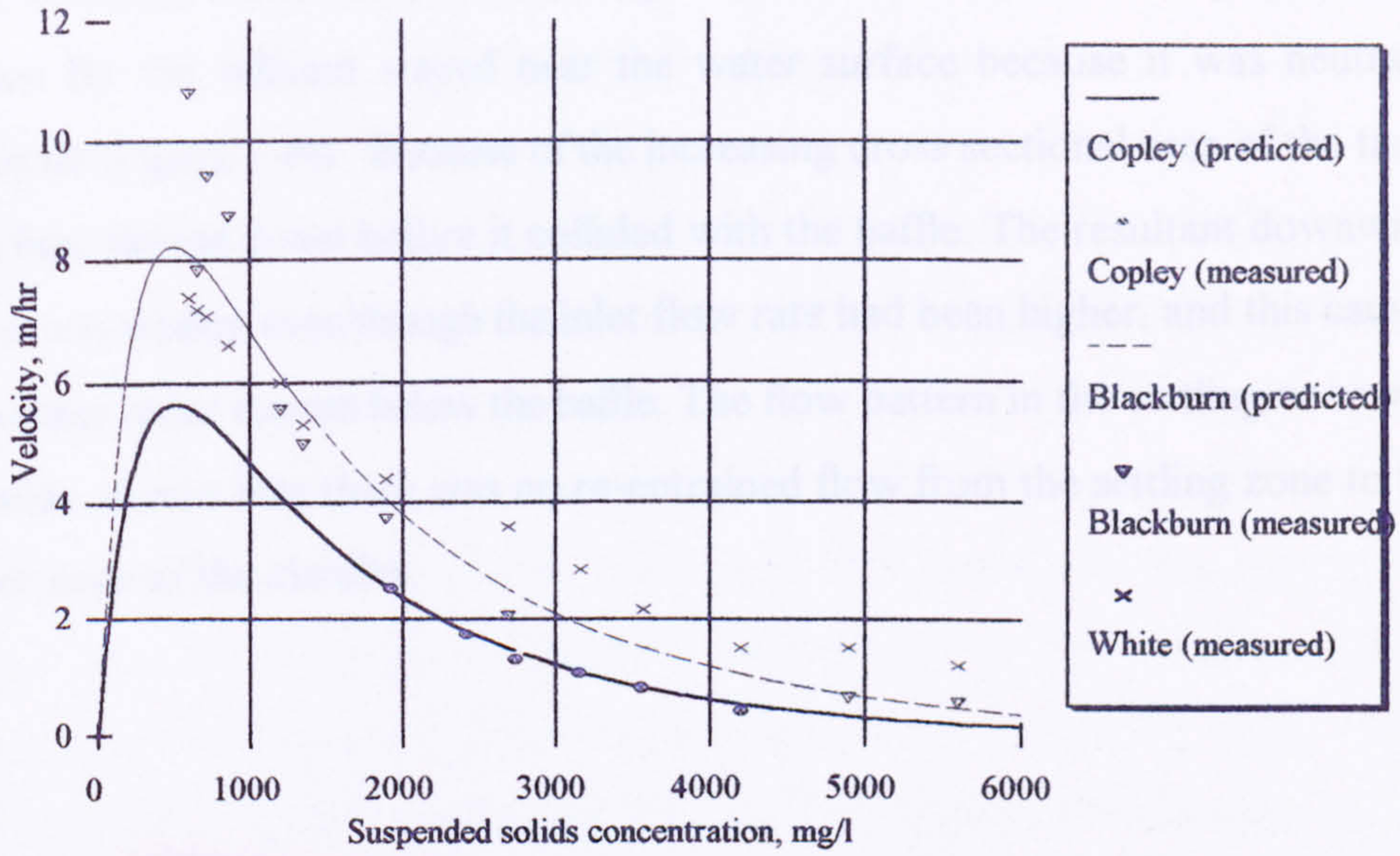

Figure 5.3 Settling velocity distributions of the solids suspension in the Copley and Blackburn Meadows clarifiers.

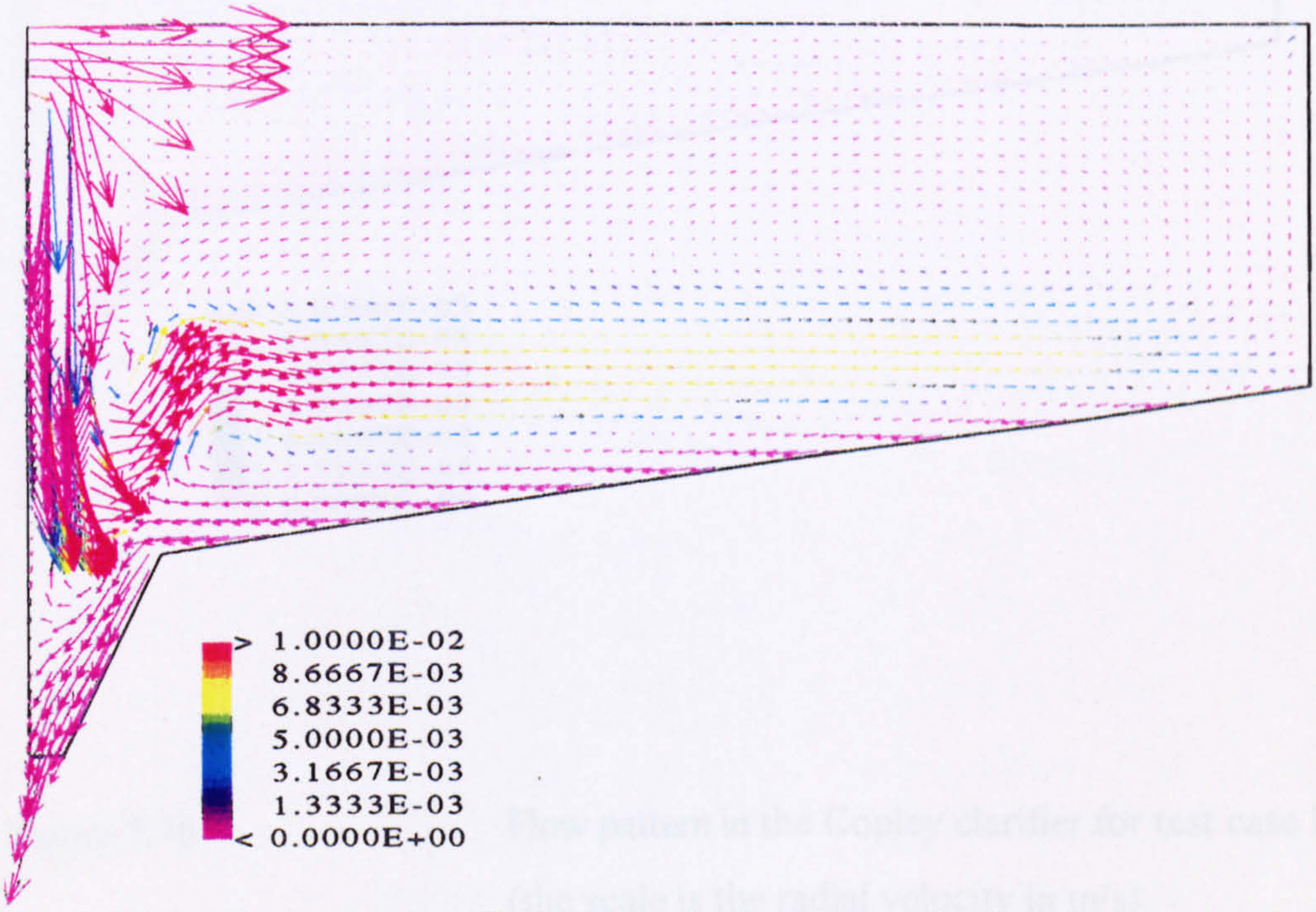

Figure 5.4a Flow pattern in the Copley clarifier for test case A (the scale is the radial velocity in m/s).

For the large baffle radius and the highest inlet flow rate to the Copley clarifier (case B), the influent stayed near the water surface because it was neutrally buoyant (Figure 5.4b). Because of the increasing cross sectional area of the tank, the flow slowed down before it collided with the baffle. The resultant downward flow was weaker even though the inlet flow rate had been higher, and this caused a weaker radial current below the baffle. The flow pattern in the settling zone was similar, except that there was no re-entrained flow from the settling zone to the inlet zone of the clarifier.

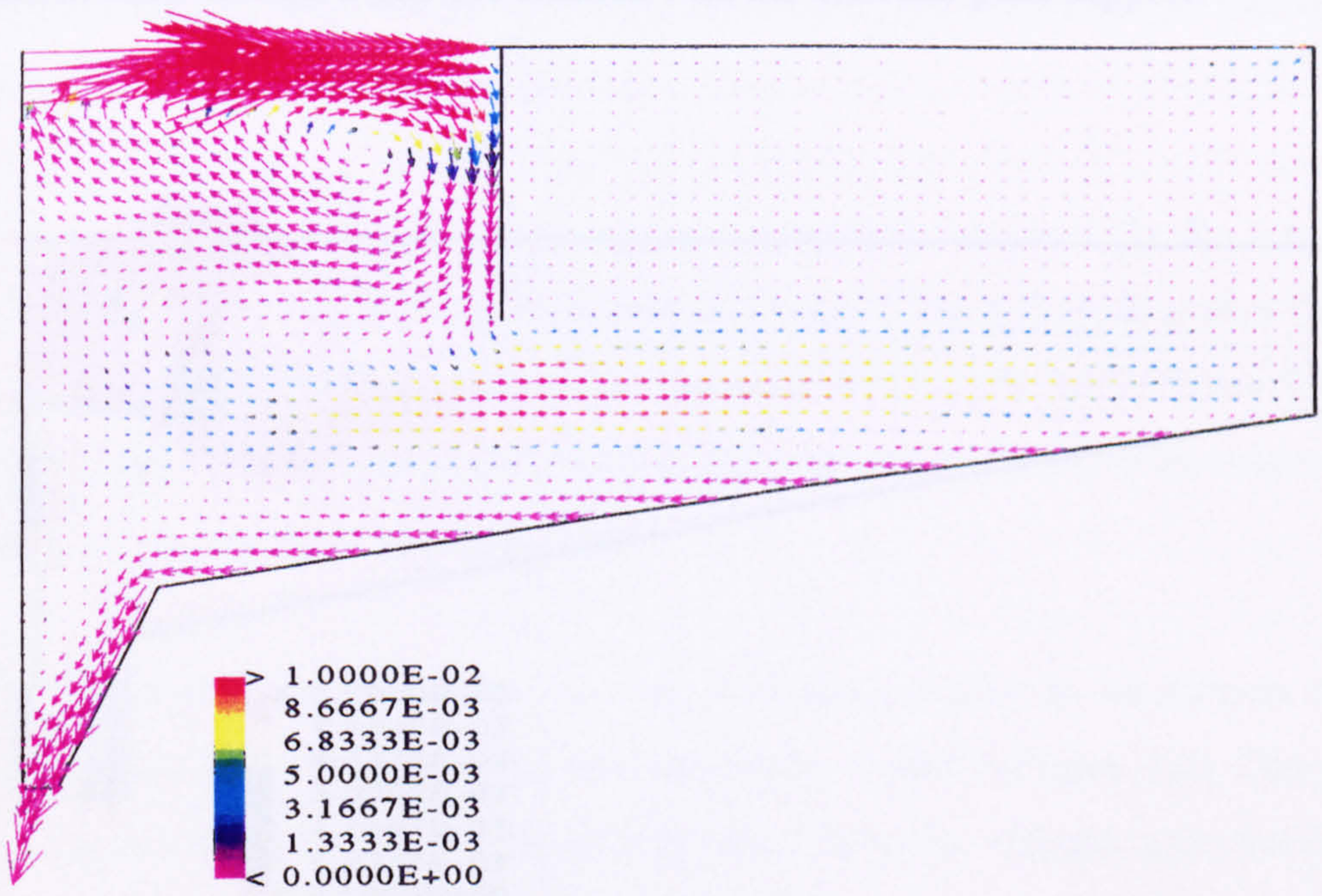

Figure 5.4b Flow pattern in the Copley clarifier for test case B (the scale is the radial velocity in m/s).

For the higher flow rate to the Blackburn Meadows clarifier (case D), the influent stream collided with the baffle to form a downward flow (Figure 5.5). The flow split upon impact with the deflector plate, and was accelerated through the gap between the baffle and the plate. A radial velocity jet was observed in the settling zone of the clarifier. The jet moved slightly upwards because of its buoyancy and slowed down, because of the increasing cross sectional area of the tank and the increasing width of the jet. The velocities in the settling zone were higher than the Copley clarifier and there was also re-entrained flow from the settling zone to the inlet zone. The return radial current in the inlet zone split on the inlet pipe, to form an upward flow towards the inlet aperture and a downward flow, which accelerated through a gap and collided with the deflector plate support.

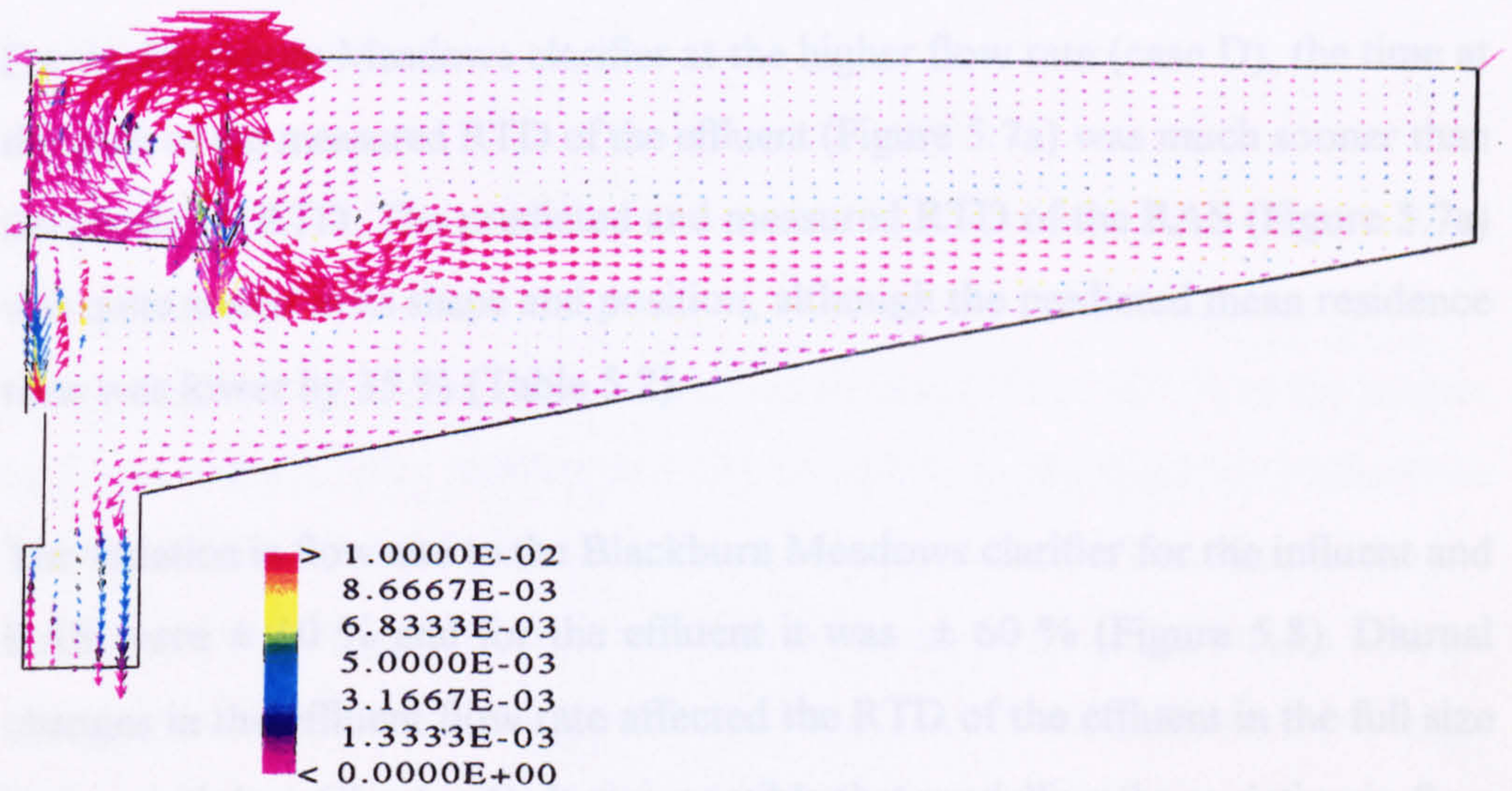

Figure 5.5 Flow pattern in the Blackburn Meadows clarifier for test case D (the scale is the radial velocity in m/s).

5.5.3 Residence time distribution

For the Copley clarifier with the small baffle radius (test case A), there was good agreement between the predicted and measured RTD's of the effluent (Figure 5.6a). However, the model under-predicted the mean residence time of the RAS (Table 5.2). For the large baffle radius (test cases B and C), the shape and position of the predicted and measured RTD's of the effluent were quite similar (Figures 5.6b and 5.6c). In all the test cases the mean residence time of the effluent was quite well predicted by the model (1 to 6 % error) but the residence time of the RAS was underpredicted by up to 41 %. The exception was in test case B, where the model was within 4% of the experimental mean residence times for both the effluent and the RAS (Table 5.2).

For the Blackburn Meadows clarifier at the higher flow rate (case D), the time at the peak of the measured RTD of the effluent (Figure 5.7a) was much sooner than the predicted RTD. The predicted and measured RTD of the RAS (Figure 5.7a) was quite similar in its shape and position, although the predicted mean residence time was lower by 35 % (Table 5.2).

The variation in flow rate to the Blackburn Meadows clarifier for the influent and RAS were ± 10 % and for the effluent it was ± 60 % (Figure 5.8). Diurnal changes in the effluent flow rate affected the RTD of the effluent in the full size humus tank (see Chapter 4). It was possible that modelling the variation in flow rate of the effluent would improve the prediction of the RTD of the effluent. Therefore, the real plant flow rates of the influent, effluent and RAS (Figure 5.8) were simulated for case D. The large variations in flow required a small numerical time step to resolve the transient nature of the flow patterns. Even though a small time step of 0.1 seconds was used, the residual of the axial velocity of the solids

phase would not go below 0.05, and so numerical convergence was not achieved. The convergence difficulties were associated with trying to resolve a transient flow field within a multi-phase flow. It had been even difficult to solve a multi-phase flow in steady-state conditions. For test case E at the lower flow rate, the difference between the predicted and experimental RTD of the effluent (Figure 5.7b) was even larger, although the positions of the RTD's of the RAS were closer together than in case D.

These results suggested that the model under-predicted the mean flow velocities towards the effluent in the Blackburn Meadows clarifier and was unable to model the turbulent jet in the clarifier. The model was able to predict the velocities to the effluent in the Copley clarifier. However, the velocities between the inlet and RAS outflow were too high in the numerical model for both the secondary clarifiers (except in case B).

The mass balance carried out on the numerical scalar showed that 109 % of the scalar had left the clarifier in 3 nominal residence times for test case B (Table C1 in Appendix C). For the chemical tracer experiments, 97 to 107 % of the lithium chloride in the Copley clarifier and 151 to 132 % in the Blackburn Meadows clarifier had left the outlets in 3 nominal residence times. These figures for the chemical tracer suggested that there was either an error with the mass balance calculation or the laboratory measurements of lithium chloride were too high. These errors were quite small for the Copley clarifier (+7%) but the mass of lithium chloride measured in the effluent and RAS were much higher than expected in the Blackburn Meadows clarifier. Indeed, these measurements should be repeated or the quantities 'modified' before comparing them to the models predictions. However, this would not help the models over-prediction of the residence time of the effluent in the Blackburn Meadows clarifier.

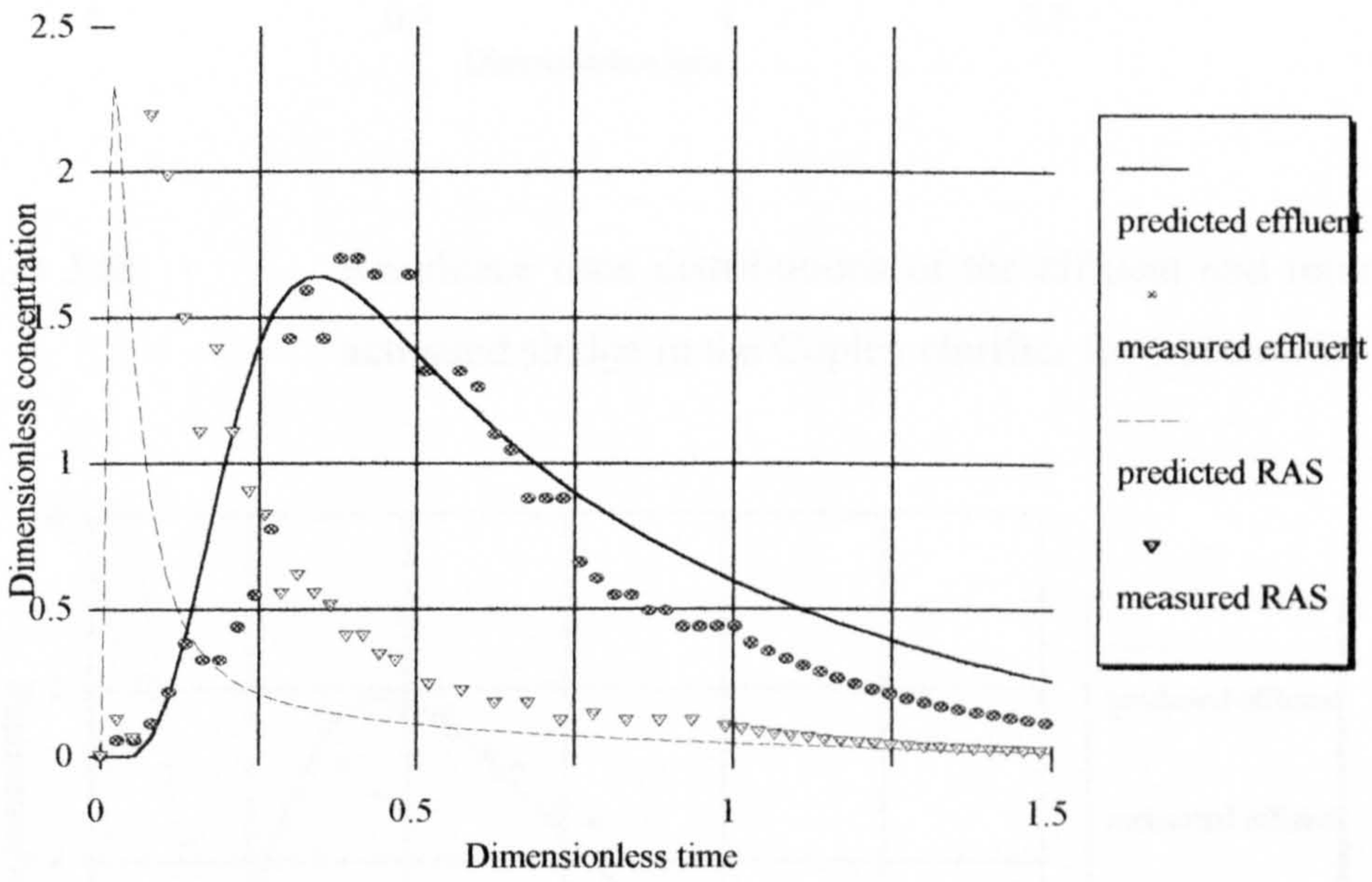

Figure 5.6a Residence time distributions of the effluent and return activated sludge in the Copley clarifier for test case A.

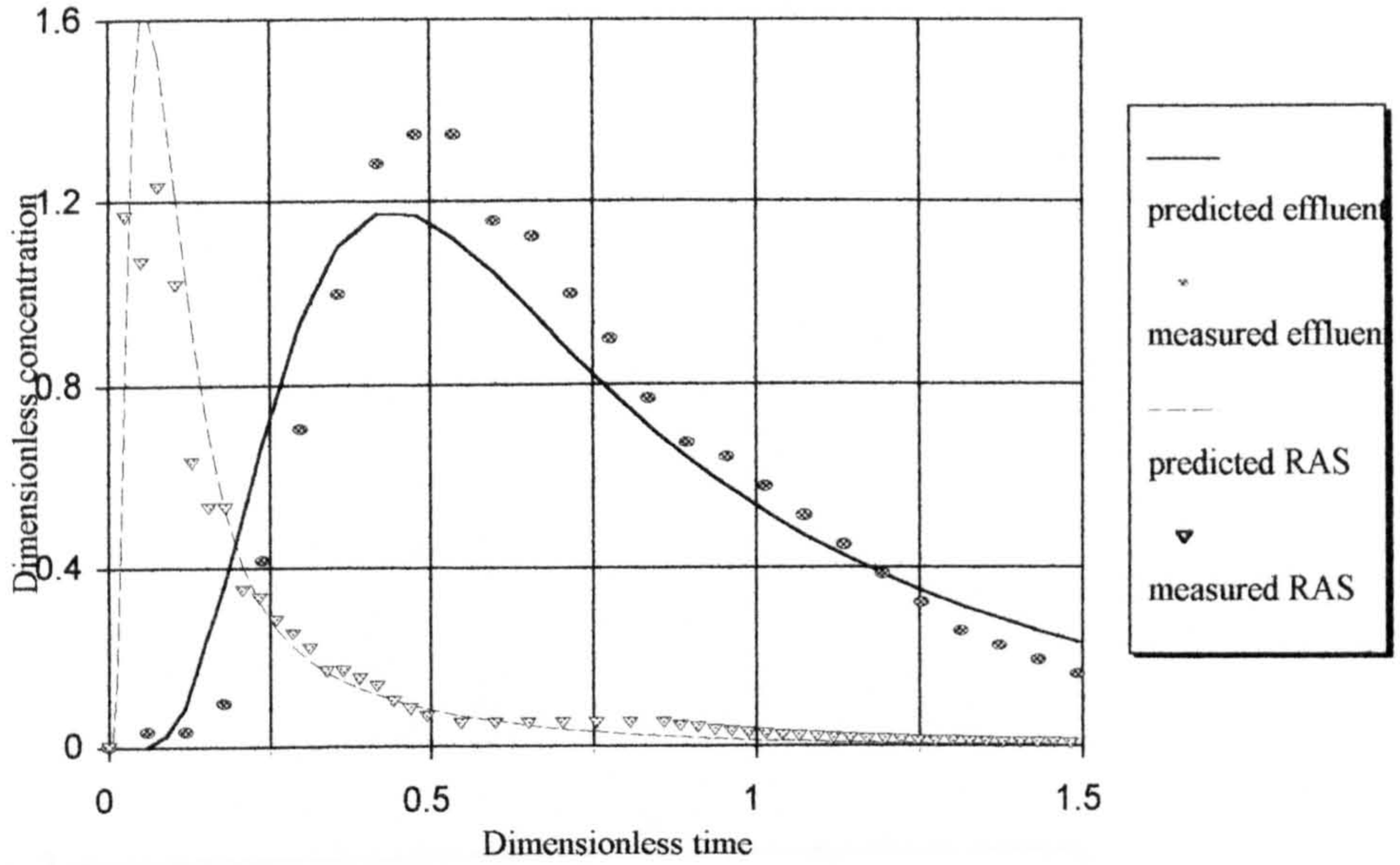

Figure 5.6b Residence time distributions of the effluent and return activated sludge in the Copley clarifier for test case B.

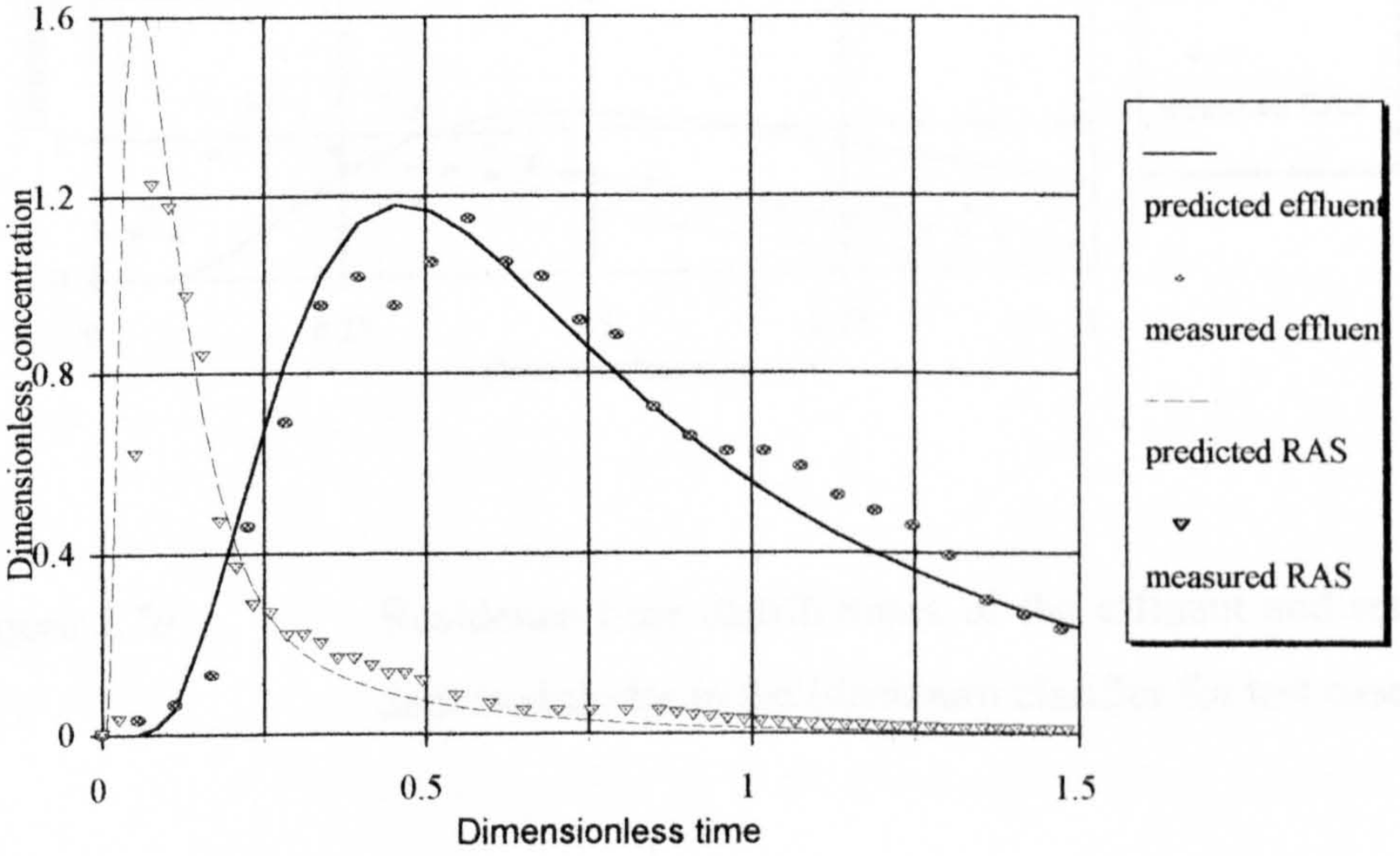

Figure 5.6c Residence time distributions of the effluent and return activated sludge in the Copley clarifier for test case C.

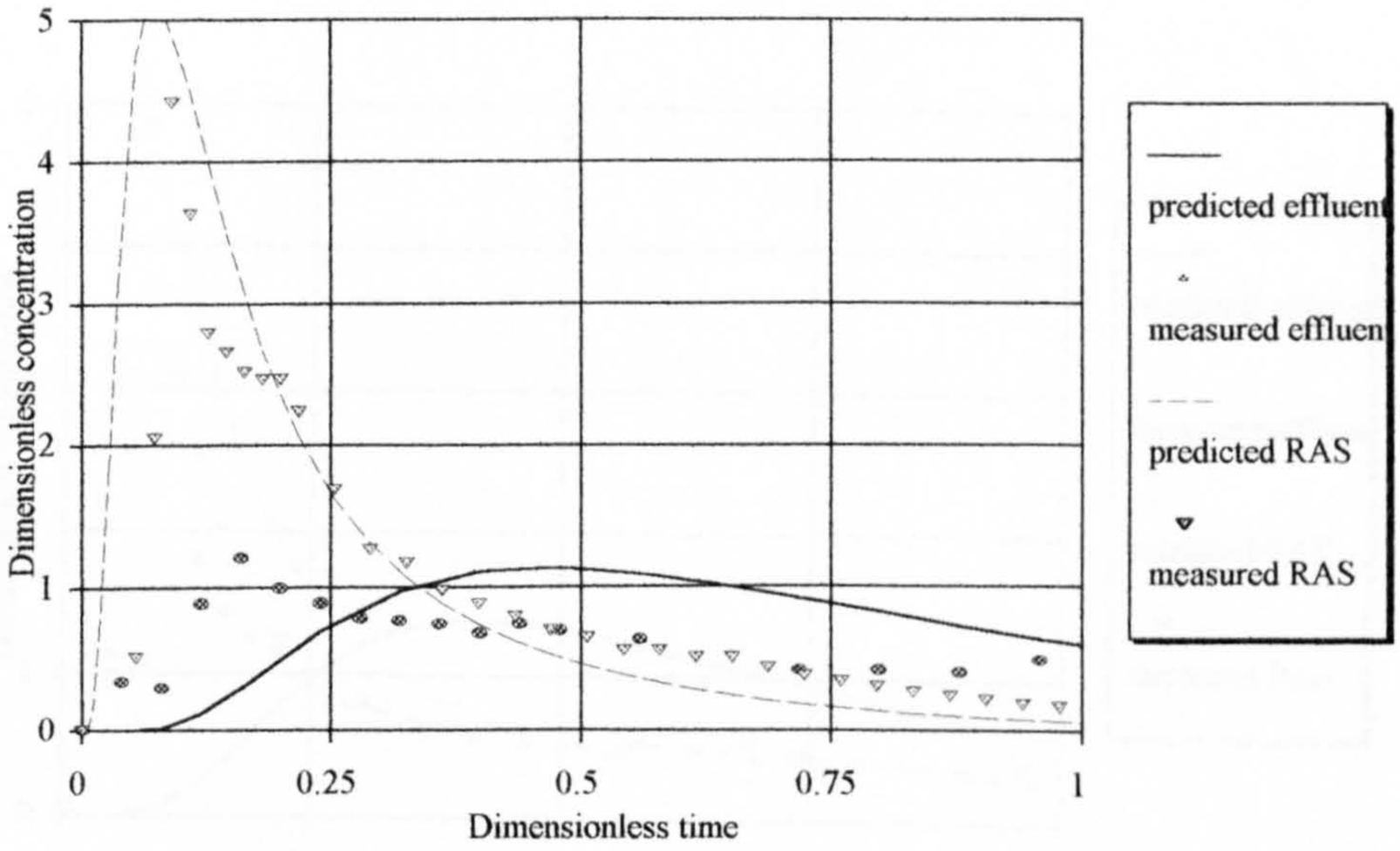

Figure 5.7a Residence time distributions of the effluent and return activated sludge in the Blackburn clarifier for test case D.

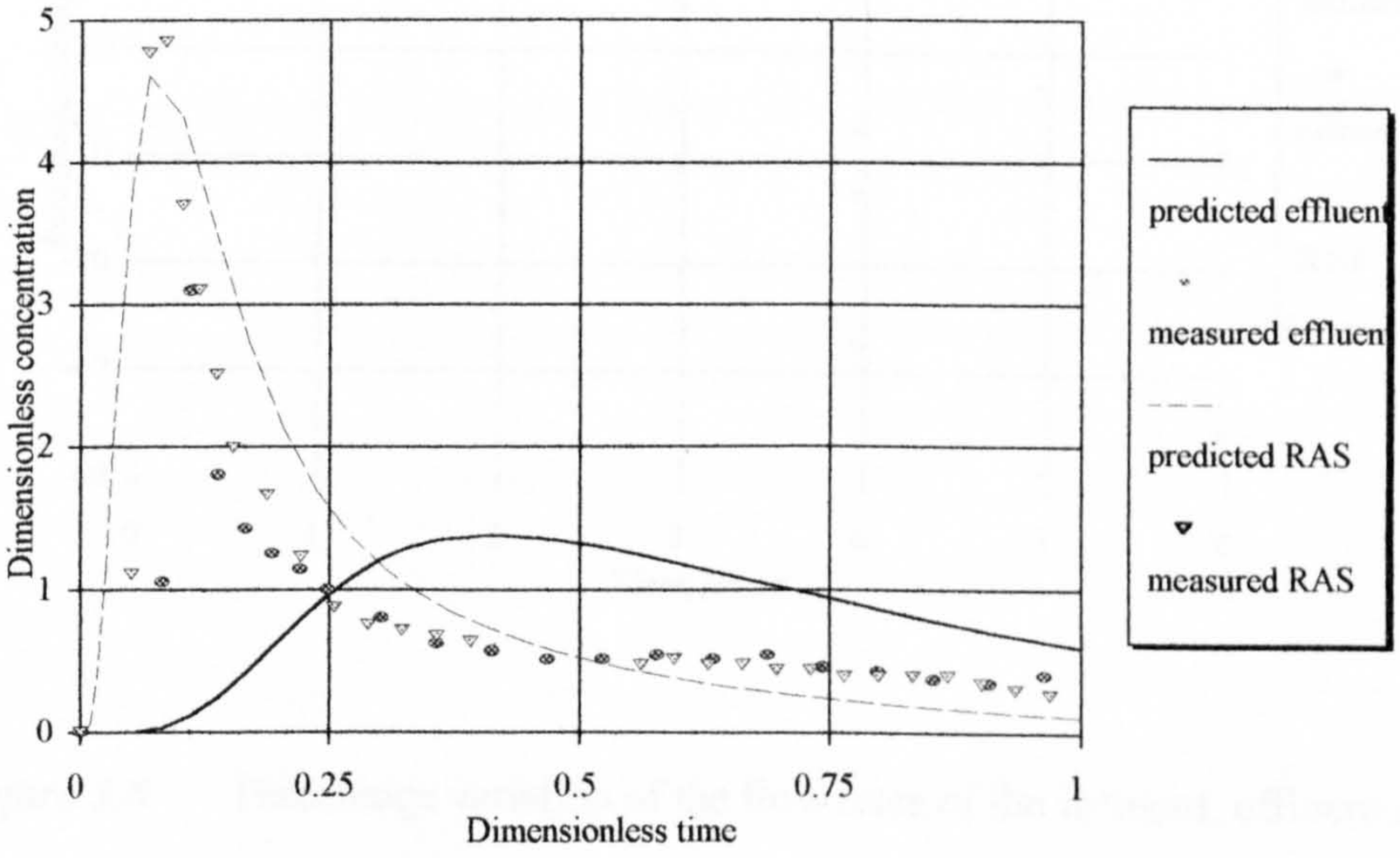

Figure 5.7b Residence time distributions of the effluent and return activated sludge in the Blackburn clarifier for test case E.

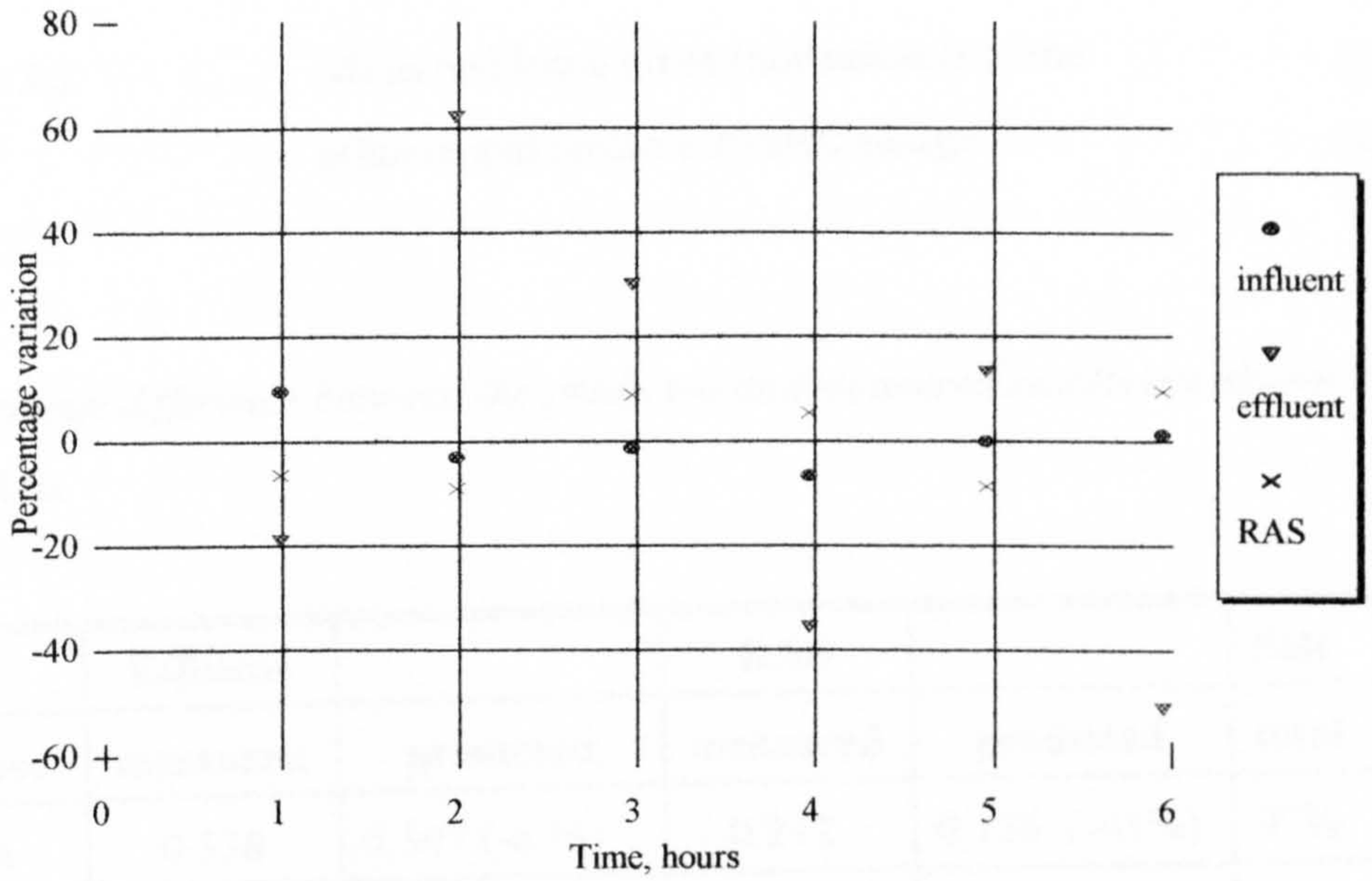

Figure 5.8 Percentage variation of the flow rates of the influent, effluent and return activated sludge in the Blackburn Meadows clarifier.

Table 5.2 Mean residence times (normalised) of the effluent and return activated sludge.

Percentage difference between the predicted and measured results are shown in brackets.

	Effluent		RAS		Salt
Case	measured	predicted	measured	predicted	total
A	0.538	0.507 (-6 %)	0.212	0.126 (-41%)	97%
B	0.648	0.674 (+4 %)	0.117	0.112 (-4 %)	107%
C	0.695	0.685 (-1 %)	0.154	0.109 (-29 %)	104%
D	0.767	0.676 (-12 %)	0.226	0.147 (-35 %)	151%
E	0.478	0.606 (+27%)	0.212	0.165 (-22 %)	132%

5.5.4 Suspended solids distribution

For the small baffle radius in the Copley clarifier (case A), a particle diameter of 130 μm was used in the model. The suspended solids concentration distribution was split by the baffle (Figure 5.9a) and the sludge blanket (@ 3000 mg/l) is shown by the blue/green interface. The highest predicted solids concentration was 6279 mg/l and the lowest was 6 mg/l, the effluent solids concentration was 16 mg/l and the RAS solids concentration was 4650 mg/l. Experimental measurements of the suspended solids concentration contour at 865 mg/l was found at water depths from 2.2 to 2.55 m across the tank, from the baffle to the effluent wall. The models predictions were at slightly shallower depths from 2.11 to 2.31 m (top of the dark purple area in Figure 5.9a). For the large baffle radius at the highest flow rate (case B) a particle diameter of 100 μm gave a sludge blanket (the lightest blue zone in Figure 5.9b) that was located higher in the tank. Consequently, the effluent concentration increased from 18 to 31 mg/l and the RAS concentration increased from 4650 to 5500 mg/l. This was probably caused by the increase of the solids loading to the clarifier (+18%) and the new position of the baffle.

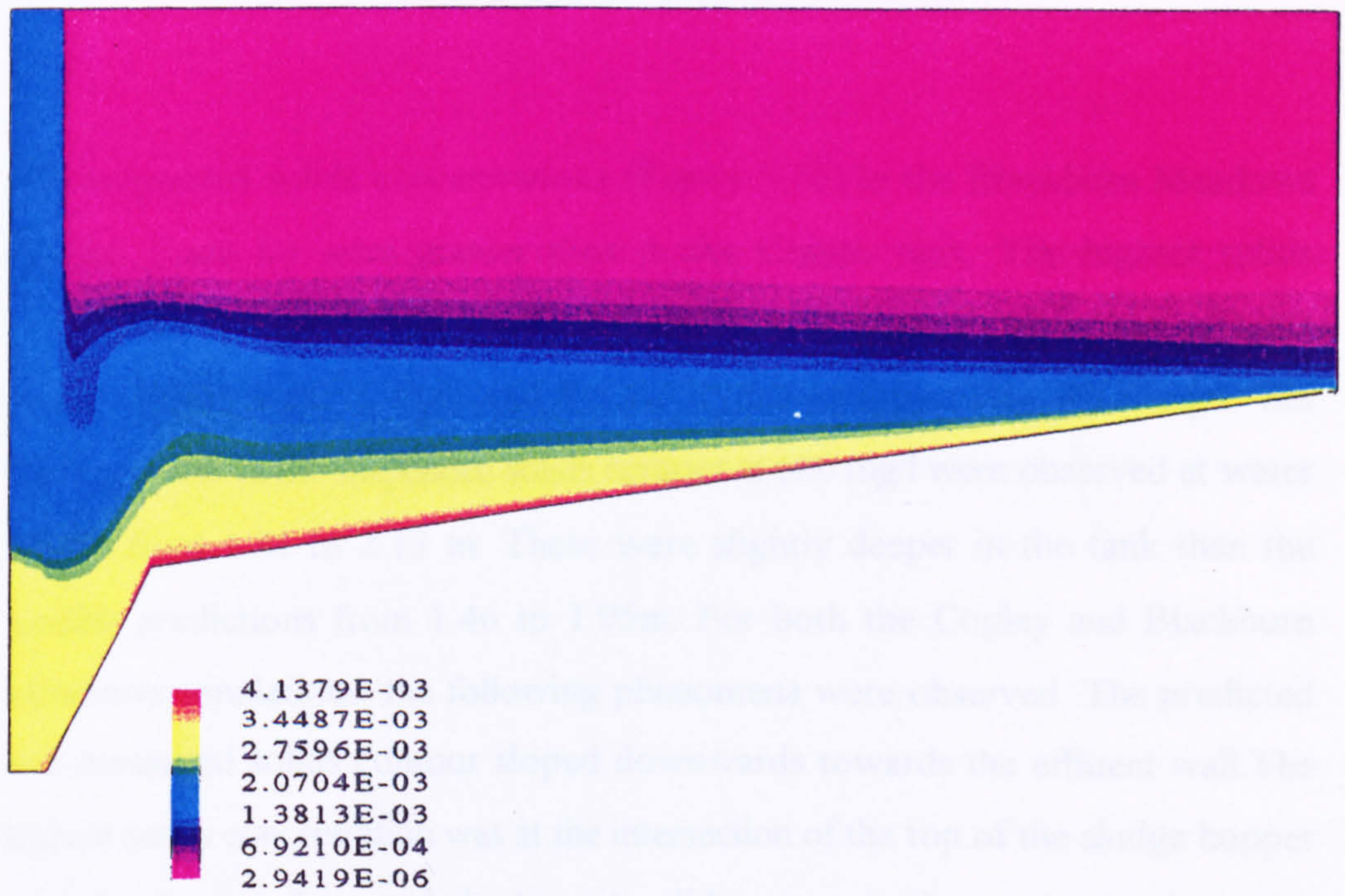

Figure 5.9a Suspended solids concentration distribution in the Copley clarifier for test case A (the scale is the volume fraction of solids).

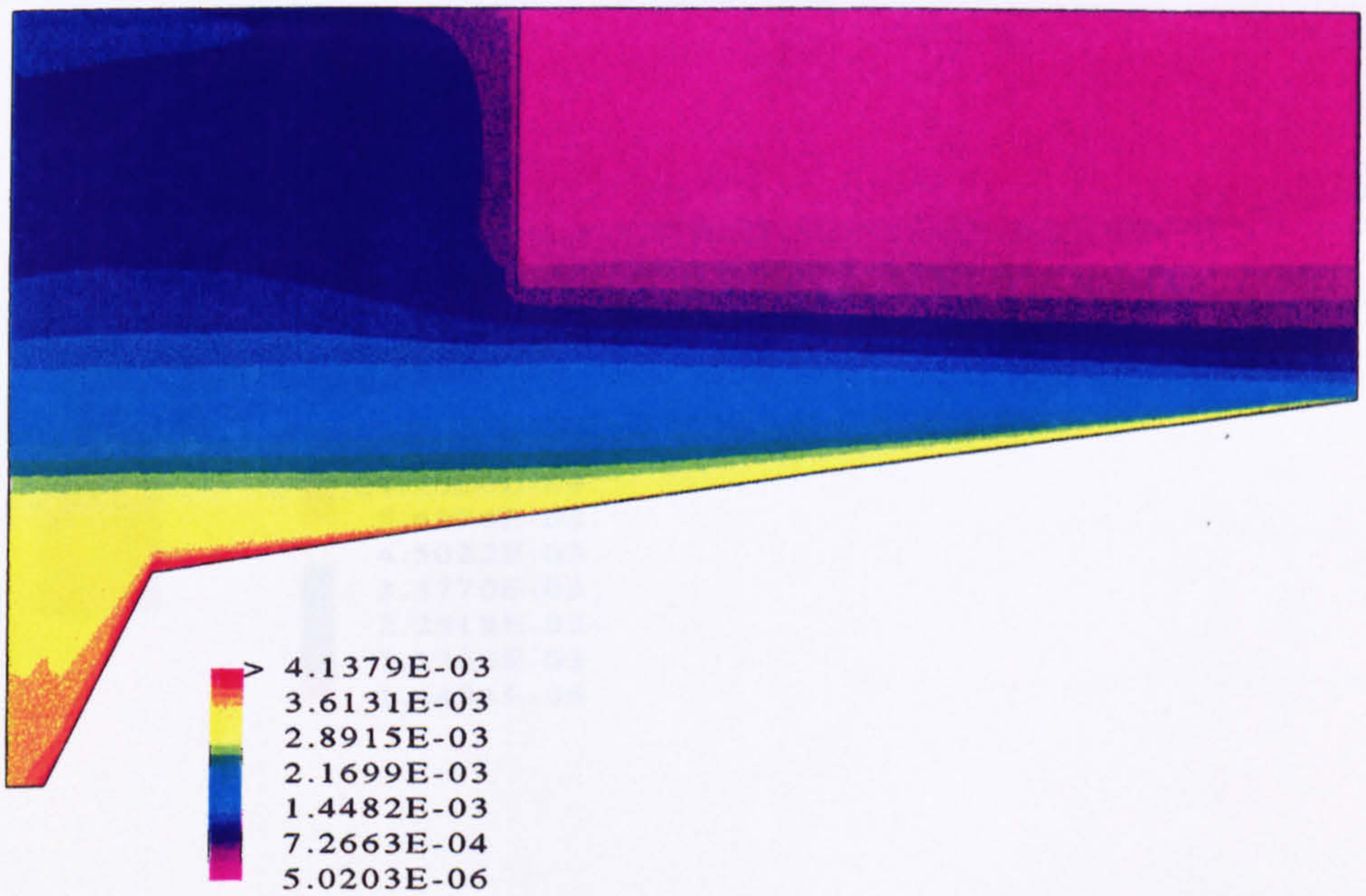

Figure 5.9b Suspended solids concentration distribution in the Copley clarifier for test case B (the scale is the volume fraction of solids).

The suspended solids concentrations (Figure 5.10) in the Blackburn Meadows clarifier (case D) were greater than in the Copley tank. The highest solids concentration was 11000 mg/l and the lowest was 8 mg/l; the effluent concentration was 81 mg/l and the RAS concentration was 8700 mg/l. Six measurements of the suspended solids contour at 600 mg/l were observed at water depths from 1.81 to 2.13 m. These were slightly deeper in the tank than the models predictions from 1.46 to 1.95m. For both the Copley and Blackburn Meadows simulations, the following phenomena were observed. The predicted and measured solids contour sloped downwards towards the effluent wall. The highest solids concentration was at the intersection of the top of the sludge hopper and the sloping floor and the lowest solids concentration was near the water surface on the outside of the baffle.

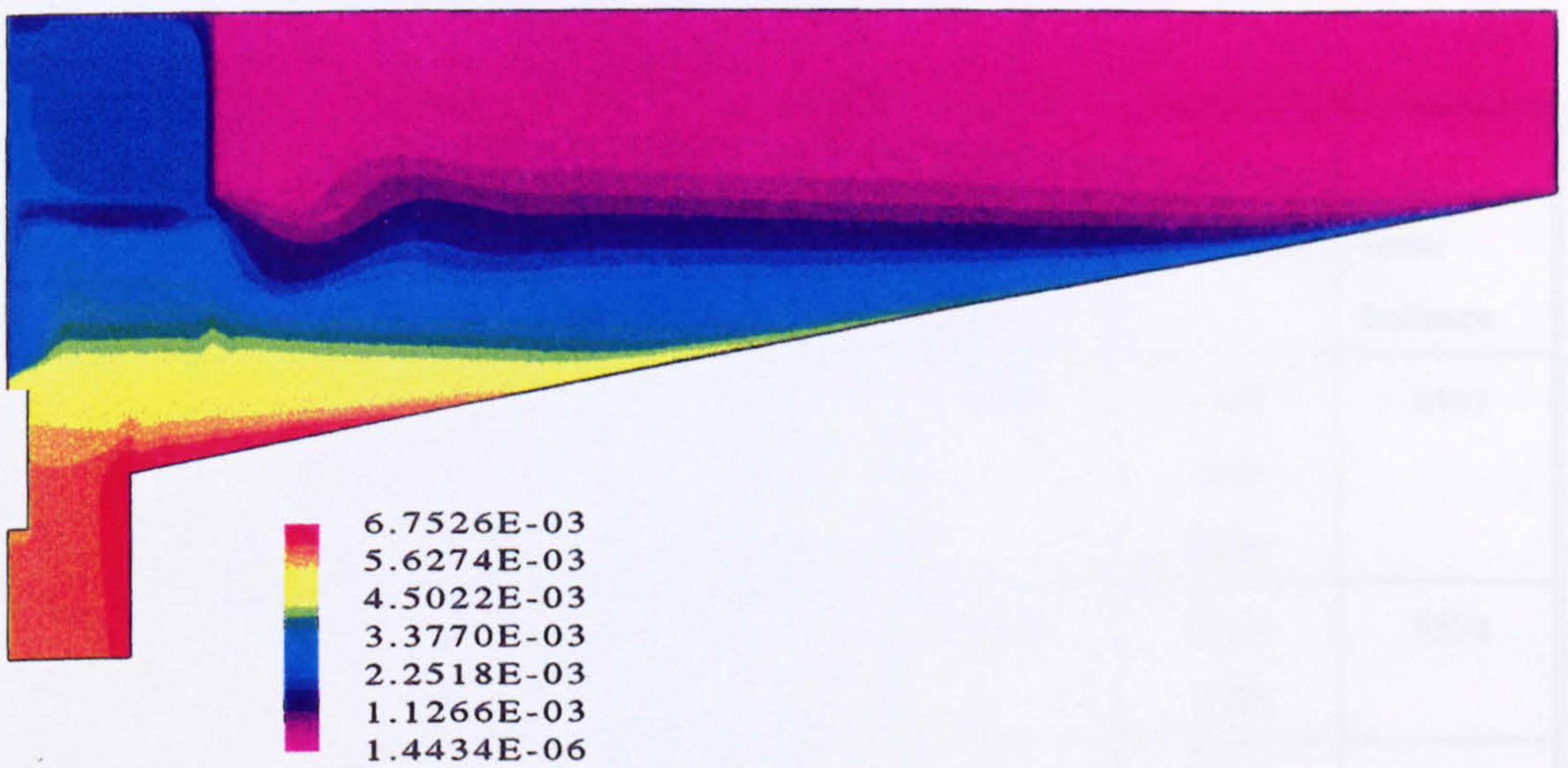

Figure 5.10 Suspended solids concentration distribution in the Blackburn clarifier for test case D (the scale is the volume fraction of solids).

5.5.6 Effluent and RAS concentrations and particle diameter

The predicted and measured effluent suspended solids concentrations in the Copley clarifier (Table 5.3) agreed when mean particle diameters of 130 μm (case A) and 100 μm (cases B and C) were used in the numerical model. In the Blackburn Meadows clarifier (Table 5.3) they agreed when particle diameters of 190 μm (case D) and 150 μm (case E) were used. The predicted solids concentration at the bottom of the sludge hopper was within 5% of the value calculated from the mass balance in all the test cases. This meant that the numerical model was mass conservative. However, the measured RAS solids concentration, for all the test cases, was unexpectedly 17-24% lower than the predicted and theoretical values.

Table 5.3 Numerical particle diameters and suspended solids concentrations.

		Effluent		RAS		
Case	**particle size, μm**	**measured mg/l**	**predicted**	**measured mg/l**	**predicted**	**mass balance**
A	100	18	25	3750	4550	4597
	130		16		4650	
	160		12		4700	
B	100	30	31	4500	5500	5534
	130		25		5750	
C	100	30	31	4500	5250	5338
	130		22		5500	
	160		16		5500	
D	170	78	85	7445	8550	8778
	190		80		8650	
E	130	49	75	6555	7700	7670
	150		50		7900	

5.6 DISCUSSION

5.6.1 Settlement tests

The graph for the double exponential equation was quite close to the settling velocity measurements made at suspended solids concentrations above 1000 mg/l for both secondary clarifiers (Figure 5.3). The equation over-predicted the measured settling velocities below solids concentrations of 1000 mg/l in the Blackburn Meadows clarifier, but were quite close to the measurements made by White (1975)[29]. A graph of the experimental settling velocity in the literature (Figure 3.5) showed that the peak settling velocity corresponded to a suspended solids concentration of 200 mg/l[28]. Therefore in the model, it was changed from 500 to 200 mg/l, but the comparison with the experimental data hardly improved. The error was really caused by the difficulties in measuring the particle settling velocity at low solids concentrations.

5.6.2 Flow patterns

Previous numerical modelling papers[5-11] on flat floored secondary clarifiers had described a strong downward flow in the inlet zone, which was caused by the high density of the influent. This was not observed in this work, possibly because the relative density of the influent to the surrounding fluid was small (Figures 5.4a, 5.4b and 5.5). Instead, the strength of the downward flow was mostly influenced by the baffle position. This work differed from previous studies, because there were 3 radial flow currents in the clarifier. This was because the RAS flow was represented by a mass flow boundary across the floor of the sludge hopper, instead of across the whole floor of the clarifier[5-11].

There has been no previous work done on simulating the jet flow between the deflector plate and the baffle, as a deflector plate is not often used in clarifiers. Although the work in this chapter, on the modelling of the jet flow was a valiant attempt; essentially the turbulent jet should have been modelled in three dimensions. In an instantaneous 2-D flow, by definition, the velocity vector would be everywhere parallel to the plane. This cannot be the case when a turbulent jet is present in the flow domain.

The calculation of the drag coefficient in the axial and radial directions was not right. The slip velocity should really not have been discomposed into two components with the relative Reynolds number and drag coefficient calculated in two directions. This is because of the non-linearity of Re and C_d. If there is only flow to consider in the axial direction then the experimental settling velocity can be substituted by the axial slip velocity. However, when the particle is also carried by the fluid's motion in the radial direction, this implies that the settling velocity will contribute to both the axial and radial directions. The axial slip velocity should therefore be lower and the radial slip velocity should be higher. Subsequently, the axial component of drag will increase, its radial component decrease, the axial velocities decrease and the radial velocities increase. Another source of error is that the drag coefficient in the radial direction was calculated using one equation only for all values of the relative Reynolds number. It should have used the same equations as those to calculate the axial drag coefficent. Experimental data for the mean flow velocities in the Copley and Blackburn Meadows clarifiers were not taken and therefore it is difficult to know how accurate the flow patterns are. However, clearly further work is needed to formulate correctly the source term of the inter-phase momentum transfer.

The water surface was represented by a symmetry plane boundary condition. Therefore, the problems encountered in Chapter 4 will also be observed in the multi-phase flow simulations. The maximum predicted radial velocity in the upper region of the secondary clarifiers is next to the water surface instead of just below it. The 'buoy' of the free surface above the inlet vertical pipe is not predicted and therefore the uniform radial velocity used for the inlet boundary will be higher than in reality. Consequently, the radial flow in the upper region of the clarifier is over-predicted and the flow is attached to the symmetry plane.

However, it was not possible to model the free surface by combining the multi-fluid model with the 'homogeous' (free surface) model in the program CFX-F3D. Separate choices can be made between these two multi-phase models for the processes of momentum, heat, turbulence and multi-component mass transfer. However, the model is not flexible enough to have momentum transfer between the water and the solid particles and no momentum transfer between the water and the air, which are the requirements of modelling the flow in a secondary clarifier with a free water surface.

The solids phase was defined as a turbulent fluid, with the transport of k and ϵ in the solids phase predicted by the standard k-ϵ model. There was no transfer of turbulence between the phases. Multi-phase turbulent flow is not well understood and it is not really known whether the disperse phase should be modelled as a laminar or turbulent phase and if the inter-phase transfer of turbulence should be included. The effect of the particles on the turbulent flow field was considered to be negligible because the particles were small ($< 200\ \mu m$) and therefore inter-phase turbulence transfer was neglected.

The molecular viscosity of the solids phase was not calculated from kinetic theory and therefore a value needed to be entered into the model. Its value was chosen to be much lower than the fluid viscosity to make it negligible in the calculation of the effective viscosity. However, its effect on the flow pattern in a secondary clarifier is not yet understood and needs further investigation.

5.6.3 Residence time distribution

In the Copley clarifier the predicted and measured RTD's showed a good agreement for the effluent, but with the RAS the comparison was only good for test case B with the large baffle radius. The numerical residuals (see Appendix A) were below 0.001 for all the 2-D simulations of the Copley clarifier (Figures A1 to A3), except for the mass continuity residual when there was a small baffle radius. Consequently, there was a significant difference between the predicted and measured RTD's of the RAS with the small baffle radius. This was probably caused by the high velocity gradients near the baffle which gave numerical instabilities[19]. The result was an over-prediction by the model of the mean flow velocities to the RAS outlet. No previous work has been done on comparing the predicted and measured RTD's in a secondary clarifier. The use of a symmetry plane for modelling the water surface has meant that the radial velocities near the liquid surface were probably over-predicted. Improvements can be made to the formulation of the momentum source term, as discussed, and this would affect the flow patterns and RTD's quite considerably.

The predicted and measured RTD's of the effluent in the Blackburn Meadows clarifier disagreed. At the higher flow the residuals were 0.005 and 0.0008 respectively for the axial and radial velocities (Figure A4 in Appendix A) which meant that the convergence criteria had not been satisfied. At the lower flow the

residuals were all below 0.001 (Figure A5). The solution from the model at the higher flow diverged when the number of cells were decreased or increased (ranging from 1583 to 12642 cells). The grid spacing was modified in the same proportion in every cell and the same in the axial and radial directions. Residuals for the velocity, turbulent kinetic energy, eddy dissipation and volume fraction are non dimensional and calculated by the sum of the residuals in each cell divided by the number of cells (see Appendix A). Therefore, the number of cells does not increase the non dimensional residual. The mass source residual is calculated as the sum of the mass flow residuals in each cell. It was expected that more cells would give a more accurate solution. However, the residuals of the axial velocity for both phases increased suddenly, even when using more cells. Increasing or decreasing the number of cells in a completely uniform fashion should not theoretically affect the aspect ratio, skewness or smoothness of a quadrilateral grid. A more plausible explanation for the divergence of the solution was that the numerical model of the Blackburn Meadows clarifier was numerically unstable and would not even allow for changes to be made to the grid.

In Chapter 4 it was shown how the diurnal variations of the flow rate could affect the RTD of the effluent. Indeed, the effluent flow rate in the Blackburn Meadows clarifier varied by ± 60% and may have the same effect. But unfortunately the solution diverged when the variable flow rate was simulated, and therefore implies that a simulation with a variable flow rate is still required. The accuracy of the variable flow data and the effect it has on the movement of the water surface in the clarifier was discussed in Chapter 4. These factors will have the same effects on secondary clarifiers.

The most plausible reason for the disagreement between the RTD's in the Blackburn Meadows clarifier, was that the 2-D axi-symmetric model was

incapable of predicting the turbulent jet. Indeed, Szalai *et al*[30] had observed that swirling flow can affect the residence time distribution of the effluent in a circular clarifier. Consequently, a 3-D simulation of the Blackburn Meadows clarifier is required.

5.6.4 Suspended solids concentration

The particle diameter in the model was adjusted to give a fit between the predicted and measured values of the effluent solids concentration. The predicted RAS solids concentration was close to the value computed from the solids mass balance. Both these results had been expected, because the effluent solids concentration was in all fairness, used as an input to the model to predict the particle diameter and the solution of the model was converged which implies mass conservation in the clarifier.

In both clarifiers the model predicted that the height of the solids contour was slightly too high. If a solids concentration of 200 mg/l (corresponding to the maximum settling velocity) had been used instead of 500 mg/l, then the settling velocities of the particles would be higher, especially at solids concentrations below 500 mg/l. The predicted solids contours at 865 mg/l in the Copley clarifier and at 600 mg/l in the Blackburn Meadows clarifier would be slightly lower down and give a better comparison to experimental data.

The measured solids concentration of the RAS was unexpectedly 20% lower than the theoretical value calculated from the solids mass balance. It was unlikely that the error was caused by the laboratory measurement of the solids concentration; which would equally have affected the influent, effluent and RAS concentrations. Indeed, the solids mass balance would still not have been satisfied. Furthermore,

the measurements of the solids concentration had been taken by different engineers and the same values were found for each person. It was possible that the error was caused by the variation in flow rate to the effluent and RAS outlets, especially for the Blackburn Meadows clarifier. When the effluent flow rate decreased by 60% (Figure 5.8), the effluent solids concentration should increase and the RAS solids concentration would decrease. Consequently, the average RAS solids concentration for the duration of the salt tracer test may have decreased.

A more plausible explanation was that the measured influent flow rate was larger or the measured RAS flow rate was lower, than it had been reported from the site test, and therefore the measured RAS concentration was indeed correct. This was possible for the Blackburn Meadows clarifier, because of the assumption of a perfect inlet flow split to all the secondary clarifiers at the plant. However, a more plausible explanation was that the RAS flow rate used in the model was too low because it had been measured downstream of the clarifiers. If some of the settled sludge coming from the bottom of the secondary clarifier had in fact been portioned off as waste sludge, then really the measured RAS flow rate used in the model would be higher than that coming from the bottom of the secondary clarifiers. That would explain why the predicted RAS concentration was about 20 % higher than the measured concentration, because the waste sludge flow was 20 % of the settled sludge. Unfortunately, if there had been an increase of 20 % to the flow rate of the RAS then it would reduce the models prediction of the residence time of the RAS and make its comparison with experimental data worse.

The flow rates to the Copley clarifier varied by only ±16% and were recorded by portable meters only once an hour, and therefore the accuracy of the flow data was worse than the Blackburn Meadows clarifier. Therefore, the arguments given

here to discuss the accuracy of the RAS solids concentration are more subjective, as far as the Copley clarifier is concerned.

5.6.5 Particle diameter

The sizes and shapes of activated sludge flocs were discussed by Atkinson and Daoud[31]. The measurements of the particle diameter have ranged from 20 μm to approximately 200 μm, in the studies of various researchers (Aiba *et al*[32], Finstein[33] and Levine *et al*[34]). Measurements of the aggregate size, floc length and maximum floc dimension have varied from 2 to 5000 μm, depending on the definition of particle size and how it was measured[25,35-42]. The floc length normal to the vertical direction was found from the settling characteristics of the floc[25,42] and the horizontal floc length gave a gross over-prediction of the floc diameter[38-40]. Other researchers used a different method for characterising the particles; by measuring the surface area (Baba *et al*[41]), cross sectional area or perimeter (Li *et al*[42]) and calculating the equivalent diameter of a sphere with the same surface area etc. Mean particle diameters from 100 to 190 μm were used in the model for the simulations of the secondary clarifiers. These figures were consistent with all the measured data of the particle diameters in the literature.

Previous research by Lyn et al[18] and Parker et al[38-39] on particle flocculation in biological wastewater treatment plants have shown that by increased mixing, particles will agglomerate and form larger sized flocs, assuming that there is no floc breakup. Higher influent suspended solids concentrations will also increase particle flocculation because the particles are closer together[18]. Indeed, with the smaller baffle radius in the Copley clarifier there was more mixing in the inlet zone and a higher influent solids concentration, and consequently the particle diameter increased from 100 μm to 130 μm. The larger particle diameters in the Blackburn

Meadows clarifier may also have been caused by more mixing in the inlet zone and because of the higher influent solids concentrations. Indeed, with the higher flow rate to the Blackburn Meadows clarifier there was the largest particle diameter for all the models.

5.7 CONCLUSIONS

1. There was a good agreement (6%) between the predicted and measured mean residence time of the effluent in a full-scale circular secondary clarifier. However, the model only compared favourably (4%) with the measured residence time of the RAS in one test case.

2. The model was unable to predict the residence time of the effluent in another secondary clarifier with a turbulent jet between a baffle and a deflector plate.

3. The model was quite comparable to the measured solids contours in both secondary clarifiers.

4. The predicted mean particle diameter was between 100 and 130 μm for the conventional secondary clarifier and between 150 and 190 μm for the secondary clarifier with the deflector plate. These values were similar to the experimental data found in the literature.

5. The predicted RAS solids concentration was 20% higher than the measured concentration.

6. Inter-phase momentum transfer was incorrectly modelled because there was no influence of radial flow on the settling velocity of the particles.

This chapter has shown that the multi-fluid model is capable of predicting the residence time distribution of the effluent in a circular secondary clarifier. However, it cannot predict the turbulent jet in another secondary clarifier. This problem may be overcome by using a three dimensional model. Unfortunately, the source term for the inter-phase transfer of momentum was incorrectly modelled. Further work is required to implement correctly inter-phase drag into the model. But without having experimental velocity data, the accuracy of the predicted flow patterns could not be verified.

However, there have been new areas of research addressed in this chapter. A new approach to modelling the flow in secondary clarifiers is given, a turbulent jet has been simulated and the model has been compared to measurements of the residence time distributions of the tank. The parameters in the model and their optimum values are investigated in a sensitivity study presented in the next chapter of the thesis.

5.8 REFERENCES

1. Matko, T., Fawcett, N., Sharp, A. and Stephenson, T. (1996). 'Recent progress in the numerical modelling of wastewater sedimentation tanks'. Transactions of the Institution of Chemical Engineers, part B3, vol. 74, 245-258.
2. Camp, T.R. (1945). 'Sedimentation and the design of settling tanks'. Transactions of the American Society of Chemical Engineers , vol. 94, 895-896.
3. DeVantier, B.A. and Larock, B.E. (1987). 'Modeling sediment-induced density currents in sedimentation basins'. Journal of Hydraulic Engineering, vol.113, 80-94.
4. DeVantier, B.A. and Larock, B.E. (1986). 'Modelling a recirculating density-driven turbulent flow'. International Journal of Numerical Methods in Fluids, vol. 6, 241-253.
5. Samstag, R.W., Dittmar, D.F., Vitasovic, Z., McCorquodale, J.A. (1989). 'Underflow geometry in secondary sedimentation.' Water Environmental Research, vol. 64, no. 3, 204-212.
6. McCorquodale,J.A., Yuen,E.M., Vitasovic,Z. and Samstag, R. (1991). 'Numerical simulation of unsteady conditions in clarifiers'. Water Pollution Research Journal of Canada, vol. 26, 201-222.
7. Krebs, P., Vischer, D. and Gujer, W. (1995). 'Inlet-structure design for final clarifiers'. Journal of Environmental Engineering, vol. 121, no. 8, 558-564.
8. Zhou, S. and McCorquodale, J.A. (1992). 'Mathematical modelling of a circular clarifier'. Canadian Journal of Civil Engineering, vol. 19, 365-374.

9. Zhou, S. and McCorquodale, J.A., (1992). 'Influence of skirt radius on performance of circular clarifier with density stratification'. International Journal of Numerical Methods in Fluids, vol. 14, 919-934.

10. McCorquodale, J.A. and Zhou, S. (1994). 'Effects of hydraulic and solids loading on clarifier performance'. Journal of Hydraulic Research, vol. 31, no. 4, 461-478.

11. McCorquodale, J.A. and Zhou, S.P. (1994). 'Use of numerical models in clarifier design - optimization of inlet structures'. 67th Annual Conference of the Water Environment Federation. Chicago.

12. Larsen, P. (1977). On the hydraulics of rectangular settling basins, experimental and theoretical studies, report no. 1001, Department of Water Resources Engineering, Lund Institute of Technology, Lund University, Lund, Sweden.

13. Anderson, N.E. (1945) 'Design of final settling tanks for activated sludge'. Sewage Works Journal, vol. 17, 50-65.

14. McCorquodale, J.A. (1989). West Point secondary clarifier model study. Program report to Mr. David Blodsoe, CH2M Hill, consulting engineers. Seattle, Washington.

15. Mousri, A. (1990). Personal communication based on Doctoral thesis in progress. University of Windsor, Windsor, Canada.

16. Rodi, W. (1980). Turbulence models and their application in hydraulics, a state of the art review. International Association for Hydraulic Research, Delft, Netherlands.

17. Celik, I., Rodi, W. and Stamou, A.I. (1985). Prediction of hydrodynamic characteristics of rectangular settling tanks. Proceedings of the International Symposium of Refined Flow Modelling and Turbulence Measurements, Iowa City, Iowa, USA.

18. Lyn, D.A., Stamou, A.I. and Rodi, W. (1992). 'Density currents and shear-induced flocculation in sedimentation tanks'. Journal of Hydraulic Engineering, vol. 118, 849-867.

19. Matko, T., Fawcett, N., Sharp, A. and Stephenson, T. (1996). 'A numerical model of flow in circular sedimentation tanks'. Transactions of the Institution of Chemical Engineers, part B3, vol. 74, 197-204.

20. Anderson, J.D. Jr. (1995). Computational Fluid Dynamics. The Basics with Applications. McGraw-Hill, Inc.

21. James, A. and Smith, E.L. (1975). Institution of Chemical Engineers, Annual Research Meeting of theBiochemical Engineering Section, University of Bradford, March.

22. Farrow, J.B. and Warren, L.J. (1989). The measurement of the floc density-floc size distributions. In: Flocculation and Dewatering (B.M. Moudgil and B.J. Scheiner, eds.) Engineering Foundation, New York, 153-166.

23. Farrow, J.B. and Warren, L.J. (1989). A new technique for characterising flocculated suspensions. In: Proceedings of the Dewatering and Technology Conference, Brisbane, Aust Inst Min Metal, Parkville, Australia, 61-64.

24. Smith, P.G. and Coackley, P. (1984). 'Diffusivity, tortuosity and pore structure of activated sludge.' Water Research, vol. 18, 117-122.

25. Lee, D.J., Chen, G.W., Liao, Y.C. and Hsieh, C.C. (1996). On the free-settling test for estimating activated sludge floc density, Water Research, vol. 30, 541-550.

26. Degremont (1991) Water Treatment Handbook. 6th English edition. Lavoisier Publishing, Paris, vol. 1, 161, 370.

27. Vesilind, P.A. (1974). Treatment and disposal of wastewater sludges. Ann Arbor Science Publishers Inc., Ann Arbor, Michigan.

28. Takacs, I., Patry, G.G. and Nolasco, D. (1991). 'A dynamic model of the clarification-thickening process. Water Research, vol. 25, 1263-1271.

29. White, M.J.D. (1975). Settleability of activated sludge. WRc technical report, TR11, May.

30. Szalai, L., Krebs, P. and Rodi, W. (1994). 'Simulation of flow in circular clarifiers with and without swirl'. Journal of Hydraulic Engineering, vol. 120, 4-21.

31. Atkinson, B. and Daoud, I.S. (1976) 'Microbial flocs and flocculation in fermentation process engineering'. Advances in Biotechnology Engineering, vol. 4, 42-124.

32. Aiba, S., Humphrey, A.E. and Millis, N.F. (1965). Biochemical Engineering. University of Tokyo Press, Tokyo, 304-305.

33. Finstein, M.S. (1965). 'Gross dimensions of activated sludge floc'. Bacterial Proceedings of the American Society of Microbiology, 13.

34. Levine, A.D., Tchobanoglous, G. and Asano, T. (1985). 'Characterization of the size distribution of contaminants in wastewater: treatment and re-use implications. Journal of the Water Pollution Control Federation, vol. 57, 805-816.

35. Li, D. and Ganczarczyk, J.J. (1986). 'Application of image analysis system for study of activated sludge flocs'. Water Pollution Research Journal of Canada, vol. 21, 130-140.

36. Magara, Y., Namby, S. and Utosawa, K (1976). 'Biochemical and physical properties of an activated sludge on settling characteristics'. Water Research, vol. 10, 71-77.

37. Schroepfer, G.J., Johnson, A.S. and Ziemke, N.R. (1955). Effect of various factors on hydraulic separation in the anaerobic contact process. Sanitary engineering report 101S, University of Minnesota, Minneapolis, Minnesota.

38. Parker, D.S., Kaufman, W.J. and Jenkins, D. (1971). 'Physical conditioning of activated sludge floc'. Journal of the Water Pollution Control Federation, vol. 43, 1817-1833.

39. Parker, D.S., Kaufman, W.J. and Jenkins, D. (1972). 'Floc breakup in turbulent flocculation processes'. Journal of the Sanitary Engineering Division, 79-98.

40. Ganczarczyk, J. and Kosarewicz, O. (1961). 'Activated sludge floc dispersing process'. Gaz Wodai Techn San, vol. 35, 19.

41. Baba, K., Yoda, M., Ichika, H. and Osumi, A. (1988). 'A floc monitoring system with image processing for water purification plants'. Water Supply, vol. 6, 323-327.

42. Li, D. and Ganczarczyk, J.J. (1987) 'Stroboscopic determination of settling velocity, size and porosity of activated sludge flocs'. Water Research, vol. 21, 257-262.

CHAPTER VI

This chapter will also be submitted to a journal and has therefore been written as a paper. Some of it will repeat what has already been written in Chapter V. The intention of the work in this chapter is to determine which parameters in the Eulerian multi-fluid model affect the flow in a circular secondary clarifier. This information can be used to determine the best values for each parameter and provide a guideline for other numerical modellers to use the model effectively. The model was modified from the computational fluid dynamics programme, CFX-F3D.

SENSITIVITY INVESTIGATION ON THE TWO-PHASE FLOW MODEL

6.1 Introduction

Secondary sedimentation has a major influence on the suspended solids concentration in the final effluent of a wastewater treatment plant, yet the impact of the fluid dynamics in a secondary clarifier is not fully understood. Several researchers have modelled the flow in secondary clarifiers[1-9] and their results have agreed with experimental measurements[1-8]. Some of the numerical parameters in these models have been studied before; i.e. the settling parameters[2-4,6,10-12], resuspension coefficient[2,6-7], the turbulent parameters[3], the inlet flow rate and inlet

solids concentration[4,8] and the number of grid cells[7]. However, a sensitivity study has not yet been carried out on all the numerical parameters.

The effect of some of the parameters in the multi-fluid model, on the flow patterns and suspended solids concentrations in the secondary clarifier without the deflector plate were investigated. Some physical parameters in the model characterise the solid particles, such as their mean density, diameter and viscosity. The parameters used to define the settling and resuspension of the solids are the settling parameter of the colloidal particles, the slip velocity between the phases and the turbulent Prandtl number of the volume fraction. Other parameters describe the flow conditions, such as the inlet flow rate and the inlet solids concentration. Finally, the numerical accuracy of the solution is affected by the number of grid cells and whether the flow is in two or three dimensions. All of these parameters were investigated and a 3-D simulation of a secondary clarifier was carried out for the first time.

6.2 Theory

6.2.1 Flow equations

The governing conservation equations for mass and momentum in an unsteady, two-phase, turbulent mean flow are :

$$\frac{\partial}{\partial t}(r_\alpha \rho_\alpha)+\frac{\partial}{\partial xi}(r_\alpha \rho_\alpha u_{\alpha i})=0 \qquad \text{- (6.1)}$$

$$\frac{\partial}{\partial t}(r_\alpha \rho_\alpha u_{\alpha i})+\frac{\partial}{\partial xi}(r_\alpha \rho_\alpha u_{\alpha i} u_{\alpha j})=r_\alpha(F_i-\frac{\partial p}{\partial xi})+\frac{\partial}{\partial xj}(\mu_{\alpha eff}\frac{u_{\alpha i}}{\partial xj})+C_{\alpha\beta}(u_{\beta i}-u_{\alpha i}) \qquad \text{- (6.2)}$$

where the phases are denoted as α and β, the volume fraction and mean density for each phase are r_α, and ρ_α, directions are labelled by subscripts i and j, mean velocities are $u_{\alpha i}$, $u_{\beta i}$, $u_{\alpha j}$ and $u_{\beta j}$, distances are given as x_i and x_j and time is t. The body force is given as F_i, the mean pressure is p and the effective viscosity is written as $\mu_{\alpha eff}$.

The third term on the right hand side of equation 6.2 is the exchange of momentum between the phases (drag force exerted on the moving fluid by the solid particles), which is a product of the slip velocity and the coefficient, $C_{\alpha\beta}$, as follows :

$$C_{\alpha\beta}=\frac{3}{4}\frac{C_d}{d_p}r_\beta\rho_\alpha(u_{\beta i}-u_{\alpha i}) \qquad \text{- (6.3)}$$

where α and β represent the liquid and solid phases respectively, C_d is the dimensionless drag coefficient, d_p is the mean diameter of the spherical particles and r_β is the volume fraction of the solids phase. Circular tanks are modelled in cylindrical coordinates, where y is the downward axial direction, r is the radial direction and θ is the tangential direction. It is assumed that there is no flow in the tangential direction because there is no deflector plate in the clarifier (see Chapter 5) and therefore a two dimensional axi-symmetric flow is modelled. A 3-D axi-symmetric flow model is also simulated to determine if there is any difference in the flow pattern.

6.2.2 Turbulence model

The turbulence model used is the standard k-ϵ model, which calculates the turbulent kinetic energy, k and the eddy dissipation, ϵ from the mean flow velocities. Because there is no standard turbulence model for multi-phase flows, the general form of the single-phase k-ϵ model is applied. For both the liquid and solid phases turbulent flow is assumed and therefore, the eddy viscosity hypothesis

holds for each turbulent phase, α. Hence molecular and turbulent diffusion of momentum is governed by an effective viscosity :

$$\mu_{\alpha eff}=\mu_{\alpha}+\mu_{t\alpha}$$

- (6.4)

where the turbulent viscosity, $\mu_{t\alpha}$ is calculated from the turbulent kinetic energy and eddy dissipation (Chapter 5).

6.2.3 Transport of suspended solids

Turbulent dispersion of the volume fraction for phase α uses the eddy diffusivity hypothesis :

$$\frac{\partial}{\partial t}(r_{\alpha}\rho_{\alpha})+\frac{\partial}{\partial xi}(r_{\alpha}\rho_{\alpha}u_{\alpha i}-\Gamma_{\alpha}\frac{\partial r_{\alpha}}{\partial xi})=0$$

- (6.5)

where

$$\Gamma_\alpha = \frac{\mu_{t\alpha}}{\sigma_\alpha}$$

- (6.6)

In these two equations, Γ_α denotes the turbulent mass diffusion of the volume fraction and σ_α is its corresponding turbulent Prandtl number. Values of 1.0, 0.5 and 0.5 were chosen respectively for the axial, radial and tangential turbulent Prandtl numbers (see Chapter 5).

6.2.4 Relative Reynolds number

The drag force exerted on a moving Newtonian, incompressible fluid (phase α) by a solid particle is expressed in terms of a non-dimensional drag coefficient, C_d which depends on the relative Reynolds number, Re, as follows :

$$Re = \frac{\rho_\alpha u_{slip} d_p}{\mu_\alpha}$$

- (6.7)

In the axial direction of the circular clarifier the slip velocity (u_{slip}) was substituted by the settling velocity of the particles, found from measurements taken in a

settling column. To investigate its sensitivity, the axial slip velocity was also calculated directly from the conservation equation of momentum. The relationships between the drag coefficient and the relative Reynolds number (given in Chapter 5) are dependent on the flow regime; i.e. Stoke's or laminar ($0 \leq Re \leq 0.2$), Allens, viscous or transitional ($0.2 < Re \leq 500$) and Newton or turbulent ($Re > 500$). In the radial direction the slip velocity was calculated directly from the momentum conservation equation.

6.2.5 Settling velocity distribution

The best equation to use for the relationship between the settling velocity and the suspended solids concentration is a double exponential relationship[12]:

$$V_s = V_0[e^{-K(C-C_{min})} - e^{-K_1(C-C_{min})}] \quad - (6.8)$$

where K denotes the floc settling parameter, K_1 is the colloids settling parameter, V_o is the free settling velocity, C is the suspended solids concentration and C_{min} is the concentration of poorly settling particles (0.002 times the inlet solid concentration). From the settling column experiments reported in Chapter 5, the values derived for K, K_1 and V_0 were 0.703 m^3/kg, 4.2 m^3/kg and 9.73 m/hr. The colloids settling parameter, K_1 was derived from these experiments, by the assumption that the transition from flocculent to hindered settling occurs at a suspended solids concentration of 500 mg/l[14]. This was compared to a colloids settling parameter corresponding to a solids concentration of 200 mg/l.

6.2.6 Boundary conditions

The flow domain in the circular secondary sedimentation tank is bounded by the flow inlet, water surface, the two flow outlets and the wall boundaries to represent the inlet pipe wall, tank bottom, effluent wall and baffle (Figure 6.1). A horizontal flow positioned between the top of the inlet pipe and the water surface represents the influent, and the inlet velocity is found by dividing the inlet flow rate by the inlet cross sectional area. Turbulent parameters for k and ϵ in the influent are calculated from the inlet velocity. The volume fraction of suspended solids in the influent is calculated by dividing the inlet solids concentration by the mean density of the solid particles, and the sum of the inlet volume fractions of the liquid and solid phases must be equal to 1. The effluent flow boundary is one cell thick between the top of the effluent wall and the water surface, and the RAS flow boundary is across the floor of the sludge hopper (Figure 6.1). Mass flow boundaries are used to represent these outflows. The boundary conditions at the solid boundaries and on the water surface for each of the phases are defined by the same equations used in the single-phase flow model[15]. The free water surface was once again simplified by using a symmetry plane. The boundary conditions are discussed in Appendix B.

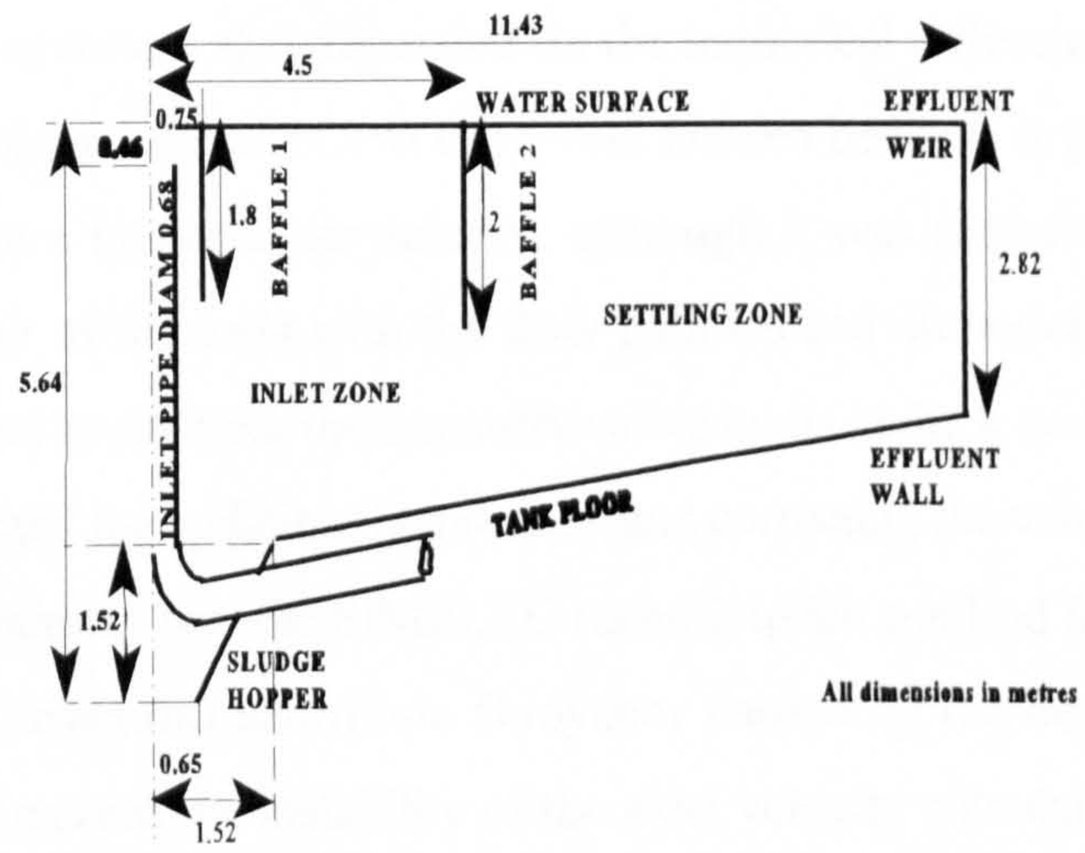

Figure 6.1 Tank dimensions of the cross section of the clarifier.

6.3 METHOD

6.3.1 Numerical scheme

The numerical methods that were used are found in the CFD program, CFX-F3D. A number of different sized 2-D grids (i.e 364, 700, 1334, 2788, 5800 and 11400 cells) were compared, to test the dependency of the flow pattern and solids concentration distribution in the clarifier on the grid size. A 3-D grid containing 29 x 46 x 60 cells was constructed, which represented the full 360° revolution of the clarifier (Figure 6.2).

The models accuracy also depended on the numerical differencing scheme used, and a first order scheme (UPWIND) was chosen because it gave a more stable solution than a higher order scheme, although it was probably less accurate[16]. Misalignment of the cells with the flow path caused numerical diffusion, which was prevented by omitting the cross-derivative terms in the k and ϵ equations. The method selected for updating the pressure and correcting the velocity components, to satisfy continuity was the SIMPLEC (semi-implicit method for pressure-linked equations correction) algorithm. Buoyancy caused by the higher density of the solids phase caused the instability of the axial velocity calculation, and therefore low values (0.15) for the under-relaxation factors were used for the axial and radial velocities.

Transient simulations were undertaken with a small initial time step (0.1 seconds) to keep the solution stable, and thereby increased incrementally to a larger time step (1200 s) which was kept constant thereafter. For each time step there were 40 iterations for the pressure-correction equation. The residuals for each variable were monitored (every time step) and a converged solution was based on all the

residuals falling below 0.001. A steady-state suspended solids distribution in the clarifier was assumed when the solids volume fraction residual was 0.000001.

The measurements taken of the suspended solids concentration of the influent and the flow rates of the influent, effluent and RAS were entered into the model (see Chapter 5). The effluent and settled sludge (RAS) solids concentrations coming from the secondary clarifier were predicted by the model. Flow patterns and suspended solids concentrations were compared for different values of the parameters in the model. Predicted and theoretical RAS solids concentrations were also compared to check that the model was mass conservative.

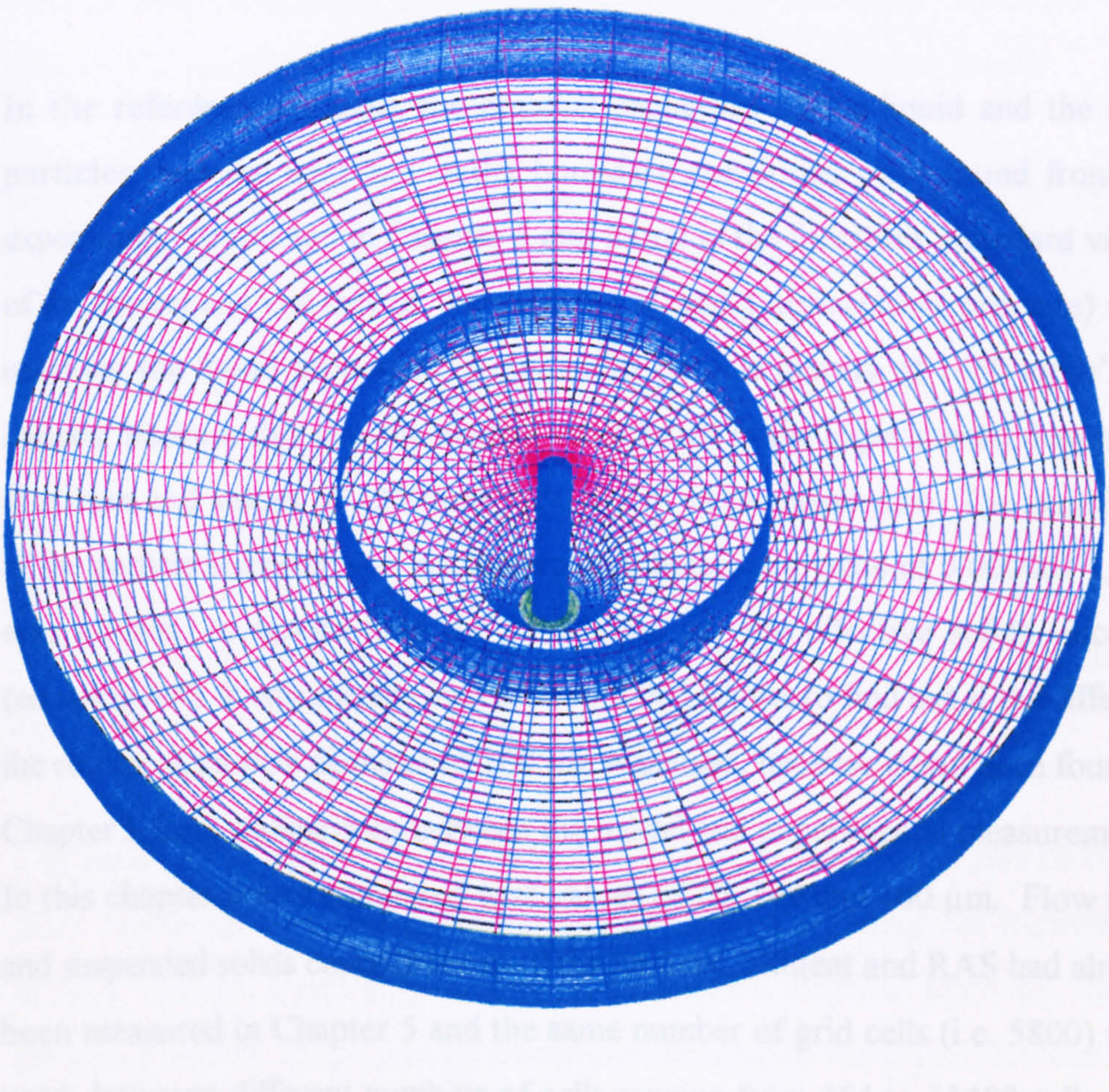

Figure 6.2 Computational grid of the three dimensional clarifier.

6.3.2 Physical parameters

The 'reference test case' refers to case C in Chapter 5 when the model was compared to experimental data. In this chapter the value of the parameters in the reference test case were changed. If there was a large change in the flow pattern (and suspended solid concentrations) in the secondary clarifier, then the new value of the parameter was considered to be outside of the acceptable range of values. However, if the solution was not really affected then the new value was accepted. By using this method the suitable range of values for each parameter was determined. However, the changes to the parameters were not validated with experimental data.

In the reference test case, the physical properties of the liquid and the solid particles, and the inlet and outlet boundary conditions were found from the experiments conducted in Chapter 5 and found in the literature. Standard values of the density and viscosity of water (at 20 °C and 1 atmospheric pressure) were used for the liquid properties. A dry solids particle density of 1450 kg/m^3 was chosen, because this was the median value found in the experimental data in the literature and values of 1250 and 1650 kg/m^3 were chosen also. The magnitude of the particle viscosity was not known and therefore a value of 0.000001 kg/ms was chosen, to ignore it in the calculation of the effective solids viscosity (equation 6.4). It was thereby increased to 0.001 kg/ms to find out if this affected the results. A particle diameter of 100 μm was used, because it had been found in Chapter 5 from comparisons between the model and experimental measurements. In this chapter it was compared with values of 70, 190 and 400 μm. Flow rates and suspended solids concentrations of the influent, effluent and RAS had already been measured in Chapter 5 and the same number of grid cells (i.e. 5800) were used, however different numbers of cells ranging from 364 to 11400 cells were compared. The values for each parameter are shown in Table 6.1.

6.4 RESULTS

6.4.1 Flow patterns

At the reference flow conditions the influent stayed near the water surface, because it was neutrally buoyant, and was deflected downwards upon impingement with the baffle (Figure 6.3a). A radially outwards current was formed below the baffle, which decreased in velocity because of the increasing tank area. It split on the effluent wall to form an upwards flow and a return current along the sloped floor. The upwards flow near the effluent wall split to form an inward return flow and the effluent discharge. The current attached to the floor of the clarifier was caused by the removal of sludge in the hopper.

An increase to the particle diameter from 100 to 400 μm increased the relative Reynolds number (equation 6.7) and decreased the drag coefficient, C_d. The momentum exchange coefficient and therefore the transfer of momentum between the liquid and the solids were reduced (equation 6.2). The lower drag force caused the momentum of the liquid to increase, which was observed by the increase to the axial and radial velocities in the clarifier (Figure 6.3b). A downward jet was formed in the mid-radius of the inlet zone of the clarifier because the decreasing radial velocity (increasing cross sectional area) caused an increase to the relative axial velocity.

The axial slip velocity (equation 6.7) was much smaller when it was calculated from the momentum conservation equation instead of using the experimental settling velocity data. In the axial direction, the relative Reynolds number decreased and the drag force increased and this caused the axial velocities in the clarifier to decrease (Figure 6.3c). In the inlet zone of the clarifier the jet collided with the baffle with a larger horizontal momentum than before and it therefore

formed a stronger downward flow which was attached to the baffle.

The axial turbulent Prandtl number of the solids volume fraction was decreased from 1.0 to 0.5. This caused the axial turbulent mass diffusion of the particles to increase (equation 6.6) and the solids concentrations in the upper region of the clarifier increased. Consequently, the axial and radial liquid velocities in the inlet zone of the clarifier were reduced (Figure 6.3d). The inlet flow did not impinge on the baffle because of the lower radial flow and therefore the downward flow in the inlet zone was separate from the baffle. However, the radial flow below the baffle showed a relative increase in relation to the axial flow.

The inlet suspended solids concentration was doubled to 3400 mg/l which can be found in most heavily loaded secondary clarifiers. This increased the mass flow rate of the solid particles in the influent and thereby increased the solids concentrations in the clarifier and reduced the axial and radial liquid velocities (Figure 6.3e). Doubling the inlet solids concentration had a very similar effect to halving the axial turbulent Prandtl number, in terms of the flow pattern.

Table 6.1 Numerical parameters and suspended solids concentrations.

Reference test conditions	New	New effluent solids concentration, mg/l	New RAS solids concentration, mg/l
Solids density = 1450 kg/m³	-	**31 (reference)**	**5275**
	1250	25	4493
	1650	41	5920
Solids viscosity = 0.000001 kg/ms	0.001	31	5213
Solids diameter = 100 μm	70	105	5105
	190	12	5151
	400	7	4911
Axial slip velocity - measured settling velocity	momentum equation	1	5016
Colloids settling parameter K_1 = 4.2m³/kg	17	11	5256
Turbulent Prandtl number axial = 1.0 radial = 0.5	Both 1.0	35	5161
	Both 0.5	450	4325
Inlet solids concentration = 1700 mg/l	100	7	273
	2260	150	6885
	3400	600	9150
Inlet flow rate = 677 m³/hr	435	13	3377
Number of cells = 5800	364	31	5200
	700	31	5182
	1334	26	5187
	2788	26	5147
	11400	32	5225
	80040	35	5155

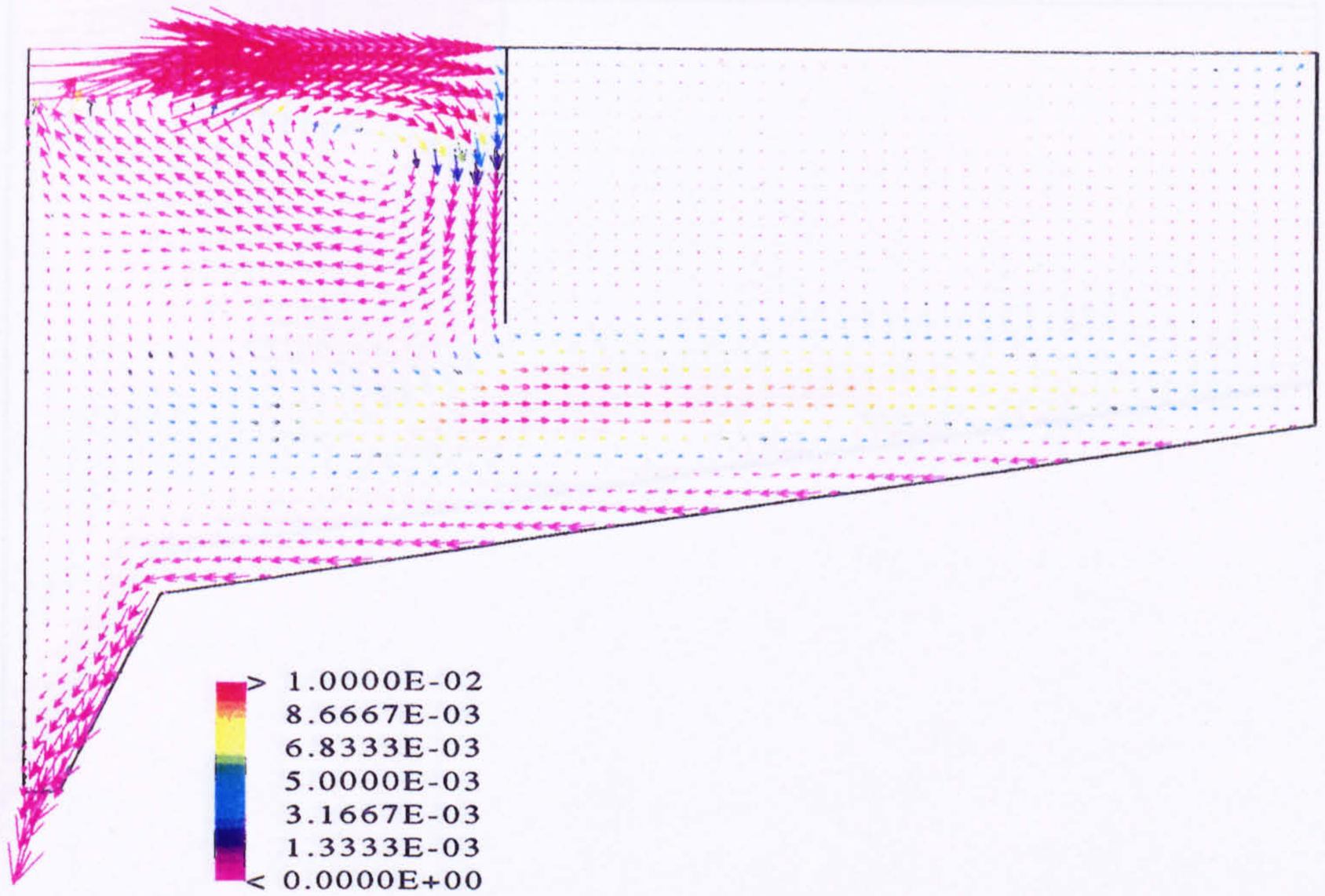

Figure 6.3a Flow pattern in the clarifier at the reference flow conditions (the scale is the radial velocity in m/s)

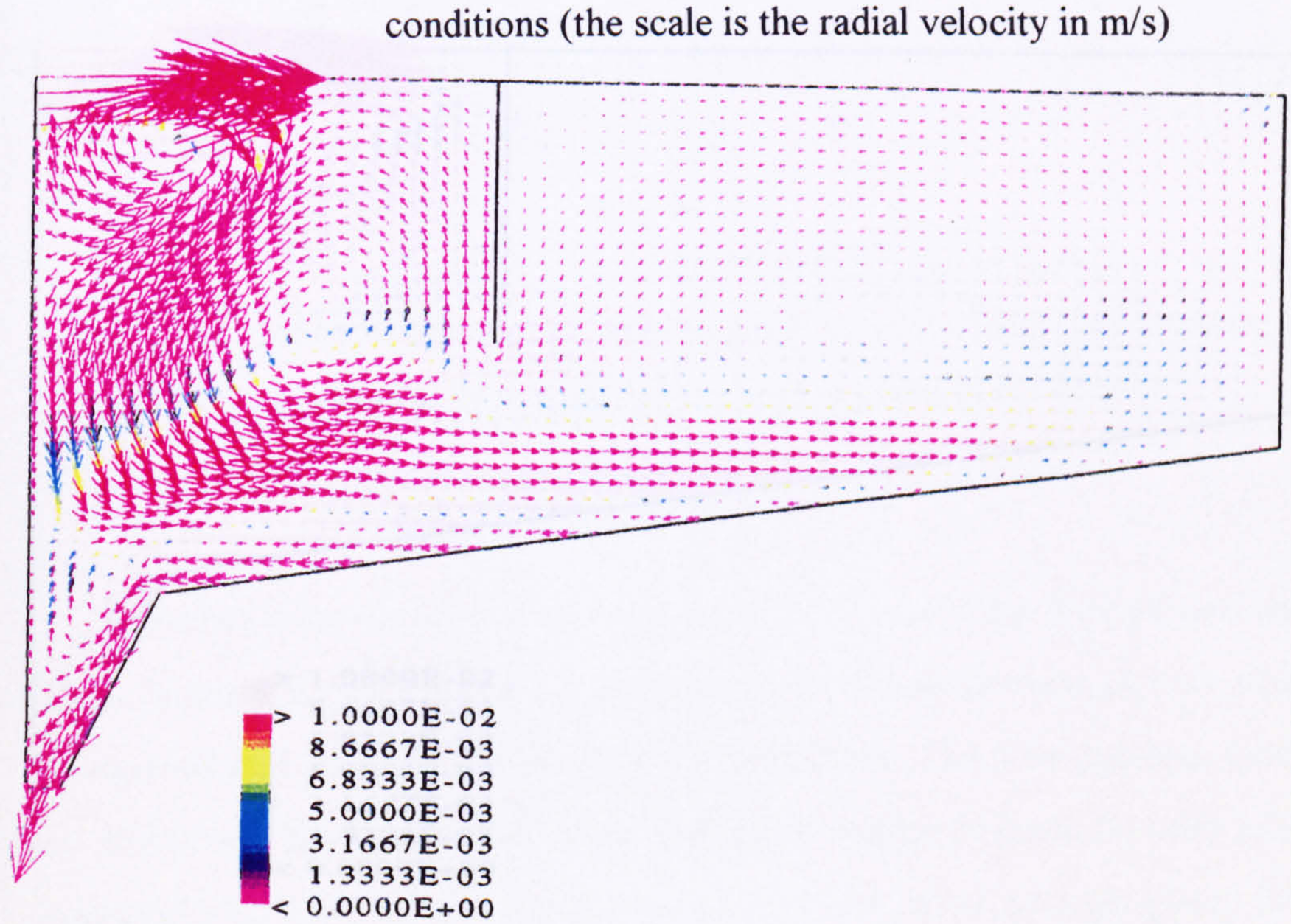

Figure 6.3b Flow pattern in the clarifier with a particle diameter of 400 μm (the scale is the radial velocity in m/s).

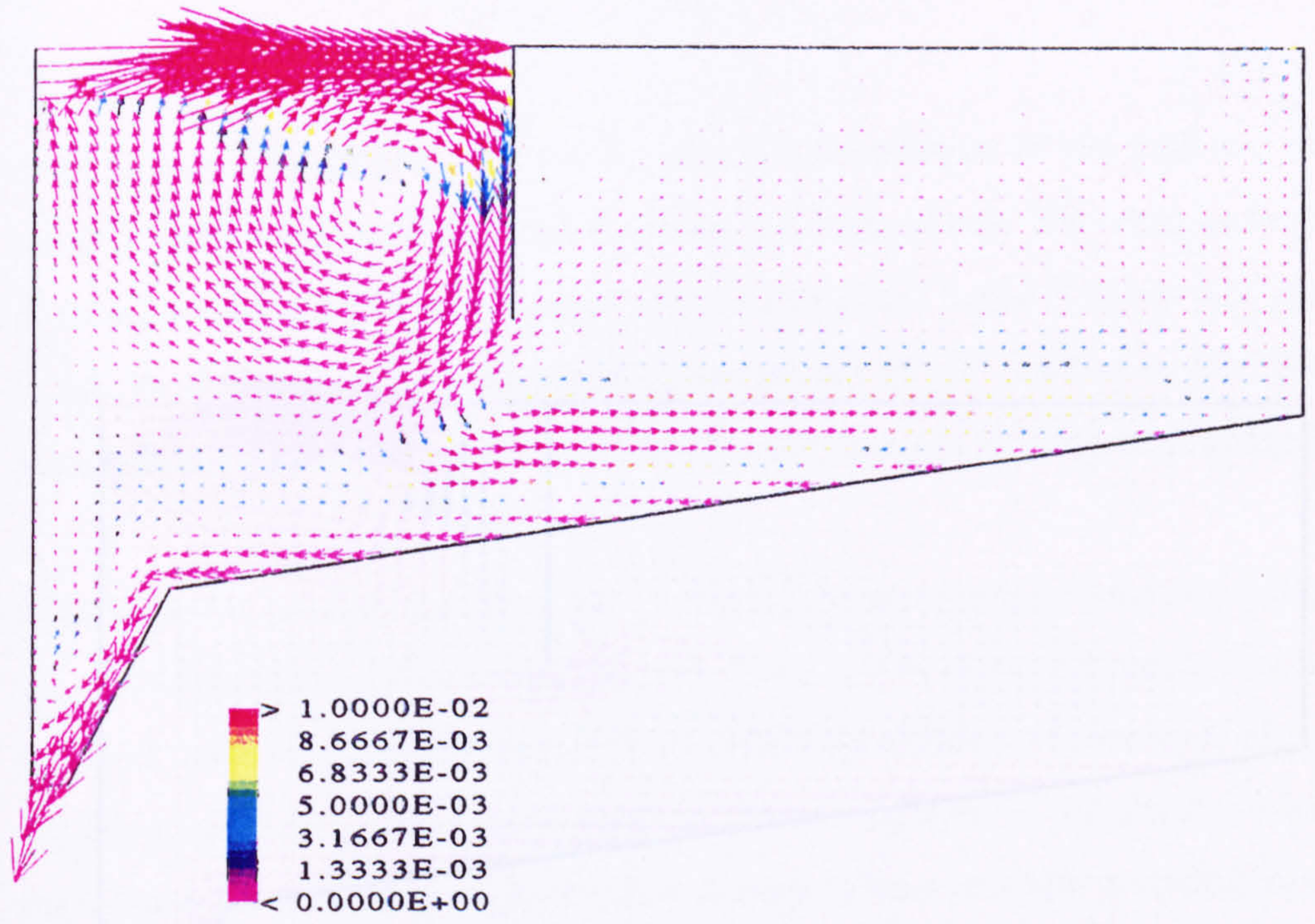

Figure 6.3c Flow pattern in the clarifier with a standard particle drag force (the scale is the radial velocity in m/s).

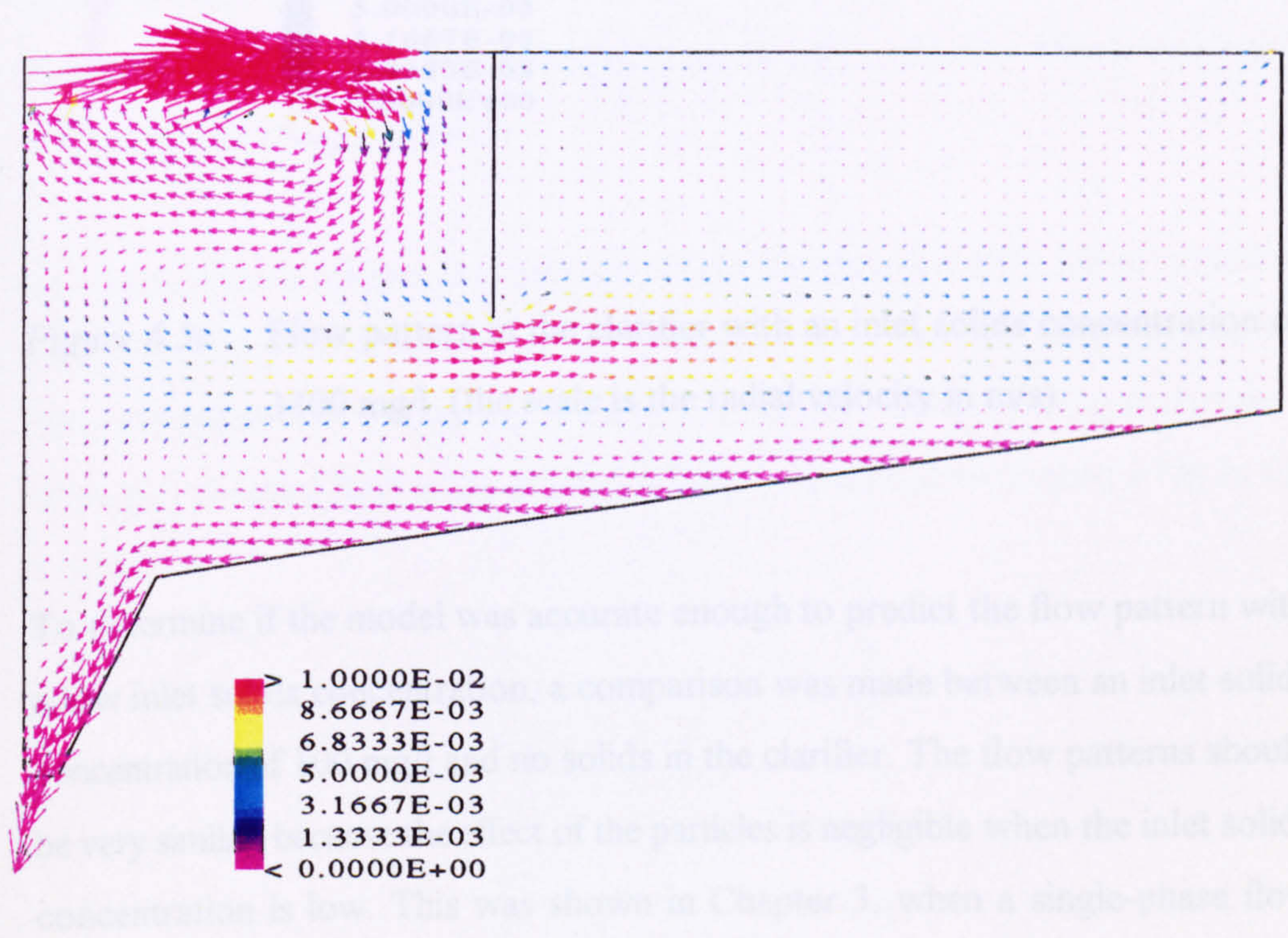

Figure 6.3d Flow pattern in the clarifier with a turbulent Prandtl number of 0.5 (the scale is the radial velocity in m/s).

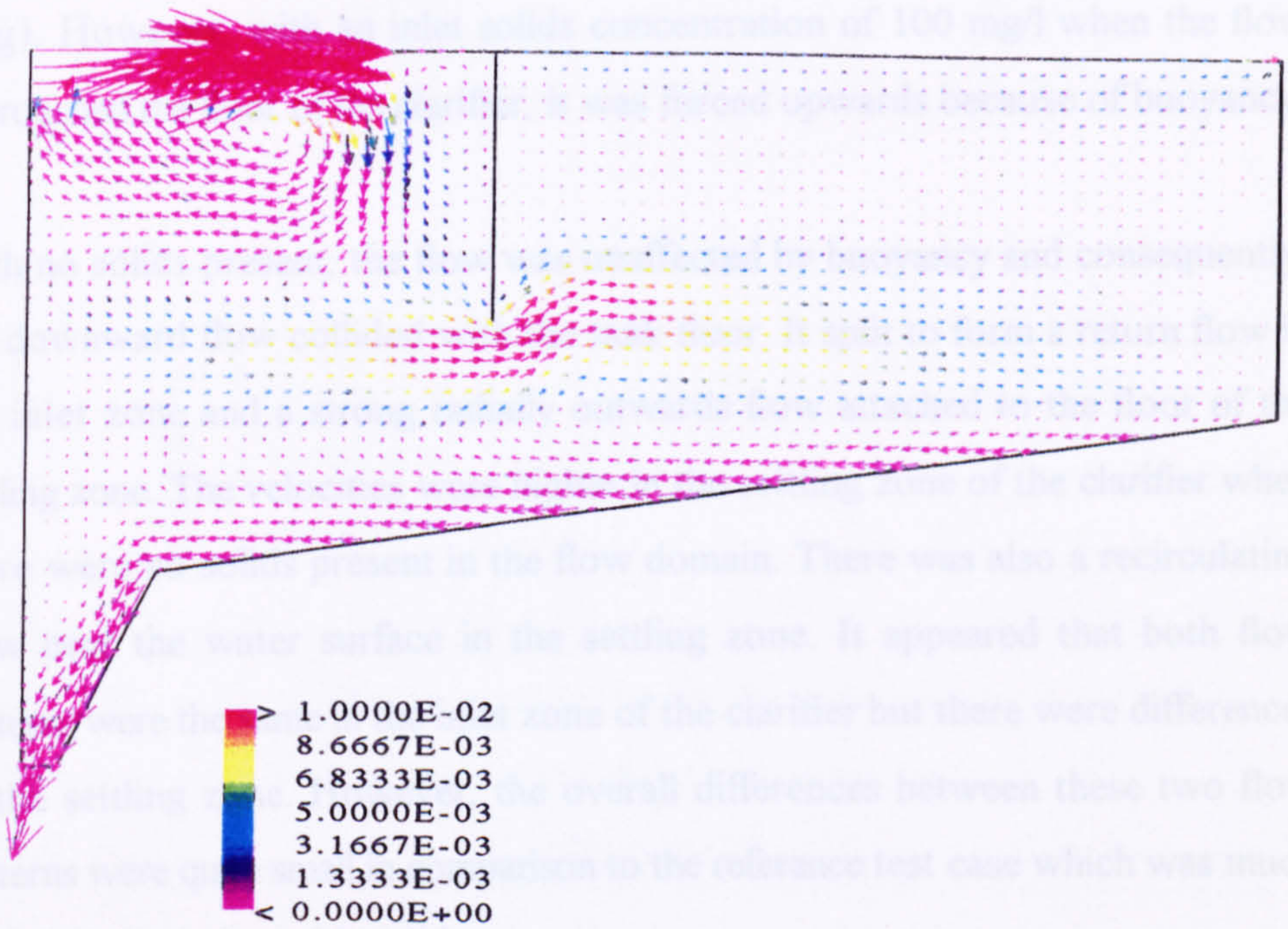

Figure 6.3e Flow pattern in the clarifier with an inlet solids concentration of 3400 mg/l (the scale is the radial velocity in m/s).

To determine if the model was accurate enough to predict the flow pattern with a low inlet solids concentration, a comparison was made between an inlet solids concentration of 100 mg/l and no solids in the clarifier. The flow patterns should be very similar, because the effect of the particles is negligible when the inlet solids concentration is low. This was shown in Chapter 3, when a single-phase flow model predicted quite well the residence time distribution of a full-scale humus tank, which had an inlet solids concentration of only 100 mg/l. The computer

simulations in this chapter with an inlet solids concentration of 100 mg/l and no solids present; both predicted that the influent jet stayed near the water surface. A strong downward flow was attached to the inside of the baffle (Figures 6.3f and 6.3g). However, with an inlet solids concentration of 100 mg/l when the flow approached the floor of the clarifier, it was forced upwards because of buoyancy.

With no solids present, the flow was unaffected by buoyancy and consequently, the downward flow collided with the tank floor. It split to form a return flow in the inlet zone and a strong radially outwards flow attached to the floor of the settling zone. The velocities were higher in the settling zone of the clarifier when there were no solids present in the flow domain. There was also a recirculating flow near the water surface in the settling zone. It appeared that both flow patterns were the same in the inlet zone of the clarifier but there were differences in the settling zone. However, the overall differences between these two flow patterns were quite small in comparison to the reference test case which was much more heavily laden with solids.

A reduction in the influent flow rate (to 435 m^3/hr) decreased the radial velocities in the clarifier, which meant that the downward flow was relatively much larger than the radial flow in the inlet zone of the clarifier. Consequently, there was a strong downward flow and a strong radially outwards flow (Figure 6.3h) in the clarifier.

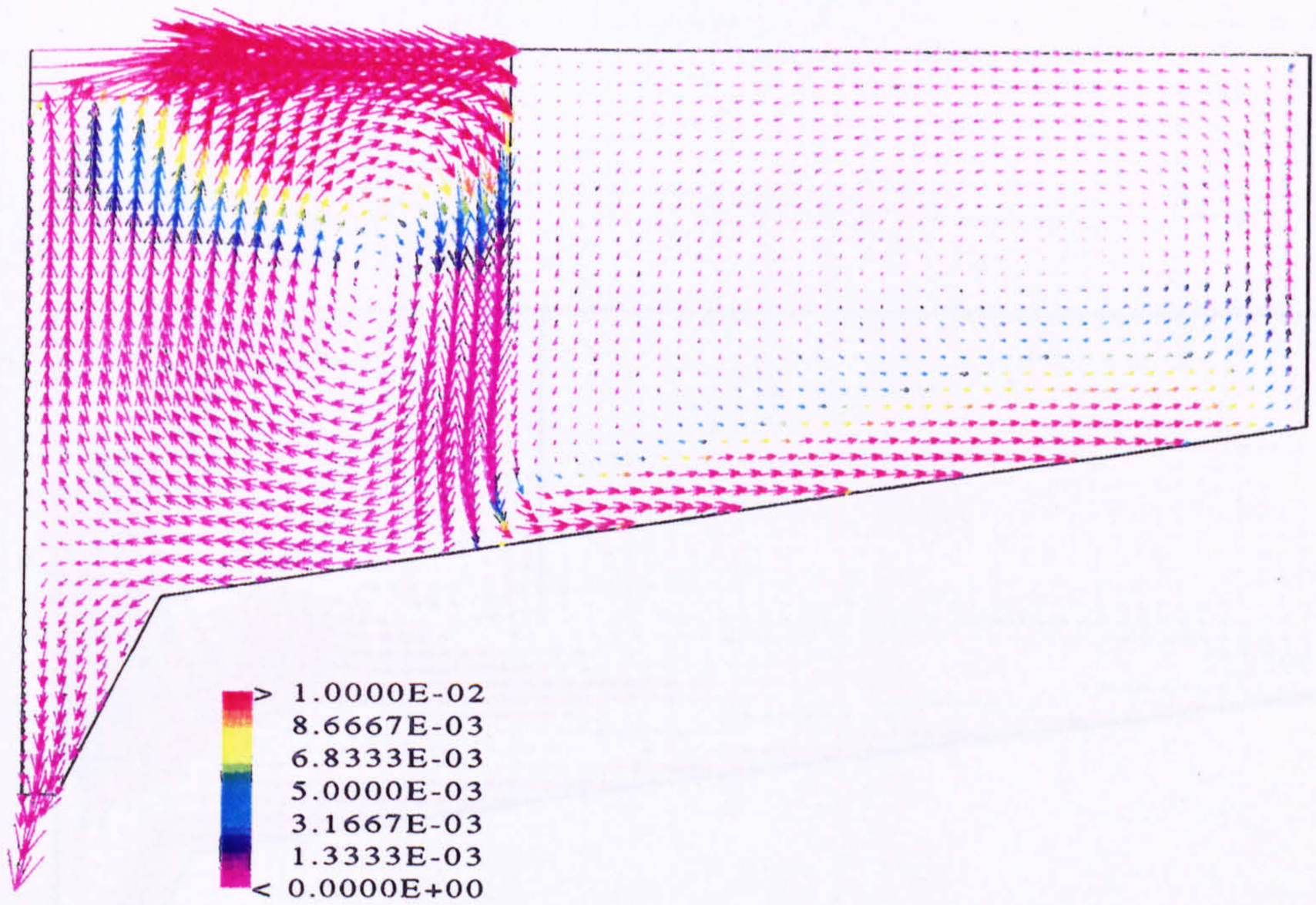

Figure 6.3f Flow pattern in the clarifier with no suspended solids (the scale is the radial velocity in m/s).

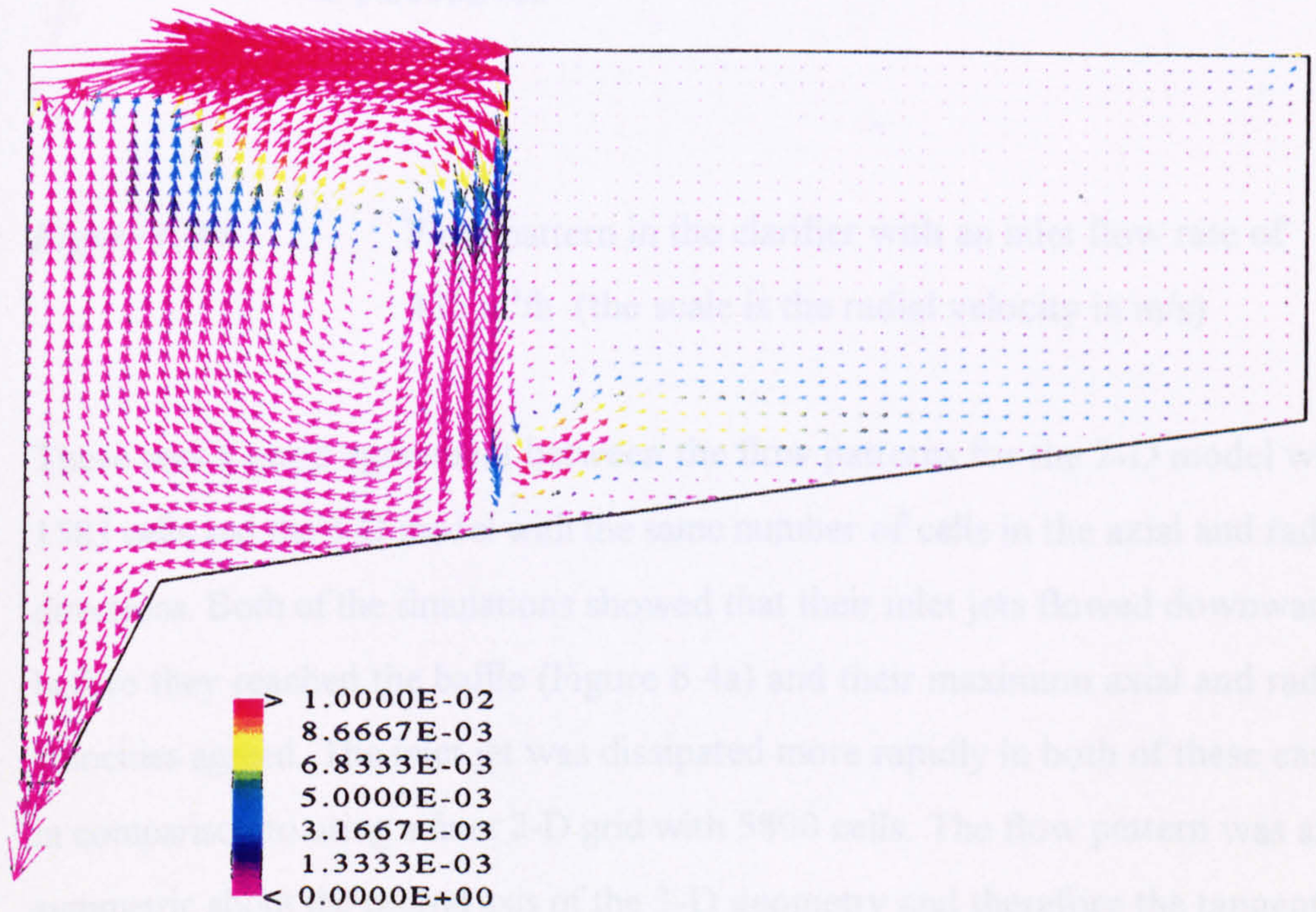

Figure 6.3g Flow pattern in the clarifier with an inlet solids concentration of 100 mg/l (the scale is the radial velocity in m/s).

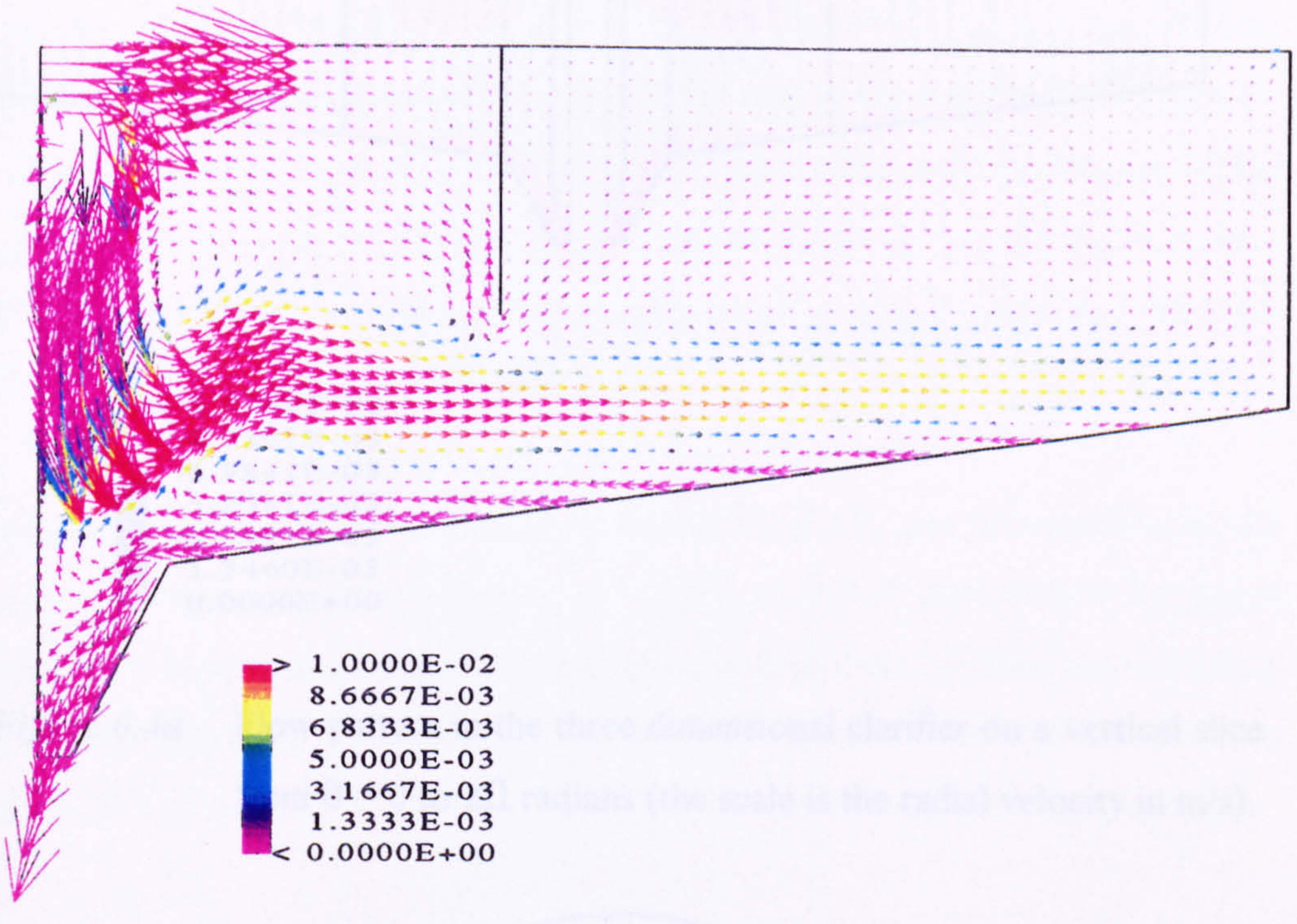

Figure 6.3h Flow pattern in the clarifier with an inlet flow rate of 435 m^3/h (the scale is the radial velocity in m/s).

There was a good agreement between the flow patterns for the 2-D model with 1583 cells and the 3-D model with the same number of cells in the axial and radial directions. Both of the simulations showed that their inlet jets flowed downwards before they reached the baffle (Figure 6.4a) and their maximum axial and radial velocities agreed. The inlet jet was dissipated more rapidly in both of these cases in comparison to using a finer 2-D grid with 5800 cells. The flow pattern was axi-symmetric about the central axis of the 3-D geometry and therefore the tangential velocities were very small compared to the axial and radial velocities (Figure 6.4b).

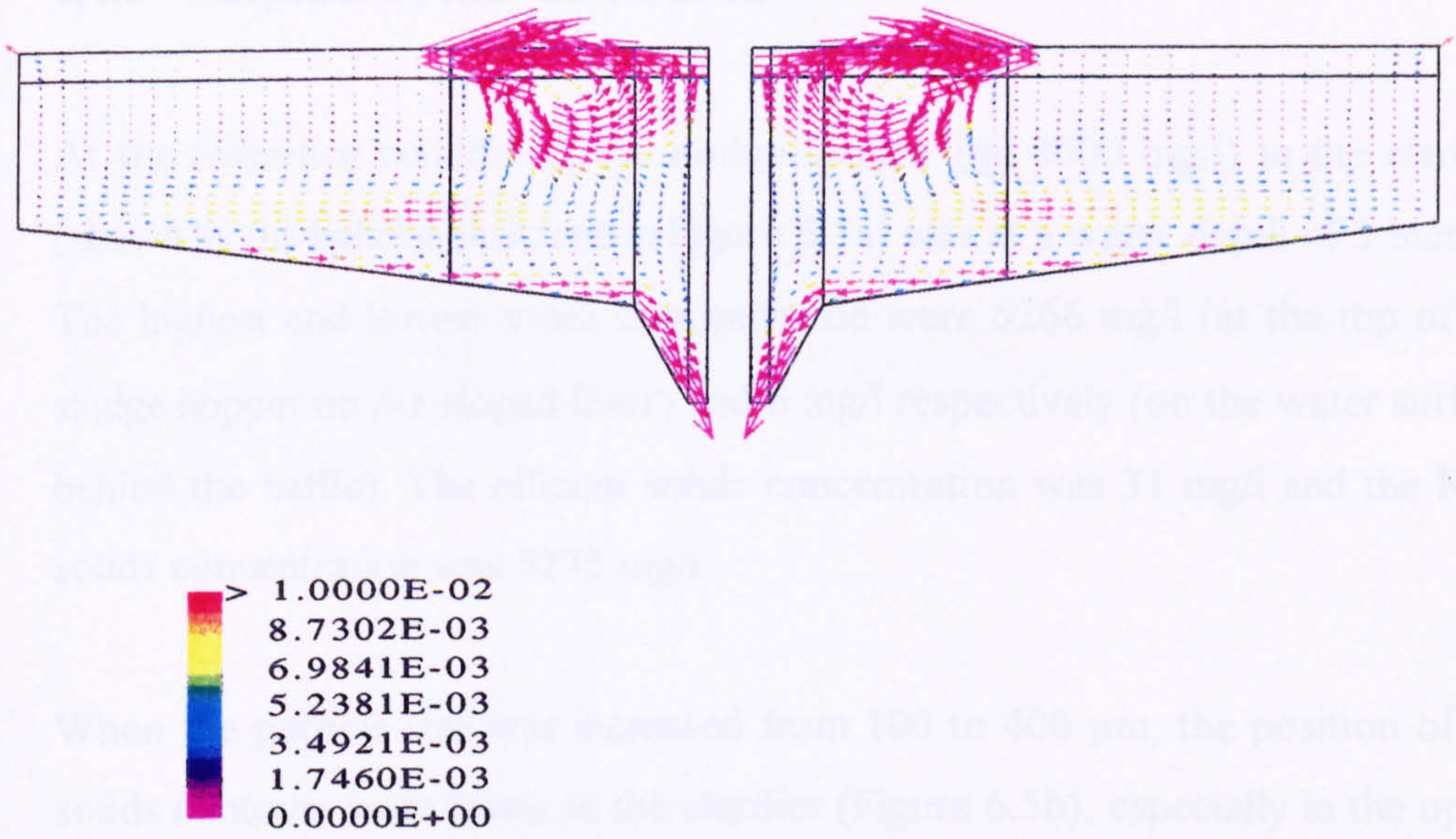

Figure 6.4a Flow pattern in the three dimensional clarifier on a vertical slice from $\theta = 0$ to 2Π radians (the scale is the radial velocity in m/s).

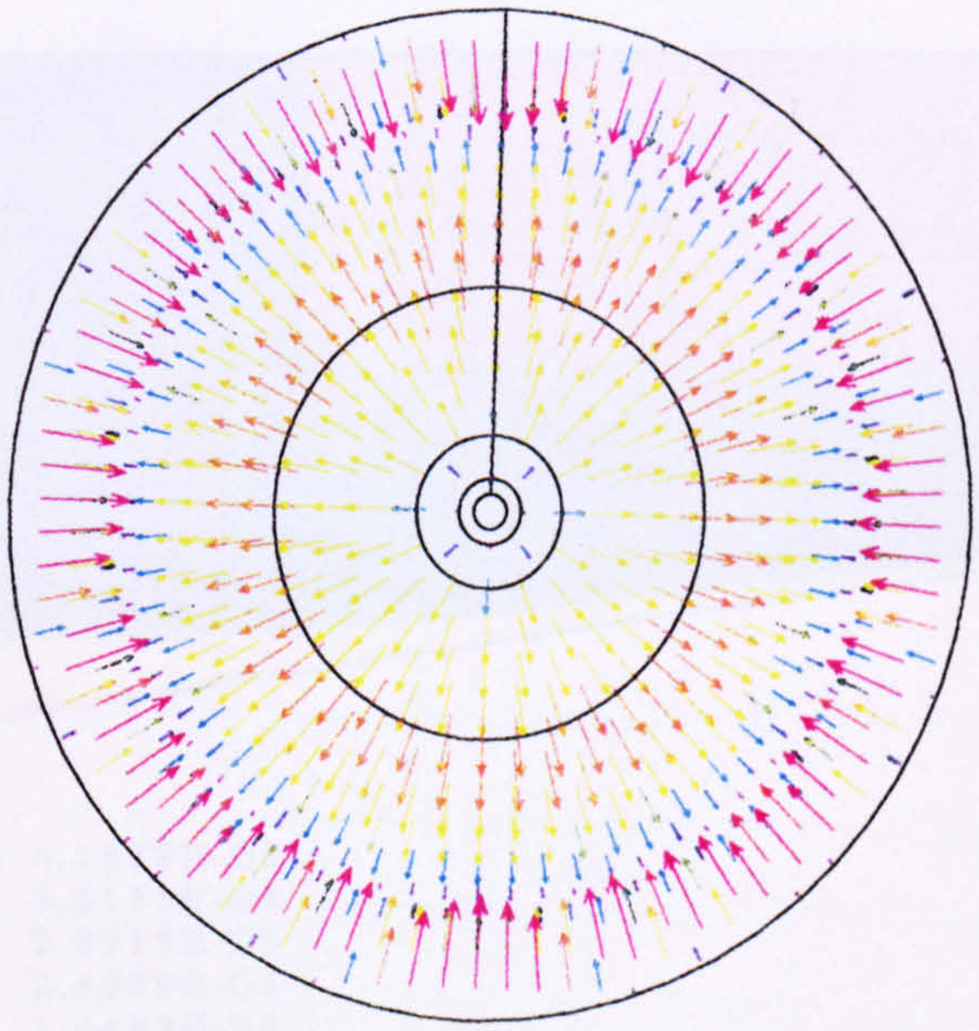

Figure 6.4b Flow pattern in the three dimensional clarifier at a water depth of 3 m (the scale is the radial velocity in m/s).

6.4.2 Suspended solids distribution

At the reference conditions, the sludge blanket (@ 3000 mg/l) in the clarifier (shown by the lightest blue zone in Figure 6.5a) was at a water depth of 3 metres. The highest and lowest solids concentration were 6266 mg/l (at the top of the sludge hopper on the sloped floor) and 6 mg/l respectively (on the water surface behind the baffle). The effluent solids concentration was 31 mg/l and the RAS solids concentration was 5275 mg/l.

When the particle size was increased from 100 to 400 μm, the position of the solids contours were lower in the clarifier (Figure 6.5b), especially in the upper region of the inlet zone when there was increased downward flow in this region. The most significant change was the reduction of the effluent solids concentration from 31 to 7 mg/l.

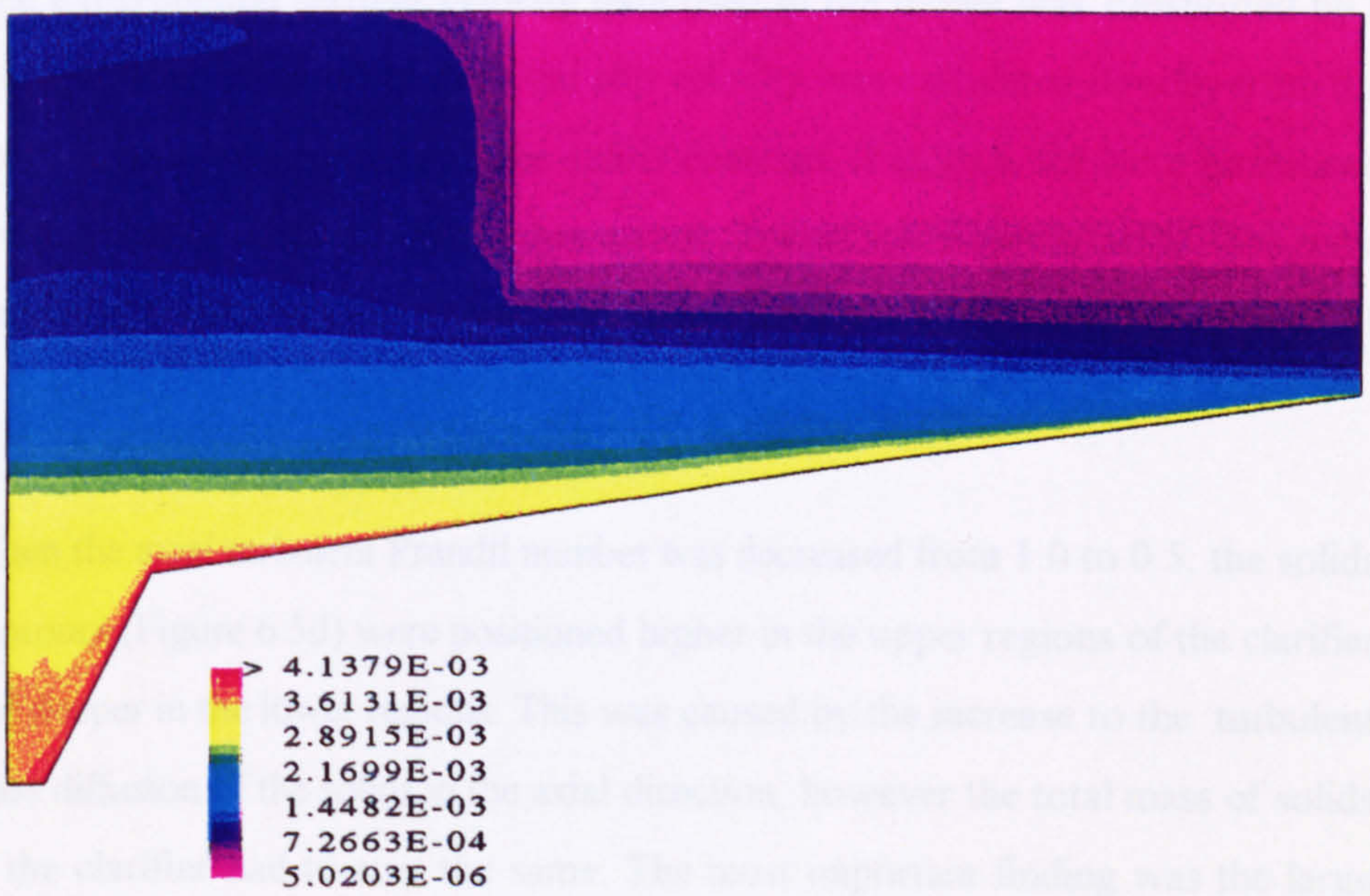

Figure 6.5a Suspended solids concentration distribution in the clarifier at the reference conditions (the scale is the volume fraction of solids).

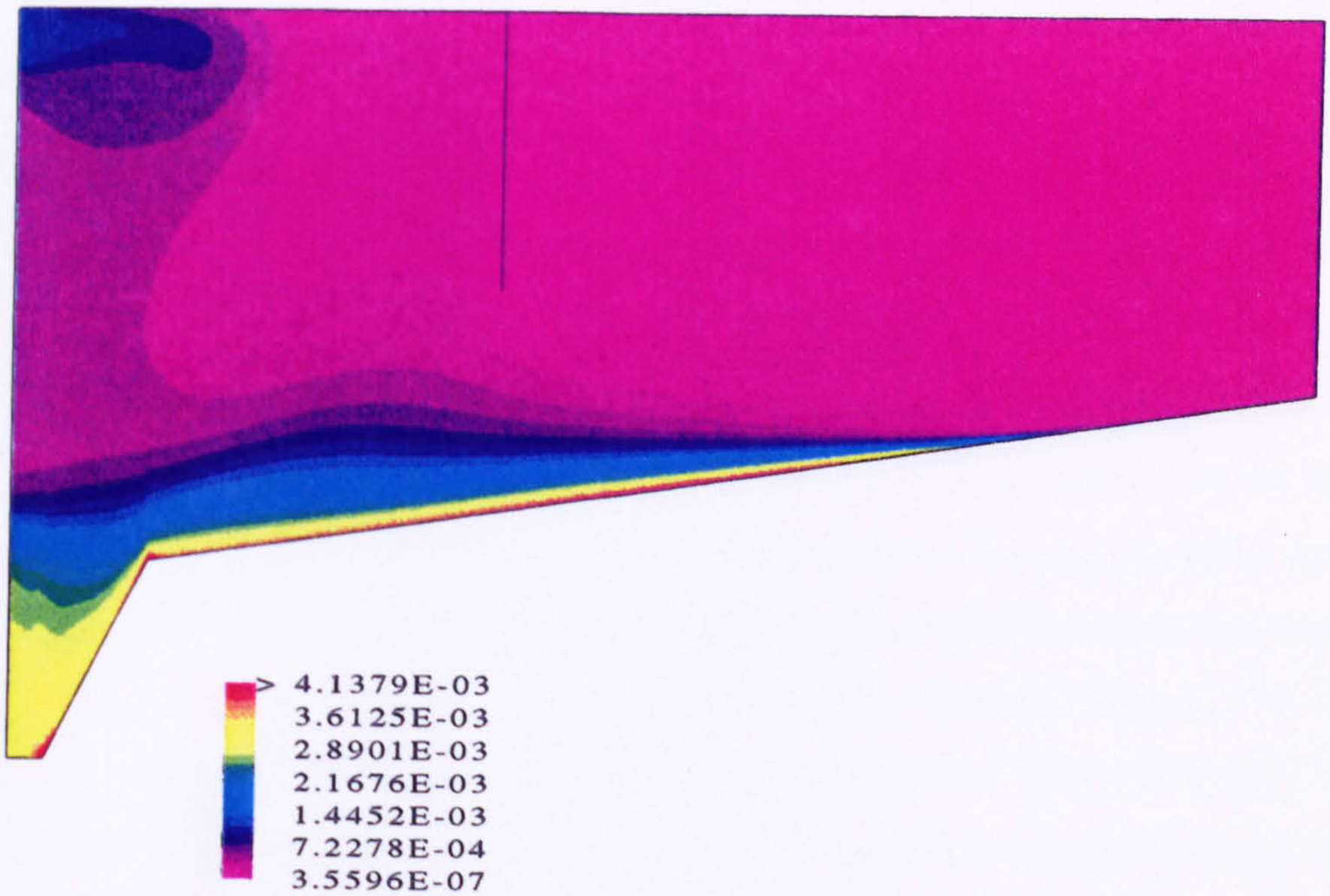

Figure 6.5b Suspended solids concentration distribution with a particle diameter of 400 μm (the scale is the volume fraction of solids).

The experimental settling velocity data used in the model was substituted by a much smaller value when the axial slip velocity was calculated directly from the conservation of momentum. The solids contours (Figure 6.5c) were positioned lower because there was more downward flow attached to the baffle. The most important finding was that the effluent solids concentration was reduced from 31 to 1 mg/l.

When the axial turbulent Prandtl number was decreased from 1.0 to 0.5, the solids contours (Figure 6.5d) were positioned higher in the upper regions of the clarifier and deeper in the lower regions. This was caused by the increase to the turbulent mass diffusion of the solids in the axial direction, however the total mass of solids in the clarifier had to stay the same. The most important finding was the large increase in the effluent solids concentration from 31 to 450 mg/l and the large decrease in the RAS solids concentration from 5275 mg/l to 4325 mg/l.

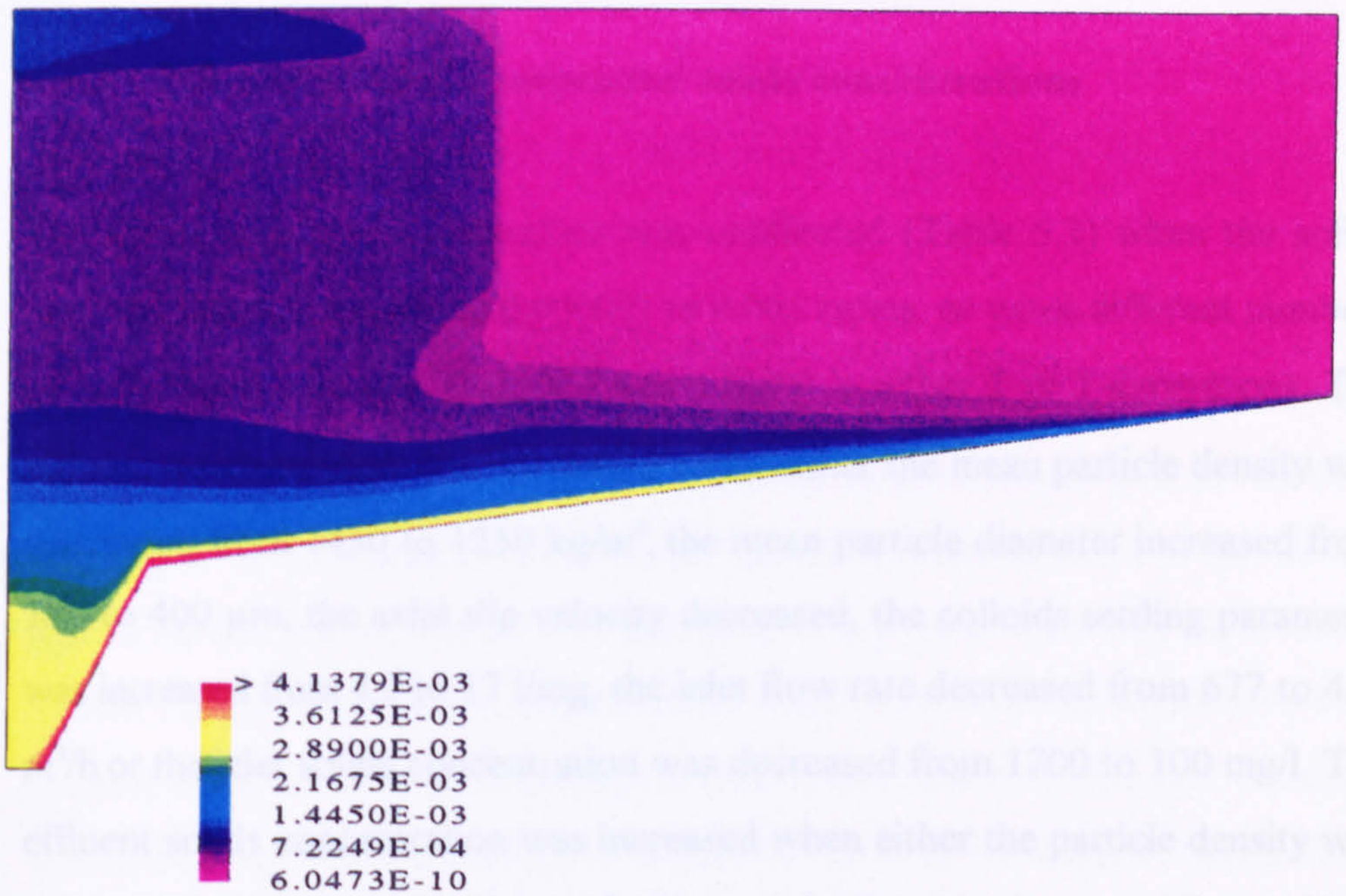

Figure 6.5c Suspended solids concentration distribution with a standard particle drag force (the scale is the volume fraction of solids).

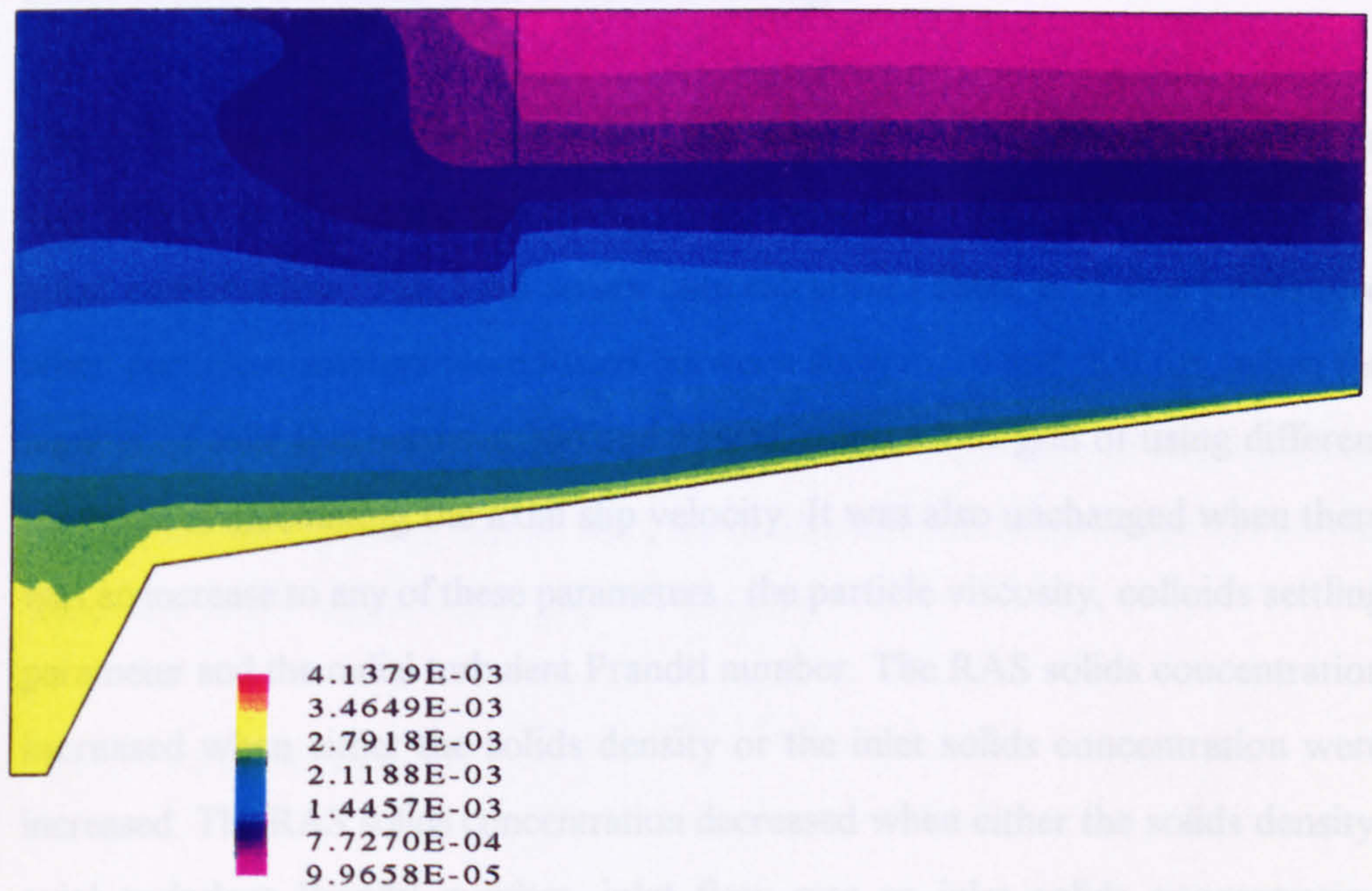

Figure 6.5d Suspended solids concentration distribution with a turbulent Prandtl number of 0.5 (the scale is the volume fraction of solids).

6.4.3 Effluent and RAS suspended solids concentrations

The effluent solids concentration was unaffected (Table 6.1) when the solids viscosity was increased from 0.000001 to 0.001 kg/ms, or when different numbers of cells were used (i.e. from 364 and 11400) in either 2 or 3 dimensions. The effluent concentration was decreased when either the mean particle density was decreased from 1450 to 1250 kg/m^3, the mean particle diameter increased from 100 to 400 μm, the axial slip velocity decreased, the colloids settling parameter was increased from 4.2 to 17 l/mg, the inlet flow rate decreased from 677 to 435 m^3/h or the inlet solids concentration was decreased from 1700 to 100 mg/l. The effluent solids concentration was increased when either the particle density was increased from 1450 to 1650 kg/m^3, the particle diameter decreased from 100 to 70 μm, the radial turbulent Prandtl number was increased from 0.5 to 1.0, the axial turbulent Prandtl number decreased from 1.0 to 0.5 or the inlet solids concentration increased from 1700 to 3400 mg/l.

The difference between the numerical and theoretical RAS solids concentration was within 7% for all the test cases, which meant that the numerical model was mass conservative. The RAS solids concentration (Table 6.1) was unchanged when particle diameters were tested between sizes of 70 and 400 μm, when the number of cells was between 364 and 11400, using a 3-D grid or using different methods of calculating the axial slip velocity. It was also unchanged when there was an increase to any of these parameters : the particle viscosity, colloids settling parameter and the radial turbulent Prandtl number. The RAS solids concentration increased when either the solids density or the inlet solids concentration were increased. The RAS solids concentration decreased when either the solids density, axial turbulent Prandtl number, inlet flow rate or inlet solids concentration decreased.

6.5 DISCUSSION

6.5.1 Particle density

The suspended solids concentration is a product of the solids volume fraction and the mean particle density. Therefore, when the particle density was increased to 1650 kg/m^3 or decreased to 1250 kg/m^3 the solids concentrations in the clarifier (and in the effluent and RAS) were changed, as expected. However, the solution did not change when the inlet particle solids volume fraction was adjusted to keep the inlet solids concentration the same as before. It is recommended that a particle density between 1250 to 1650 kg/m^3 is chosen, which is the range of values found in the literature (see Chapter 5).

6.5.2 Particle viscosity

Particle viscosity had no effect on the flow pattern and solids concentration distribution in the clarifier, for the range of values studied. The values chosen had not changed the value of the effective solids viscosity in equation 6.4. This was because the turbulent viscosity of the solids phase had been much greater than the solid viscosity (i.e. 0.000001 and 0.001 kg/ms) for the range of values studied. Therefore, it was not surprising that these values chosen did not affect the flow patterns. Consequently, future work should be undertaken to study the particle viscosity with a higher value (e.g. 0.1 kg/ms).

6.5.3 Particle diameter

The particle diameter had a significant effect on the flow pattern and the solids concentration distribution in the clarifier. It is used to calculate the exchange of momentum between the phases, in terms of the drag force on the fluid from the

particles. For example, by increasing the particle diameter from 100 to 400 μm, the relative Reynolds number increased and the drag coefficient was reduced. Consequently, the axial and radial velocities were increased in the clarifier (Figure 6.3b). Conversely, the velocities were decreased using a lower particle diameter (i.e. 70 μm). The particle diameters found in Chapter 5 (100 and 130 μm) were derived by comparing the predicted and measured effluent solids concentrations in the Copley clarifier and will be the best values to use.

6.5.4 Axial slip velocity

The settling velocity data of the particles influence the suspended solids concentrations in the secondary clarifier, especially in the withdrawal zone[2-4,6]. When the experimental settling velocity data (in the axial direction) was not substituted for the axial slip velocity, then the downward flow attached to the baffle increased and the effluent solids concentration was under-predicted (1 mg/l).Therefore, the axial slip velocity calculated directly from the momentum equation will be suitable for predicting the flow in a secondary clarifier. The measured settling velocities of the particles were used as a substitution for the axial slip velocity[12]. However, care must be taken because if they are substituted for the axial slip velocity then this does not consider the influence that radial flow in a sedimentation tank will have on the settling velocity of a particle.

6.5.5 Colloids settling parameter

Increasing the colloids settling parameter reduced the effluent concentration, but had no effect on the RAS solids concentration. If there had been more accurate measurement data for the settling velocities at low solids concentrations then the colloids settling parameter could have been directly found from the experiments. However, it was assumed that the transition from flocculent to hindered settling

occurred between 200 mg/l and 500 mg/l[12,14]. Indeed, the 2 parameters in the multi-fluid model that had been hardest to measure were the particle diameter and the colloids settling parameter. If the particle diameter had been accurately measured then the colloids settling parameter could have been found instead of the particle diameter by comparing the predicted and measured effluent solids concentration.

6.5.6 Turbulent mass diffusion of the particles

Reducing the axial turbulent Prandtl number from 1.0 to 0.5 made a large difference to the suspended solids concentration in the clarifier. Therefore, this parameter should really not be changed from a value of 1.0. Changing the radial turbulent Prandtl number however had little effect. Consequently, any value between 0.5 and 1.0 would be suitable for the radial turbulent Prandtl number. The tangential turbulent Prandtl number was not an influential parameter in the 3-D flow model in this work because the tangential velocities were very low. However, if swirling flow had been included in the 3-D model then the turbulent Prandtl number would probably have an influence on the flow patterns.

6.5.7 Inlet flow rate and suspended solids concentration

The effluent and RAS solids concentrations were dependent on the solids loading to the clarifier, which was a product of the inlet solids concentration and the inlet flow rate. Therefore when the inlet flow rate was decreased the effluent and RAS solids concentrations decreased. When the inlet solids concentration was increased the effluent and RAS solids concentrations and the maximum bottom current increased, which had been observed by other researchers[2,8]. The flow rates and solids concentrations of the influent, effluent and RAS should always be measured when modelling a secondary clarifier.

6.5.8 Number of cells and dimensionality

The minimum number of cells that was able to capture the flow pattern in the secondary clarifier was 2788. In fact, the radial flow in the upper region of the clarifier was not captured fully when fewer cells were used (i.e. 1334). The 2-D axi-symmetric model predicted the same flow pattern as the 3-D axi-symmetric model, which had been expected. Swirling flow could have been included in the 3-D simulation, if the tank's geometry had been non-symmetrical about the central axis, or if the effect from wind or the rotating sludge scraper had been included in the model.

6.6 CONCLUSIONS

1. In a circular secondary clarifier, the effluent and RAS suspended solids concentrations were unaffected by the solids molecular viscosity and the 3-D simulation. The RAS concentration was also unaffected by the particle diameter, the axial slip velocity, the colloids settling parameter and the radial turbulent Prandtl number of the volume fraction.

2. The effluent solids concentration was affected by the particle density, particle diameter, axial slip velocity, colloids settling parameter, axial turbulent Prandtl number, inlet flow rate and the inlet solids concentration.

3. The RAS solids concentration was affected by the particle density, axial turbulent Prandtl number, inlet flow rate and the inlet solids concentration.

4. Recommended values for the particle density are between 1250 to 1650 kg/m^3, particle diameter is 100 μm, colloids settling parameter is between 4.2 to 17 l/mg, axial and radial turbulent Prandtl numbers are 1.0 and between 0.5 to 1.0 respectively, and the number of cells is 2788.

This chapter has shown how most of the important parameters in the multi-fluid model affect the flow pattern and suspended solids concentrations in a secondary clarifier and has recommended the best values to use for some parameters. This should allow the model to be used to predict the flow in other circular secondary clarifiers. The contents of this study and the 3-D simulation of the secondary clarifier are novel areas of research. There are concerns however about the way the transfer of momentum between the phases has been defined in this work and the use of a symmetry plane to represent the water surface. These assumptions will indeed have a major influence on the flow patterns and suspended solids concentrations presented in Chapters 5 and 6 of this thesis. The criticisms of these assumptions are given in Chapter 5 and in the overall discussion of the thesis which is presented in the next chapter.

6.7 REFERENCES

1. DeVantier, B.A. and Larock, B.E. (1986). 'Modelling a recirculating density-driven turbulent flow'. International Journal of the Numerical Methods in Fluids, vol. 6, 241-253.
2. DeVantier, B.A. and Larock, B.E. (1987). 'Modeling sediment-induced density currents in sedimentation basins'. Journal of Hydraulic Engineering, vol. 113, 80-94.
3. Samstag, R.W., Dittmar, D.F., Vitasovic, Z., McCorquodale, J.A. (1989). 'Underflow geometry in secondary sedimentation'. Water Environmental Research, vol. 64, no. 3, 204-212.
4. McCorquodale,J.A., YuenE.M., Vitasovic,Z. and Samstag, R. (1991). 'Numerical simulation of unsteady conditions in clarifiers'. Water Pollution Research Journal of Canada, vol. 26, 201-222.
5. Krebs, P., Vischer, D. and Gujer, W. (1995). 'Inlet-structure design for final clarifiers'. Journal of Environmental Engineering, vol. 121, no. 8, 558-564.
6. Zhou, S. and McCorquodale, J.A. (1992). 'Mathematical modelling of a circular clarifier'. Canadian Journal of Civil Engineering, vol. 19, 365-374.
7. Zhou, S. and McCorquodale, J.A. (1992). 'Influence of skirt radius on performance of circular clarifier with density stratification'. International Journal of Numerical Methods in Fluids, vol. 14, 919-934.
8. McCorquodale, J.A. and Zhou, S. (1994). 'Effects of hydraulic and solids loading on clarifier performance'. Journal of Hydraulic Research, vol. 31, no. 4, 461-478.
9. McCorquodale, J.A. and Zhou, S.P. (1994). Use of numerical models in clarifier design- optimization of inlet structures. 67th Annual Conference of the Water Environment Federation, Chicago.

10. Larsen, P. (1977). On the hydraulics of rectangular settling basins, experimental and theoretical studies. report no. 1001, Department of Water Resources Engineering, Lund Institute of Technology, Lund University, Lund, Sweden.

11. Vesilind, P.A. (1974). Treatment and Disposal of Wastewater Sludges. Ann Arbor Science Publishers Inc., Ann Arbor, Michigan

12. Takacs, I., Patry, G.G. and Nolasco, D. (1991). 'A dynamic model of the clarification-thickening process'. Water Research, vol. 25, 1263-1271.

13. Matko, T., Fawcett, N., Sharp, A. and Stephenson, T. (1996). 'Recent progress in the numerical modelling of wastewater sedimentation tanks'. Transactions of the Institution of Chemical Engineers, part B3, vol. 74, 245-258.

14. Degremont (1991). Water Treatment Handbook. 6th English edition. Lavoisier Publishing, Paris, France, vol. 1, 161, 370.

15. Matko, T., Fawcett, N., Sharp, A. and Stephenson, T. (1996). 'A numerical model of flow in circular sedimentation tanks'. Transactions of the Institution of Chemical Engineers, part B3, vol. 74, 197-204.

16. Anderson, J.D. Jr. (1995). Computational Fluid Dynamics. The Basics with Applications. McGraw-Hill, Inc.

CHAPTER VII

DISCUSSION

Sedimentation may be a conceptually simple process but it is complex in practise. A numerical model for predicting the flow in sedimentation tanks needs therefore to be simplified, otherwise the computational effort is very large. Indeed, there were several modelling assumptions made in this project, as follows :

The 3-D effects on flow are more pronounced in rectangular clarifiers in the corners of the tank, but the flow in a circular clarifier can also be affected by swirling flow. This is caused by the intense energy dissipation in the inlet zone of the clarifier, the wind forces on the water surface, a non-symmetrical tank geometry and the rotation of the sludge scraper. The model may be simplified, because in the absence of wind the flow has been observed to be essentially 2-D in a vertical plane[1-2]. Therefore, a 2-D axi-symmetric model was used for nearly all the simulations in this study and saved a considerable computational effort[3-14]. A 3-D axi-symmetric simulation of a secondary clarifier was also undertaken, but there were no differences in the simulated flow pattern. This was because there was a symmetrical geometry and the wind and rotation of the sludge scraper were not modelled.

If there is not much swirling flow in a circular clarifier and the flow is fully turbulent, then the standard k-ϵ turbulence model should be sufficiently accurate and the more advanced turbulence models may not be required. The standard k-ϵ turbulence model has been used in most of the secondary clarifier models[8-13,15].

However, the numerical modelling of turbulent multi-phase flow is not as well understood as single-phase flow and there is no standard industrial multi-phase model like the single-phase k-ϵ model.

Both the liquid and solid phases were assumed to be turbulent and used the same turbulence model with no inter-phase transfer of turbulence. There was an option in the program CFX-F3D to model the solids phase as laminar and the liquid phase as turbulent. The effect of turbulence on the solids phase is enabled by setting the solids phase viscosity proportional to the continuous phase eddy viscosity. It may have been better to have a laminar dispersed phase rather than modelling all the phases as turbulent. This is because the turbulent constants in the standard k-ϵ model have been traditionally found from experiments conducted on viscous fluids and are not really known for particles.

There is additional production and dissipation of turbulence in the multi-fluid model which is not captured by the single-phase flow source terms in the transport equations of k and ϵ. Large particles are known to enhance turbulence, due to the production of a turbulent wake behind the particles and small particles are known to suppress turbulence. However, to avoid a further complexity in the model this was assumed to be negligible. Indeed, the magnitude of these terms is not really known.

Single-phase wall functions are known to be inadequate for multi-phase flow near a wall. The use of single-phase wall functions will only be safe if the flow is sufficiently stratified that mostly one phase is adjacent to any one wall. This will be true because the volume fraction of the liquid phase is much greater than the solids phase in all regions of a secondary clarifier.

The water surface was simplified by a symmetry plane, which neglected the effect of wind, the buoy of the surface above the inlet vertical jet and the movement of the water surface caused by the variation in flow. In the program CFX-F3D it is possible to model a free surface (e.g. an air-water interface) without a discrete phase (e.g. no solid particles or air bubbles). This could have been compared to the single-phase flow predictions with the symmetry plane. However, it is not possible using version 4.1 of the software to model a free surface when the Eulerian multi-fluid model is being used. Moreover; the program does not have the capability to model two continuous phases (liquid and air) and a discrete phase (solids) when using the Eulerian multi-fluid model on its own. The influence of the wind could not be modelled because the shear forces acting on the water surface were not known. However, it would have been very desirable to model the free water surface because there were disadvantages to assuming a symmetry boundary plane at the water surface. The mean radial velocities near the water surface were over-predicted and this was observed by the under-prediction of the mean residence times of the effluent for the single-phase flow model. No free surface modelling of the water surface in a sedimentation tank has been reported before in the literature.

When the influent enters at a different temperature to the surrounding fluid, density stratification will occur, which mostly affects primary clarifiers[16-20]. In secondary clarifiers, the high inlet solids concentration will have a much more significant effect on density stratification. Therefore, heat transfer was ignored and saved computational effort. Most circular secondary clarifiers have a sloping floor to encourage the solids to move towards the sludge hopper after settling on the floor, and this type of tank was modelled in this study. Only secondary clarifiers with flat floors have been simulated before[6-13].

The single-phase flow model agreed qualitatively with the measured residence time distribution of the effluent in a full-scale humus tank. Modelling an upward velocity at the top surface of the inlet pipe gave a very similar flow pattern to a horizontal inlet velocity. This was expected, because the symmetry boundary condition at the water surface caused the vertical inlet jet to be rapidly dissipated and converted into a radial jet along the water surface. In the past, this comparison has never been made as the horizontal influent was always used, most probably to make convergence easier. It has nevertheless been useful to check which inlet flow boundary is preferable.

Modelling the variable flow to the full-scale humus tank improved the correlation with the measured RTD of the effluent. This suggested that modelling the real plant flows would also be an important consideration for the two secondary clarifiers. A variable flow to a secondary clarifier has been simulated before, but without any comparisons to experimental data[8]. There are concerns about the modelling of the water surface as a symmetry plane because the water depth in the clarifier is therefore not affected by the variable flow. The peripheral weir keeps the level of the water constant at the weir, but does not prevent the water surface rising away from the weir. The model will not be able to predict that the suspended solids can be carried into the effluent channel when the water depth in the clarifier is changing. The variability of the measured flow rate upstream of the clarifier will be reduced (damped) by the time it reaches the inlet of the clarifier and the time lag can also affect the magnitude of the inlet flow to the clarifier. The inlet flow should be measured as close as possible to the inlet of the clarifier in the future.

The double exponential equation[3-4,8-13], that best represents the settling velocity distribution of the particles was used. The experiments to measure the settling

velocity were conducted in a settling column, in quiescent flow conditions, and did not mimick the turbulent flow conditions in a full-scale clarifier. Particle resuspension is less in a settling column, and therefore the measured settling velocities in the column will be higher than in the full-scale clarifier. Radial flow reduces the downward settling velocity of a particle in a clarifier but is ignored in a settling column. Another concern was that the settling velocities at low solids concentrations had been difficult to measure and therefore, an assumption had to be made to find the colloids settling parameter. Nevertheless, the settling column method is still the best technique for measuring settling velocities.

The biggest problem in the modified multi-fluid model used in this work was the incorrect implementation of the term in the momentum equation for the inter-phase momentum transfer. By making the axial drag of the particles equal to the settling velocity and using the default calculation for the radial drag coefficient, consequently the effect of the radial flow on the particle settling velocity was not considered. It was probably also incorrect to split the drag force on the particle into two components because the relative Reynolds number and the drag coefficient are related non-linearly. The flow patterns and suspended solids concentrations are affected by the drag coefficient in both the axial and radial directions and therefore the multi-phase flow patterns in this work are incorrect. Until the correct particle drag is implemented into the model then clearly the effect it has on the flow patterns will not be clearly understood.

Particle settling is normally opposed by particle resuspension in the axial direction of a circular secondary clarifier. Indeed, the suspended solids concentrations in the secondary clarifier (without the deflector plate) were sensitive to the axial turbulent Prandtl number. Therefore, the solution was sensitive to particle resuspension in the axial direction. The particle resuspension near the floor of a

secondary clarifier has been represented before using a resuspension coefficient[8-12], but this was not needed in the multi-fluid model. The sensitivity of the turbulent Prandtl numbers have not been studied before in other secondary clarifier models[4, 8-9,13].

The particle size distribution in a wastewater was simplified to a mean particle diameter. While this causes the particle drag distribution of the solids suspension to be unrealistic, it is unreasonable in terms of the computational effort to use a number of dispersed phases to account for the particle size distribution. It is difficult to measure the mean particle diameter because activated sludge flocs are irregularly shaped. Therefore, the particle size was used really as an output from the model by comparing the predicted and measured effluent solids concentration. Measurements of the particle diameter in the literature have ranged from 20 to 200 μm[22-24], which were very similar to the multi-fluid model's predictions, i.e. 100-190 μm. Previous clarifier models have not used a particle diameter, nor calculated the drag force. Instead, they used a single-phase flow transport equation for the liquid and a density stratified transport equation for the suspended solids. Therefore, the multi-fluid model represents a more fundamental approach to modelling multi-phase flow.

Good correlations were found between the predicted and measured residence time distributions of the effluent for the secondary Copley clarifier. The residence time distributions of the RAS agreed for only one of the test cases. This can be attributed to the incorrect formulation of the interphase momentum coefficient, the assumption of a symmetry plane to represent the water surface, the measurement of the inlet flow rate upstream of the clarifier and the measured RAS flow rate downstream of the secondary clarifiers. A solids contour in each of the secondary clarifiers was predicted quite well by the model, but this was partly caused by

making the effluent solids concentration an input to the model. Unfortunately, no measurements of the flow velocities were taken in the clarifiers and therefore it is not known how accurate the predicted flow patterns are. The flow velocities in the single-phase flow simulations are expected to be closer to experimental data than the multi-phase flow predictions because there is no inter-phase momentum term. However, if the free surface is included then the comparison to experimental data will probably improve. Comparisons have been made between the predicted and measured flow velocities[3,6-8,10-12] and solids concentration contours[4,9] in other models of secondary clarifiers.

The residence time of the effluent in the secondary clarifier with the deflector plate was not well predicted and this can be attributed to not using a 3-D model. The turbulent jet between the deflector plate and the baffle is essentially 3-D, because the jet spreads out tangentially as it moves radially outwards and because turbulence is 3-D. It might also be interesting to find out what is the effect of modelling the variable plant flow rates on the predicted residence time of the effluent. Few secondary clarifiers have a deflector plate and a turbulent jet flow is difficult to model, especially with a multi-phase flow. These are probably the reasons why it has not been reported before in the literature.

When the parameters were changed in the multi-fluid model in the sensitivity study, it would have been desirable to compare the results with experimental data. However, this was not necessary because the effects that the parameters have on the models predictions were being investigated. It was concluded that several parameters can be kept constant in the multi-fluid model for most flow conditions in secondary clarifiers; i.e. the fluid density and viscosity, particle density and viscosity and the axial and radial turbulent Prandtl numbers of the volume fraction. The axial and radial slip velocities should not be calculated directly from the

momentum equation, but as a function of the particle settling velocity. There needs to be more information to determine the correct value of the molecular viscosity of the particles. The flow rates and suspended solids concentrations at the inlet and outlets of the clarifiers should always be measured. A 2-D model of the flow in a circular clarifier is probably sufficient, but a comparison with a 3-D simulation with a rotating sludge scraper is desirable.

The most sensitive parameters on the simulated flow patterns in the secondary clarifier were found to be the particle density, particle diameter, axial slip velocity, colloids settling parameter, axial turbulent Prandtl number, inlet flow rate and the inlet solids concentration. Sensitivity studies have been carried out before, on some of the settling parameters[4,7-9,24], the resuspension coefficient[7,9-10], turbulent parameters[4], inlet flow rate[8,12], inlet solids concentration[8,12] and the number of grid cells[10].

Finally, novel research work was undertaken in this project. The Eulerian multi-fluid model was used to predict the flow in circular secondary clarifiers. Secondary clarifiers with sloping floors and a deflector plate were simulated. The direction and variability of the influent were investigated. Comparisons were made between the predicted and measured residence time distributions. Sensitivity studies were undertaken on the density, size and viscosity of the particles, the axial slip velocity, colloids settling parameter and the axial and radial turbulent Prandtl numbers. A 3-D simulation of a secondary clarifier was carried out.

References

1. Schamber, D.R. and Larock, B.E. (1981). 'Numerical analysis of flow in sedimentation basins'. Journal of the Hydraulic Division (American Society of Civil Engineers), vol. 107, 575-591.
2. Tay, A.J. and Heinke, G.W. (1983). 'Velocity and suspended solids distribution in settling tanks'. Journal of the Water Pollution Control Federation, vol. 55, 261-269.
3. Zhou,S., McCorquodale, J.A. and Vitasovic,Z. (1992c). 'Influences of density on circular clarifiers with baffles'. Journal of Environmental Engineering (American Society of Civil Engineers), 829-847.
4. Samstag, R.W., Dittmar,D.F., Vitasovic,Z., McCorquodale, J.A. (1989). 'Underflow geometry in secondary sedimentation'. Water Environmental Research, vol. 64, no. 3, 204-212.
5. Krebs, P., Vischer,D. and Gujer,W. (1995). 'Inlet-structure design for final clarifiers'. Journal of Environmental Engineering, vol. 121, no. 8, 558-564.
6. DeVantier,B.A. and Larock,B.E. (1986). 'Modelling a recirculating density-driven turbulent flow'. International Journal of Numerical Methods in Fluids, vol. 6, 241-253.
7. DeVantier,B.A. and Larock,B.E. (1987). 'Modeling sediment-induced density currents in sedimentation basins'. Journal of Hydraulic Engineering, vol. 113, 80-94.
8. McCorquodale,J.A.,Yuen,E.M., Vitasovic,Z. and Samstag,R. (1991). 'Numerical simulation of unsteady conditions in clarifiers'. Water Pollution Research Journal of Canada, vol. 26, 201-222.
9. Zhou,S. and McCorquodale,J.A. (1992). 'Mathematical modelling of a circular clarifier'. Canadian Journal of Civil Engineering, vol. 19, 365-374.

10. Zhou,S. and McCorquodale,J.A., (1992). 'Influence of skirt radius on performance of circular clarifier with density stratification'. International Journal of Numerical Methods in Fluids, vol. 14, 919-934.

11. Lyn,D.A., Stamou,A.I. and Rodi,W., (1992). 'Density currents and shear-induced flocculation in sedimentation tanks'. Journal of Hydraulic Engineering, vol. 118, 849-867.

12. McCorquodale, J.A. and Zhou, S. (1994). 'Effects of hydraulic and solids loading on clarifier performance'. Journal of Hydraulic Research, vol. 31, no. 4, 461-478.

13. McCorquodale, J.A. and Zhou,S.P. (1994). Use of numerical models in clarifier design - Optimization of inlet structures. 67th Annual Conference of the Water Environment Federation. Chicago.

14. Szalai,L., Krebs, P. and Rodi, W. (1994). 'Simulation of flow in circular clarifiers with and without Swirl'. Journal of Hydraulic Engineering, vol. 120, no. 1, 4-21.

15. Dahl,C., Larsen,T., Petersen,O. (1994). 'Numerical modelling and measurement in a test secondary settling tank'. Water Science Technology, vol. 30, 219-228.

16. Zhou, S. and McCorquodale, J.A. (1994). 'Short circuiting and density interface in primary clarifiers'. Journal of Hydraulic Engineering, vol. 120, no. 9, 1060-1080.

17. Heinke, G.W. (1974). Design and performance criteria for settling tanks for the removal of physical-chemical flocs. Summary Report. University of Toronto.

18. Heinke, G.W., Qazi, M.A. and Tay,A. (1975). Design and performance criteria for settling tanks for removal of physical-chemical flocs. Research report. University of Toronto.

19. McCorquodale, J.A. (1987). Density currents in clarifiers. Proceedings of the National Conference on Hydraulic Engineering. ASCE. New York. N.Y.

20. McCorquodale, J.A. (1976). Hydraulic study of the circular settling tanks at the West Windsor pollution control plant. Report submitted to Lafontaine, Cowie, Buratto and Associates limited, consulting engineers. Windsor, Ontario.

21. Aiba, S., Humphrey, A.E. and Millis, N.F. (1965), Biochemical Engineering. University of Tokyo Press, Tokyo, 304-305.

22. Finstein, M.S. (1965). 'Gross dimensions of activated sludge floc'. Bacterial Proceedings of the American Society of Microbiology, 13.

23. Levine, A.D., Tchobanoglous, G. and Asano, T. (1985). 'Characterization of the size distribution of contaminants in wastewater: treatment and re-use implications. Journal of the Water Pollution Control Federation, vol. 57, 805-816.

24. Larsen, P. (1977). On the hydraulics of rectangular settling basins, experimental and theoretical studies. report no. 1001, Department of Water Resources Engineering, Lund Institute of Technology, Lund University, Lund, Sweden.

CHAPTER VIII

CONCLUSIONS

1. The single-phase flow model predicted the residence time of the effluent from both a pilot-scale and full-scale clarifier to within 24 % of the experimental data.

2. The inlet boundary, represented as a vertical flow showed no added value to the single-phase flow prediction in the pilot-scale tank and therefore, a horizontal inlet flow was preferred.

3. The single-phase flow model predicted the residence time distribution of the effluent in the full-scale clarifier much better when using a variable inlet flow rate.

4. There was a good agreement (5%) between the predicted and measured residence time distribution of the effluent in a full-scale circular secondary clarifier using the modified Eulerian multi-fluid model. However, the model only compared well with the mean measured residence time of the RAS in one test case.

5. The modified multi-fluid model could not predict the residence time of the effluent in another secondary clarifier with a turbulent jet on a deflector plate.

6. The modified multi-fluid model compared quite well with the measured solids contours in both secondary clarifiers.

7. The predicted mean particle diameter was between 100 and 130 μm for the conventional secondary clarifier, and between 150 and 190 μm for the secondary clarifier with the deflector plate. These values were similar to the experimental data found in the literature.

8. The predicted RAS solids concentration was 20% higher than the measured data.

9. Inter-phase momentum transfer was incorrectly modelled because there was no account of the influence of the radial flow on the settling velocity of the particles.

10. The symmetry boundary condition that represents the water surface in the clarifiers did not allow for its movement and therefore the radial velocities near the water surface were probably over-predicted.

11. The most sensitive parameters in the multi-fluid model, for the prediction of flow in circular secondary clarifiers, were the particle density, particle diameter, axial slip velocity, colloids settling parameter, axial turbulent Prandtl number, inlet flow rate and the inlet solids concentration.

13. Overall, computational fluid dynamics techniques were able to give some reasonable predictions of the residence time distribution of the effluent and RAS and the mean particle diameter in circular wastewater clarifiers.

CHAPTER IX

FUTURE WORK

There are improvements that can be made to the multi-phase flow model presented in this work, which should improve it's comparison with experimental data. Before progressing to multi-phase flow it is sensible first to improve the model for single-phase flow.

The water surface in a sedimentation tank is not stationary and should preferrably not be represented by a symmetry plane. It can be affected by the wind, velocities near the water surface and variable flow. In the program CFX-F3D the 'homogeneous' model is similar to the free surface model in other programs and uses the same velocity field for each of the phases. There is also no inter-phase transfer of mass, momentum or energy between the phases. The water surface can be represented by modelling the interface between two phases, namely air and water. Air stays above the water because of its lower density difference. The homogeneous model may be used to predict the inlet flow pattern more accurately and lower the radial velocities near the water surface. This could improve the prediction of the residence time distribution of the effluent in the pilot-scale and full-scale humus tank.

The variable inlet flow rate to all full-scale clarifiers should be measured as close as possible to the inlet of the clarifier. This would reduce the time it takes for the flow to reach the inlet and reduce the damping effect on variable flow. The return activated sludge flow rate should be measured as close as possible to the bottom of the secondary clarifier and the waste sludge flow rate (from the RAS) should be zero.

There is a need to measure flow velocities in sedimentation tanks to validate numerical models because the residence time distribution is not a useful method for determining the flow patterns in a clarifier. It is easier to measure flow velocities in a pilot-scale tank using water as the simulant because there is good flow visualisation. A simple method would be to inject dye and measure how long it takes to travel a known distance in the tank. A better method is to use a portable velocity meter which is capable of measuring low velocities and can indicate the direction of the flow. A much more expensive but accurate method is Laser Doppler Anemometry (LDA). Probably, the best compromise between accuracy and cost is to use a velocity meter. In a full-scale clarifier the meter can be lowered into the tank, similarly to using a sludge blanket detector and the direction of the flow can be read by the velocity meter.

Using the homogeoneous model for the water surface, a 3-D model can be used to model the sludge scraper in a circular clarifier. It can be modelled explicitly by modelling a rotating solid scraper. Alternatively, an implicit momentum source model can be used to fix the velocity, turbulent kinetic energy and eddy dissipation on the tips of the sludge scraper so that these values do not change. The preferred method is the explicit model because it infers that the geometry of the sludge scraper affects the flow pattern. The rotation of the sludge scraper can also be modelled for multi-phase flows in secondary clarifiers in the program CFX-F3D.

Temperature induced density stratification is more predominant in primary full-scale clarifiers where there are lower inlet suspended solids concentrations. The temperature difference between the influent and the contents in the clarifier induces thermal gradients. It is worth measuring the temperature distribution in a clarifier and for the influent and effluent. This data can be used to validate the numerical model which can solve the conservation equation of energy. Some work

has already been carried out on the effect of the inlet temperature on the flow patterns in pilot-scale clarifiers.

To investigate the effect of wind on any full-scale clarifier is difficult to carry out because a measuring device (i.e. wind vanes) needs to be located on the water surface to measure the velocity and direction of the wind. An alternative method may be to measure the profile of the water surface. Comparisons can be made with a numerical model of the free water surface.

Progressing to a multi-phase flow model, the most important work that is needed is the modelling of the inter-phase drag term in the momentum equation. The flow in a secondary circular clarifier can be simplified to a two dimensional flow. The drag coefficient of the particles has a non-linear relationship with the relative Reynolds number. This makes it undesirable to split the flow into two directions and calculate the anisotropic drag coefficient, however this is the only option in the program CFX-F3D. One method may be to calculate the direction of the settling velocity vector from the local values of the axial and radial liquid velocities. Then discompose the magnitude of the measured settling velocity into its axial and radial components and substitute these values into the model for the axial and radial slip velocities respectively. Consequently, calculate the inter-phase momentum transfer separately in the axial and radial directions from these values. Further work is required to implement the right equations into the inter-phase drag term.

The liquid and solid phases of the flow in a secondary clarifier have been modelled as a turbulent fluid with no inter-phase transfer of turbulence. It is not known whether the solids phase should have been modelled as a laminar or turbulent fluid. It will be useful to represent the solids phase as a laminar fluid to determine

if the comparison with experimental data is improved. So far, the production and dissipation of turbulence due to the presence of the particles have been ignored. The source terms of production and dissipation can be included in the k and ϵ transport equations using the standard k-ϵ model. However, it may not be sensible to include them in the equations because their magnitudes are unknown.

The free surface modelling of an interface between two continuous fluid phases which includes a disperse phase is not available in version 4 (release 1) of the CFX-F3D program. But, it is very desirable to be able to model the free surface between air and water along with the solid particles in the water. This would be an important breakthrough in secondary clarifier modelling but could also be a difficult step in the development of the Eulerian multi-phase model.

A 3-D simulation of the secondary clarifier with the deflector plate is needed because the turbulent jet in the clarifier has to be modelled in 3 dimensions. The model had been difficult to converge in 2 dimensions, but this may have also been caused by the incorrect formulation of the drag force.

The mean particle density of the solids suspension in a secondary clarifier was assumed to be the average of the experimental data found in the literature. However, it is desirable to measure the mean particle density in a laboratory for the particular wastewater that is also being tested in a settling column. The method is as follows. Samples of wastewater are taken from secondary clarifiers and a number of suspensions at different solids concentrations are made up. Known volumes of the suspensions are weighed and the particle density can be calculated from the suspended solids concentration of the sample and its volume and weight. A range of solids concentrations should be measured to find its relationship with the particle density. Density is sensitive to the temperature of the

fluid and therefore the temperature of the sample in the laboratory should be the same as the sample in the treatment plant.

The mean particle diameter was an output from the numerical model of the secondary clarifiers, but it is preferrable to measure this quantity in an experiment and use it as an input to the model. A number of wastewater samples with different solids concentrations can be measured for the particle size distribution. At each solids concentration the mean particle size can be determined from the area under the particle size distribution curve. The measurement of size has to be the diameter of a sphere. The amount of mixing of the sample in the laboratory will probably be less than in the full-scale secondary clarifier and therefore the amount of particle flocculation and breakup will differ. This can cause an error between the laboratory measured particle diameter and the real field data. It is preferable to use an averaged particle diameter in the Eulerian multi-fluid model instead of a particle size distribution. This is because each discrete particle diameter has to be represented by a different disperse phase in the Eulerian multi-fluid model.

The sensitivity study found that the molecular viscosity of the solid particles did not affect the flow patterns in a secondary clarifier for the range of values studied. However, this was probably because the particle viscosity was much less than the turbulent viscosity of the solids phase and it was therefore ignored when calculating the effective solids viscosity. Higher values of the particle viscosity should be tested to see their effect on the flow pattern in a secondary clarifier.

An important breakthrough in the modelling of multi-phase flow in a secondary clarifier would be to progress to a variable flow. This requires the convergence criteria in the model to be satisfied at the end of every time step. It would be a

substantial step forward for modelling the real flow conditions in full-scale secondary clarifiers.

The effect of the flow in a secondary clarifier on particle growth and breakup would be an interesting study to conduct in order to be able to calculate a distribution of particle diameters in the clarifier. Particle flocculation and breakup are essentially comprised of statistical relationships between the particle diameter, suspended solids concentration and the dissipation of kinetic energy (i.e. a function of the mixing intensity).

Denitrification is a series of chemical reactions which takes place during the biological treatment of wastewater. The nitrate content (NO_3^-) in wastewater is reduced to nitrogen gas in the absence of oxygen. The effect of the oxygen concentration on the nitrate concentration can be studied in the flow of a secondary clarifier to determine how much nitrogen is produced. Homogeneous chemical reactions (e.g. gaseous reactions) are available when using the Eulerian multi-fluid model in the program CFX-F3D.

Finally, when the multi-fluid model has been suitably modified to accurately predict the flow in a secondary clarifier, geometrical studies can be conducted and validated against experimental data. There are some sedimentation tank design studies which have not been studied before using CFD models, as follows: the angle of the floor, side wall depth, the design of the sludge hopper and a comparison between peripheral and launder weirs. The most eagerly awaited study is to find the optimum position of the internal baffle which has a major influence on the flow patterns in sedimentation tanks.

APPENDIX A

RESIDUALS OF THE NUMERICAL PARAMETERS

The Eulerian multi-fluid model was used to predict the flow patterns and suspended solids concentrations in two full-scale circular secondary clarifiers. The method to check the accuracy of the solution was to monitor the residuals for the computed variables. The history of the residuals are presented in this chapter, for the axial and radial velocities, mass continuity, turbulent kinetic energy and eddy dissipation of the liquid phase and the volume fraction of the solids phase. The definition of the residuals are at the end of this Appendix.

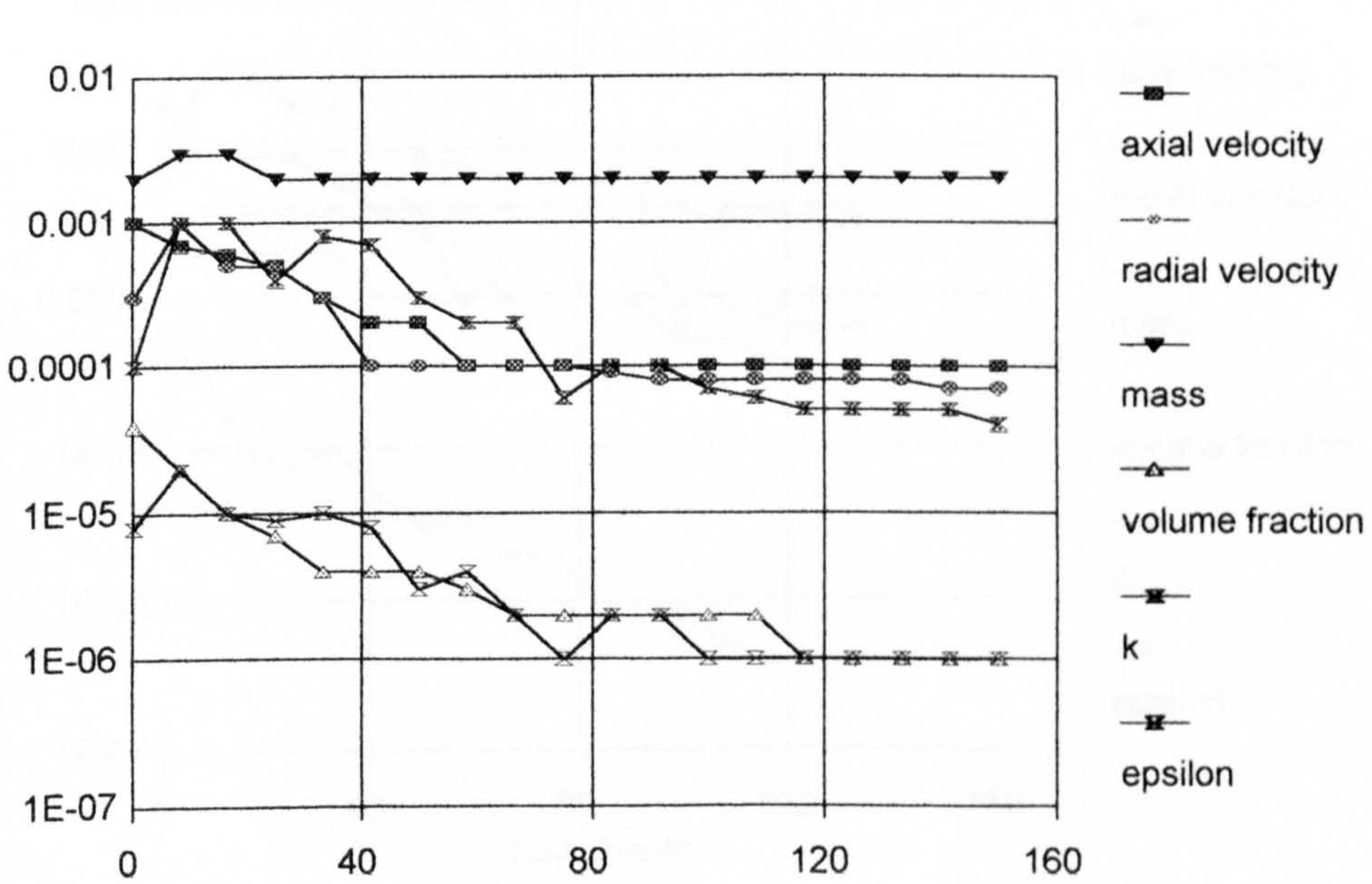

Figure A1 Numerical residuals of the Copley clarifier for test case A.

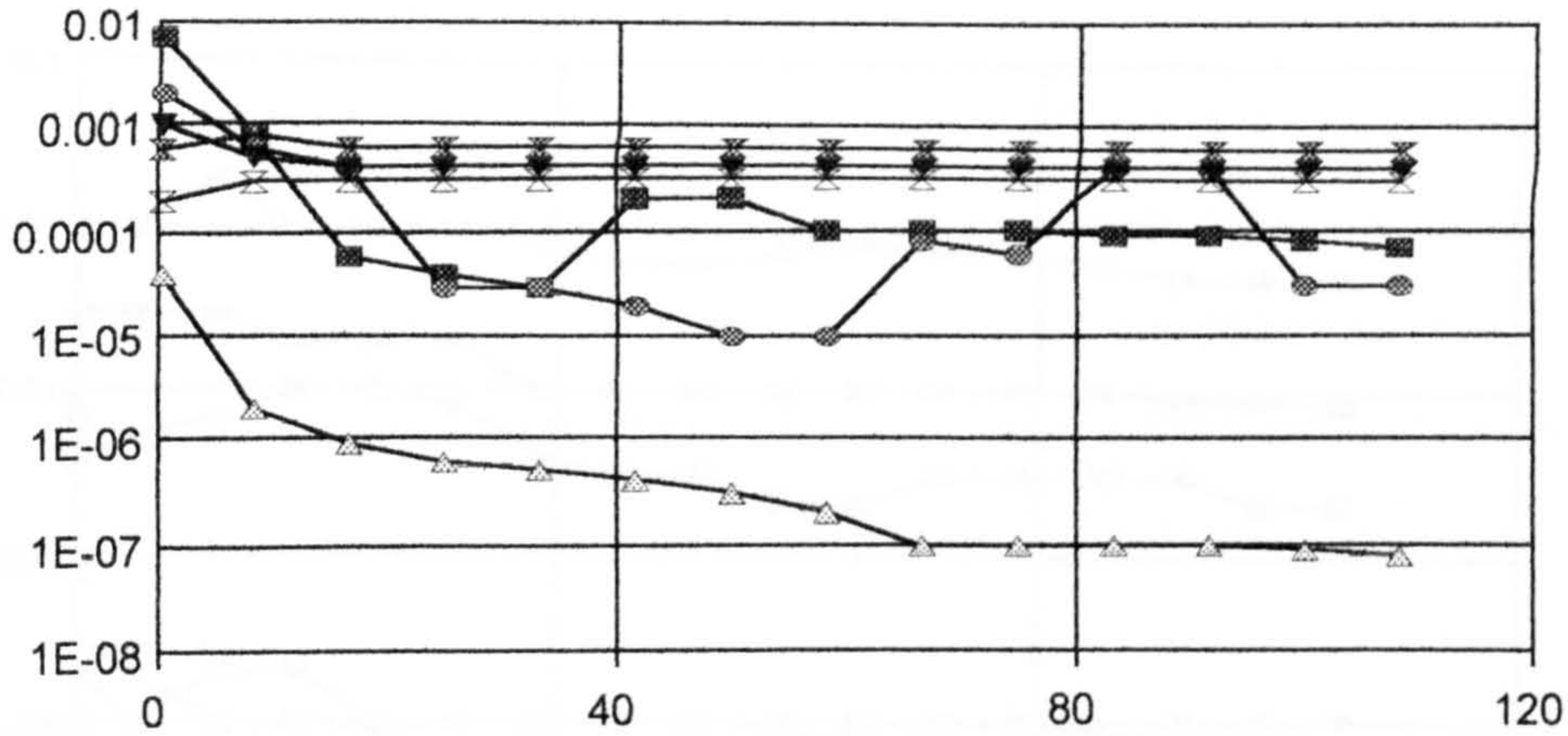

Figure A2 Numerical residuals of the Copley clarifier for test case B.

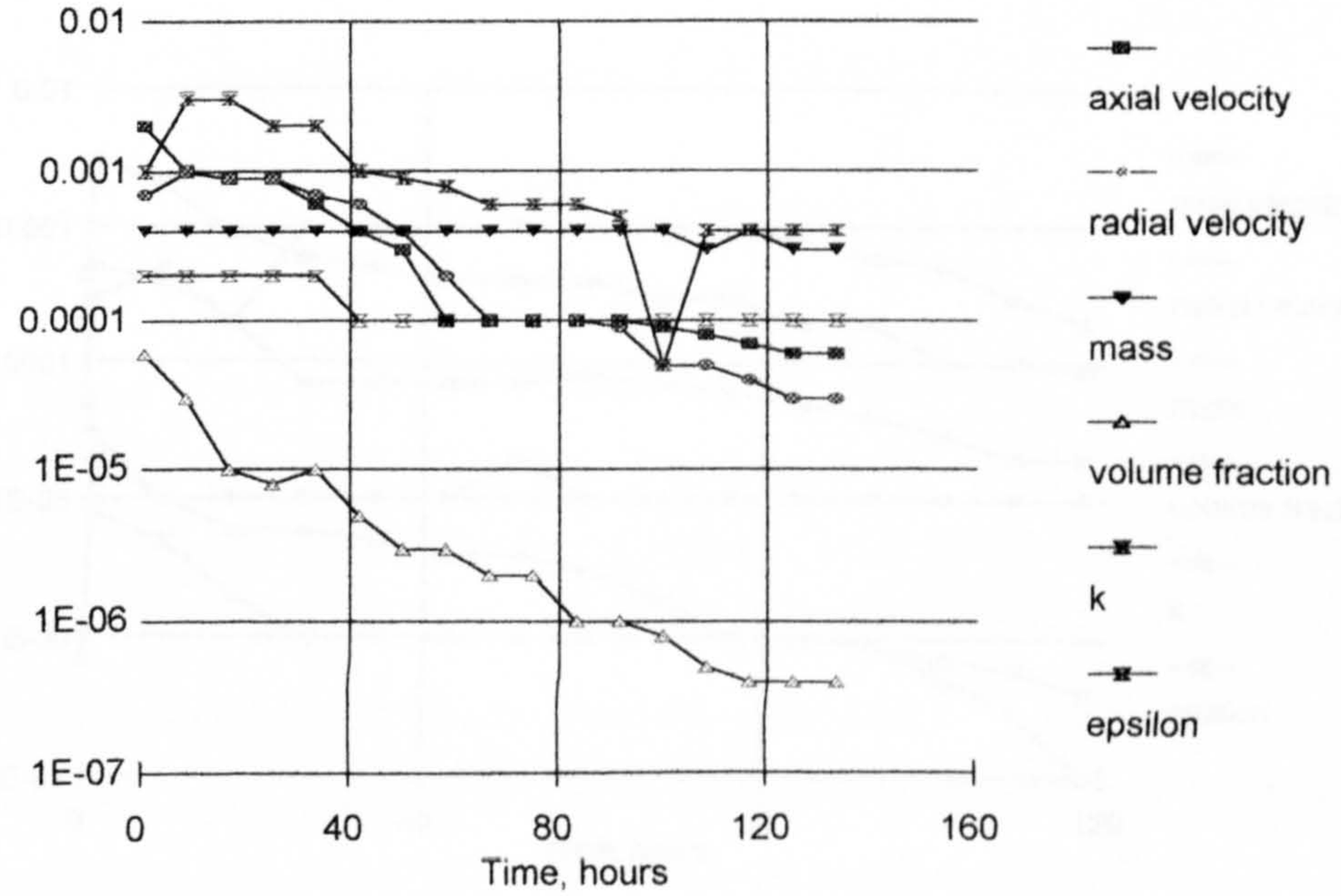

Figure A3 Numerical residuals of the Copley clarifier for test case C.

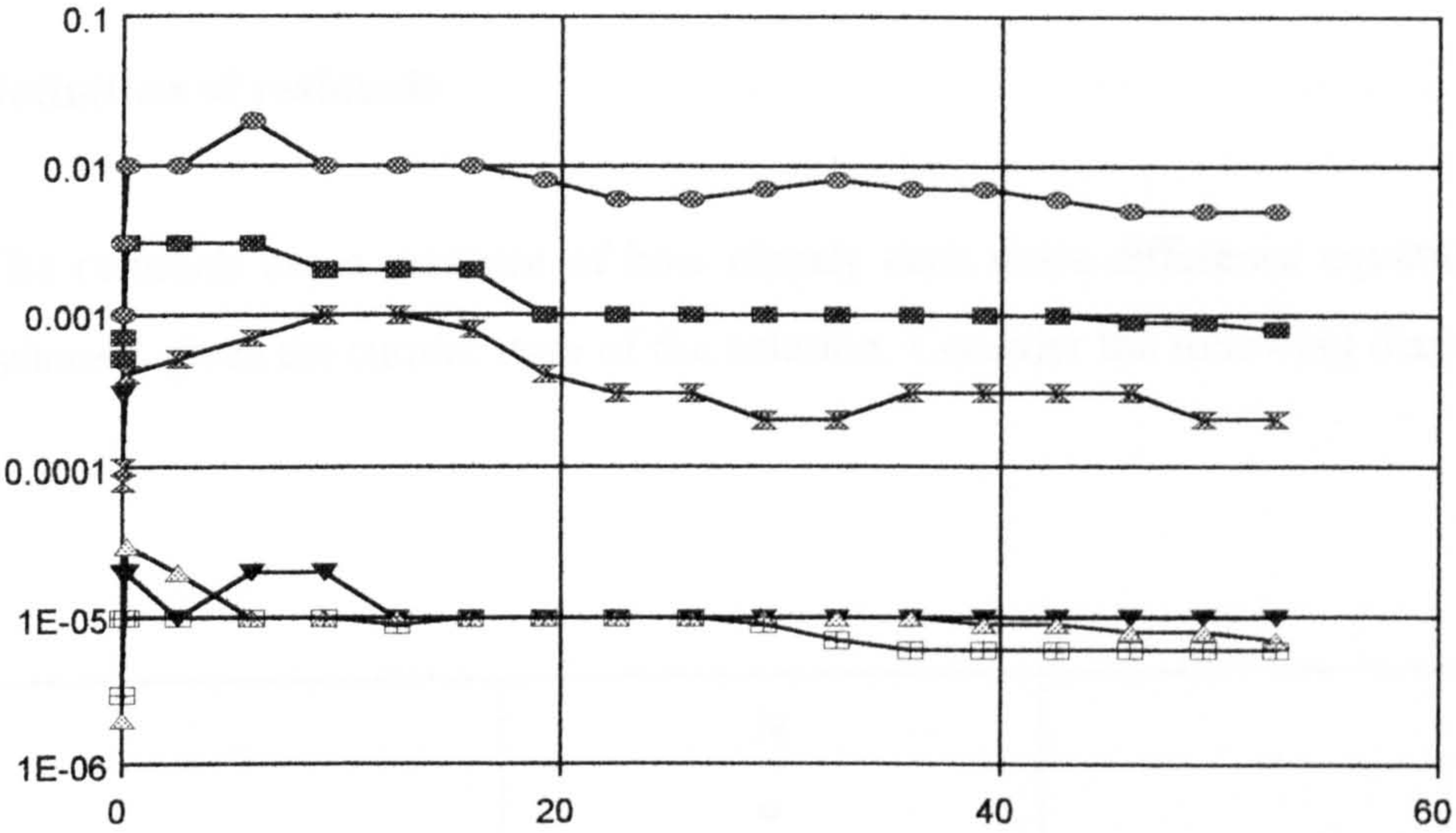

Figure A4 Numerical residuals of the Blackburn Meadows clarifier for test case D.

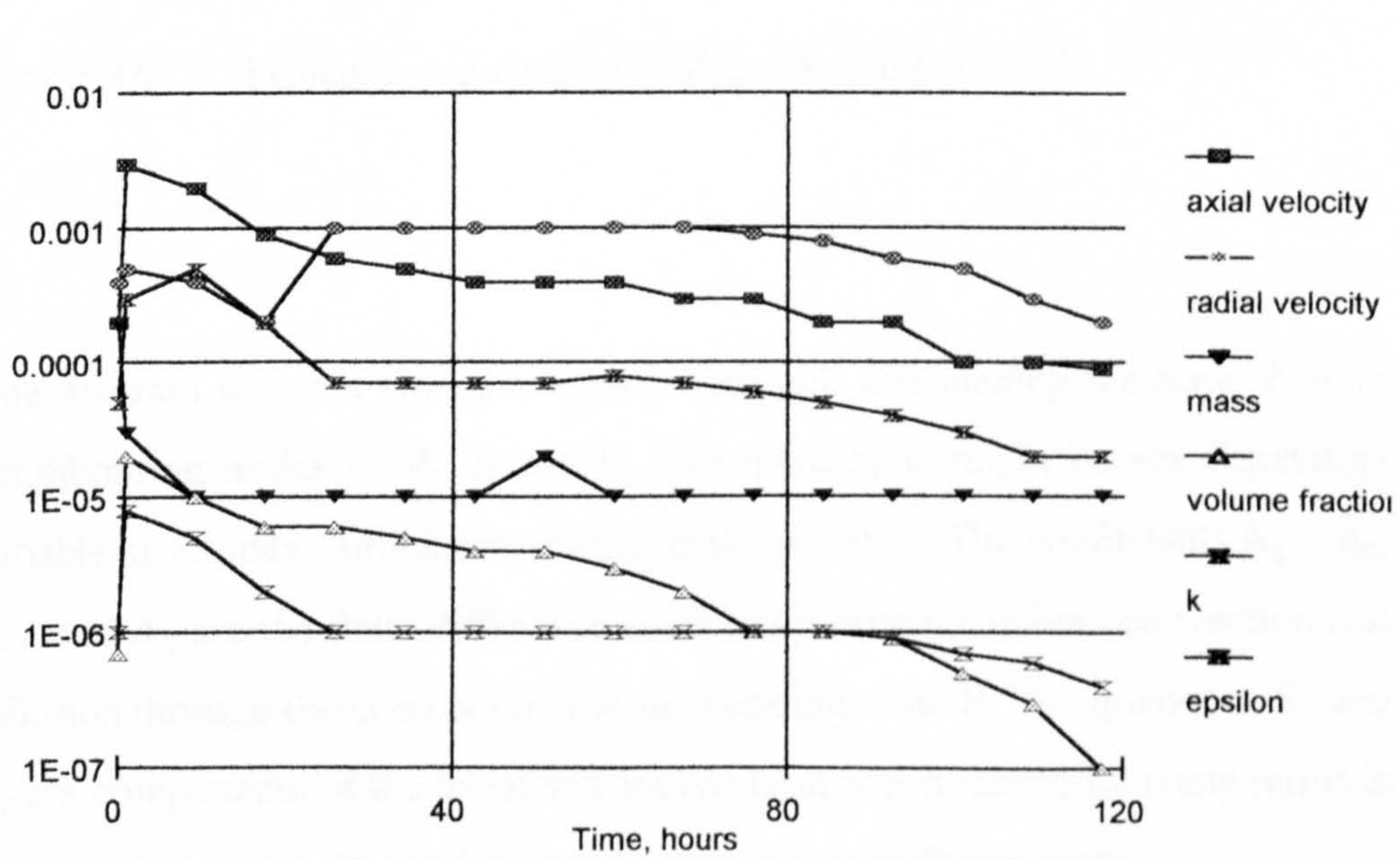

Figure A5 Numerical residuals of the Blackburn Meadows clarifier for test case E.

Definition of residuals

The residuals are a measure of how closely each finite difference equation is balanced, given the current state of the solution. Consider the following diagram:

	N ●	
W ●	**P** ●	**E** ●
	S ●	

Figure A6 Typical computational cell surrounding node P.

The diagram shows a typical computational cell surrounding the node P, with neighbouring nodes E, W, S and N. The quantity ϕ might be any dependent variable (u velocity, turbulence energy, enthalpy, etc.). The coefficients A_E , A_W A_N and A_S are the finite difference coefficients which combine convection and diffusion through the control volume surrounding point P. The quantities S_C and S_P are components of the linearised source term which incorporate any terms in the equation which do not fall into the convection/diffusion form.

The residuals in the program CFX-F3D are normalised, except for the mass source residual. The normalised residual is the sum of the imbalance in the equations for all cells in the domain, divided by the sum of the quantity ϕ at node P, as follows:

$$R=\frac{\sum_{nodesP}|A_E\phi_E+A_W\phi_W+A_N\phi_N+A_S\phi_S+S_C-A_P\phi_P|}{\sum_{nodesP}|A_P\phi_P|}$$

-(A)

The mass source residual is not dimensionless: it is equal to the numerator in the above equation and therefore has the dimensions mass ÷ time. It can be normalised by comparing it with the total mass flow through the inlets into the domain.

APPENDIX B

NUMERICAL BOUNDARY CONDITIONS

Inlet boundary

Velocity inlet boundary conditions are used to define the velocity and scalar properties of the flow at inlet boundaries. In some instances, velocity inlet boundaries may also be used to define the velocity at flow outlets. The alternative inlet boundary condition is a pressure boundary which is specified in terms of the pressure difference from inlet to outlet instead of the mass flow rate. However, for a sedimentation tank the inlet flow rate is known and therefore a velocity inlet boundary condition is more physically sensible. Incompressible and weakly compressible flow at a velocity inlet has all variables specified, except pressure which is extrapolated from the downstream quantity.

The velocity at an inlet can be specified as either normal to the boundary or as the components of the velocity (e.g. swirling flow). A boundary is defined as a patch in the program CFX-F3D and a non-uniform velocity profile on a patch can only be specified in a user defined subroutine. In a circular sedimentation tank with an inlet vertical pipe, there are alternative inlet boundary locations. It can be located as far upstream in the inlet pipe as physically possible to allow for the flow to become fully developed. If measurements of the inlet velocity magnitude and profile are available then this would be the most sensible place to locate the inlet patch, as long as it does not extend the geometry too much. Because there was no measured inlet velocity data a uniform profile was used. Comparisons were made

between an axial velocity at the top of the inlet pipe and a radial velocity above the pipe.

The flow enters the circular clarifier as a vertical inlet jet which disturbs the water surface and flows radially outwards. To model this accurately there should be a free surface to represent the water surface, however it was modelled using a symmetry plane. It was not surprising therefore that the flow patterns for the vertical and horizontal inlet velocities were very similiar above the vertical pipe. It was therefore sensible to assume a uniform radial velocity inlet above the inlet pipe.

In general it is difficult to specify values for all the quantities across an inlet. This is particularly true for turbulence quantities. In the absence of experimental data the inlet values of k and ϵ are based on the mean flow characteristics. Uniform profiles for the turbulence quantities k and ϵ may be approximated for a relatively small inlet into a large domain for example in a clarifier, but are less good when the inlet is as wide as the domain. The inlet effective viscosity is obtained by extrapolation from downstream rather than by computing it from the inlet k and ϵ values. This is due to the fact that k, ϵ and hence μ_t may vary extremely rapidly at the inlet, and the estimated inlet values of k and ϵ may be far from their true physical values. This can lead to large numerical errors in the computation of viscosity gradients which contribute to the momentum equation source terms. The empirical constants C_{p1} and C_{p2} which are used to calculate the inlet values of k and ϵ have values 0.002 and 0.3 respectively. These values should not be changed because they have been derived from experiments on turbulent flows that have been well documented. All the inlet turbulence quantities and velocities were assumed to be the same for each of the phases in the multi-phase flow. This is the most common practise when there is no measured data for the disperse phase,

however different values of the inlet velocity and turbulence quantities can be specified for each phase.

Volume fractions of the liquid and solid phases are specified as a uniform profile in the inlet. This is realistic when there is a homogeneous concentration such as in a fully developed pipe flow. For the vertical inlet at the top of the pipe this is quite reasonable. However, the radial velocity inlet boundary condition has a volume fraction gradient in the vertical direction because of the higher density of the dispersed phase. The assumption of a uniform inlet volume fraction is not too problematic with a small inlet into a large domain but will have an effect when the inlet is as wide as the domain.

Wall boundaries

Many of the variables vary rapidly in the near-wall regions of the flow and, instead of using extremely fine grids in these regions, their behaviour is specified with wall functions. A more fundamental problem is that the model equations, as defined, do not accurately represent the the turbulence in the near-wall region. The wall function is derived by considering the flow in a fully developed boundary layer over a stationary wall. Near the wall it is found that the wall shear stress τ is related to the turbulence kinetic energy. The equation for the turbulent kinetice energy k is solved in the control volume immediately adjacent to the wall. From this the value of the wall shear stress is obtained. A special treatment of the production terms in the k equation is necessary in order to use only quantities interior to the flow and the specified boundary conditions of the velocities and temperature. The turbulence dissipation has a unique relationship with the turbulence kinetic energy near the wall.

The shear stress on the fluid at the wall is calculated from the properties of the flow adjacent to the wall/fluid boundary. In laminar flows this calculation is dependent on the velocity gradient at the wall, while in turbulent flows the well known log law of the wall is applied. Fluid flow over rough surfaces are encountered in diverse situations and wall roughness affects drag (resistance). If a turbulent wall bounded flow has considerable wall roughness these effects can be included through the law-of-the-wall modified for roughness. The flow properties in the near wall regions of the clarifier were defined using the standard wall function in CFX-F3D.

A thin surface boundary condition was used to define the internal baffle and deflector plate in the clarifiers. This boundary is composed of two walls which are separated by an infinitely small thickness and the boundary conditions are the same on both sides of the thin surface. The standard wall function was probably adequate for the modelling of the flow near the walls, baffle and deflector plate in the clarifier because the boundary layer flow was really not being investigated. It was believed that using a more advanced wall function to resolve the near wall flow would not have a significant effect on the overall flow pattern in the clarifier.

Planes or axes of symmetry

Symmetry boundary conditions are used when the physical geometry of interest, and the expected pattern of the flow have mirror symmetry. It assumes a zero flux of all quantities across a symmetry boundary and no convective flux, i.e the normal velocity component at the symmetry plane is thus zero. There is no diffusion flux across a symmetry plane, i.e the normal gradients of all variables are thus zero. The symmetry boundary conditions are identical to those of a frictionless wall.

Symmetry boundaries are used to reduce the extent of the computational domain to a symmetrical subsection of the overall physical system. An axis boundary condition can be used at the centerline of axisymmetric problems whenever the grid lines converge to a point at the centerline. This is appropriate for defining the centre line of a circular clarifier when the radius becomes zero (indeed it can also be used for a very small inner radius). A 3-D circular clarifier can be simplified to a 2-D polar grid in CFX-F3D using the axis boundary condition on the centreline.

Whereas a symmetry boundary may be appropriate for dividing a symmetrical flow pattern, it should not be used for the interface between two fluid phases such as at the water surface in a clarifier. Clearly, the impact of the inlet vertical jet on the free water surface has a major influence on the flow patterns in a clarifier. When it collides with the water surface the normal velocity at the surface is zero and therefore the axial momentum is transferred to a radial velocity parallel to the water surface. Therefore, the highest radial velocities are found in the computational cells adjacent to the water surface. Normally there is air/water shear at a water surface instead of fluid/fluid shear and the largest radial velocities should be normally a distance below the water surface. The radial velocities in the clarifier will be over-predicted when using a symmetry plane to represent the water surface.

Future work is required to model the particle laden flow in the pilot-scale and humus tanks using the 'homogenous' multi-phase model in CFX-F3D with a free surface between the air and surface water. Progress to modelling particle transport in the water phase with a free water/air surface will depend on the availability of combining the Eulerian multi-fluid and homogeneous models in the program CFX-F3D.

Mass flow (Neumann) outlet boundary

The fraction of the total inlet mass flow rate to a secondary clarifier was specified in the effluent and RAS outlets to make sure that mass conservation was satisfied. This is implemented at a mass flow boundary as follows :

(1) Apply a nominal Neumann boundary condition to the velocity field, i.e

$$\frac{\partial U^i}{\partial n} = 0 \qquad \text{- (B1)}$$

The gradient of the normal velocity with respect to distance is zero, which corresponds to a fully developed flow.

(2) Compute the discrepancy between the actual mass flow rate out of the domain, and the desired flow rate M.

(3) Add an increment to U^i on the boundary, in the direction of the outward going unit normal n^i, to force the outward mass flow rate to the desired value.

This is equivalent to

$$\frac{\partial U^i}{\partial n} = \lambda n^i \qquad \text{- (B2)}$$

A mass flow boundary condition is one at which values for all variables are extrapolated from the interior cells adjacent to the outlet and have no impact upon the upstream flow. The outlet velocity and pressure are updated in a consistent manner which is analogous to fully developed flow when there is no area change at the outlet. In subsonic flows, the normal velocities at the outlet are adjusted to satisfy an overall mass balance for the computational domain. The correction is updated at each iteration so that the exit flow balances the inlet flow. The mass flow boundary is most suitable when the outlet area is not changing, for example in a uniform duct well away from the main flow region.

However, it can also be applied to regions of flow which are not fully developed if it is expected to have a small impact on the flow. This is as long as it is not placed where there is expected to be recirculating flow. This is important because a mass flow boundary at an outlet cannot define the properties of recirculating flow. In this case it is better to use a pressure boundary or extend the domain downstream to position the outlet where there is fully developed flow.

In the multi-fluid model the fractional total mass flow rate through each outlet was specified and therefore the velocity components of all phases, were adjusted proportionately to the local volume fraction. There is however a difficulty using mass flow boundary conditions with multi-phase flow. The volume fraction

equations solve the mass conservation equation for each phase and are coupled with the pressure correction equation, which imposes mass conservation for all phases together. But there can be difficulties in achieving the correct mass flow for the individual phases.

Pressure boundaries are an alternative when there is knowledge of the pressure difference between the inlet and outlet. Because there were two outlets in the secondary clarifier, pressure boundaries can only be specified at both outlets if the static pressure was known in each. The flow is only influenced by the relative pressure differences at pressure boundaries. If the split in flow between the outlets is known then it is better not to specify the outlets as pressure boundaries otherwise the correct split may not be predicted.

Velocity inlet boundaries can be specified as a negative velocity at an outlet and thereby suck the flow out of the domain. However, both outlets cannot be specified as 'velocity inlets' because there will be a mass conservation problem. Unless the areas of the outlet boundaries are known to machine accuracy, then the mass flowrates calculated in the velocity outlets will not satisfy mass conservation in the domain. Therefore, the RAS outlet was instead specified as a velocity inlet and the effluent outlet as a pressure boundary with a zero static pressure. The convergence of the solution was very similar to using two mass flow boundaries. The overall flow pattern was the same except for the velocity profile across the bottom cells of the sludge hopper. When using a 'mass flow boundary' for the RAS outflow the velocities were in both the upward and downward directions at the boundary, which was probably because the flow was not yet fully developed. However, the flow pattern at the bottom of the sludge hopper did not have much of an effect on the overall flow pattern in the clarifier. This was possibly because the vertical solids concentration gradients were large in the sludge hopper, which

inhibited the movement of flow upwards. However, specifying the correct boundary at the effluent outlet was more important than the RAS outflow because it was closer to a recirculating eddy. The static pressure was unknown for the effluent and it was decided not to use a pressure boundary but two mass flow boundaries instead.

The main concern with using mass flow boundaries for the outlets were that they were not situated in a region of fully developed flow. However, the effluent boundary was only one cell thick which meant that there could not be any return flow through the boundary and mass continuity could be quite easily achieved. Moreover, the RAS boundary was in a region of mostly downward flow and well away from the main recirculating flow in the clarifier.

APPENDIX C

SALT TRACER EXPERIMENTS

Dose of lithium chloride

The mass of lithium chloride dosed to the inlet of the full-scale sedimentation tank is calculated on the basis of detecting 3 times the minimum measurable concentration of lithium ions in the clarifier. Therefore, assuming there is a homogeneous lithium ions concentration of 0.3 mg/l in the clarifier, the required dosage of lithium chloride (in kg) is equal to :

$$0.3\frac{V}{100}\frac{MWLi^{+}}{MWLiCl} \qquad \text{- (C1)}$$

where V is the volume of the clarifier in m^3, MW is the molecular weight in g, and Li^+ and LiCl are the chemical formulae for lithium ions and lithium chloride respectively. For example, the Copley secondary clarifier has a volume of 1365 m^3 and 3 x the detectable concentration of Li^+ in the tank is 0.3 mg/l. Therefore:

Mass of Li^+ in tank = 0.3 V/1000 kg

= 0.3 x (1365 / 1000) kg

= 0.410 kg

Dosage of LiCl = mass of Li^+ (MW LiCl / MW Li^+) kg

= 0.410 ((35.453 + 6.941) / 6.941) kg

= 2.504 kg

The calculated dosages of lithium chloride compared to the actual used dosages are given below in Table C1.

Table C1 Salt dosage and percentage of salt/scalar in the outlets in 3 nominal residence times.

Test case / flowrate m^3/s	Tank volume m^3	Salt dosage calculated kg	Salt dosage actual	% salt in outlets	% scalar in outlets
Copley, Q=0.121	1365	2.50	5	97	-
Q=0.195	1365	2.50	3.5	107	109
Q=0.188	1365	2.50	3.5	104	-
Blackburn, Q=0.709	3665	6.73	10	151	-
Q=0.544	3665	6.73	10	132	-
Humus, Q=0.091	1518	2.79	3.5	-	-

Residence time distribution

The experimental test rig for the salt tracer experiment on the pilot-scale clarifier is shown in Figure C1 and the experimental method is described in Chapter 4. The conductivity probe was used to detect the voltage reading of the sodium chloride in the effluent channel of the clarifier and the probe was calibrated beforehand by measuring the voltage of sodium chloride at different salt concentrations. The sodium chloride concentration was found from the voltage reading of the six channel signalling box. The method to non-dimensionalise the residence time distribution is given in Table C2.

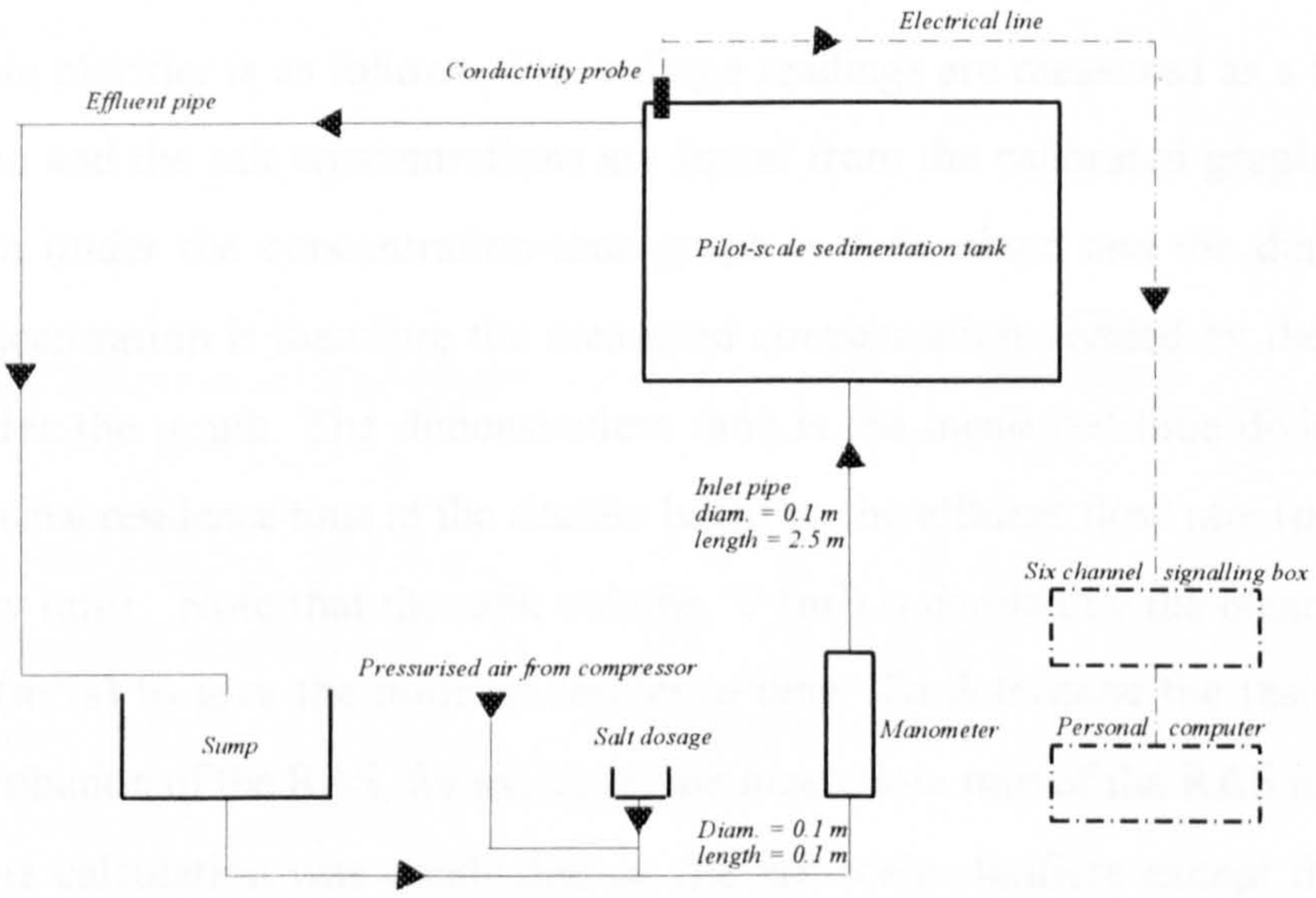

Figure C1 Schematic diagram of experimental test rig of pilot-scale clarifier.

Table C2 Non-dimensionalisation of residence time distribution.

Time sec.	Voltage V	Salt conc. mg/l	Area	Dim.less. time	Dim.less conc.
t1	v1	c1	c1 (t1-0)	t1/τ	c1 /Σ cΔt
t2	v2	c2	c2 (t2-t1)	t2/τ	c2 /Σ cΔt
t3	v3	c3	c3 (t3-t2)	t3/τ	c3 /Σ cΔt
tn	vn	c4	cn(tn-tn-1)	tn/τ	cn /Σ cΔt
			Σ cΔt		

To find the residence time distribution of the effluent (for example) in the pilot-scale clarifier is as follows. The voltage readings are measured as a function of time and the salt concentrations are found from the calibrated graph. The total area under the concentration-time graph is determined and the dimensionless concentration is therefore the measured concentration divided by the total area under the graph. The dimensionless time is the measured time divided by the nominal residence time of the clarifier based on the effluent flow rate (not the inlet flow rate). Note that the tank volume, V (m^3) is divided by the mean flow rate, Q (m^3/s) to give the nominal residence time. To determine the residence time distribution of the RAS, for example, the mean flow rate of the RAS is used. The same calculation was conducted on the full-scale clarifiers except that the salt concentration was measured directly from the samples taken instead of measuring the voltage. The flow sheet of the secondary sedimentation process for the Copley and Blackburn Meadows secondary clarifiers is shown in Figure C2.

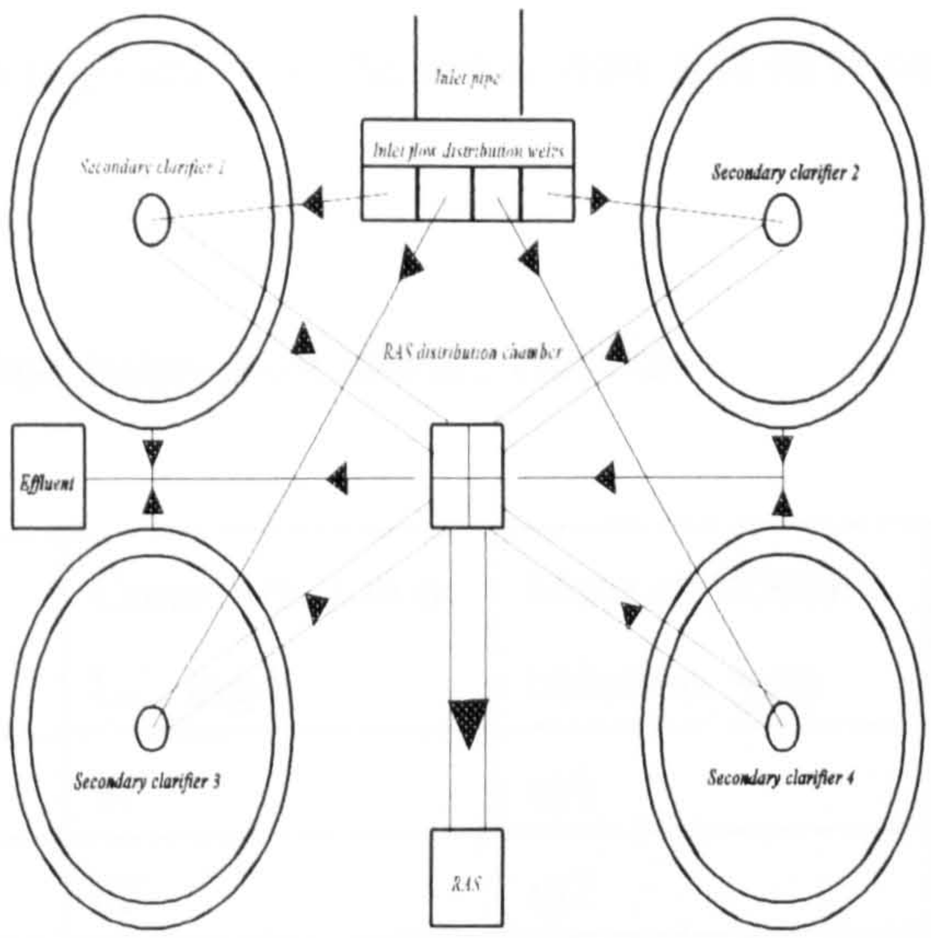

Figure C2 Process flow sheet of secondary sedimentation process at the Copley and Blackburn Meadows wastewater treatment plants.

Mass balances on the experimental and numerical tracers

The percentage of salt to reach the outlets of the sedimentation tank are calculated to check that there is mass conservation of the salt and the numerical scalar. The lithium chloride concentration is calculated from the measured lithium ion concentration as follows :

$$m = c\frac{\%}{100}\frac{MWLiCl}{MWLi^{+}} \qquad \text{- (C2)}$$

where m is the mass flow rate of lithium chloride in kg/s, c is the concentration of lithium ions in mg/l and Q is the mean flow rate of the effluent (or RAS) in m^3/s.

Table C3 Mass balance on lithium chloride.

Time, s	Concentration of Li^+, mg/l	Mass of lithium chloride, kg/s	Mass of lithium chloride, kg
t1	c1	m1	m1 (t1-0)
t2	c2	m2	m2 (t2-t1)
t3	c3	m3	m3 (t3-t2)
tn	cn	mn	mn (tn-tn-1)
			Σ m Δt

The total area under the concentration-time graph (bottom right entry in Table C3) for the mass flow rate of lithium chloride corresponds to the total mass of lithium chloride in the effluent (or RAS). It is calculated for the effluent and RAS outflows separately and the percentage of salt to pass through the outlets for any length of time is as follows :

$$\frac{(\sum m\Delta t)_{effluent}+(\sum m\Delta t)_{RAS}}{doseLiCl} x100\% \qquad \text{- (C3)}$$

The same calculation is carried out on the numerical scalar and the results are given in Table C1.